DIGITALCOMMONS
@WAYNESTATE

Wayne State University

Wayne State University Theses

1-1-2010

Effect Of Alternative Fuels On Aftertreatment Device

Bunpreet Singh
Wayne State University,

Follow this and additional works at: http://digitalcommons.wayne.edu/oa_theses

Part of the Mechanical Engineering Commons

Recommended Citation
Singh, Bunpreet, "Effect Of Alternative Fuels On Aftertreatment Device" (2010). *Wayne State University Theses.* Paper 64.

This Open Access Thesis is brought to you for free and open access by DigitalCommons@WayneState. It has been accepted for inclusion in Wayne State University Theses by an authorized administrator of DigitalCommons@WayneState.

www.manaraa.com

EFFECT OF ALTERNATIVE FUELS ON AFTERTREATMENT DEVICE

by

BUNPREET SINGH

THESIS

Submitted to the Graduate School

of Wayne State University,

Detroit, Michigan

in partial fulfillment of the requirements

for the degree of

MASTER OF SCIENCE

December 2010

MAJOR: MECHANICAL ENGINEERING

Approved by**:**

Advisor Date

www.manaraa.com

ACKNOWLEDGEMENTS

The research work as described in this Masters' thesis dissertation was conducted on the multi cylinder diesel engine at the Compression Ignition Direct Injection laboratory at the Center for Automotive Research (CAR) at Wayne State University Detroit MI. This work would not have been possible without the guidance and direction of my professor and advisor Dr. Dinu Taraza. He has been a teacher and my mentor and I would like to express my deepest gratitude and thank him for all the help and assistance he has made available to me that has made this work possible. His kind words, his watchful ever eyes for perfection, his constant encouragement and valuable insights has driven me to achieve betterment in all the work I have done and I will ever do. His immense experience and his in depth knowledge, has given me both the confidence and comfort in carrying out this research. This work could never be reality without his presence, for which I am eternally indebt to his kindness and support. I would like to say that it was my privilege and pride to have worked under the leadership and guidance of Dr Dinu Taraza.

Dr. Naeim Henein has also been very instrumental in this research work. I will never forget the advice and support that he has rendered to me with a smile on his face. I thank you from the bottom of my heart for always welcoming me to your office every time I needed help.

Special thanks to Dr. Walter Bryzik, Dr. Marcis Jansons and Dr. Trilochan Singh for all the help and advice and for your mere presence in the lab that helped us solve the most complex of the problems in the simplest of way. I will have to add that I was most unfortunate for not having worked with you for a longer period of time. I would have learnt so much more from your vast knowledge and experience.

I was fortunate to get all the support regarding tricks of the trade in the lab from my colleagues Florin Mocaanu and Elena Florea. More than my colleagues they have been my good friends, this thesis would not be complete without thanking them for their advice and their nature to go out of their way teach me everything I needed to know.

www.manaraa.com

TABLE OF CONTENTS

www.manaraa.com

www.manaraa.com

www.manaraa.com

www.manaraa.com

www.manaraa.com

www.manaraa.com

LIST OF FIGURES

www.manaraa.com

www.manaraa.com

www.manaraa.com

www.manaraa.com

www.manaraa.com

www.manaraa.com

www.manaraa.com

www.manaraa.com

www.manaraa.com

www.manaraa.com

LIST OF TABLES

www.manaraa.com

www.manaraa.com

www.manaraa.com

1. INTRODUCTION

1.1. Introduction:

In a diesel engine air is first compressed to self ignition temperature (a temperature high enough to cause the fuel to ignite) and then the fuel is injected in the combustion chamber. In 1893, a German engineer named Rudolf Diesel successfully developed an engine on this principle and obtained a patent of the type which bears his name till date. In 1897, after four years of rigorous experiments, he finally marketed his engine capable of developing 20 hp and gave a thermal efficiency of 26%. The thermal efficiency of a diesel engine is the highest as compared to any internal combustion engine due to its high compression ratio. Diesel engine has a advantage of higher torque at lower speeds. Modern diesel engines are much cleaner, quieter and fuel efficient in operation. In order to compete with the specific power being produced by a spark ignited engine, diesel engines are making use of turbochargers. Nowadays, with the advent of new technical features such as common rail injection system, turbochargers, etc, diesel engines have become very useful in automotive industry.

1.2. Emissions of diesel engines and regulations (history and forecast):

Diesel engines produce higher level of certain pollutants such as NO_x and particulate matter (soot). The smoke form a diesel engine is characterized as per the color. Black smoke is due to the presence of carbonaceous particles, blue smoke is due to presence of lube oil and white smoke is due to the presence of unburnt fuel. However, black smoke has drawn maximum attention as it contains very small particles and is not pleasing to the eye. The exhaust emissions pertaining to diesel engines have been in the process of constant regulation since the early 1960s

www.manaraa.com

and up to 2013. The emission regulations are becoming much more stringent with time. In order to meet these severe emission requirements, an overall optimization of various processes such as type of the fuel, the aftertreatment system and the in- cylinder combustion is necessary.

Diesel engines are categorized into light duty diesel engines and heavy duty diesel engines.

1.2.1. Light duty diesel engines:

Light duty diesel engines fits good for light commercial vehicle applications. NO_X requires the utmost attention for these types of engines, diesel particulate filters takes care of the particulate matter very efficiently and hydrocarbons are generally not an issue with light duty diesel engines (1). Figure 1.1 shows a comparison of Euro 6 regulation and US tier 2 bin 5 standard.

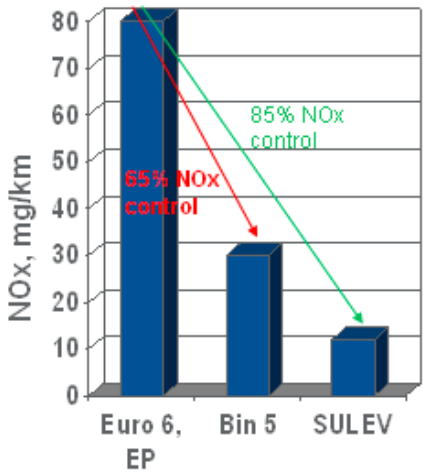

Figure 1.1 Euro 6 NO_X Regulations as compared to US Tier 2 Bin 5 (1)

By adding 65% more deNO_X control to the aftertreatment system, Euro 6 (2014) type engines can be compared with US Bin 5 standards. In order to compare it to the California SULEV standards, the control has to be increased up to 85% and at present

www.manaraa.com

this is the standard being targeted for deNOX technology as far as cold start emissions are concerned. The Japanese proposed target for light duty diesel engines are illustrated in table 1.1.

Standard	NO_X	PM
JP 2009	.08 g/km	.005g/km

Table 1.1 JP 2009 standards (for passenger cars < 1250 kg)

1.2.2. Heavy duty diesel engines:

As most of the fuel in a heavy duty diesel engine is combusted under high load conditions, research engineers are targeting more on traditional diesel combustion hardware and strategies and are making progress towards their goals. Since this experimental investigation involves a heavy duty engine, therefore hereafter, this study will lay more emphasis on heavy duty diesel engines.

Diesel emission standards are becoming tougher with time. Table 1.2 illustrates the U.S.Federal diesel emission standards vs. years (2).

www.manaraa.com

Year	CO (g/bhp-hr)	NMHC (g/bhp-hr)	NO_X (g/bhp-hr)	NMHC-NO_X (g/bhp-hr)	PM(Truck) (g/bhp-hr)	PM(Bus) (g/bhp-hr)
1988	15.5	1.3	10.7		0.60	0.60
1990	15.5	1.3	6		0.60	0.60
1991	15.5	1.3	5		0.25	0.25
1993	15.5	1.3	5		0.25	0.10
1994	15.5	1.3	5		0.25	0.07
1996	15.5	1.3	5		0.10	0.05
1998	15.5	1.3	4		0.10	0.05
2002	15.5			2.5	0.10	0.05
2004	15.5	2.0	0.5	2.5	0.10	0.05
2007	15.5			1.1	0.01	0.01
2010	13.3			0.2	0.01	0.01

Table 1.2 U.S. Federal diesel emission standards vs. time **(2)**

NMHC is basically nonmethane hydrocarbons. The goal of standard per EPA, CARB and heavy duty diesel manufacturer is to reduce heavy-duty highway NOx emissions to a specified limit. For example, in 2004, the specified value for NO_X + NMHC is 2.5 g/bhp-hr which corresponds to an actual breakup of 2.0g/bhp-hr NO_X and 0.5 g/bhp-hr NMHC. The manufacturers can certify their engines either way.

The emphasis of all the emission legislation worldwide is to reduce the gaseous and particulate emissions to close to zero levels. Figure 1.2 shows the emission regulations laid by the three major market sectors (U.S.A., Japan and Europe) which the

www.manaraa.com

heavy duty engines must comply with extremely low exhaust emission limits, without neglecting the fuel economy (3).

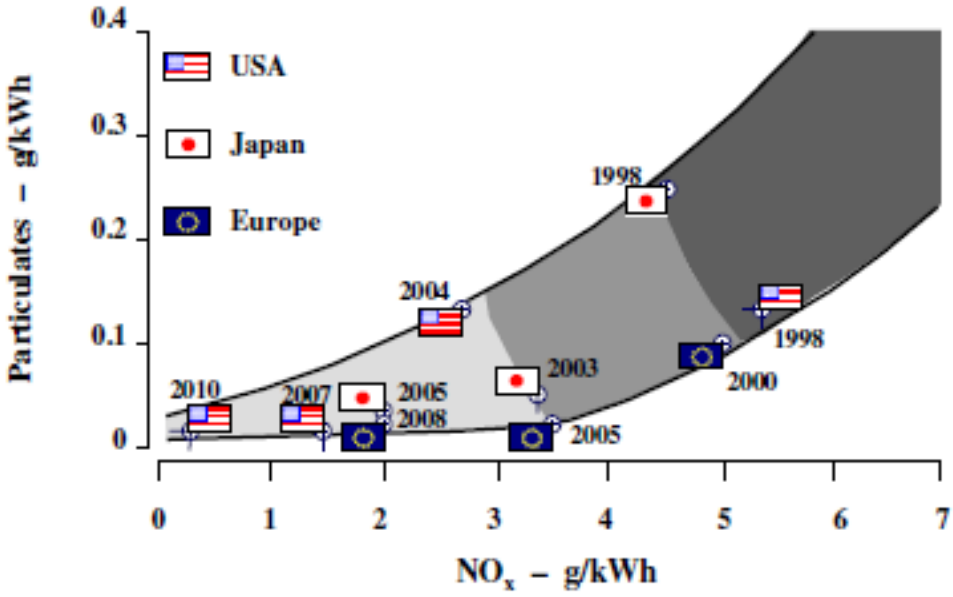

Figure 1.2 Global trend in emission regulation

The three countries follow different duty cycles to conduct engine testing. The new European testing cycle is focused more on medium engine speeds. Figure 1.3 shows the European transient cycle. Figure 1.4 shows the Japan's transient cycle.

In U.S., in order to cover the emission behavior in highway and city traffic conditions, the F.T.P. cycle basically concentrates on high engine speed and also on low idling speeds. Figure 1.5 shows the U.S. transient cycle. The Japanese testing cycle is focused more on low engine speed and low load conditions simulating the typical driving conditions in Japan (especially in big cities).

www.manaraa.com

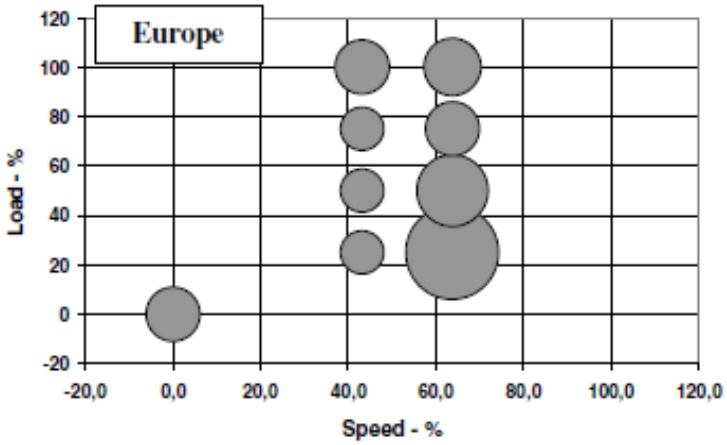

Figure 1.3 European test cycle (3)

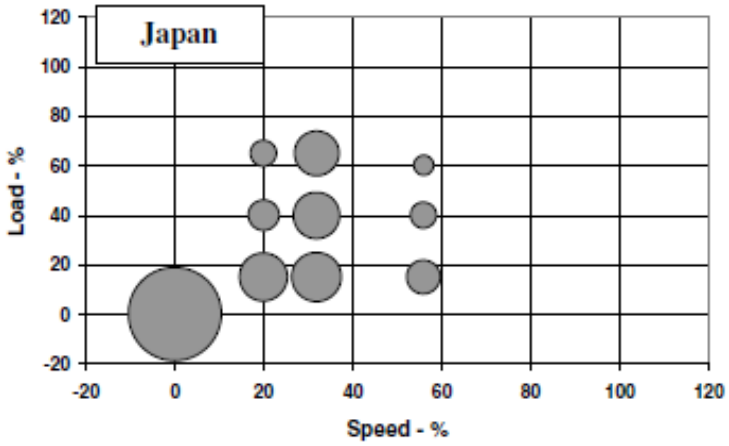

Figure 1.4 Japan's test cycle (3)

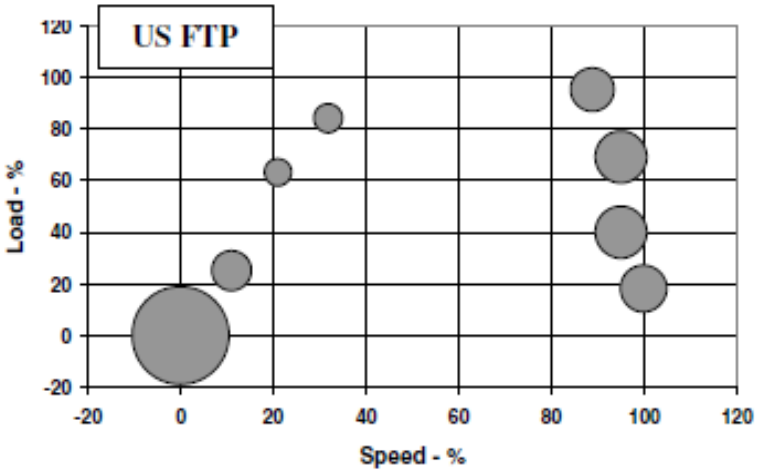

Figure 1.5 U.S.test cycle (3)

www.manaraa.com

The basic comparison of all these three transient cycles is shown in figure 1.6.

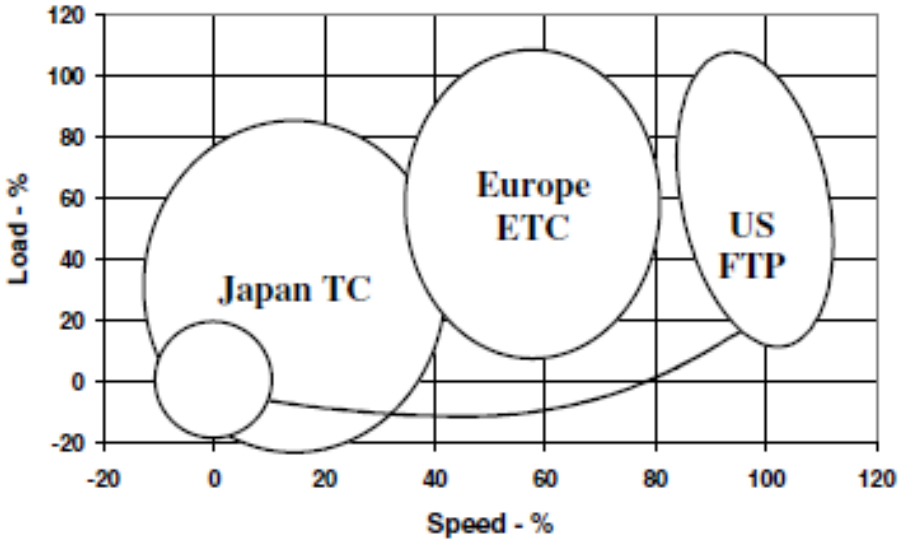

Figure 1.6 Comparison of three test cycles (3).

Table 1.3 illustrates the European standards. Europe is in the process of finalizing the EURO VI heavy-duty regulations for 2013. A new particle number shall be adopted (1).

Standards	**CO** (g/kw-hr)	**HC** (g/kw-hr)	**NO_X** (g/kw-hr)	**PM** (g/kw-hr)	**Smoke** (m^{-1})
Euro IV(2005)	1.5	0.46	3.5	0.02	0.5
Euro V(2008)	1.5	0.46	2	0.02	0.5
Euro VI(2013)	1.5	0.13	0.4	0.01	

Table 1.3 European emission standards

www.manaraa.com

Table 1.4 illustrates the Japanese emission standards. The proposed 2009 emission regulation's details for Japan are also shown in the table.

Standards	**NO_X** (g/kw-hr)	**PM** (g/kw-hr)
JP 2005	2.0	0.027
JP 2009(proposed)	0.7	0.01

Table 1.4 Japanese emission standards

www.manaraa.com

2. LITERATURE REVIEW

2.1 Different arrangements for meeting the emission requirements:

2.1.1. Exhaust gas recirculation (EGR):

Oxides of nitrogen are formed when the temperature inside the combustion chamber exceeds the critical temperature so that the molecules of nitrogen and oxygen combine (6). Basically, there are two types of EGR: internal and external. External EGR uses external piping to direct the exhaust gases back to the combustion chamber whereas Internal EGR normally uses devices such as variable valve timing in order to retain a certain fraction of exhaust from the previous cycle. Figure 2.1.1 shows the arrangement of an External EGR system.

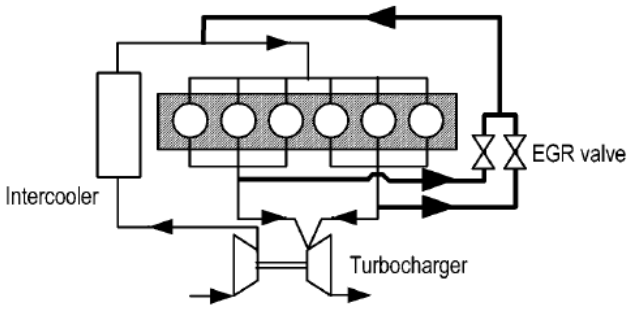

Figure 2.1.1 External EGR system (6)

www.manaraa.com

EGR basically cuts off some percentage of the oxygen going into the combustion chamber and also increases the specific heat of the charge inside the combustion chamber which ultimately reduces the in cylinder temperature. There is no doubt that EGR is very effective in reducing oxides of nitrogen, but it also has adverse effects on the engine efficiency. As it contains a lot of particulate matter, it may also contaminate the lubricating oil and can also foul the intake manifold (6).

2.1.2. Diesel oxidation catalyst (DOC):

It basically consists of a substrate, an oxide mixture which is known as a washcoat and precious metals such as platinum, palladium or rhodium (4). Fig 2.1.2 shows the function of a DOC.

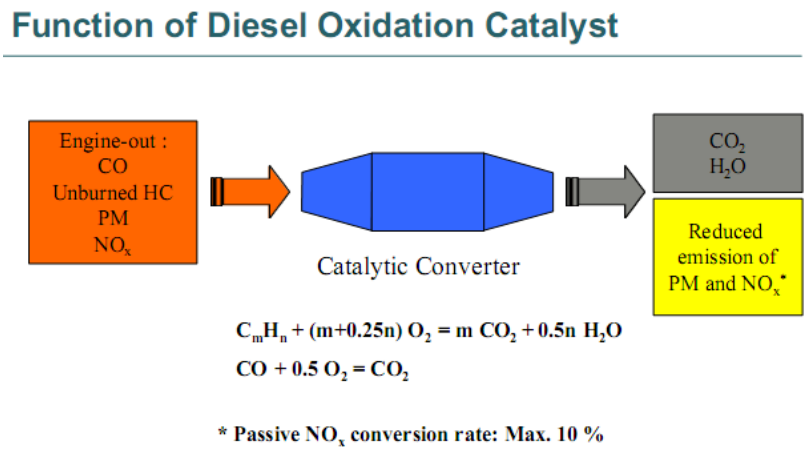

Figure 2.1.2 Purpose of a DOC (4)

www.manaraa.com

The DOC performs the following functions:

- Carbon monoxide (CO) and unburnt hydrocarbons (HC) are oxidized to CO_2 and H_2O.
- NO is oxidized to NO_2 in a DOC. NO_2 is a better oxidizer as compared to oxygen for the oxidation of the soot (5).
- The D.O.C's effectiveness after reaching the light-off temperature is high and it is quite satisfactory at the moment.
- Doc also helps in reducing the soluble organic fraction of the diesel particulate.
- However, there is a problem due to the CO and HC emissions during cold start and warm up conditions.

There is no doubt that the oxidizing catalyst is one of the important aftertreatment devices which is playing a key role in reducing tail pipe emissions. An oxidizing catalyst basically oxidizes the carbon monoxide and unburnt hydrocarbons. Also, it reduces the particulate matter emissions. Particulate matter mainly comprises of a carbonaceous or soot component which constitutes most of the insoluble fraction, and a complex cocktail of high molecular weight organic compounds known as the soluble organic fraction (SOF) (22). Hence, the conversion efficiency of an oxidizing catalyst for particulate matter is limited by the net percentage of SOF in the total amount of particulate matter. In case of diesel engines, no additional measure is required to ensure sufficient oxygen for a catalyst to operate since the exhaust gas is always rich in oxygen. Therefore, diesel exhaust temperatures can fall sufficiently to cause the catalyst to light down (22).

www.manaraa.com

Lubricating oil can also contribute to the PM emissions. The need for extremely low consumption, with minimal contribution to PM, can be relaxed somewhat if the oil is oxidized by the catalyst (22).

2.1.2.1. Architectural design of D.O.C.:

A diesel oxidizing catalyst is a flow through device that consists of a canister which contains a substrate. The substrate is a honeycomb like structure. The large surface area of the substrate is coated with a layer of active layer of catalyst. The precious materials such as platinum or palladium are well dispersed over this layer. As the exhaust gases passes through the catalyst, carbon monoxide, gaseous hydrocarbons and SOF are effectively oxidized, which eventually results in the reduction of harmful emissions. The schematic of a D.O.C. is shown in figure 2.1.3.

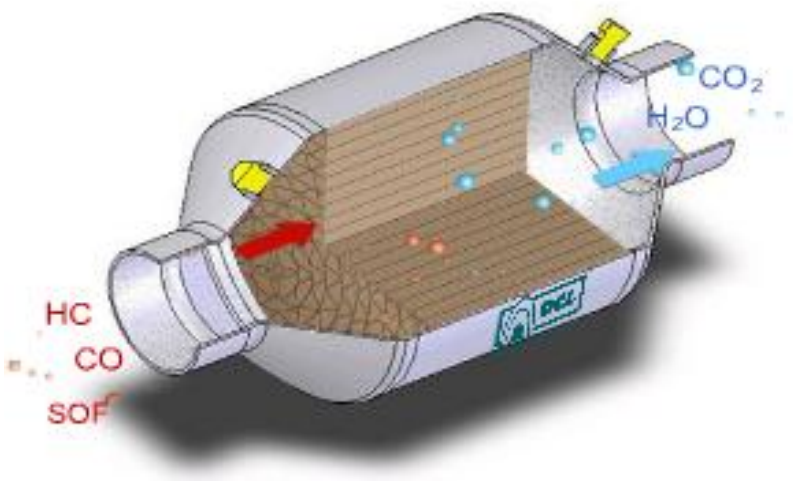

Figure 2.1.3 Schematic of a D.O.C.

Different configurations are possible for a D.O.C. These are mainly one brick system and two brick system types. Figure 2.1.4 and figure 2.1.5 shows the respective one brick system and two brick system type configurations (23).

www.manaraa.com

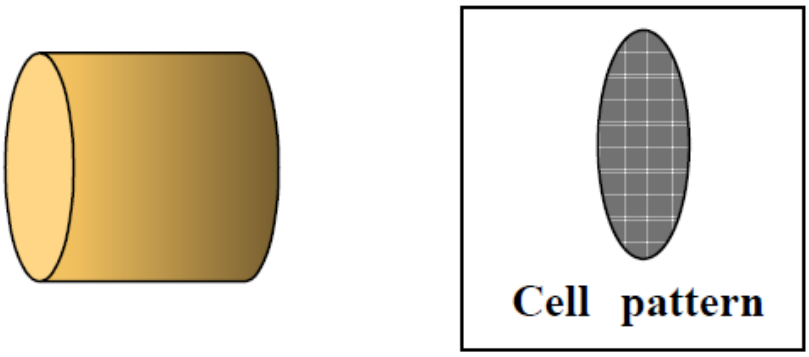

Figure 2.1.4 One brick type configuration (23).

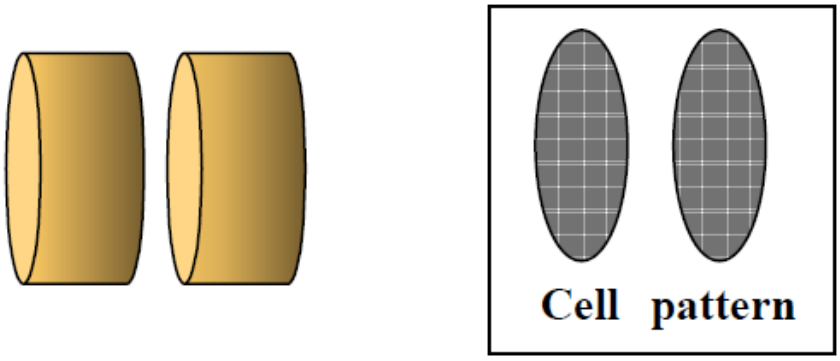

Figure 2.1.5 Two brick type configuration (23).

Higher SOF conversion was observed in a two brick DOC system at lower temperatures (200°C) under non-steady state (23). However, two brick system showed the same SOF conversion efficiency under steady state or at higher temperatures (240°C). The advantage of a two brick system is assumed to be a thermal mass effect. Smaller volume catalysts are well known to have better light off performance for gas species such as CO and HC (23).

www.manaraa.com

2.1.2.2. Catalyst warming-up period:

Four temperature regimes can be possibly identified in the course of a catalyst warming up period (22).

1) Storage period: Hydrocarbons adsorb or condense onto the cold catalyst surface. This leads to pseudo-conversion efficiency.
2) Release period: During this period, the catalyst has become too warm to retain the stored hydrocarbons; therefore they desorb. The conversion efficiency falls, and can become negative.
3) Intermediate period: The catalyst has finished releasing hydrocarbons. It is too warm for storage, but still too cold for oxidation. This leads to zero conversion efficiency.
4) Light off: The catalyst becomes active for oxidation, and so the conversion efficiency again becomes positive.

Since the operating temperature is test-cycle dependent, it is quite possible for a vehicle to satisfy the legislation of one country and to fail that of another (22). At high loads, Johnson and kittleson (1994) found the formation of calcium sulfate because the catalyst was hotter, and because of high oil consumption.

2.1.2.3. Advantages of DOC:

1) DOC reduces the HC, CO and PM emissions effectively. Normally, methane remains stable after passing through DOC due to its high oxidation stability. Moreover, a part of the methane may come from conversion of higher hydrocarbons (24).

www.manaraa.com

2) The design is flow through type so therefore, it does not exert any back pressure and the fuel economy is not compromised.
3) With the lower sulfur content in the fuels being used at present, the risk of sulfate formation is minimized.
4) DOC converts NO to NO_2. NO_2 is found to be a better oxidizer then oxygen at lower temperatures. NO_2 reacted subsequently to N_2 with hydrocarbons, diesel particulates or CO (25).

2.1.3. Diesel particulate filter (DPF):

DPF is designed to collect the particulates and burn the particulates either through passive mode or through active mode. It is very efficient in removing the soot particles which are emitted by the diesel engines. It consists of a honeycomb structure which has a lot of parallel channels. The channels are closed by the ceramic plugs at the either ends. As soot particles travel through the walls, they diffuse into the walls where they finally adhere (deep-bed filtration). Figure 2.1.6 shows the pictorial view of a DPF.

www.manaraa.com

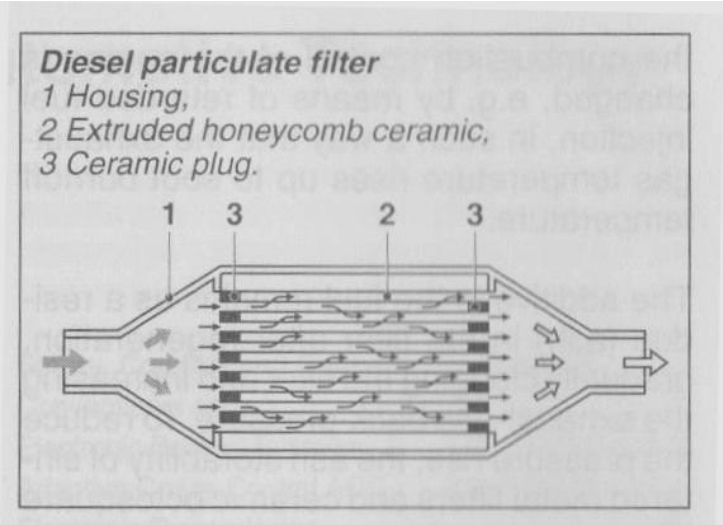

Figure 2.1.6 Pictorial view of a DPF (4)

Diesel particulate filters play a key role in removing particulates from the exhaust gas. A schematic of a diesel particulate filter is shown in figure 2.1.7. Basically, it is designed to collect the particulates and to burn the particulates either through passive mode or through active mode.

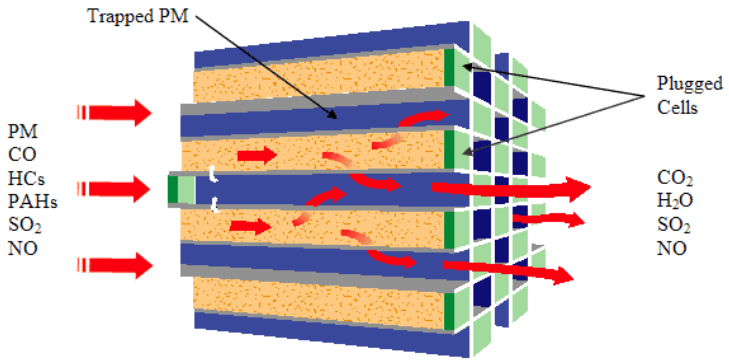

Figure 2.1.7 Schematic of a diesel particulate filter.

www.manaraa.com

Particulate matter combusts at or above 600°C in the presence of oxygen. Therefore, the filter needs to be regenerated either passively or actively. The filter is catalyzed with precious metals in case of passive regeneration. The catalyst coating lowers the combustion temperature to around 250°C (26). Active regeneration can be accomplished by supplementing the exhaust gas temperature with extra heat as regeneration is required (27).

2.1.3.1. Filtration process:

Diffusion is largely responsible for collecting nuclei and small accumulation mode particles (<200 nm). In addition to diffusion, particle collection of these nano-, ultra-fine, and fine particles can be attributed to van der waals attraction and electrostatic force. The effect of diffusion decreases as the size of particle increases. Beyond a size of about 200 nm, this effect becomes negligible (28).The collection of accumulation-mode and coarse-mode particles involves different filtration mechanisms, namely interception and inertial impaction

While inertial impaction is effective for removing large coarse-mode particles (>2000 nm), it becomes insignificant as the particle size decreases to the large accumulation-mode, so that the interception and diffusion become the dominant filtration mechanisms. The effect of interception also decreases with diesel particle size in the accumulation-mode, becoming negligible for nuclei-mode particles.

Diffusion is dominant with small particles with diameters in range from .1μm and below tend to make random interactions with the zigzagging gas molecules. As these small particles bump into gas molecules they too begin moving randomly about, bumping into other particles as well. Diffusion is predominant with low gas velocities and smaller

www.manaraa.com

particles (28). The smaller a particle is and the slower the flow, the more time it will have to zigzag around, therefore giving it much better chance of hitting and sticking to a filter. As more and more particles collect, the collision of other particles is enhanced, but with an associated increase in pressure drop.

Inertial impaction occurs when the particle is so large that is unable to quickly adjust to the abrupt changes in the streamline direction near a filter. The particle, due to inertia, will continue along its original path and hit the filter. As dust particles collect, they themselves become part of the filter media, therefore increasing the efficiency by adding to the number of possible collisions for other suspended particles (28).

Interception occurs when a particle following a gas streamline comes within one particle radius of the filter. The particle touches the filter and is captured, thus being removed from the gas flow. For a given particle size, there are certain streamlines which will move close enough to the filter so that the particle will be captured. Streamlines further than one particle radius away from a filter will not contribute towards this mechanism (28).

There exists a region in the accumulation-mode where none of the mechanisms have an overwhelming effect on suspended diesel particles in the exhaust gas, corresponding to the low efficiency gap. This region is referred to as Greenfield Gap, where the particle size correlating to the minimum efficiency is defined as the most penetrating particle size (28). Figure 2.1.8 shows the Greenfield gap.

www.manaraa.com

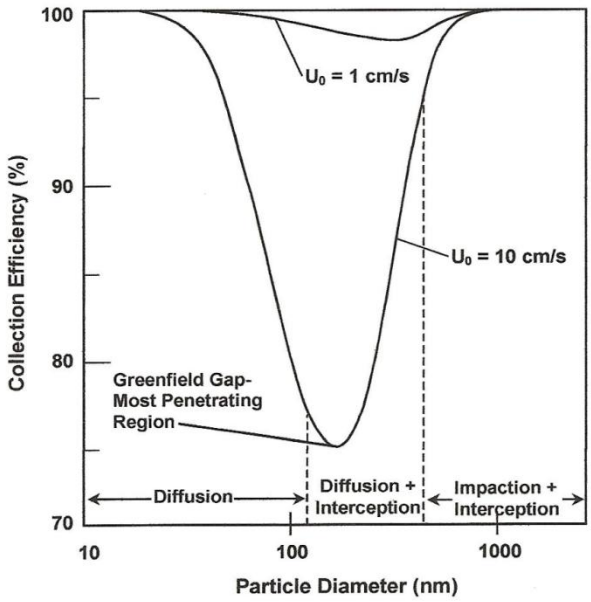

Figure 2.1.8 Greenfield gap (28).

2.1.3.2. Filter efficiency:

The filtration efficiency is inversely proportional to the unit size of the filtering material. Here, the unit size refers to the single fiber diameter for composite fibrous media or solid granular granular size for cordierite and SiC media (28). As the fiber or grain size decreases, the minimum efficiency improves as shown in figure 2.1.9.

www.manaraa.com

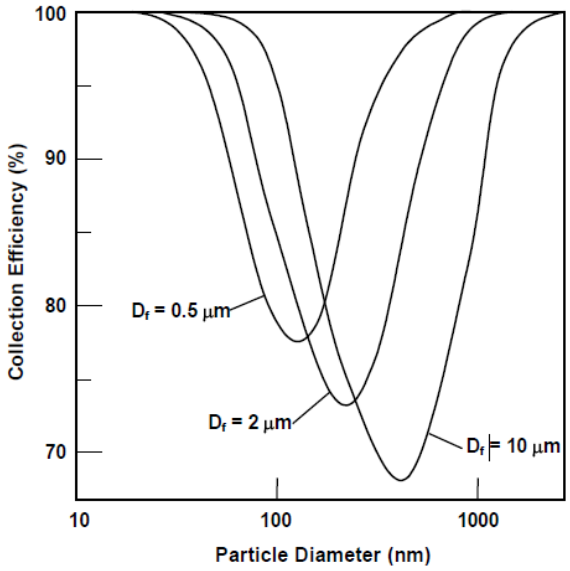

Figure 2.1.9 Filter efficiency as a function of particle size (28).

2.1.4. Lean NO_X Trap:

The NO_X trap is only able to store NO_2. Therefore, NO is initially converted to NO_2. The NO_2 stored in there reacts with the catalysts such as barium carbonate and oxygen from the lean diesel exhaust to form nitrates. This operation is only possible within a range of exhaust gas temperature of 250 to 450° C, below which oxidation of NO is too slow and above which NO_2 is unstable (4). Figure 2.1.10 and 2.1.11 shows the arrangement of a lean NO_X trap.

www.manaraa.com

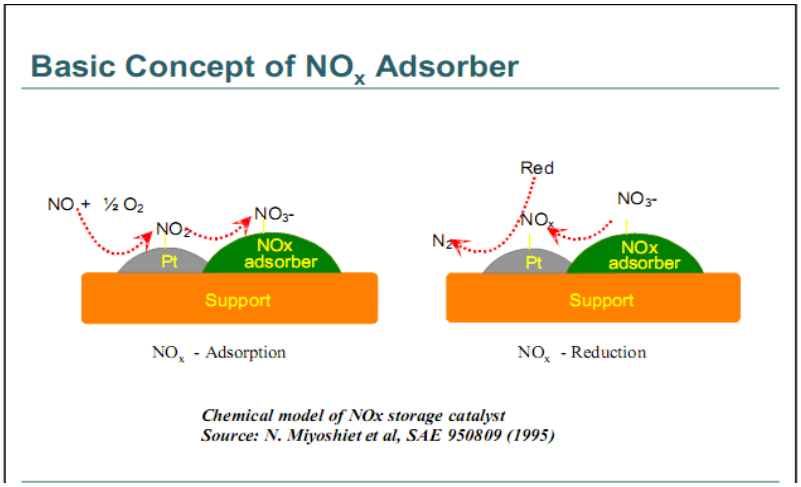

Figure 2.1.10 Basic concept of NO_X trap

At the end of storage period, the trap must be regenerated. Rich conditions must be set in the exhaust gas in order to achieve regeneration. The reactions take place in presence of reducing agents such as CO, H_2 and the nitrate compound is decomposed to N_2 in the presence of the catalyst.

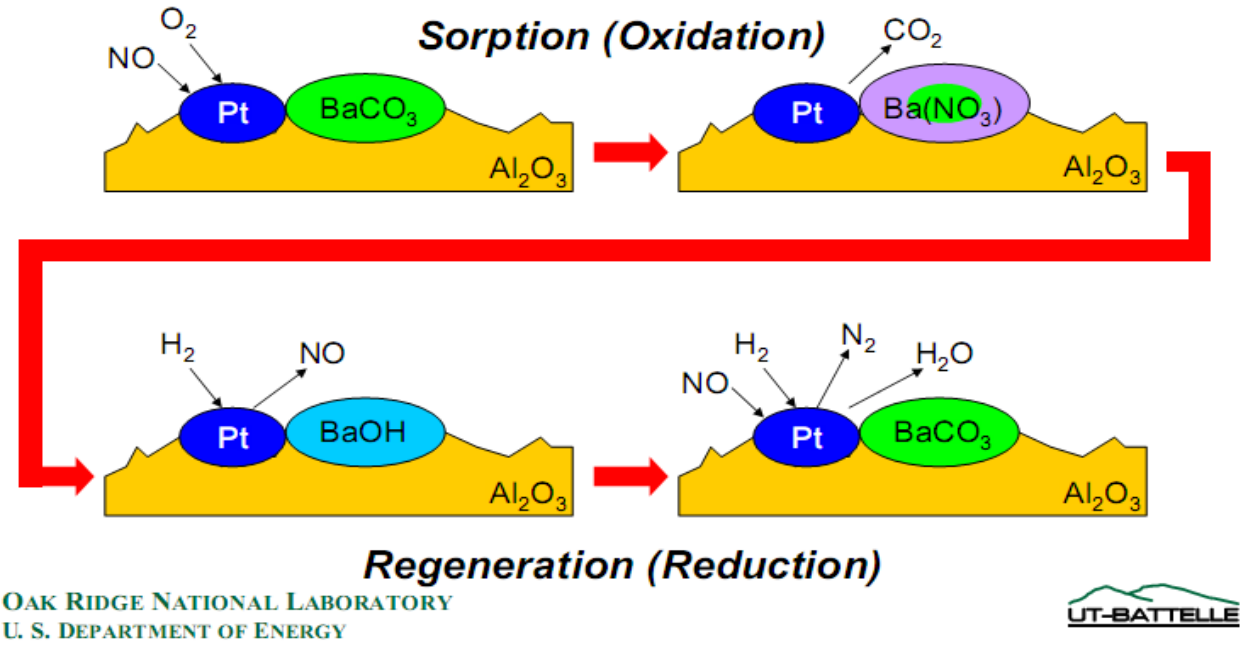

Figure 2.1.11 Basic concept of L.N.T.

www.manaraa.com

The different reactions involved in this mechanism are summarized as under:

$6NO + 3O_2 \rightarrow 6NO_2$

$6NO_2 + 3BaO + 3/2\ O_2 \rightarrow 3Ba(NO3)_2$

$6NO_2 + 2CH_3OCH_3 \rightarrow 3N_2 + 4CO_2 + 6H_2O$

For a hydrocarbon fuel, its NO_X conversion efficiency increases with its H/C ratio. This may suggest that B.D.F. have a higher NO_X efficiency than diesel fuel. H_2 is found to be the best reductant even at 150^0 c at which diesel fuel as a reductant does not work.

2.1.5. Selective catalytic reduction of oxides of nitrogen:

The word selective means that the reducing agent oxidizes selectively with the oxygen contained in the nitrogen oxides instead of with the molecular oxygen present in the exhaust gas (4). Ammonia is a highly reducing agent in this mechanism but as it is toxic, therefore, urea is used. Urea first forms ammonia before the actual SCR reaction starts. At first, ammonia and isocyanic acid are formed in a thermolysis reaction.

$(NH_2)_2CO \rightarrow NH_3 + HNCO$ (thermolysis)

The isocyanic acid is converted with water in a hydrolysis reaction to form ammonia and carbon dioxide.

$HNCO + H_2O \rightarrow NH_3 + CO_2$ (hydrolysis)

Ammonia produced reacts according to the following equations:

$4NO + 4NH_3 + O_2 \rightarrow 4N_2 + 6H_2O$

$NO + NO_2 + 2NH_3 \rightarrow 2N_2 + 3H_2O$

$NO_2 + 8NH_3 \rightarrow 7N_2 + 12H_2O$

Conversion usually takes place as per reaction 2 when the exhaust gas temperature is less than 300^0 C. Figure 2.1.12 shows the arrangement of a SCR.

www.manaraa.com

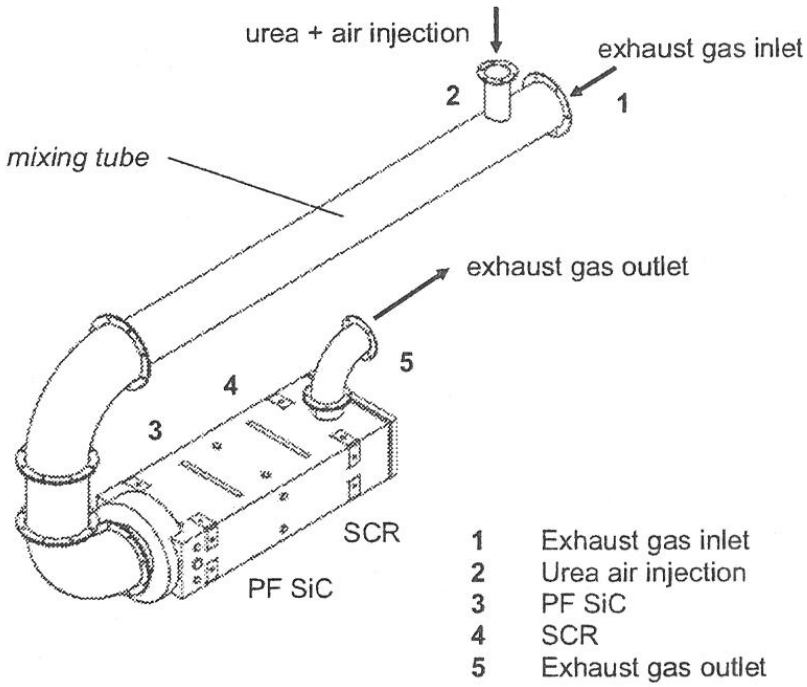

Figure 2.1.12 Arrangement of a SCR (4)

- A classical SCR consists of four catalytic parts:

  - Precatalyst converting NO to NO_2.
  - Injection of AdBlue (with the intention of best distribution and evaporation in the exhaust gas flow).
  - Hydrolysis catalyst (production of NH_3)
  - Selective catalyst (several deNO_X reactions).
  - Oxidation catalyst (minimizing of NH_3 slip)

www.manaraa.com

Conclusions:

1. The emission control in a diesel engine is still in progress.
2. There is a continuous effort being made in order to get rid of the aftertreatment device. The aftertreatment device for diesel engines (cars) is huge in size and they also increase the fuel consumption. However, they are more compatible with heavy duty (truck or bus) type engines.
3. Modern diesel engines specifications under Euro V legislation are fairly efficient and are optimized to reduce the emission levels to meet the desired challenges. For example, Peugeot has introduced a new Euro V compliant 1.6 litre HDi FAP 82 KW turbo diesel engine. The key design features are:
    - ❖ Lower compression ratio (16 compared to 17.5 previously) for enhanced performance and reduced emissions including NO_X.
    - ❖ An increase in diameter of the combustion chamber (+10%) helps to reduce the quantity of the incompletely burnt fuel as a result of less contact with the walls of the combustion chamber.
    - ❖ A reduction of the swirl (10%) reduces the heat loss against the walls.
    - ❖ The variable geometry turbocharger has also been optimized in terms of size. Being smaller, it has a lower inertia, reducing response times to a minimum.
    - ❖ Finally, the use of an optimized exhaust gas recirculation system (EGR valve) and the reduction of internal friction losses improves efficiency.

www.manaraa.com

2.2.Multi fuel operation of a diesel engine:

Engine research is an important task for emission reduction and fuel economy improvement in vehicles. As the diesel engine vehicles are gaining interest all over the world, a lot of emphasis have been directed towards the exploration of alternative fuels with a desire to reduce dependency on imported petroleum. A fuel that permits full design performance is known as the primary fuel. An alternative fuel is the fuel which provides acceptable performance (operational) as compared to the primary fuel and moreover the performance characteristic of the engine should not fall below a required specified level. There is a big need to come up with some form of alternative fuel in order to fulfill the energy demand worldwide and this field is gaining much more popularity as the fossil fuels are depleting day by day. This chapter mainly describes the use of the alternative fuels on diesel engines, and their impact on emissions. Alternative fuels such as biodiesel fuel, gas-derived synthetic fuel (gas to liquid, GTL), jet petroleum fuel have been tried on diesel engines with or without little modifications on the engine. A lot of research has been done pertaining to the use of the biodiesel fuel on diesel engines and a lot of the results show that the engine fueled with soy diesel/diesel fuel blends reduced unburnt hydrocarbons, particulate matter, and carbon-monoxide. However, the oxides of nitrogen depend upon the engine duty cycle. With increasing emissions restrictions, alternative fuels have been recommended to help reduce engine emissions. Studies have shown that biodiesel can significantly reduce CO, PM and HC emissions but may show an increase in nitrogen oxide emissions. If the NOX emissions can be reduced, conventional diesel engines, which feature a high thermal efficiency, may be most able to capitalize on the use of alternative fuels by burning fuels such as biodiesel rather than conventional diesel.

www.manaraa.com

2.2.1 Fischer-Tropsch liquid (FTL) fuels:

There is no doubt that GTL (gas to liquid) type fuel has many desirable properties and is a good potential source of diesel fuel. These fuels are derived from a process known as Fischer-Tropsch process and are also known as Fischer-Tropsch fuels (FTL). In a Fischer-Tropsch process, a carbon containing fuel such as gas, coal or biomass, are converted to a mixture of carbon monoxide and hydrogen gases with the aid of oxygen and water. The two gases formed then reacts over a Fischer-Tropsch catalyst to produce a paraffinic hydrocarbon molecules which is commonly known as white crude as opposed to petroleum (black or dark crude) (7). The GTL fuel type has significantly lower sulfur content and aromatic content and higher cetane number as compared to the standard diesel fuel. Atkinson, et al., had reported a 31% reduction in particulate matter and 20% reduction in NOX in comparison to the regular diesel fuel (8). S8 is a natural gas derived fuel. A large supply of natural gas is available in the United States. FTL and GTL synthetic fuels could play a very important role in meeting future diesel engine emission regulations and meeting the power requirements at the same time.

www.manaraa.com

2.2.1.1 Properties of FTL fuels:

1) Sulfur content:

Lowering the sulfur content of the fuel reduces the engine out emissions of particulate matter (9). Due to the use of low sulfur fuels, diesel engines can effectively use cooled exhaust gas recirculation without any severe corrosion or fouling of the exhaust gas recirculation system (10).

2) Cetane number:

NOx emissions generally reduce when using a fuel having higher cetane numbers (7). A very important property which is known as the ignition delay depends on the cetane number of the fuel. The ignition delay generally governs the mixing of the fuel and the subsequent combustion. A higher cetane number corresponds to the shorter ignition delay which results in smaller fraction of the premixed combustion (9). The reduced fraction of the premixed combustion leads to the reduction of NO_X emissions.

3) Aromatics:

One would expect lower NO_X emissions if the aromatic content of a fuel is low. It can also reduce the particulate matter emissions as there will be lesser amount of polycyclic aromatic hydrocarbons production during the process of combustion.

4) Distillation properties:

It has been well known that by reducing the distillation temperatures, the particulate matter and the total hydrocarbon emissions reduce significantly (11).

Table 2.2.1 illustrates the effect of all these properties on NO_X and PM emissions (7).

www.manaraa.com

Property	Change	Effect on NO_x	Effect on PM
Sulfur	reduce from 350 to 50 (or 15) ppm	0%	↓10-20%
Cetane number	Increase from 40 to 60	↓5-10%	↓0-5%
T90	Reduce from 370°C to 320°C	↓0-5%	↓0-5%
Total Aromatics	reduce from 30% to 10%	↓0-5%	↓0-5%
Oxygenates	10% by vol. blend of DMM	↓0-5%	↓5-15%

Table 2.2.1 Effect of fuel properties on NO_X and PM emissions (7).

2.2.2 JP8:

JP8 is a coal derived aviation fuel. In 1988, the NATO nations took a decision in order to move towards a single fuel for all military applications. They introduced the concept of single fuel concept. JP8 gained popularity because of this single fuel concept. If a kerosene type fuel such as JP8 is used in place of conventional diesel in a diesel engine, the combustion process tends to be more complete. As, JP8, is used for all the applications in the military, therefore, it has a large domain of cetane number (33 to 60) to fulfill different demands.

www.manaraa.com

2.2.3 Biodiesel fuel:

There is no doubt that biodiesel fuel is a promising alternative to conventional diesel fuel for diesel engines. Biodiesels are carbon neutral, even though burning those releases CO2. The carbon in the biodiesel comes from a process known as photosynthesis, where CO2 is absorbed by a plant from the atmosphere and stored as glucose. The glucose once stored is then converted into molecules such as starch, sugar etc. Sugars and starches can be easily converted into bio-ethanol, while oils can be converted into biodiesel. In other words, for every gram of CO2 released into the atmosphere by burning a biodiesel fuel, there was a gram removed from the atmosphere through the process of photosynthesis. Therefore, the use of biodiesel is a very effective way to reduce CO2 emissions. It's a high time for the reduction of CO2 emission from the automobiles as 90% of the CO2 emission from the transportation sector is generated by automobiles (12).

Biodiesel fuels are produced from a process known as transesterification. In this process, the fuel is produced from renewable agricultural resources such as soybean, canola, animal fat etc. In this process, the triglyceride (vegetable oil or animal fat) reacts with an alcohol (methanol) in the presence of a catalyst in order to produce glycerol and a mono-ester (biodiesel) (13).

www.manaraa.com

2.2.3.1 Determination of oxidation stability:

The oxidation stability is determined with the Rancimat, a method known from food industry.10g samples are aged at a constant temperature (95°C, 110°C, 120°C) with an airflow passing through at the rate of 10 l/h. The airflow is passed through a measuring cell filled with distilled water. There the conductivity is determined continuously and recorded automatically.

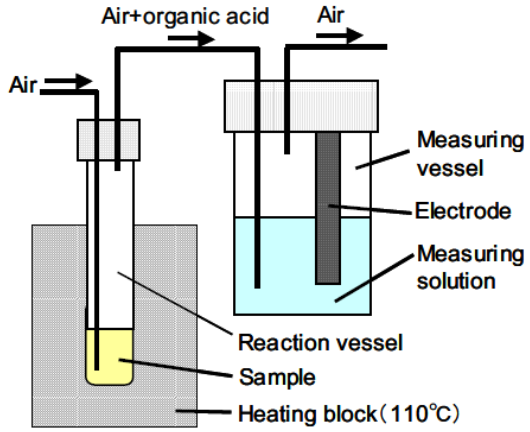

Figure 2.2.1 Apparatus of Rancimat test (14)

During the oxidation process volatile acids are formed. At the end of the ageing period the conductivity increases rapidly. The period up to this point is called 'induction period (14).

2.2.3.2 Oxidation stability of Biodiesel fuel:

6 identical samples of rape oil methyl ester produced by BLT Wiesel burg were aged. The samples were stored in translucent plastic bottles under various conditions for 14 weeks. Every week the induction period was determined by Rancimat. After 14 weeks the induction period of those samples stored at 4°C was 70% of the initial value, while that of the samples stored in the dark was 50%. The induction period of the samples stored in the ambient conditions was 30% of the initial value. Sample which was exposed to the sunlight lost its color. Its

www.manaraa.com

induction period decreased to 0. This sample showed the highest increase in viscosity and acid number (15). Table 2.2.2 illustrates different storage conditions and figure 2.2.2 shows their impact on the relative induction period.

sample	quantity	storage conditions	temp.
A1	250 ml	cooled, dark	4°C
A2	250 ml	dark	ambient
A3	250 ml	daylight	ambient
A4	250 ml	sunlight (window)	ambient
A5	250 ml	daylight, open bottle	ambient
A6	1000 ml	cooled, dark	4°C

Table 2.2.2 Biodiesel samples (15)

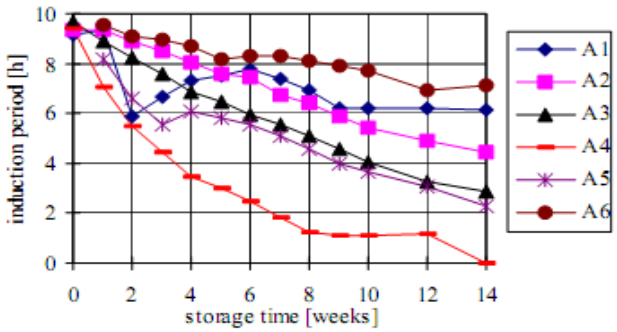

Figure 2.2.2 Induction period of the samples (15)

2.2.4. Effect of Biodiesel on D.O.C:

1) Carbon monoxide and unburned hydrocarbons are the exhaust gas components which can be effectively removed by the Diesel Oxidation Catalyst (D.O.C.).
2) The D.O.C's effectiveness after reaching the light-off temperature is high and it is quite satisfactory at the moment.
3) However, there is a problem due to the CO and HC emissions during cold start and warm up conditions.

2.2.4.1 Effect of biodiesel on D.O.C (HC emissions):

1) Pure biodiesel contains approximately 10 percent oxygen by weight. The presence of oxygen in the fuel leads to a reduction in emissions of unburned hydrocarbons (16).
2) The HC emissions were decreased by 3% for B30 and were decreased by 11% for B5.

www.manaraa.com

3) The HC emissions were increased by 6% for B30 which shows that not only the presence of oxygen but other physical and chemical properties of the blended fuels are of significant importance.

4) With the increase of the biodiesel percentage, fuel volatility reduces and which leads to improper combustion.

5) Test fuels included 2007 certification diesel fuel and various biodiesel blends made from RME biodiesel feedstock.

Figure 2.2.3 shows the HC emissions for different fuel blends and figure 2.2.4 shows the changes in HC emissions in percentage for different fuel blends.

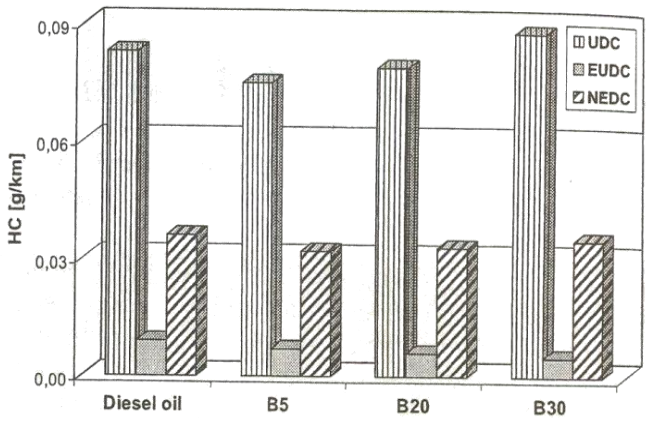

Figure 2.2.3 HC emissions for different fuel blends (16)

www.manaraa.com

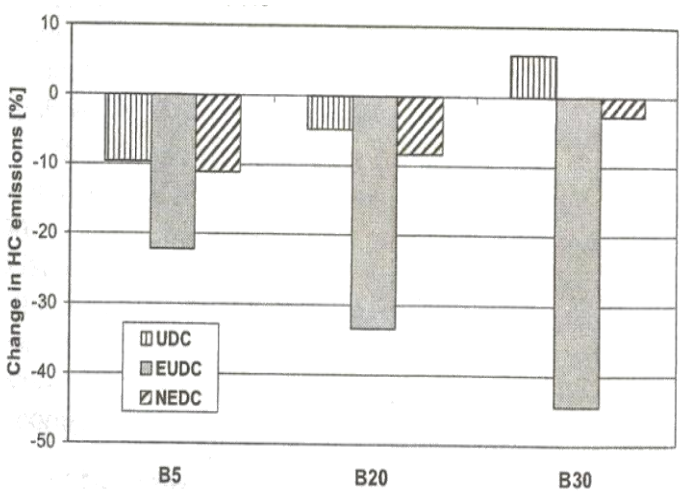

Figure 2.2.4 Change in HC emissions for different fuel blends (16)

www.manaraa.com

2.2.4.2 Effect of biodiesel on D.O.C (CO emissions):

1) Pure biodiesel contains approximately 10 percent oxygen by weight. The presence of oxygen in the fuel leads to a reduction in emissions of carbon monoxide (16).
2) There was 15% reduction for B5, no change for B20 and 6% increase for B30 at 95% confidence level.
3) The CO emissions were increased by 6% for B30 which shows that not only the presence of oxygen but other physical and chemical properties of the blended fuels are of significant importance. With the increase of the biodiesel percentage, fuel volatility reduces and which leads to improper combustion.

Figure 2.2.5 shows the CO emissions for different fuel blends and figure 2.2.6 shows the changes in CO emissions in percentage for different fuel blend

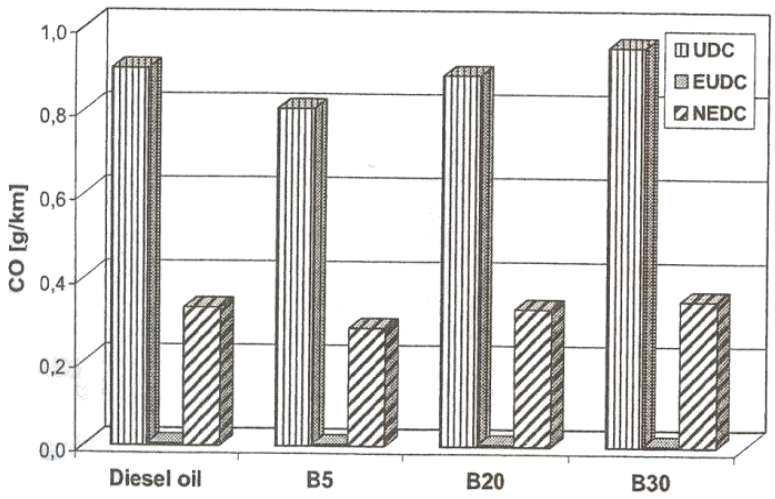

Figure 2.2.5 CO emissions for different fuel blends (16).

www.manaraa.com

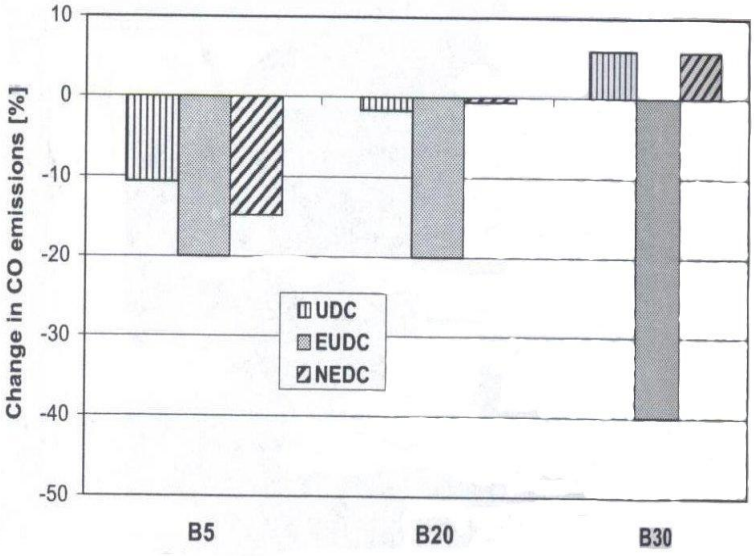

Figure 2.2.6 Changes in CO emissions for different fuel blends (16).

www.manaraa.com

2.2.4.3 Effect of biodiesel on D.O.C. (PM emissions):

1) The use of biodiesel decreases the solid carbon fraction of particulate matter, reduces the sulfate fraction, while the soluble organic fraction either remains the same or is increased.
2) Therefore, biodiesel works well with new technologies such as oxidation catalyst (which reduces the soluble organic fraction of diesel particulate) and exhaust gas recirculation (16).

Figure 2.2.7 shows the PM emissions for different fuel blends and figure 2.2.8 shows the changes in PM emissions in percentage for different fuel blends.

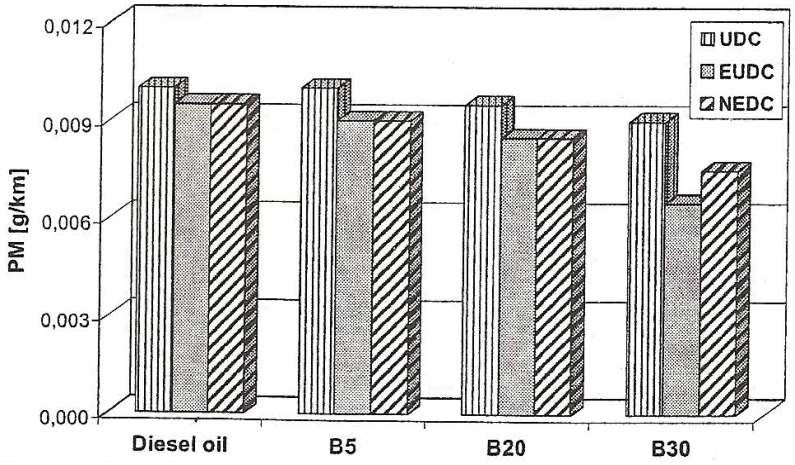

Figure 2.2.7 PM emissions for different fuel blends (16)

www.manaraa.com

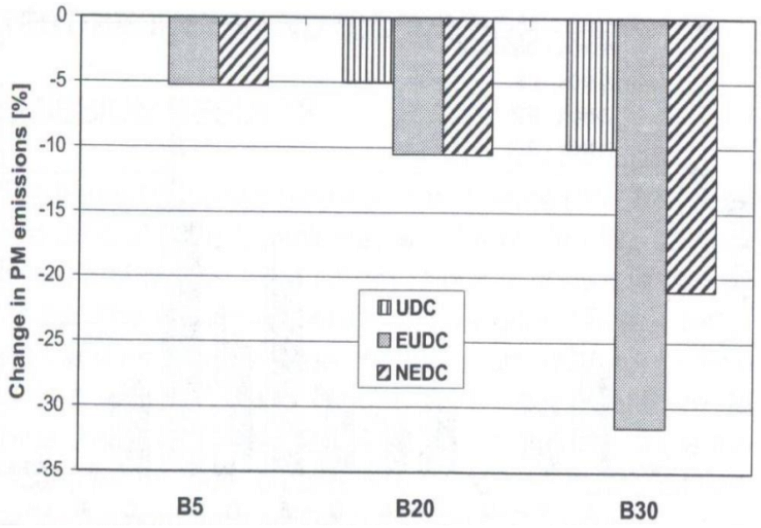

Figure 2.2.8 Changes in PM emissions for different fuel blends (16)

2.2.4.4 Effect of biodiesel on D.O.C (Opacity measurements):

1) Opacity measurements using biodiesel blends B20 and B30 were about 8-25% lower than those with diesel fuel, supporting low carbonaceous particulate emissions with biodiesel (16).

Figure 2.29 shows the opacity measurements during UDC cycle for different fuel blends and figure 2.2.10 shows the opacity measurements during EUDC cycle for different fuel blends.

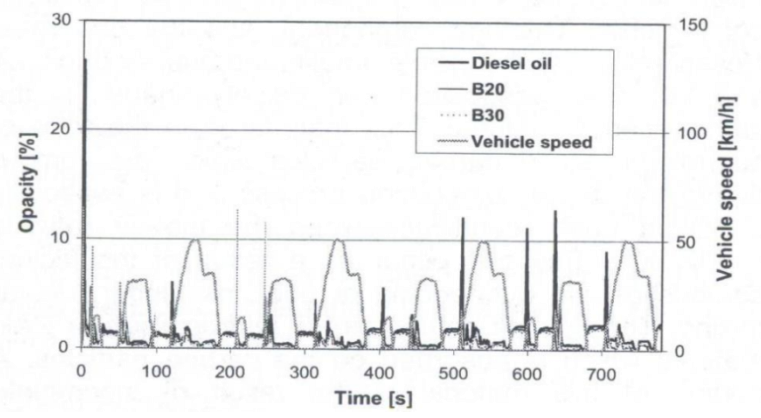

Figure 2.2.9 Opacity during UDC phase (16)

www.manaraa.com

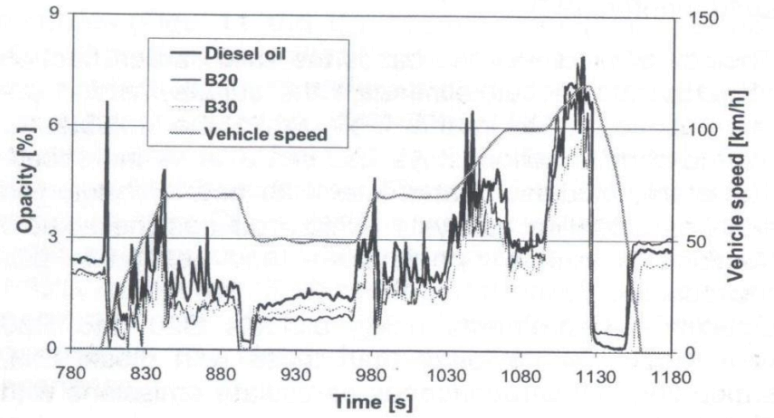

Figure 2.2.10 Opacity during EUDC phase (16)

2.2.5. Effect of biodiesel on D.P.F:

2.2.5.1. Experimental investigation:

The test setup consisted of a 2002 model year 5.9L 300 hp Cummins engine equipped with a diesel particulate filter. The DPF is a 12L catalyzed diesel particulate filter employing catalyzed continuously regenerating technology (CCRT) (17).The CCRT filter is a diesel oxidation catalyst followed by a catalyzed soot filter. It is used in applications with average exhaust temperatures as low as 200°C - 250°C.The DPF is mounted 152 cm from the engine turbo flange outlet. Temperatures were measured with K-type thermocouples mounted 8 cm from the face of the pre-catalyst on the inlet side and 8 cm from the face of the DPF on the outlet side. Inlet and outlet pressures as well as differential pressures were measured from the same location. Test fuels included 2007 certification diesel fuel and various biodiesel blends made from soy biodiesel feedstock. A schematic of the experimental investigation is shown in figure 2.2.11.

www.manaraa.com

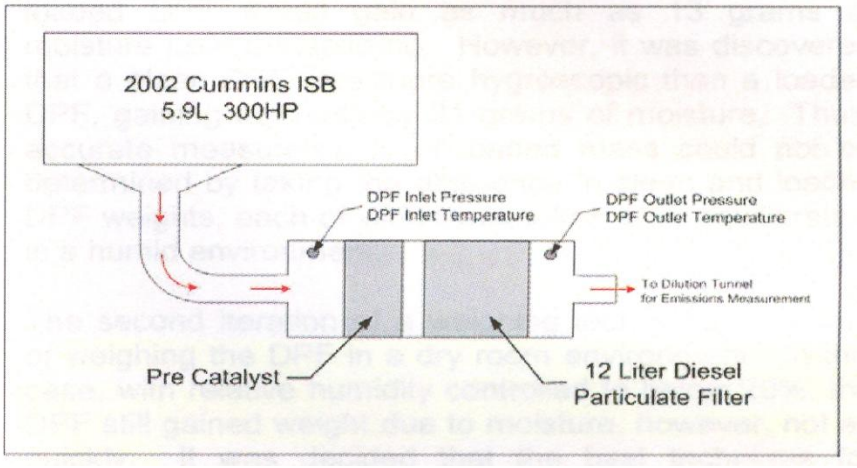

Figure 2.2.11 Experimental investigation (17)

2.2.5.2. Effect of the level of particulate loading on the performance of d.p.f.:

1) For each fuel type the D.P.F. was loaded to 1.5 g/L (17).
2) However, the amount of time to produce 18 grams of PM at the 2000 rpm and 20 ft-lb preload conditions is different for each fuel.
3) Weighing the DPF was carried out in dry room environment. In this case , the relative humidity was controlled to below 20% and it was decided to remove the DPF as quickly as possible following engine operation and take immediate measurements in the dry room conditions.
4) Samples were collected onto 47 mm Teflon membrane every 20 minutes for the entire 340 minutes duration.

www.manaraa.com

5) Assuming that the D.P.F. captures and stores all of PM at the preload condition, total collection of 18 grams would take 332, 314 and 239 minutes for B100, B20 and 2007 Cert. respectively. Figure 2.2.12 shows the PM rate study result.

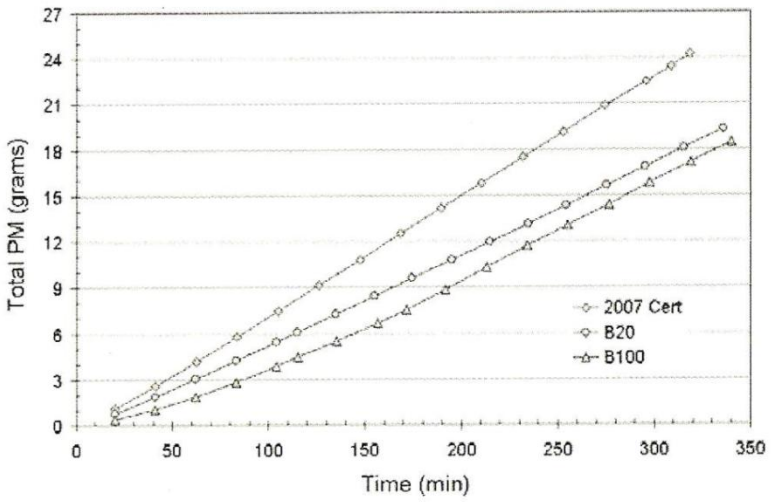

Figure 2.2.12 PM rate study results (17)

2.2.5.3. Balance point temperature:

The B.P.T. is defined as the D.P.F. inlet temperature at which the rate of particle oxidation approximately equals the rate of particle collection (17). At the balance point temperature during steady state operation, the D.P.F. should not experience a net gain or loss of particulate matter and consequently differential pressure across the D.P.F. should not change.

2.2.5.3.1. Determination of Balance Point Temperature:

The D.P.F. was completely regenerated by operating at near rated power (2500 rpm and 575 ft-lbs) for 120 minutes (17). The D.P.F. was then preloaded with PM at 2000 rpm and 20 ft-lbs over the appropriate amount of time to achieve an approximate 1.5g/L loading of PM on the D.P.F. The preloaded D.P.F. was then operated at 1700 rpm while torque was increased to achieve specified exhaust temperatures. The D.P.F. pressure drop was monitored continuously to

www.manaraa.com

determine slope of increase or decrease of the differential pressure across the D.P.F. at a given inlet temperature. Figure 2.2.13 shows the procedure for determination of balance point temperature.

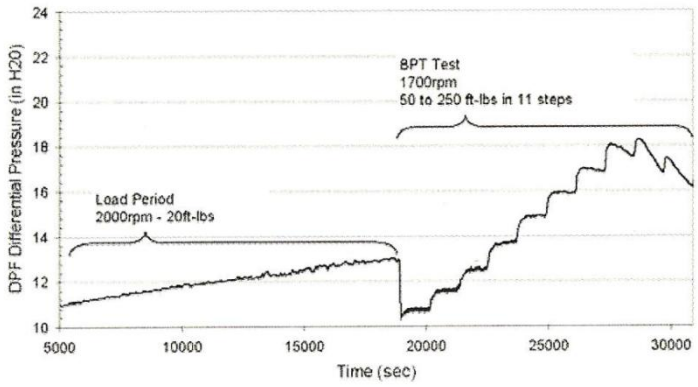

Figure 2.2.13 Determination of balance point temperature (17)

2.2.5.3.2. Balance point temperature test results:

The B.P.T. determination is made by plotting the slope of the differential pressure versus the D.P.F. temperature for each of the steps (17). If the slope is positive (backpressure is increasing) than it is assumed that the DPF is collecting particulate matter. Once the slope becomes negative (backpressure is decreasing) that temperature is above the balance point temperature. A linear curve fit is made between the two steps where the differential pressure slope transitions from positive to negative value. The point where the curve fit crosses the Y-intercept is determined as the best estimate of the balance point temperature. On average, the balance point temperature is 45°C lower than 2007 certification diesel for B20 blends

www.manaraa.com

and 112°C lower for neat biodiesel. Figure 2.2.14 shows the balance point temperature test results.

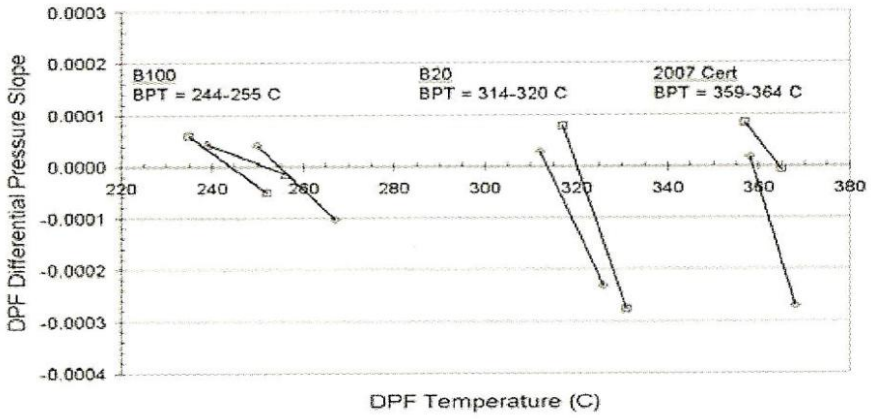

Figure 2.2.14 Balance point temperature test results (17)

2.2.5.4. Regeneration rate:

This plot shows the normalized D.P.F. differential pressure for the final 15 minutes of steady state operation at the active regeneration point (17).The differential pressure slope for 2007 certification fuel is slightly positive for repeated runs at 1700 rpm, 250 ft-lb operating condition with temperatures around 354°C..Both biodiesel blends at the B5 and B20 level show measurable decrease in D.P.F. differential pressure with similar amounts of D.P.F. preloading. These tests show that when fueled with biodiesel blends, PM appears to oxidize more quickly as compared to 2007 certification diesel fuel. Increased levels of biodiesel in the fuel appear to increase the rate of D.P.F. regeneration at a given engine operating condition. Figure 2.2.15 shows the regeneration rate for different fuels.

www.manaraa.com

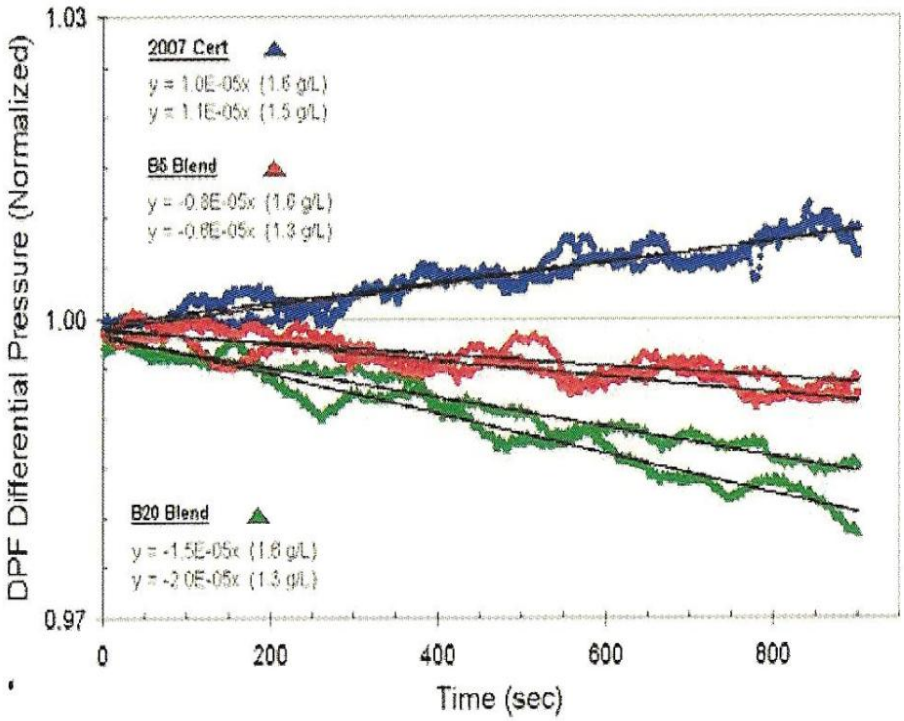

Figure 2.2.15 Regeneration rate for different fuels (17)

2.2.6. Particulate matter emissions:

PM emissions can be divided into three components:

1) The first component, and the most closely related to visible smoke and opacity often associated with diesel exhaust, is the carbonaceous material. This material is in the form of sub-micron sized carbon particles which are formed during the diesel combustion process and is especially prevalent under conditions when air- fuel ratio is overly rich (16).
2) The second component is hydrocarbon or PAH material which is absorbed on the carbon particles. A portion of this material is the result of incomplete combustion of the fuel, and the remainder is derived from the engine lube oil.

www.manaraa.com

3) The third particulate component comprises of sulfates and bound water. The amount of this material is directly related to the fuel sulfur content.

The USEPA defines diesel particulate matter as the mass collected on the filter from the exhaust that has been diluted and cooled to 52^0 C or below. The composition of exhaust particles depends upon where and how they are collected. As the exhaust is diluted and cooled, nucleation, condensation, and absorption transform volatile materials to solid and liquid particulate matter. In the tail pipe, where the temperatures are high, most volatile materials are in gas phase. The details of the dilution and cooling processes determine the relative amounts of material that absorb or condense onto existing particles and nucleate to form new particles (18).

Particle size influences the environmental impacts of engine exhaust particles size in many ways: it influences the atmospheric residence time of the particles, the optical properties of the particles and the health effects of the particles. The residence time of the particles in the atmosphere is longest for particles in the 0.1-10μm diameter range and is typically about one week. Larger particle are removed from the atmosphere quite quickly by settling and smaller ones by diffusion and coagulation.

2.2.6.1. Particle composition:

Diesel exhaust particles consist mainly of highly agglomerated solid carbonaceous material and ash, and volatile organic and sulfur compounds. Solid carbon is formed during combustion in locally rich regions (18). Much of it is subsequently oxidized. The residue is exhausted in the form of solid particles consist mainly of highly agglomerated solid carbonaceous material and ash and volatile organic and sulfur compounds. A tiny fraction of the fuel and atomized and evaporated lube oil escape oxidation and appear as volatile or soluble organic compounds in the exhaust (generally

www.manaraa.com

described as SOF). The SOF contains polycyclic aromatic compounds containing oxygen, nitrogen and sulfur. Most of the sulfur in the fuel is oxidized to SO_2, but a small fraction is oxidized to SO_3 that leads to sulfuric acid and sulfates in the exhaust particles. Metal compounds in the fuel and lube oil lead to a small amount of inorganic ash. SOF values are highest at light engine loads when exhaust temperatures are low. Figure 2.2.16 shows the particle distribution.

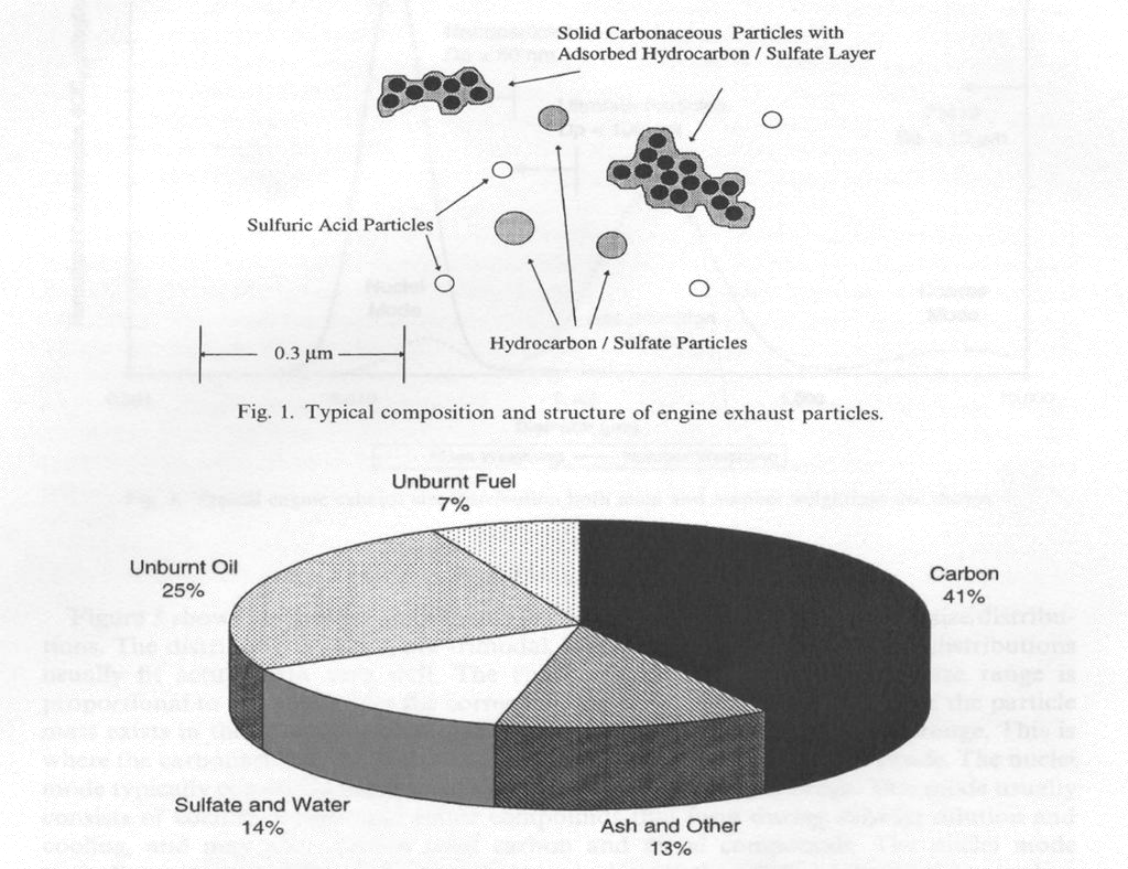

Figure 2.2.16 Particle composition (18)

www.manaraa.com

2.2.6.2. Particle distribution:

1) The distributions shown are trimodal (18).
2) Most of the particle mass exists in the so-called accumulation mode.
3) The nuclei mode typically contains 1-20% of the particle mass and more than 90% of the particle number.
4) The coarse mode contains 5-20% of the particle mass. It consists of accumulation mode particles that have been deposited on the cylinder and the exhaust system surfaces and later re entrained.
5) Note that by number; nearly all of the particles emitted by a diesel engine are nanoparticles.

Current emission standards are mass based. Mass tends to be conserved during the dilution and sampling process. On the other hand, particle number is not conserved and may be changed significantly by homogeneous nucleation and coagulation. This in turn may change particle size, especially if a numbered weighted size is used. Concern about particle emissions from vehicles tends to focus on those powered by diesel engines, because of their much higher mass concentrations. However, if nanoparticles are a problem, not only diesel, but also spark ignition engines may be important sources. Figure 2.2.17 shows the particle distribution.

www.manaraa.com

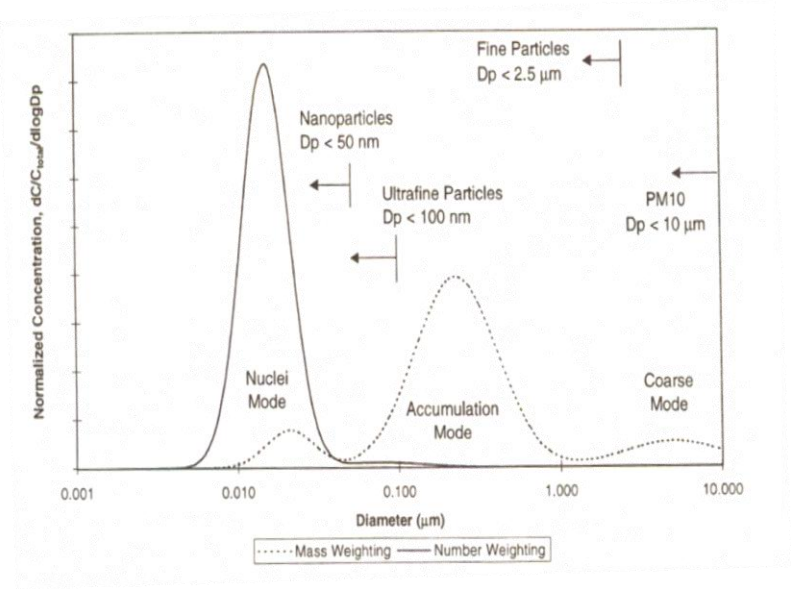

Figure 2.2-17 Particle distribution (18)

The fact that diesel exhaust gases are comprised of large amounts of volatile compounds makes it difficult to accurately measure the particle size distribution downstream of a D.P.F. After exhaust gases penetrate the D.P.F, some of the saturated and super-saturated volatile gases will nucleate and condense to form particles during dilution and cooling. These particles do not represent the D.P.F. performance, since it is designed to control upstream liquid and solid particles, rather gaseous compounds.

2.2.7. Effect of biodiesel on particulate matter:

1) Generally, PM decreases with the use of biodiesel fuels. This effect is attributed to higher oxygen content in the biodiesel fuels, which enables more complete oxidation in the engine cylinder.
2) The use of biodiesel decreases the solid carbon fraction of particulate matter, reduces/eliminates the sulfate fraction, while the soluble, or hydrocarbon, fraction stays the same or is increased. Therefore, it reduces the particles in the accumulation mode but nanoparticles either remain the same or are increased.

www.manaraa.com

3) Besides reducing the number of nuclei-mode sulfur compound particles, the low sulfur content prevents the nucleation and condensation of those volatile organic compounds that typically use sulfur compounds as nuclei.
4) For diesel engines, the load is roughly proportional to equivalence ratio.
5) Higher equivalence ratios are used during cold starts, warm-ups, and high loads which increases the rate of carbon formation and decrease the rate of oxidation.
6) At light loads, the exhaust temperatures are low and unburned fuel and oil are not effectively oxidized. When the exhaust is diluted and cooled, these materials nucleate and form large numbers of tiny particles in the nuclei mode [4].
7) These particles lead to large number concentrations, but because of small particle size, they do not usually contribute significantly to the volume or mass concentrations. As load is increased, the exhaust temperature increases and the SOF is more effectively oxidized causing the exhaust number concentrations to fall.

www.manaraa.com

2.2.8 Effect of biodiesel on NO_X:

1) The change in NO_X emissions for a biodiesel blend compared to its base diesel fuel is the result of two effects (19).
2) A fundamental combustion effect, driven by fuel chemistry and fluid dynamics.
3) An effect caused by the interaction of lower specific energy content of the biodiesel with the engine control system which was calibrated using conventional diesel fuel.
4) The combustion effect can itself be separated into two factors: flame temperature effects and ignition delay effects.
5) At higher loads, characterized by diffusion flame combustion, the flame temperature effect is dominant. One would expect that a B20 blend would have lower NO_X because of lower aromatics content of the blend compared to the base diesel fuel. However, the methyl ester compounds in the biodiesel have more double bonds than the base diesel fuel. These double bonds have the effect of increasing the flame temperature.
6) At light load, much of the fuel is burned in a "premixed" mode. For EGR engines, premixed combustion generally produces lower NO_X than diffusion flame combustion. B20 blends have higher cetane number and thus shorter ignition delay time than their base diesel fuel. This means the fundamental combustion effect of B20 blends is to increase NO_X at light loads.
7) At higher speeds and loads, the change in engine control settings due to the lower energy content of the blended fuel could lead to a NO_X increase on the order of 3-4%. However, studies show that this factor does not play an important role in engines which have common rail fuel injection systems.

www.manaraa.com

8) Biodiesel has a higher bulk modulus of compressibility then petroleum diesel and this was proposed to cause a more rapid transfer of the fuel pump pressure wave to the injector needle. This caused earlier needle lift and a small advance in injection timing that was proposed to account for fraction of NO_X increase observed under some conditions (20).
9) Another fuel chemistry might be the formation of prompt NO, which can account for 30% of the NO_X formation. Prompt NO is formed by the reaction of radical of HC species with nitrogen ultimately forming NO. Unsaturated compounds may form higher radicals during combustion (20).
10) Engine manufacturers could go in for higher E.G.R. rates.
11) Lower NO_X Emissions could be achieved with multiple injections. Length of time between injections does effect NO_X Emissions; when the time is short, high temperature region exists, promoting the formation of NO_X (21).

www.manaraa.com

3. EXPERIMENTAL SETUP

3.1. Experimental engine:

The investigative study is focused on effect of alternative fuels on a multi cylinder engine. The experimental work is performed on a six cylinder, inline, single stage turbocharged, water cooled, four stroke, direct-injection, MBE 926 diesel engine. Each cylinder has two intake valves and one exhaust valve. Each unit has a separate electronic unit pump (EUP) with a short injection line to the injection nozzle, which is located in the center of the combustion chamber. The engine is equipped with a fully electronic control system. The firing order is 1-5-3-6-2-4. Besides the engine and its related sensors, this system is composed of the Motor Control Module (MCM), and the Common Powertrain Controller (CPC). The two units are connected by a proprietary datalink through which all the necessary data and information can be exchanged. Inorder to meet the on-highway EPA 2007 regulation applications, the engine uses a water cooled EGR system along with an Aftertreatment System to meet the emission standards. The engine uses an asymmetric turbocharger with two entries (pulse turbocharging), and the EGR is fed from first three cylinders. The EGR system consists of a Turbocharger, an EGR cooler, an EGR valve and an EGR mixer. The exhaust with a maximum temperature of 730^{o} C (1346^{o} F) is cooled to a maximum of 150^{o} C (302^{o} F) in the EGR cooler. The EGR cooler is a single pass type cooler and is fairly effective. Table 3.1 gives the engine's specifications.

www.manaraa.com

Descriptions	6–Cylinder EGR Engine
Engine Type	Vertical, inline cylinder block with turbocharger and charge–air cooler
Engine Length	1057 mm (41.6 in.)
Engine Width	862 mm (33.9 in.)
Engine Height	1138 mm (44.8 in.)
Cooling System	Liquid Circuit
Combustion Principle	4–Stroke direct–injection diesel
Number of Cylinders	6
Bore	106 mm (4.17 in.)
Stroke	136 mm (5.35 in.)
Displacement (total)	7.2 liters (439 in^3)
Compression Ratio	18:1
Starting Speed	Approximately 100 rpm
Direction of Engine Rotation (viewed from flywheel)	Counterclockwise
Starter	Electric Motor
Coolant Capacity of Engine (Does not include capacity of cooling system.)	Max. 12.5 liters (13.2 qt.)
Lubricating Oil Fill Capacity **(In standard pan, including oil filter.)**	Max. 29.0 liters (30.6 qt.)
Cold–Start Temperature Limit (Without starting aids and with battery 75 percent charged)	Down to –15°C (+5°F)
Engine "Dry" Weight — Single -Stage Turbocharger Engine "Dry" Weight — Dual -Stage Turbocharger	613 kg (1362 lb) 648 kg (1428 lb)
Valve Lash (with engine cool)	Intake = 0.40 mm (0.016 in.)
	Exhaust = 0.60 mm (0.024 in.)
Valve Lift (at maximum valve clearance)	Intake = 9.7 mm (0.38 in.)
	Exhaust = 10.7 mm (0.42 in.)
Engine Oil Pressure	At idle rpm = 50 kPa (7 psi)
	At maximum rpm = 250 kPa (36 psi)
Fuel Injectors	Minimum opening pressure = 24,500 kPa (3553 psi)
	Maximum opening pressure = 25,700 kPa (3727 psi)
Coolant Thermostat	Opening temperature = 81° to 85°C (178° to 185°F)
	Normal operating temperature = 95°C (203°F)

Table 3.1 Technical specifications (29)

www.manaraa.com

Figure 3.1 shows the performance map of the experimental engine.

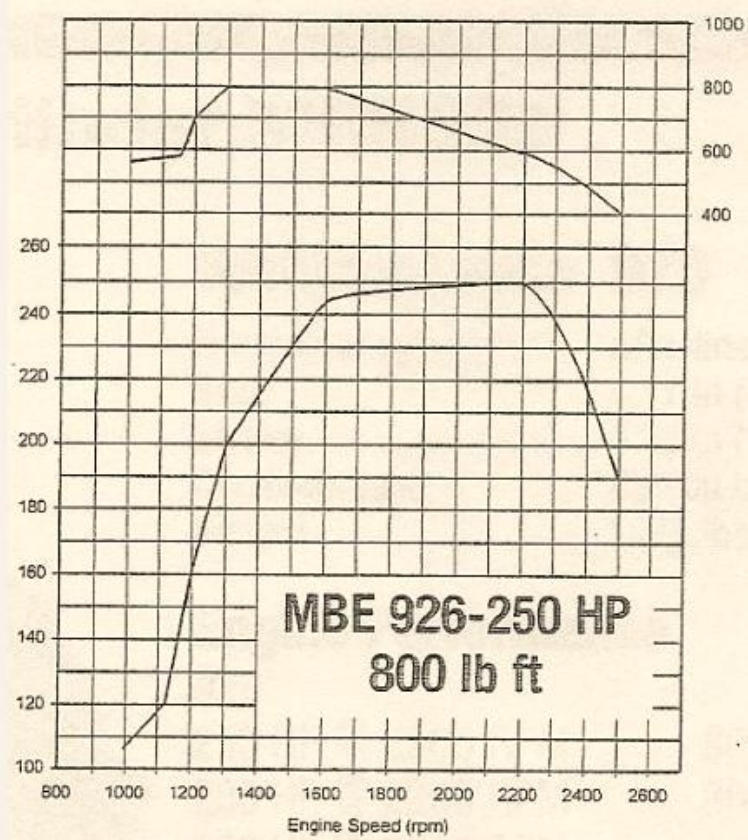

Figure 3.1 Performance mapping of the experimental engine

From the figure it is clear that the engine torque increases with the increase in speed till 1600 rpm and thereafter it falls gradually with the increase in speed. The engine develops a maximum torque of 800 lb ft in the speed range of 1300 to 1600 rpm.

The engine components are shown in figure 3.2 and 3.3.

www.manaraa.com

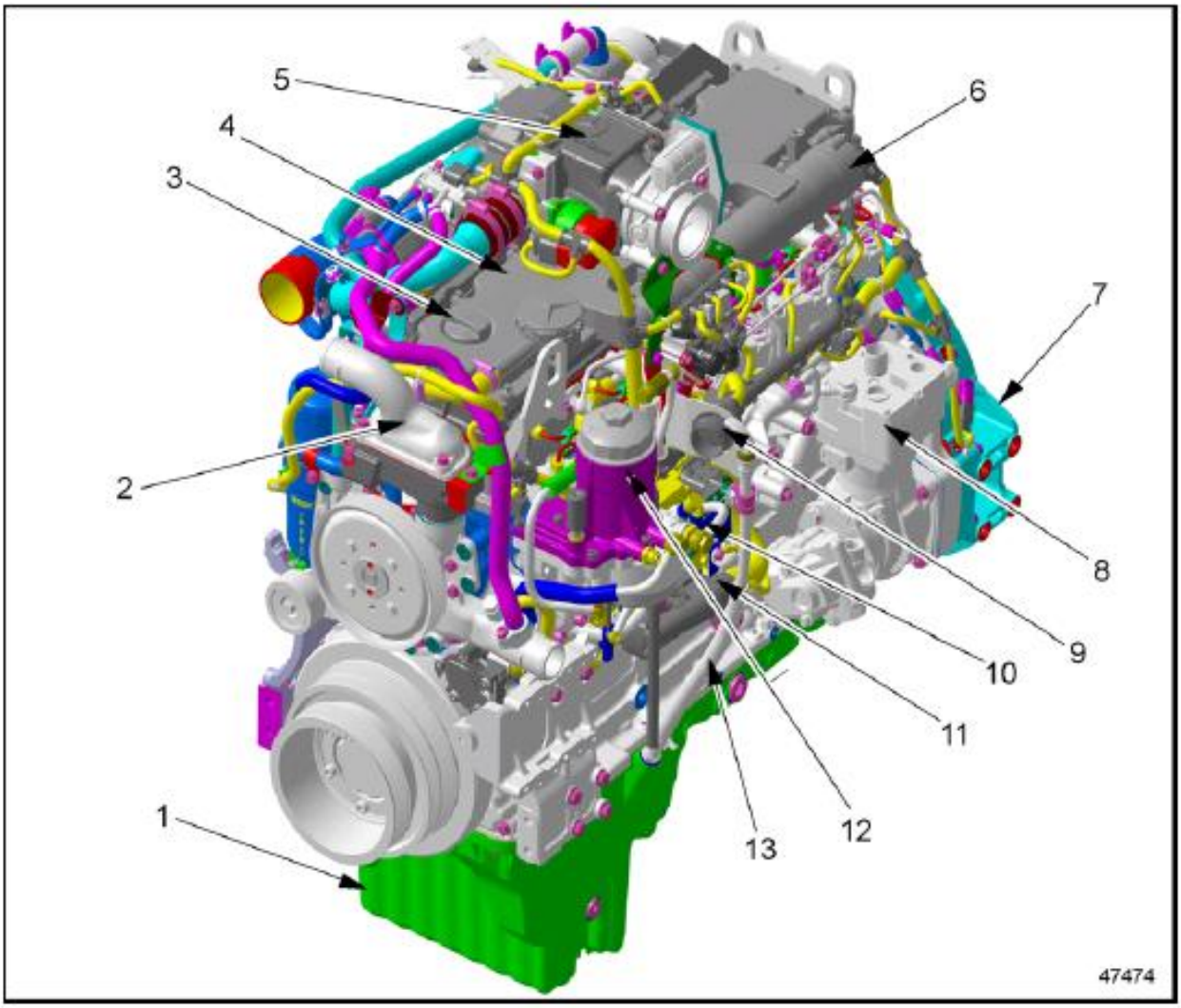

1. Oil Pan
2. Thermostat Housing
3. Oil Fill Cap
4. Cylinder Head Cover
5. EGR Mixer
6. Electrostatic Oil Separator
7. Flywheel Housing
8. Air Compressor
9. 31–Pin Connector
10. Motor Control Module (MCM)
11. 120–Pin Connector
12. Fuel Filter/Water Separator
13. Oil Dipstick Tube

Figure 3.2 Left side view of engine components (29)

www.manaraa.com

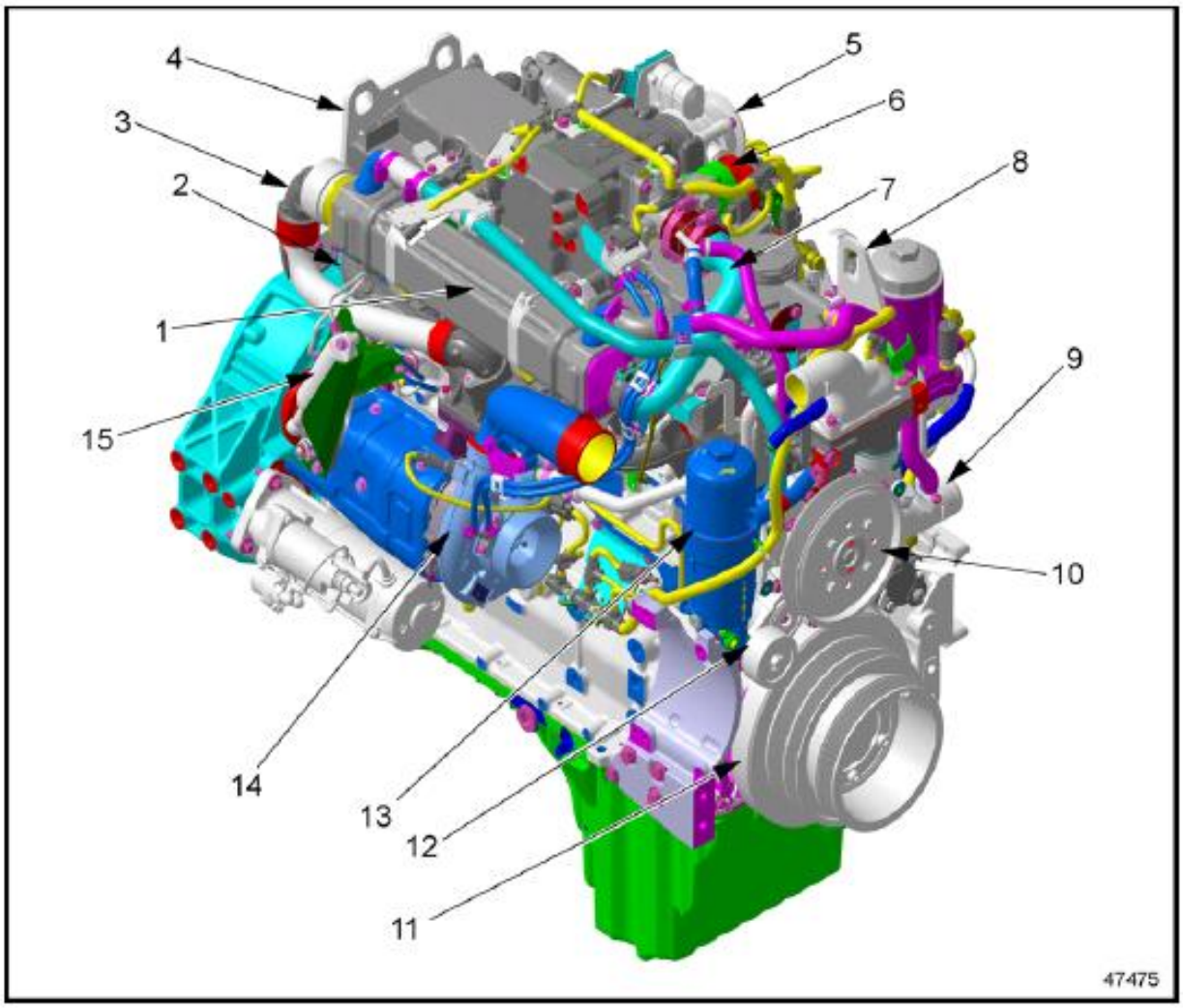

1. EGR Cooler
2. EGR Exhaust Elbow
3. Rear Lifting Bracket
4. Air Intake Throttle Valve
5. EGR Valve
6. EGR Delivery Pipe
7. Front Lifting Bracket
8. Water Pump
9. Fan Pulley
10. Crankshaft Vibration Damper
11. Belt Tensioner
12. Oil Filter
13. Turbocharger (Single-Stage)
14. Exhaust Brake

Figure 3.3 Right side of engine components (29)

www.manaraa.com

3.2. Test bench setup:

The loading on the engine is achieved by coupling the engine to the A/C dynamometer (AVL APA series 045) controlled by PUMA V 1.2 software as shown in figure 3.4. The engine parameters such as speed, torque etc were controlled by AVL Puma V 1.1 test bench.The data from the fuel meter is fed to the PUMA for the instantaneous fuel consumption of the engine. The aftertreatment device has 35 thermocouples incorporated in it and the data is fed to Puma. The soot concentration in the exhaust is measured by AVL 415 smoke meter and the data is fed to AVL PUMA.

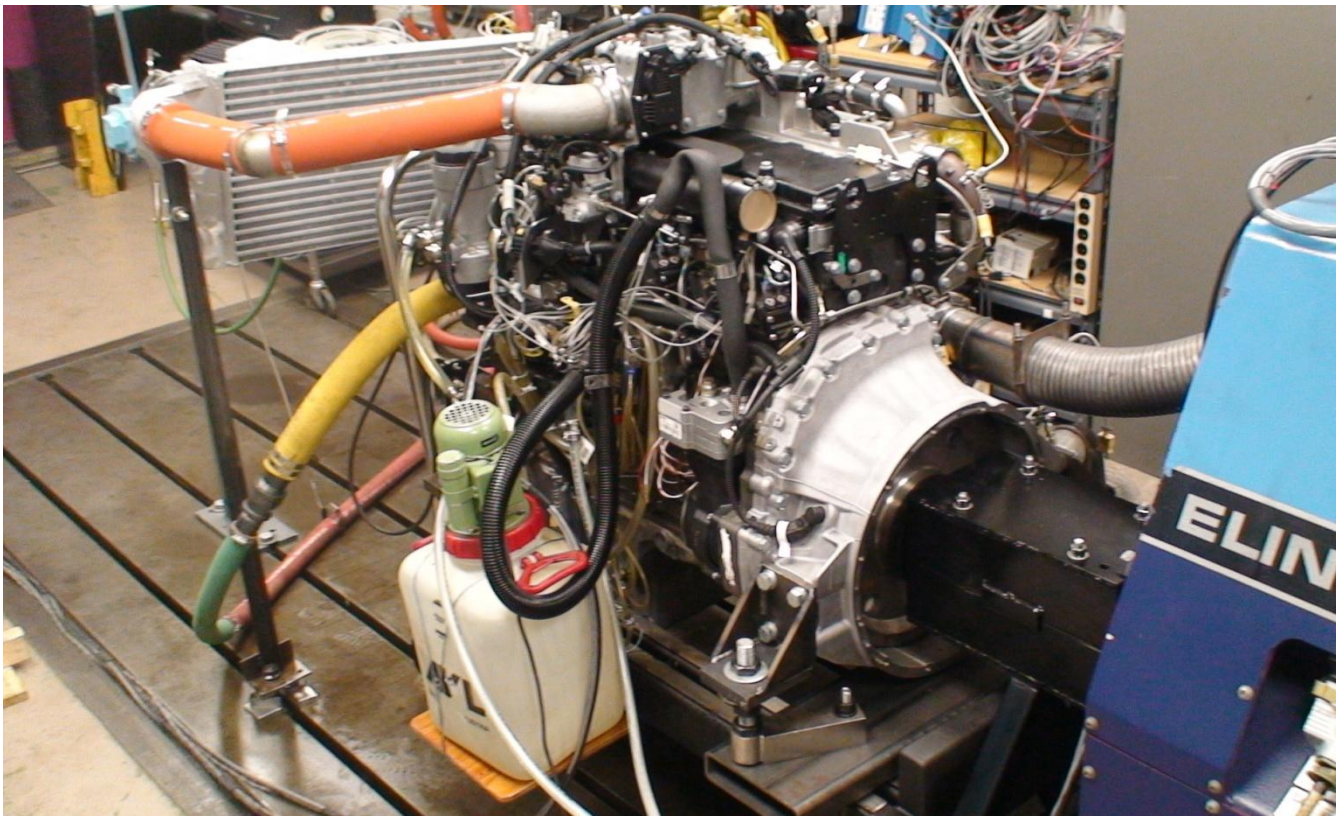

Figure 3.4 Engine coupled to dynamometer (29)

www.manaraa.com

3.2.1. Crank Angle Encoder:

In order to record the data on crank angle basis, an optical shaft encoder was used. The output from various transducers is usually recorded on a crank angle basis in order to synchronize the data recorded from the transducers to the position of the piston. An AVL angle encoder (type 356CC) was used in this investigation and was installed on the free end of the crank shaft. The sensitivity of this encoder was 0.1 of a crank angle degree. The optical encoder is made up of an optical pickup with permanently connected cable and the optical transmitter. The marker disk has 720 angle marks, one of them "trigger" is longer. The marker disk is scanned with infra red light via fibre optic cables fed through a flexible hose between the pickup and the optical transmitter. The light signal is converted to an analog voltage signal in the optical transmitter. The marker disk is scanned using the reflection method. Table 3.2 shows the technical specifications of the shaft encoder used for this investigative study.

SPECIFICATIONS	DESCRIPTION
Model	AVL Optical Encoder 365CC
Speed range	50 rpm……20,000 rpm
Supply voltage	5V Standard; 9V TO 36V Optional
Temperature	-40 ^{o}C – 70 ^{o}C
Moment of inertia of rotating masses	3.8 x 10^{-5} kgm^{2}

Table 3.2 Specifications of shaft encoder

www.manaraa.com

3.2.2. Data Acquisition System:

Two data acquisition systems were used in the present setup. A high speed data acquisition system (Indiset Advanced Plus 641) was used for crank angle based signals. It includes 2 data acquisition modules with 08 analog input channels each for high speed data acquisition as typically required in engine indicating. The AVL Indiset Advanced Plus 641 is a multi- channel indicating system for combustion engines. Its main application area is the recording of measurement data, such as cylinder pressure, fuel rail pressure etc in relation to the crank angle.

Parameterization, measurement control, data display and data evaluation are performed using the AVL Indicom software. It has 16 channels with a resolution of 12 bit each, and the output voltage range is from -10V to +10 V. Data is recorded at an overall throughput rate of up to 800 kHz/channel.

Time averaged values of the shaft end torque, throttle actuation control, brake power, speed, temperature measurements and many more were recorded on a time basis by Front End Module (FEM-A) incorporated to the dynamometer control interface. This hardware recorded 48 channels with a sampling rate of maximum 100 kHz. The engine parameters such as speed, torque etc were controlled by AVL Puma V 1.1 test bench.

AVL Puma is a low speed data acquisition system and it records 48 channels whereas AVL Indicom is a 16 channel high speed data acquisition system and it records 14 channels.

www.manaraa.com

3.2.3. Data channels – PUMA (low speed):

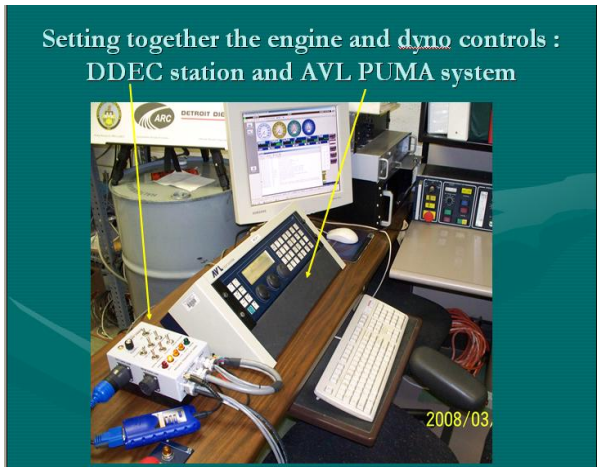

Figure 3.5 AVL Puma

Torque.

Speed.

Fuel consumption.

DOC (11 thermocouples).

DPF (24 thermocouples).

Exhaust gas temperature for cylinder 6.

Exhaust gas temperature at the exit of the turbocharger.

Gas temperature at the entrance in the EGR.

Gas temperature at the exit from the EGR.

Temperature of gases at the entrance in the turbocharger for cylinders 1,2 and 3.

Temperature of gases at the entrance in the turbocharger for cylinders 4, 5 and 6

Cooling water temperature at outlet.

Intake air temperature before intercooler.

www.manaraa.com

3.2.4. Data channels INDICOM (16 high speed channels):

In-cylinder Pressure#1

In-cylinder Pressure#2

In-cylinder Pressure#3

In-cylinder Pressure#4

In-cylinder Pressure#5

In-cylinder Pressure#6

Fuel Rail Pressure

Current Probe Signal

Air inlet manifold pressure.

Figure 3.6 AVL Indicom

Total exhaust manifold pressure (after the t/c)

Exhaust manifold pressure (for cylinders 1,2,3 before t/c)

Exhaust manifold pressure (for cylinders 4,5,6 before t/c)

EGR cooler inlet pressure

EGR cooler outlet pressure

www.manaraa.com

3.2.5. Fuel System:

This engine has a unit injection pump system which is mechanically actuated with the aid of the camshaft and is electronically controlled. This configuration can reach a maximum injection pressure up to 2200 bar. Each unit has a separate electronic unit pump (EUP) with a short injection line to the injection nozzle, which is located in the center of the combustion chamber. The fuel tank has a capacity of 10 gallons. The fuel consumption is measured with the aid of a fuel balance and the data is fed to PUMA.

3.3. Instrumentation:

3.3.1. Engine instrumentation:

The engine is heavily instrumented to measure cylinder pressure on each cylinder, intake manifold pressure, exhaust manifold pressure, EGR cooler inlet and outlet gas pressures, exhaust gas pressure before and after the turbocharger, and various thermocouples installed on the engine and on the aftertreatment device to measure temperature at different locations. Fuel rail pressure sensor is installed on the fuel high pressure line (after the electronic unit injection pump) on cylinder # 6 due to the ease of mounting. The engine has a stock ECU. The needle lift sensor could not be incorporated in the injector due to space constraints. The engine schematic is shown in figure 3.7.

www.manaraa.com

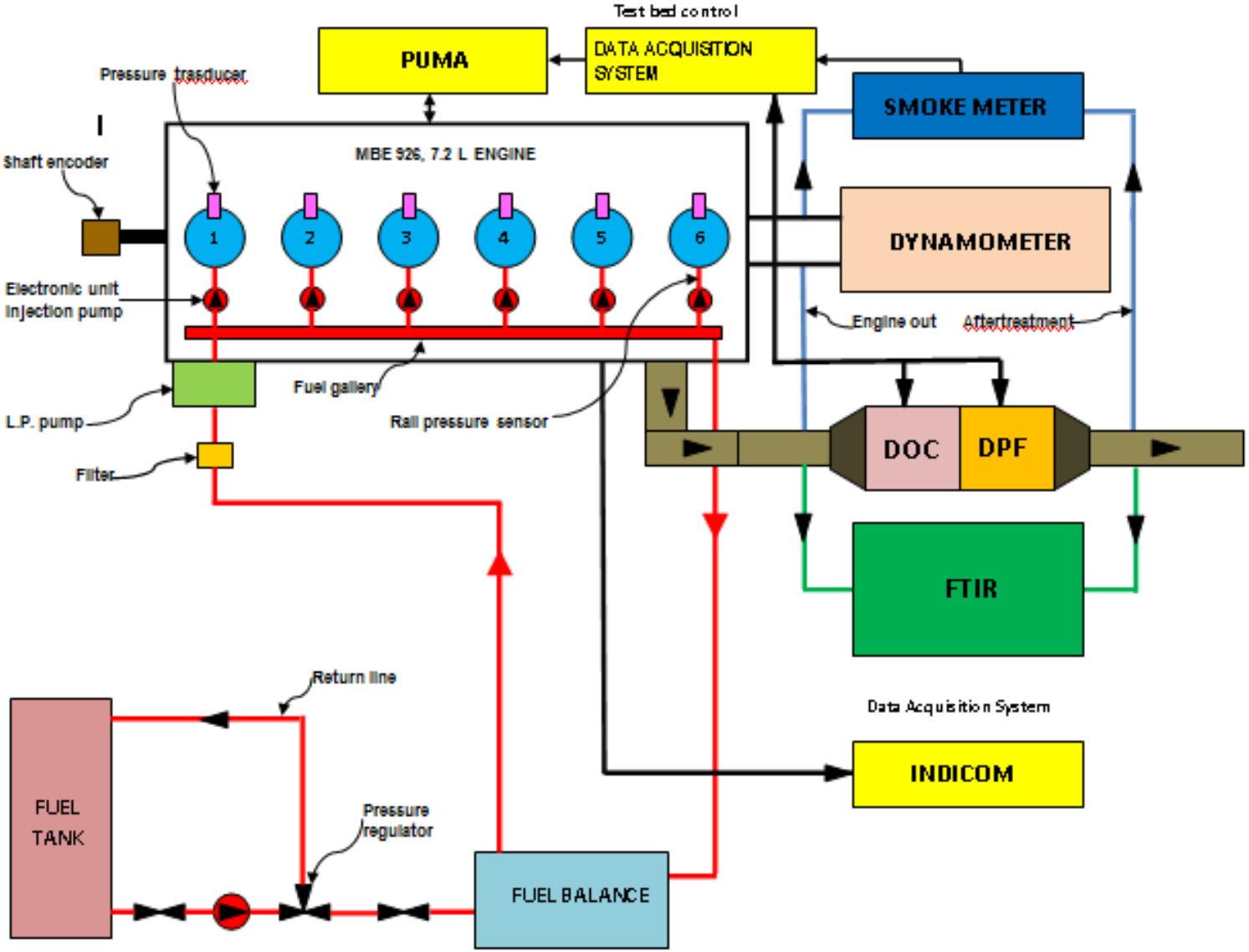

Figure 3.7 Schematic of engine instrumentation

www.manaraa.com

3.3.1.1. Pressure Transducers:

The cylinder head of the engine was replaced with a customized cylinder head. The sleeves for installing the in-cylinder pressure transducers could be mounted in the customized cylinder head. Six Kistler (Type 7061B) pressure transducers were used in this investigation. The signal from these in-cylinder transducers was amplified by six Kistler (5010) amplifiers respectively. Figure 3.8 shows the Kistler (Type 7061 B) pressure transducer and table 3.3 illustrates the technical specifications of the in-cylinder pressure transducer.

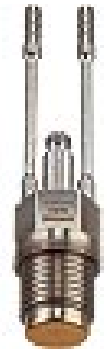

Figure 3.8 In cylinder pressure transducer

SPECIFICATIONS	DESCRIPTION
Measuring range	0 to 250 bar
Overload	300 bar
Sensitivity	5.52 pC/psi
Natural frequency	45 khz
Operating temperature range	-58 to 662 °F

Table 3.3 Specifications of in cylinder pressure transducer

These transducers were water cooled. The technical specifications of the Kistler (5010) amplifier are illustrated in table 3.4.

www.manaraa.com

SPECIFICATIONS	DESCRIPTION
Measurement range	+10,-10 to 999000 pC
No. of channels	1
Frequency range	0 to 180 khz
Supply voltage	115 V(AC)
Operating temperature range	32 to 122 °F

Table 3.4 Specifications of the Kistler (5010) amplifier

There were seven additional pressure transducers which were installed on the engine. The transducers were installed for the measurement of intake manifold pressure, EGR cooler inlet pressure, EGR cooler outlet gas pressure, gas pressure in the exhaust manifold for units # 1,2,3, gas pressure in the exhaust manifold for units # 4,5,6, fuel rail pressure (installed on unit #6), exhaust gas pressure after the turbocharger. Figure 3.9 shows the location of pressure transducers on the engine. Table 3.5 illustrates the types of pressure transducers.

www.manaraa.com

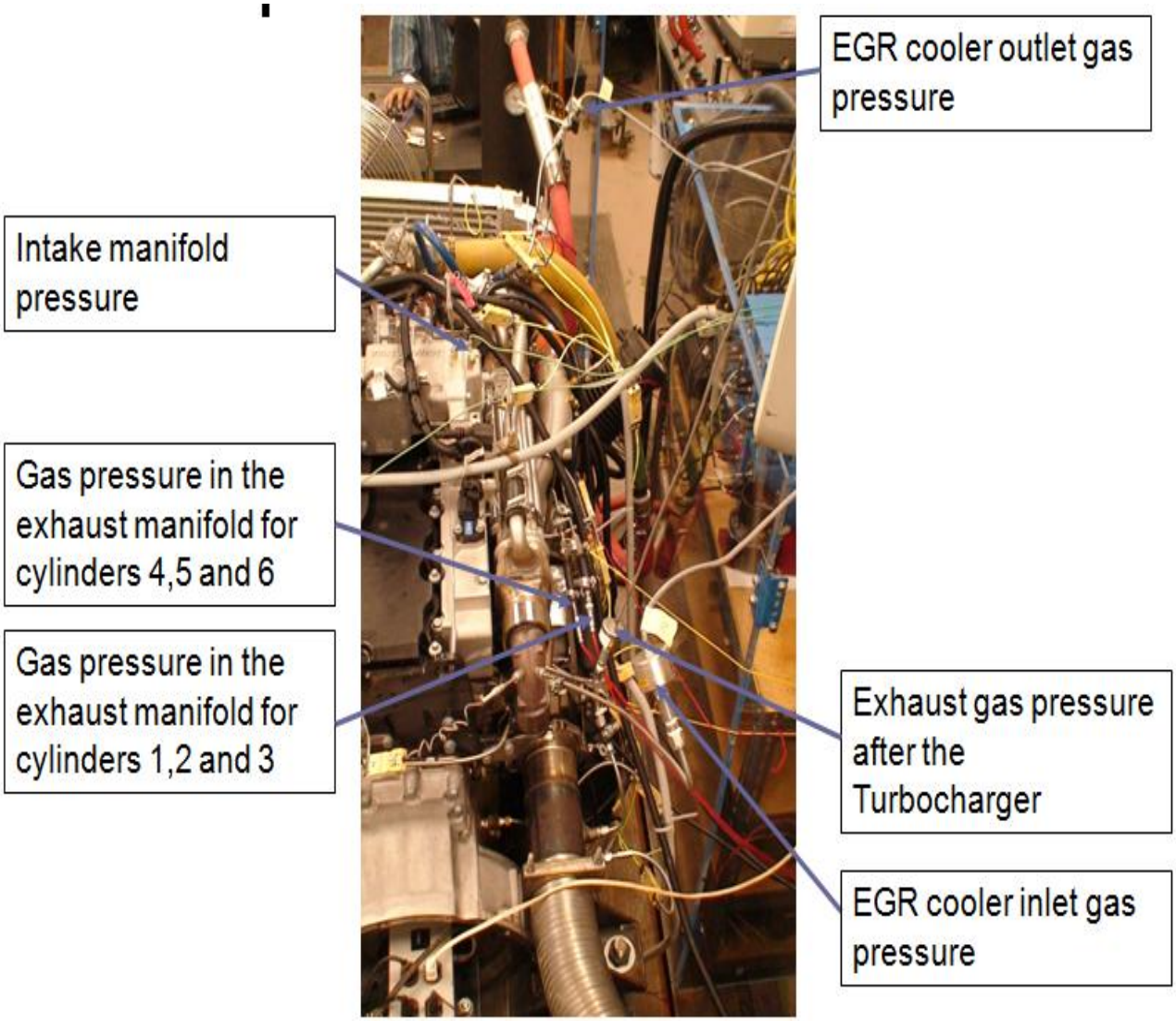

Figure 3.9 Location of pressure transducers on the engine

www.manaraa.com

Transducer Type	Description
Kistler 4005AA5R	Intake Air Manifold
Kistler 4067	Fuel Rail Pressure
Omega PX-176-050A5V	EGR Inlet Pressure
Omega PX-176-050A5V	EGR Outlet Pressure
Omega PX-176-050A5V	Total Exhaust Pressure
Fischer 102	Exhaust Gas Pressure(unit # 1,2,3)
Fischer 102	Exhaust Gas Pressure(unit # 4,5,6)

Table 3.5 Types of pressure transducers

The signal from the exhaust gas pressure (unit#1,2,3), exhaust gas pressure (4,5,6), Intake air manifold pressure and fuel rail pressure sensors is amplified by the the respective Kistler (4618A0) amplifiers. The technical specifications of Kistler (4618A0) are illustrated in table 3.6.

SPECIFICATIONS	DESCRIPTION
Input signal	-50,+50 to 1000 mV
Excitation current	1.5 mA
Frequency range	0 to 40 khz
Input voltage	18 to 30 V
Operating temperature range	32 to 140 °F

Table 3.6 Specifications of Kistler (4618A0) amplifier

www.manaraa.com

3.3.1.2. Thermocouples:

Omega k type thermocouples were used for this investigation. The diameter of the wire was 1875 inches and the junction was grounded. The temperature range for measurement was from -200°C to 1250°C and the standard limit of error was 2.2°C or 0.75% (whichever was greater). Figure 3.10 shows an omega K type thermocouple.

Figure 3.10 Omega K type themocouple used in temperature measurement

3.3.1.3. Current Probe:

Due to space limitations, the needle lift sensors for the fuel injectors could not be installed on this engine. Instead of that a current probe (fluke 80i-110s) is used for this investigation. This probe is jaw shaped and it is clamped around all the six conductors through which the electrical signal goes to the respective fuel injectors.

The arrangement of this current probe is shown in figure 3.11.

www.manaraa.com

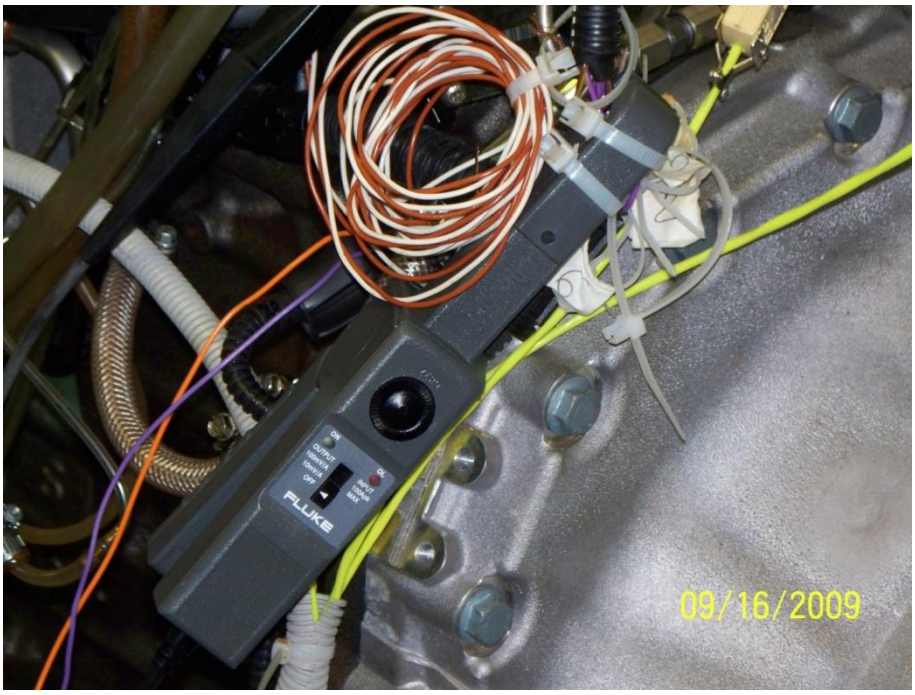

Figure 3.11 Arrangement of the current probe

This device is used to measure current through any conductor. The magnetic flux strength around the conductor is measured, from which the current is calculated.

The technical specifications are illustrated in table 3.7.

SPECIFICATIONS	DESCRIPTION
Dimensions	67 x 231 x 36 mm
Weight	330 gm (battery included.)
Max conductor size	11.8 mm
Max jaw opening	12.5 mm
Operating temperature	-30 to 70°C

Table 3.7 Technical specifications of the current probe.

www.manaraa.com

3.3.1.4. Electronic Control Unit

The engine is equipped with a stock Electronic Control Unit (ECU) which is a fully electronic control system. This system is composed of a Motor Control Module (MCM), and the Common Powertrain Controller (CPC). The two units are connected by a proprietary data link through which all the necessary data and information is shared. The MCM monitors both the engine and the data link. When a malfunction or other problem is detected, the system selects an appropriate response.

a. Motor Control Module

The engine mounted MCM includes control logic to provide overall engine management. The MCM processes the data received from the CPC, for example the position of the accelerator pedal. This data is evaluated together with the data from the sensors on the engine, such as, charge and oil pressure and coolant and fuel temperature. The data is then compared to the characteristic maps stored in the MCM. From this data, quantity and timing of injection are calculated and the electronic unit pumps are actuated accordingly through the solenoid valves. Figure 3.12 shows the arrangement of motor control module.

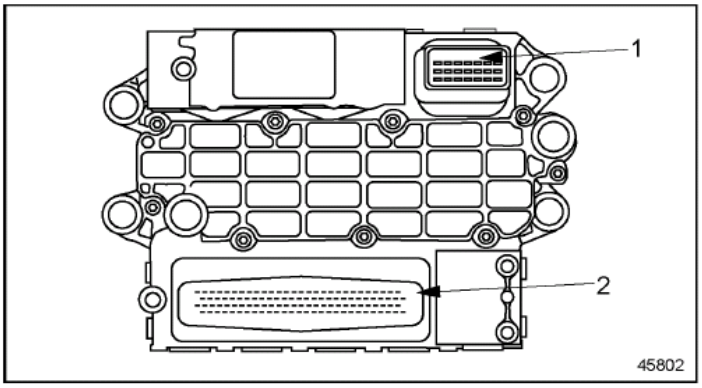

Figure 3.12 Motor control module (29)

www.manaraa.com

b. Common Powertrain Controller

The CPC has three 18-pin connectors and one 21-pin connector. The CPC is the interface between the MCM and the vehicle/equipment for engine control. The CPC receives data from the operator (accelerator pedal position, switches, and various sensors). Figure 3.13 shows the arrangement of common powertrain controller.

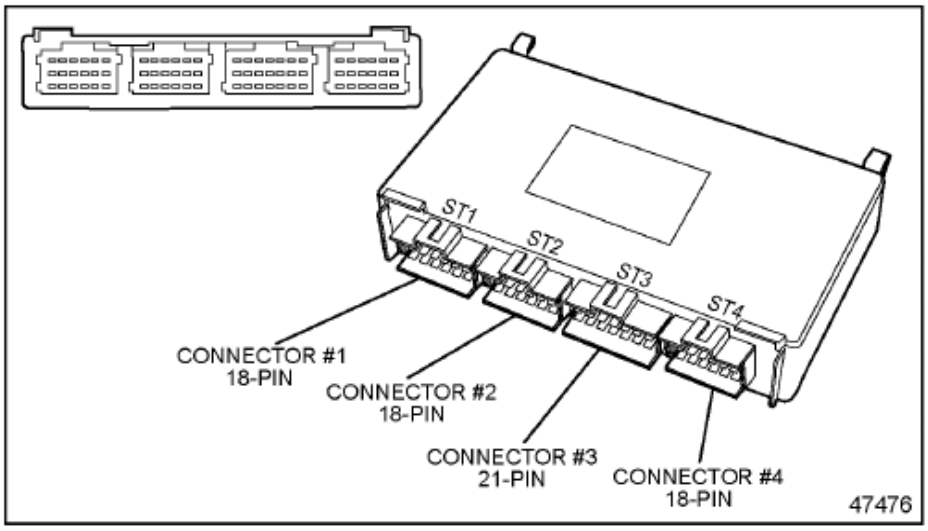

Figure 3.13 Common powertrain controller (29)

From the data received by the CPC , instructions are computed for controlling the engine and transmitted to the MCM via the proprietary data link. Within the CPC, sets of data for specific applications are stored. These include idle speed, maximizing running speed, and the speed limitation.

3.3.2. Aftertreatment Device:

The device's primary function is to oxidize unburnt hydrocarbons and carbon monoxide and to capture and burn off (regenerate) the particulate matter (soot) in the engine exhaust gas. The exhaust gas first enters the Diesel Oxidation Catalysts (D.O.C) and then flows through the

www.manaraa.com

Diesel Particulate Filter (D.P.F.). Through constant monitoring of exhaust gas temperature and the system back pressure, the E.C.U. is able to manage regeneration.

The E.C.U. processes the signals from the sensors (such as exhaust gas temperature, exhaust gas back pressure), initiates regeneration and controls the filter regeneration temperature by actively adjusting the position of the throttle valve at the intake manifold.

Thus it provides a rich mixture which results in the continuation of the oxidation reactions in the exhaust manifold which in return increases the temperature of the exhaust gases.

An exhaust port fuel injector placed upstream of the diesel oxidation catalyst can also be utilized to increase the exhaust gas temperature. It provides micro-diesel fuel injections in the exhaust gas when required. Based on the exothermal catalytic combustion of the fuel over the oxidation catalyst, the exhaust temperature can reach the suitable temperature level for soot combustion and filter's regeneration.

3.3.2.1. Instrumentation at the Aftertreatment Device:

The thermocouples are located axially and radially along the aftertreatment device. Figure 3.14 shows the arrangement of the thermocouples in the D.O.C. and figure 3.15 shows the arrangement of the thermocouples in the D.P.F.

www.manaraa.com

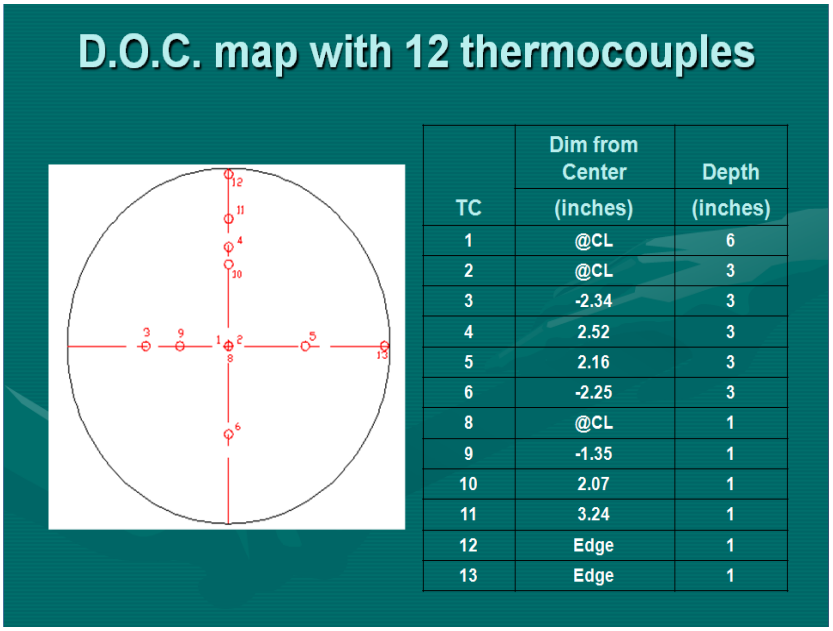

TC	Dim from Center (inches)	Depth (inches)
1	@CL	6
2	@CL	3
3	-2.34	3
4	2.52	3
5	2.16	3
6	-2.25	3
8	@CL	1
9	-1.35	1
10	2.07	1
11	3.24	1
12	Edge	1
13	Edge	1

Figure 3.14 Location of thermocouples in D.O.C.

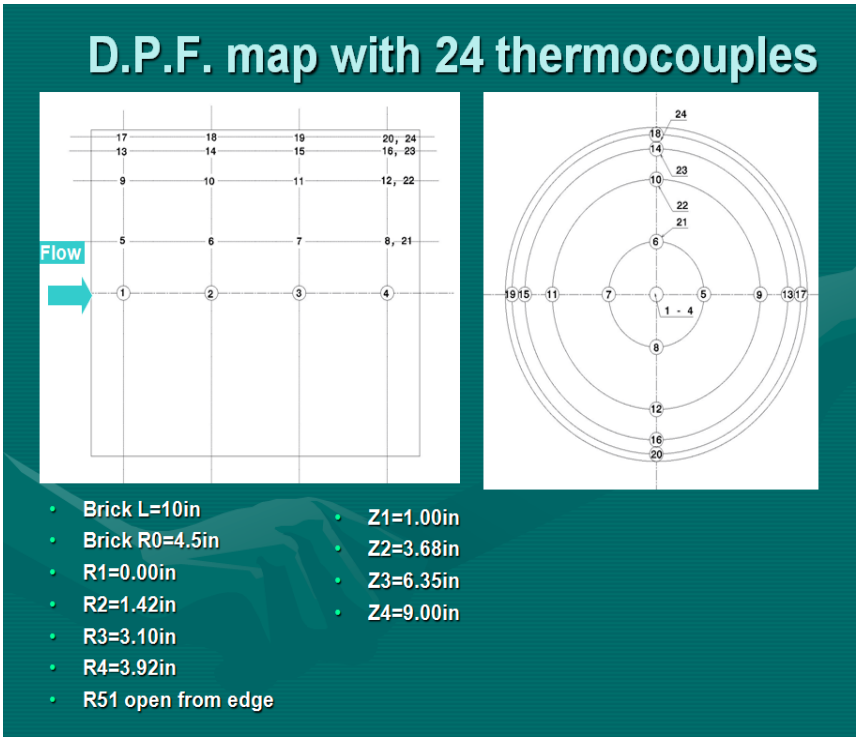

Figure 3.15 Location of thermocouples in the D.P.F.

www.manaraa.com

The emissions can be measured both before and after the aftertreatment device through a combo valve. The arrangement of the combo valve is shown in figure 3.16.

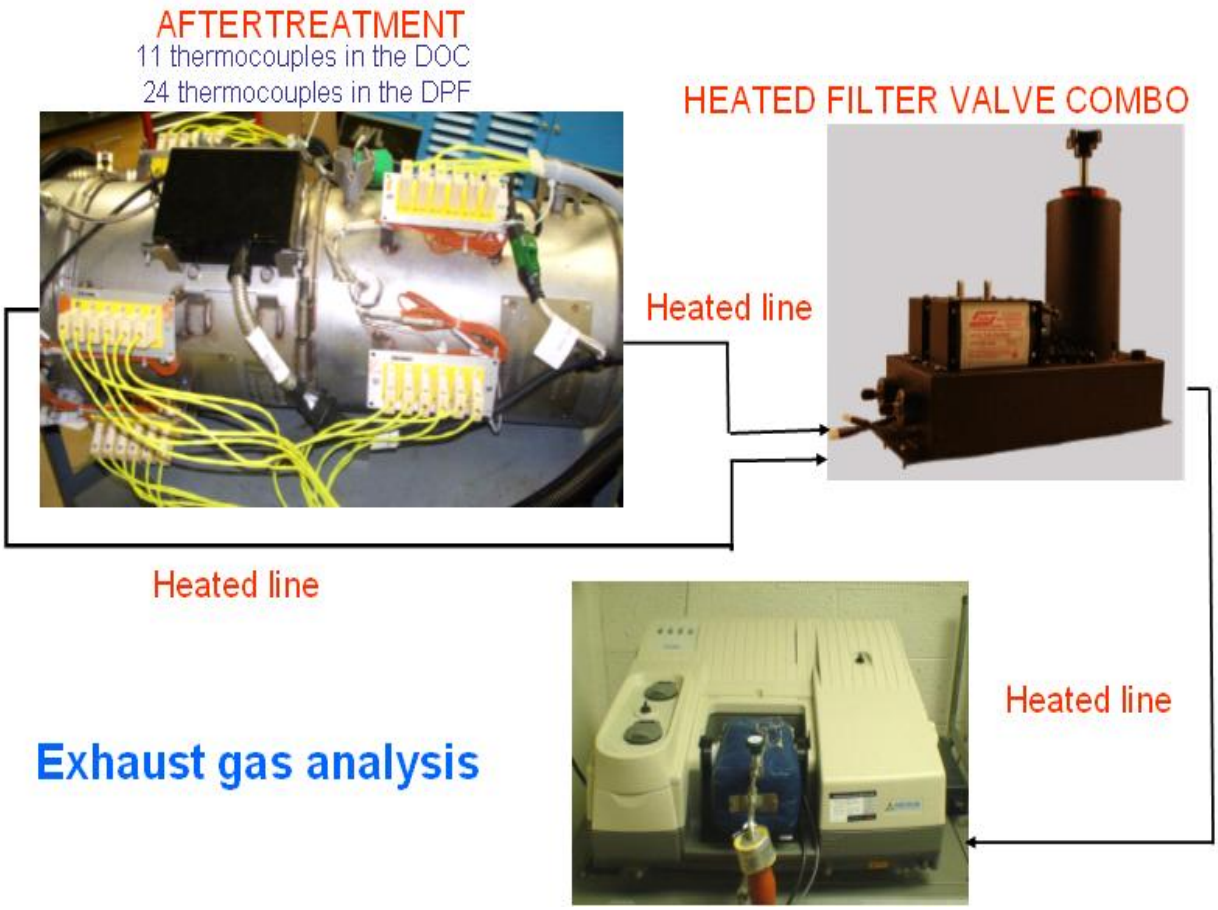

Figure 3.16 Arrangement of the combo valve

3.4. Emission Measurement:

In order to measure the engine out emissions, a F.T.I.R (Nexus 670 Analyzer) was used. F.T.I.R spectroscopy is a useful solution to the analytical problems of exhaust measurement. While traditional on-line analyzers require exhaust to be diluted and cooled before sampling, F.T.I.R can directly measure data from the raw exhaust. Many highly reactive species in the exhaust can be measured by F.T.I.R down to low part-per-million levels. 5-6 discrete analyzers

www.manaraa.com

could be replaced by one single F.T.I.R. analyzer. Figure 3.17 shows the diagram of the instrument used in this investigation.

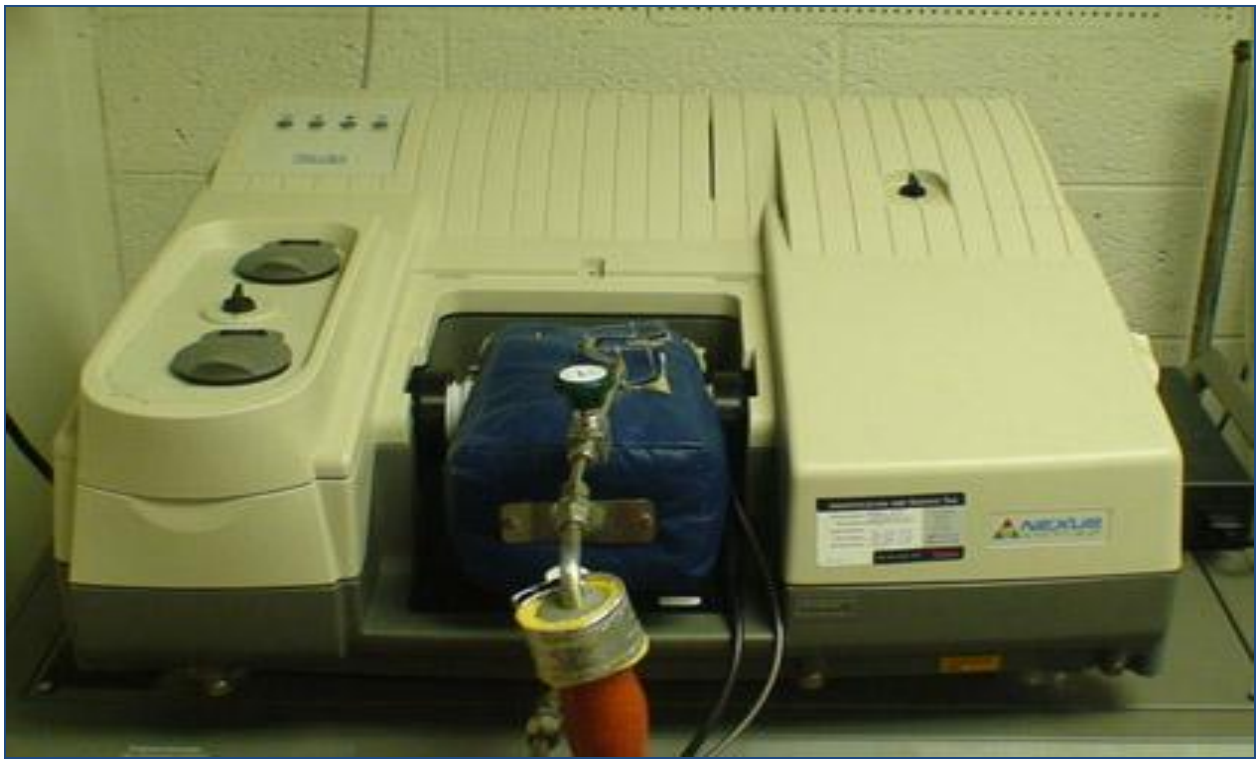

Figure 3.17. F.T.I.R (Nexus 650 Analyzer)

The working principle is illustrated in figure 3.18.

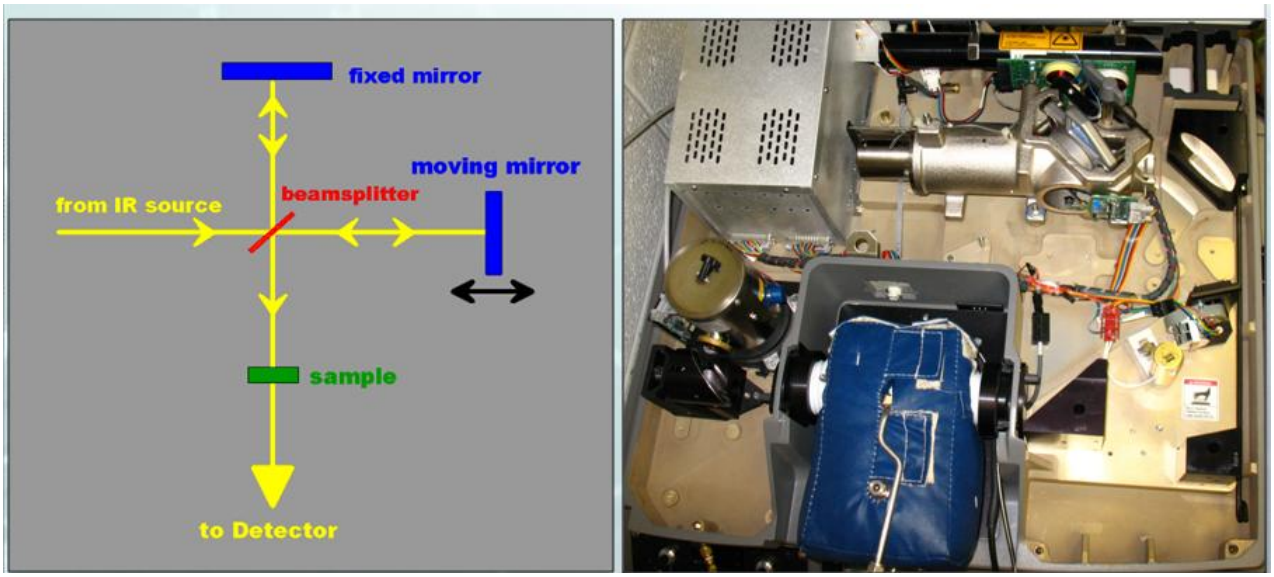

Figure 3.18 Working principle of an Inferometer

www.manaraa.com

From the IR source, the light travels to the beam splitter from where half (50%) of the light is reflected to the fixed mirror and the remaining half portion of the light is transmitted to the moveable mirror. Light travels to each of these mirrors and reunites at the beam splitter before passing through the sample and then it reaches the detector. As the light intensity of the recombined beam is recorded at the detector, the moveable mirror travels towards the beam splitter, producing an interferogram.

The instrument has a 2m gas cell. The small volume (200 ml) of the 2m gas cell is ideal for sample streams where the component concentrations are varying with time and therefore it is ideal for internal combustion engines. This gas cell gives an exceptionally good mixing rate, which allows accurate recording of concentration changes over time.

A wide range of species can be measured with this instrument. Measurement of carbon dioxide is very simple. Carbon monoxide levels vary greatly with different applicators, which require the careful selection of infrared absorbance bands to stay within the desired absorbance range. As the oxides of nitrogen is not a single compound and is actually sum of two separate compounds NO and NO_2 and therefore an equivalent NO_X value can be obtained by adding these two values. Also both NO and NO_2 absorb only in regions with very high levels of water interference, as well as CO and CO_2 interferences.

F.T.I.R. measures hydrocarbons differently from the flame ionization detector (F.I.D.) typically used in the exhaust measurements. F.T.I.R. can measure 15-20 hydrocarbons individually in the exhaust, whereas the F.I.D. measures all hydrocarbons in a single bulk reading. By weighting the calculated levels of individual hydrocarbon species with their carbon numbers, the F.T.I.R. values can be combined into an F.I.D. equivalent reading.

www.manaraa.com

OMNIC software is designed to meet the requirements for gas phase calculations. Interference from water or other compounds may be minimized by careful selection of the windows which blank out the interfering bands.

3.4.1. Smoke Measurement:

This instrument is for automatically measuring the soot content of the exhaust gas of an internal combustion engine that uses standard diesel fuel. The variable intake volume means that even extremely low soot concentrations in the exhaust can be measured. In this investigation, the device is operated via the computer port and from a test bench host (PUMA). The smoke can be measured both before and after the aftertreatment device. Figure 3.19 shows the arrangement of the smoke test bench.

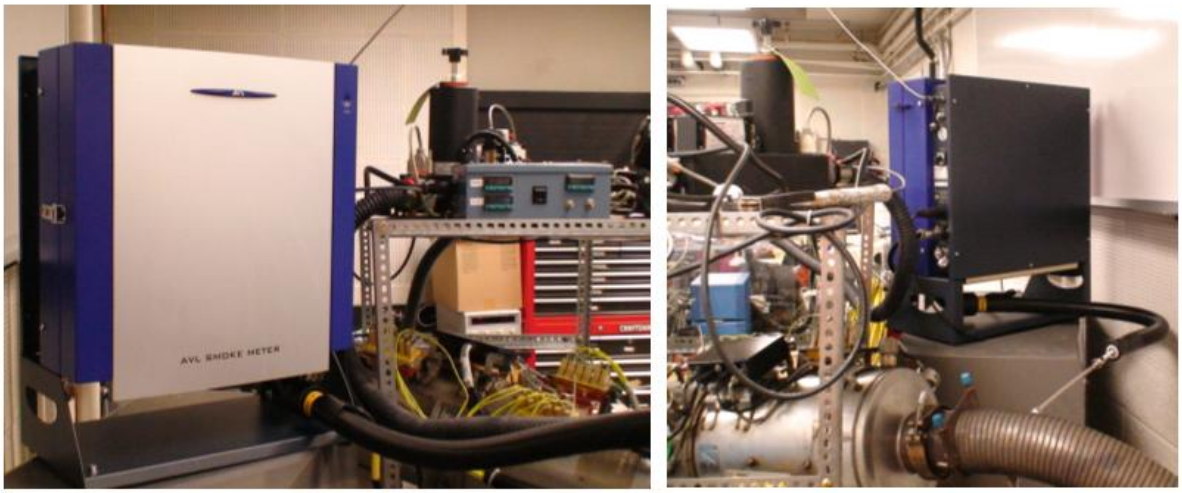

Figure 3.19 Arrangement of the smoke bench

www.manaraa.com

3.4.1.1. Working Principle:

The device works on an auto range mode and samples a definite volume of exhaust from the exhaust line using a probe. In the present setup, the device uses two probes and is able to measure the soot content before and as well as after the aftertreatment device. The volume of the exhaust drawn through the filter paper is measured by the flow meter. The effective length is calculated. The blackening of the filter paper due to soot is detected by an optical reflectometer head. The soot content in the exhaust is determined by the paper blackening and the effective length. The soot content is the output as F.S.N. or soot concentration (mg/m3). Figure 3.20 shows the working principle of the device.

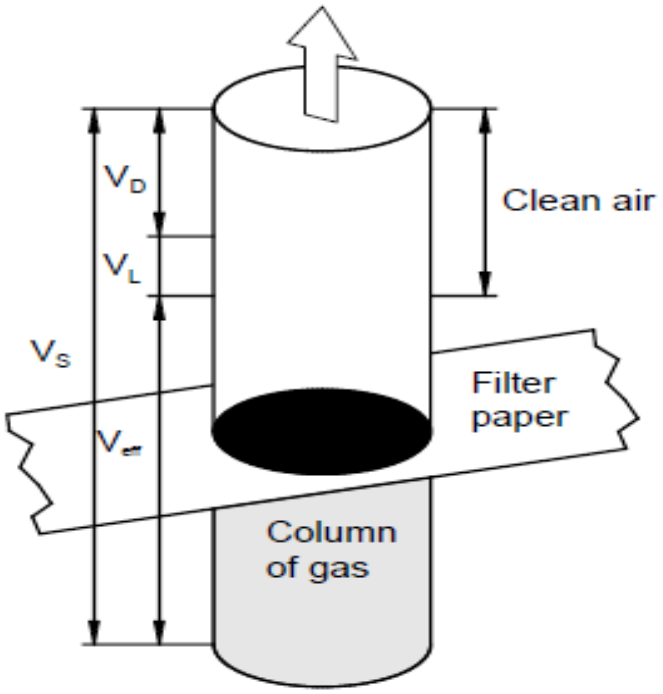

Figure 3.20 Working principle of the smoke meter (30)

www.manaraa.com

Where,

- Effective length (L_{eff}) is the column of the exhaust gas drawn through the filter paper. Mathematically, $L_{eff} = V_{eff} / A$, where A is the area of the blackened paper.
- Sampling time is the time over which the sample is taken.
- Effective sampling time is the time over which the mean soot content is determined.
- Sampled volume (V_s) is the total volume of the gas drawn in by the device through the filter area.
- Dead volume (V_D) denotes the geometric volume from the sampling probe through the hose to the filter paper. Before each measurement it is purged with clean air and therefore does not contribute to paper blackening.
- Leak volume (V_L) defines the volume of the clean air that is drawn in together with exhaust gases due to leaks.
- Effective volume (V_{eff}) is the volume of the exhaust gases drawn to the filter paper.

Mathematically, $V_{eff} = V_S – V_D – V_L$.

www.manaraa.com

4. Test matrix and testing conditions

4.1. Test matrix:

The engine testing for this investigation study was done using four different fuels (ULSD, S8, JP8 and B20). The engine is capable of producing a net power of 250 hp and a net torque of 1085 Nm. However, due to limitations of the dynamometer, the maximum torque which can be put on the engine is 400 Nm. Moreover, taking into consideration the factor of safety, the engine is only loaded up to 360 Nm. Therefore, the engine is only loaded 33.3% of the maximum load which the engine is capable of delivering.

For steady state conditions, the data is recorded once the exhaust gas temperature stabilizes. An average of 100 cycles is considered for every test point in order to get away with cycle to cycle variations.

Tests are also conducted with and without EGR in order to see the effect of EGR on the emissions.

For steady state points, the emissions are recorded before and after the aftertreatment device in order to have a better understanding regarding the efficiency of the aftertreatment device.

The engine is calibrated for ULSD, but it is run on alternative fuels such as S8, JP8 and B20 in order to see the effect of these fuels on the performance of the engine and the emissions.

www.manaraa.com

Table 4.1 illustrates the test matrix.

Speed \ Torque	237 Nm	360 Nm
1300 rpm		
1500 rpm		
2000 rpm		
2200 rpm		

Table 4.1 Test matrix

5 bar imep corresponds to 237 Nm torque, and 7.5 bar imep corresponds to the 360 Nm torque. Tests have been conducted at 5 bar IMEP in order to compare it with high speed single cylinder diesel engine in one of the test cells (lab 1356) at center of automotive research. On the other hand, 7.5 bar IMEP is the maximum limit the engine could run on due to the limitation of the dynamometer. At 7.5 bar IMEP, the investigation pertains to the effect of speed on the in cylinder combustion and the emissions (before and after the aftertreatment device).

www.manaraa.com

5. Tested fuels and properties

5.1. Tested fuels:

The different fuels tested for this investigative study were ULSD, JP8, S8, and B20. The engine is calibrated for ULSD. Due to the lack of the lubricity in S8, an additive named NALCO was added to the fuel. For 5 gallons of S8, 0.859 g (60 ppm by weight) of NALCO was added. . It is well known from the literature that biodiesel blends tends to react with plastic storage tanks and hence stainless steel tanks are used. Moreover, when exposed to atmosphere, biodiesel blends to form precipitates owing to it poor oxidation stability which can clog fuel filters and injectors. Therefore, for biodiesel, another fuel tank was used which was pressurized by compressed nitrogen.

5.2. Fuel properties:

Different fuels have different physical and chemical properties. These properties greatly affect the in-cylinder combustion and the tail pipe emissions. Table 5.1 illustrates the physical properties of the different fuels used for this investigation study.

www.manaraa.com

Properties	Units	ULSD	Source	S8	Source	JP8	Source	B100	Source
Bulk modulus (400 bar)	Mpa	1775	CAR	1484	CAR	1411	CAR	1854	CAR
Density (@40°C)	(Kg/L)	0.837	CAR	0.737	Tardec	0.785	Tardec	0.890	
Viscosity	(cst)	2.35	RKA	1.29	NREL				
Heating value	(MJ/Kg)	41.66	CAR	42.29	CAR	42.11	CAR	36.6	
Heating value	(MJ/L)	34.87		31.16		33.05		32.57	

Table 5.1 Physical properties of different fuels.

The physical properties of fuels will have a great influence on spray injection, which is a critical physical property of mixture preparation. The mixture preparation will no doubt affect the in-cylinder combustion. Under the same pumping conditions, different bulk modulus values of different fuels will develop different injection pressures. Lower bulk modulus value will develop lower injection pressure and higher bulk modulus value will develop higher injection pressure. As the injection pressure is increased, the spray gets narrow and it leads to a better atomization of the fuel. The width of the current probe signal depends upon the bulk modulus of the fuel. Higher the bulk modulus of the fuel, lower is the width of the current probe signal. The density of a fuel also plays an important role as it determines how much a fuel has to be injected on volumetric basis to meet the same power requirement. The injection system is designed to deliver a certain amount of fuel to the engine. If for instance, the density of the fuel is less, therefore, in order to develop the same power the amount of fuel injected on volumetric basis has to be increased and vice-versa. The heating value on volumetric basis is also shown in table 7.1. It is obtained by the product of lower heating value of the fuel and the density of the fuel.

Table 5.2 illustrates the chemical properties of the different fuels used for this investigation study.

www.manaraa.com

Properties	Units	ULSD	Source	S8	Source	JP8	Source	B20	Source
Composition (vol %)	Aromatics	31.1	Batch 1 Halterman	0.45	Tardec	17.7	Chevron		
	Olefins	1	Batch 1 Halterman			2.3	Chevron		
Cetane number		45.3	South west	56.1	NREL	44.1	South west	54	NREL

Table 5.2 Chemical properties of different fuels

Cetane number is a measure of fuel's ignition delay. Ignition delay is the time period between the start of injection (SOI) and the start of combustion (SOC) of the fuel. Start of combustion (SOC) is considered when the firing RHR curve crosses the motoring RHR curve. Higher cetane number shortens the ignition delay and promotes faster combustion.

JP8 is a jet fuel. The cetane number is not included in the specifications. Due to this, the cetane number varies over a wide range (30 to 60). The exact value of cetane number for JP8 in our case is 44.1 from the results of South West lab.

5.3. Effect of fuel volatility on ignition delay:

The vaporization and the combustion of the fuel is greatly affected by a property known as fuel's volatility. If the fuel is having a low boiling point, it evaporates and mixes with the air at a faster rate in order to form a combustible mixture. This eventually shall lead to a more intense premixed fraction burn and heat release in a diesel engine combustion process. Figure 6.15 shows the distillation curves for ULSD, JP8 and S8.

www.manaraa.com

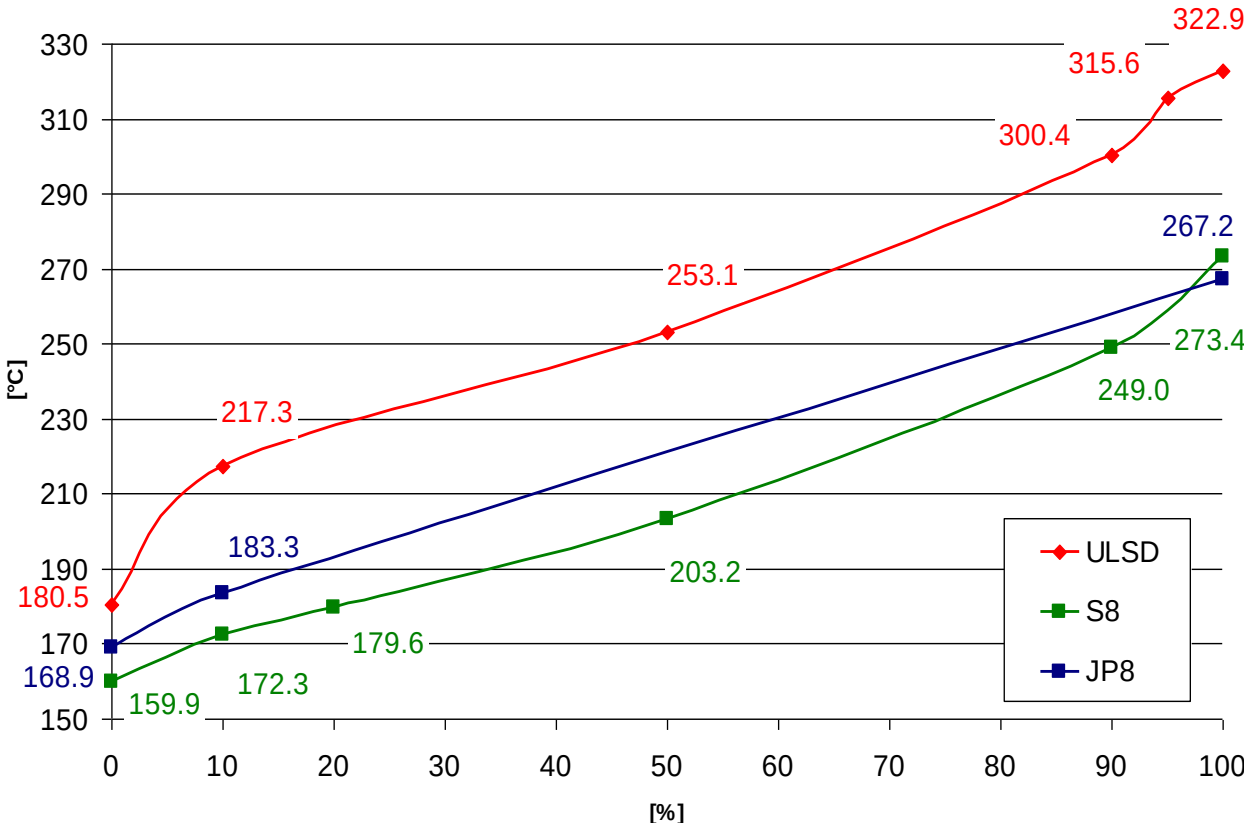

Figure 5.1 Distillation curve for ULSD, JP8 and S8

S8 has hydrocarbons with the lower boiling point followed by JP8. In case of ULSD, boiling temperatures are much higher.

www.manaraa.com

6. Experimental results and analysis (5 BAR IMEP)

6.1. In cylinder combustion data analysis:

6.1.1. Reference data using ULSD (In cylinder combustion):

First set of experiments were conducted at 5 bar IMEP at 1500 rpm. As the engine is calibrated for ULSD, therefore, initially the engine was run on ULSD in order to know how the engine behaves with ULSD and to set the results as a benchmark in order to compare it with other results obtained using other alternative fuels. Also, the 5 bar IMEP was chosen so that the emission results could be compared with a single cylinder HSDI engine running at the same conditions. The study was diverted to investigate any variability of in-cylinder combustion, emissions, and the efficiency of the aftertreatment device. The effect of EGR was also studied. Table 6.1 illustrates the few critical parameters at this running point.

Running point	Throttle valve opening	LPPC	RHR peak	Peak compression pressure	Peak combustion pressure	Fuel Consumption	Exhaust gas temperature
ULSD(With EGR)	44%	11.6^0 ATDC.	226 KJ/m^3	55 bars	60 bars	7.7 kg/hr	316 ^{0} C

Table 6.1 Critical parameters with ULSD (with EGR) at 5 bar IMEP.

Figure 6.1 shows the running point with ULSD (with EGR). The pulse width for the current probe signal is 9.6 CA, the peak of rail pressure is 1130 bars and the location of peak of rail pressure is 4.8° ATDC. Figure 6.2 shows the exploded view of RHR. The ignition delay of was calculated from the motoring RHR and the firing RHR. The ignition delay in this case is 3.7 CAD.

www.manaraa.com

Figure 6.3 shows the same running point without EGR. Table 6.2 illustrates the few critical parameters at this running point.

Running point	Throttle valve opening	LPPC	RHR peak	Peak compression pressure	Peak combustion pressure	Fuel Consumption	Exhaust gas temperature
ULSD(Without EGR)	46%	9.2^{0} ATDC.	254 KJ/m^3	65 bars	70 bars	8.1kg/hr	287 ^{0} C

Table 6.2 Critical parameters with ULSD (without EGR) at 5 bar IMEP.

Figure 6.4 shows the exploded view of RHR. The combustion takes place at a faster rate (evident from the slope of the curve) and the LPPC shifts closer to TDC and its location is 9.2° ATDC. The pulse width of the current probe remains the same as the fuel used is the same and there is no difference in the value of the bulk modulus and the viscosity of the fuel. The ignition delay gets shortened and it is reduced to 3.2 CAD.

This engine is optimized for the use of EGR. By removing the electrical connection of the EGR, the calibration of the engine was disturbed. Since, there was no possibility to optimize the effect, the combustion was shorter but the overall efficiency was lower.

Without EGR, there is a larger amount of exhaust gases hitting the turbine blades and therefore, there is a higher value of the air intake pressure. Higher work is consumed during the compression process. Therefore, it can be concluded that the injection timing is not optimized for these conditions.

www.manaraa.com

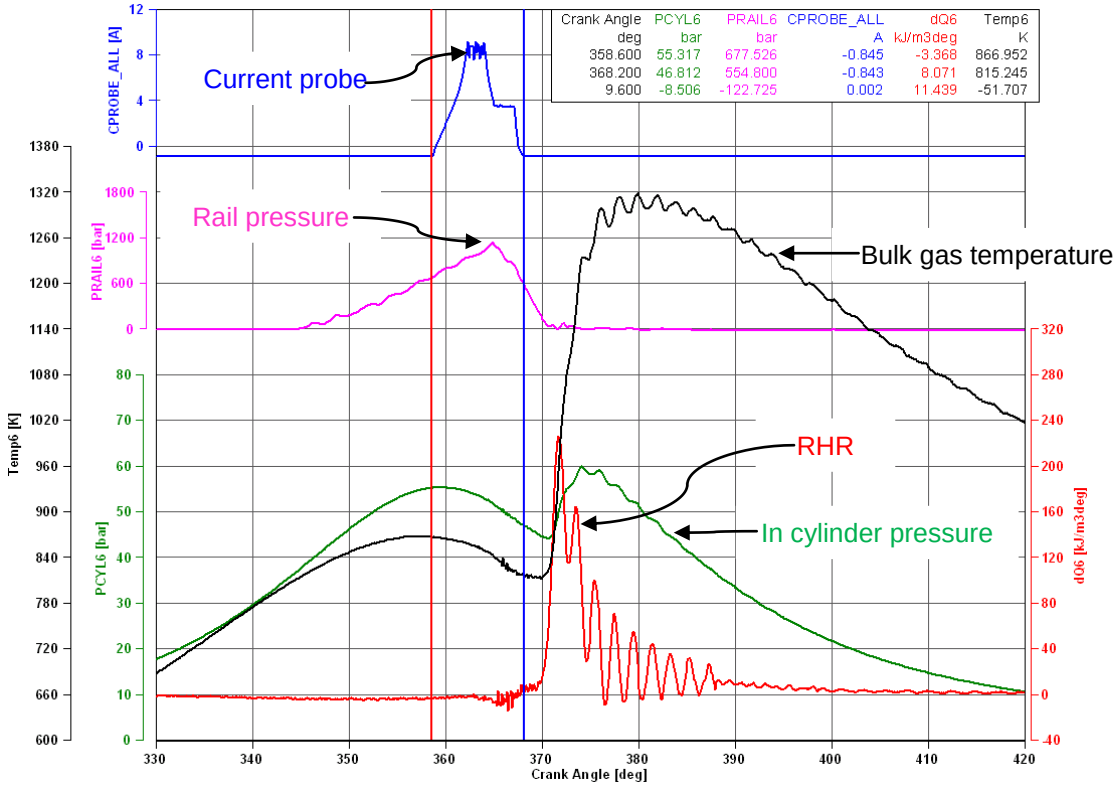

Figure 6.1 (5 bar) data point with ULSD (with EGR)

www.manaraa.com

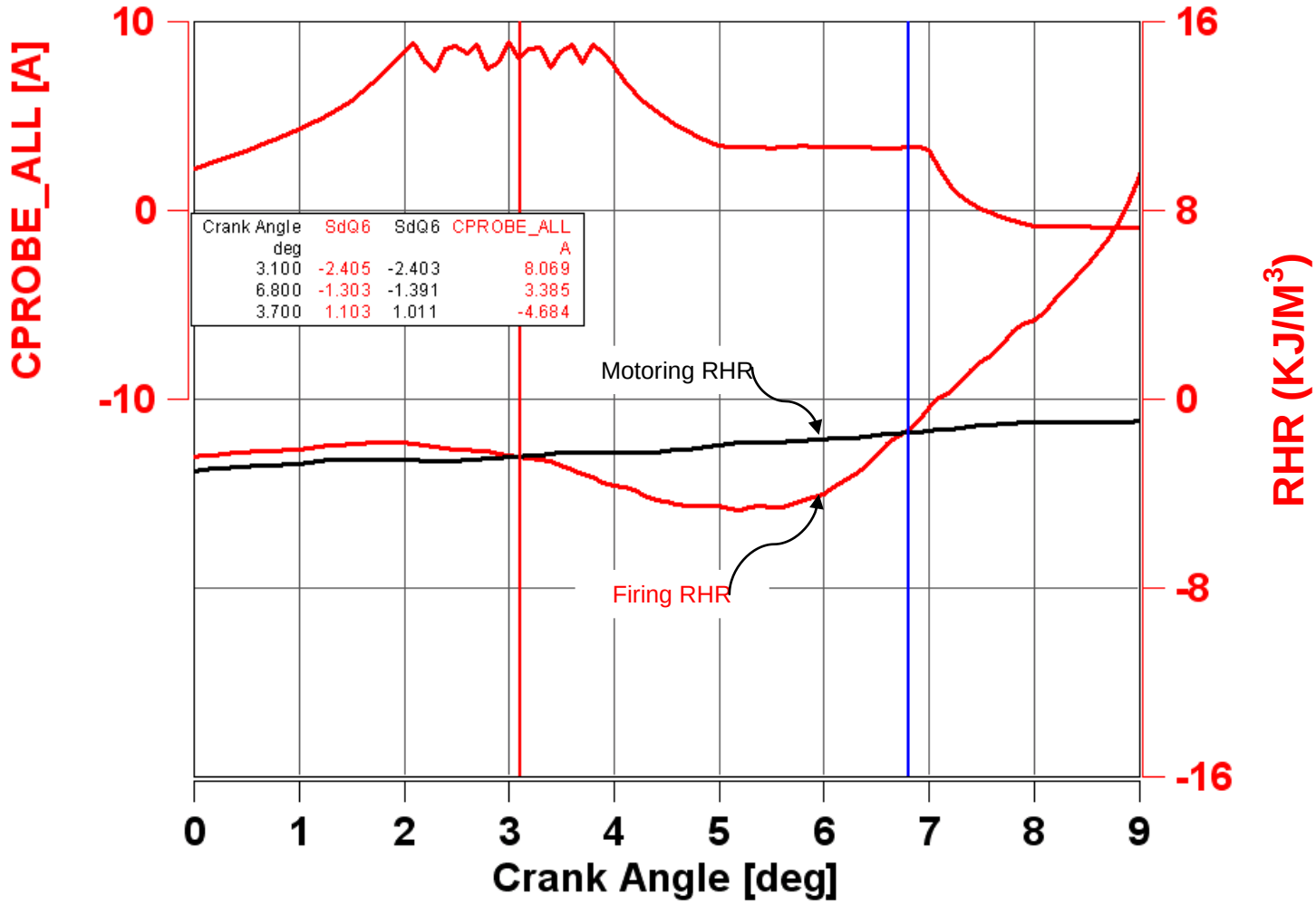

Figure 6.2 Exploded view of Apparent RHR for ULSD (with EGR)

www.manaraa.com

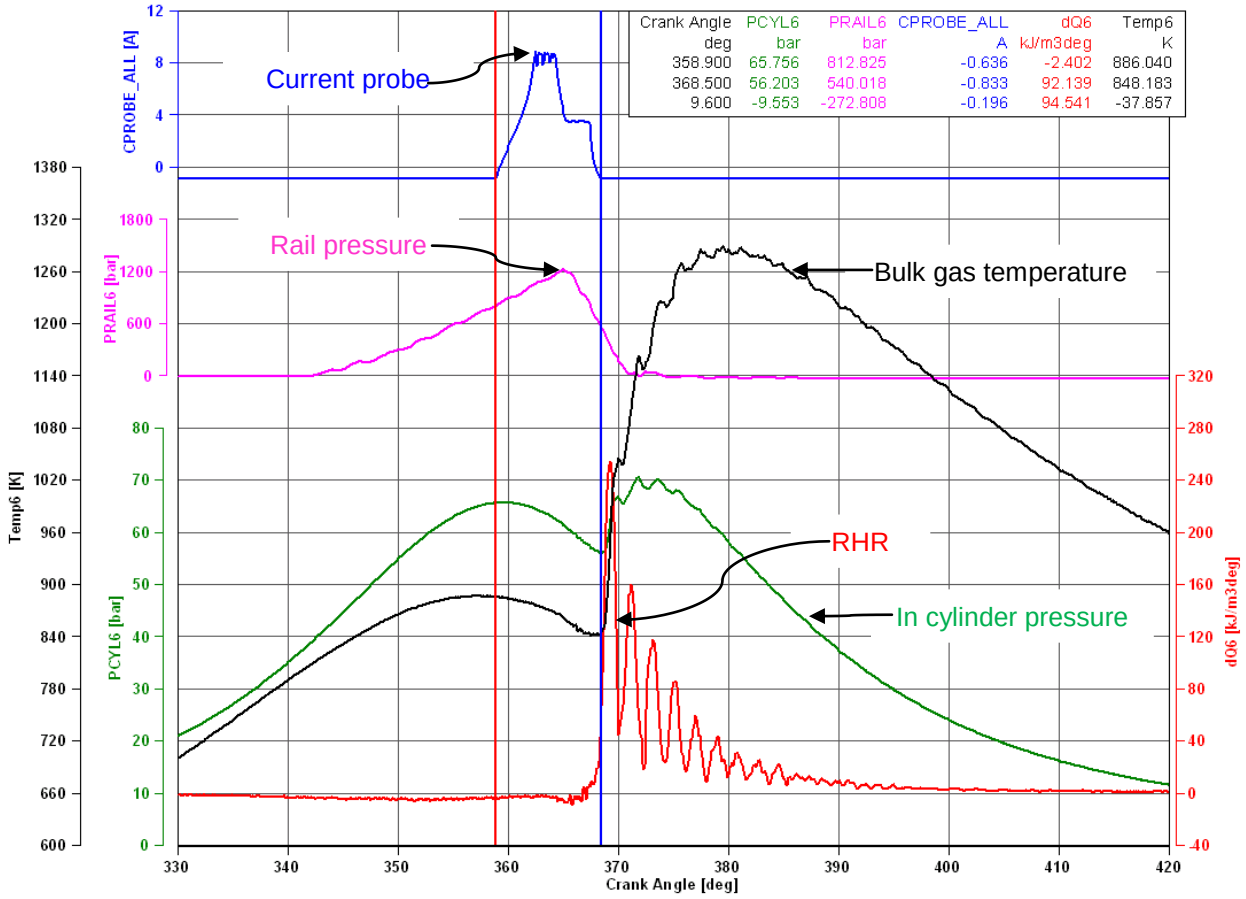

Figure 6.3 (5 bar) data point with ULSD (without EGR)

www.manaraa.com

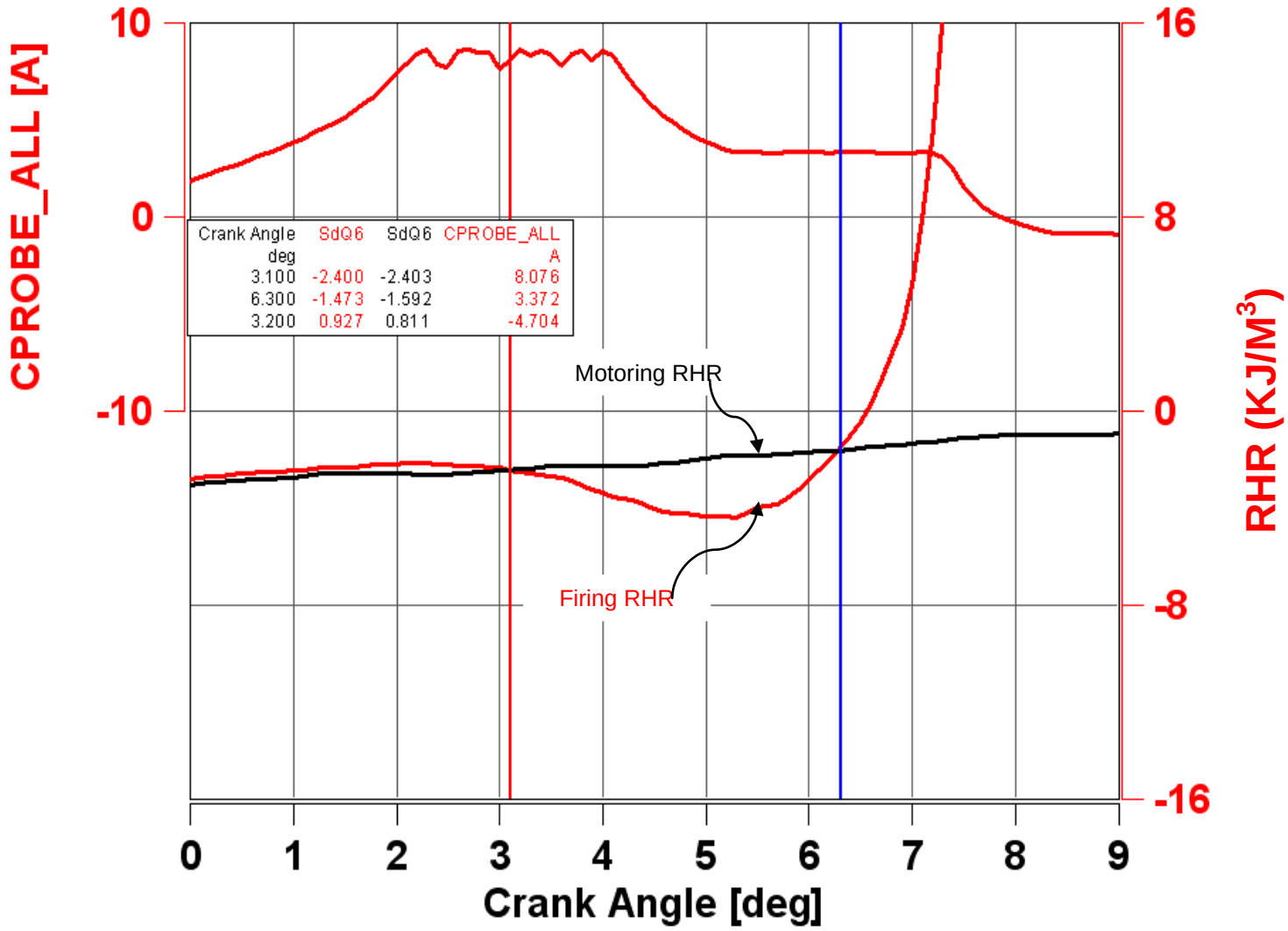

Figure 6.4 Exploded view of Apparent RHR for ULSD (without EGR)

www.manaraa.com

6.1.2. Effect of alternative fuels on in-cylinder combustion:

The engine was also run at 5 bar IMEP with S8, JP8 and B20. Figure 6.5 shows the run made with JP8 (with EGR) at 5 bar IMEP. Table 6.3 illustrates the few critical parameters at this running point.

Running point	Throttle valve opening	LPPC	RHR peak	Peak compression pressure	Peak combustion pressure	Fuel Consumption	Exhaust gas temperature
JP8 (With EGR)	48%	12.9^0 ATDC.	233 KJ/m^3	56bars	58 bars	7.6 kg/hr	301 ^{0} C

Table 6.3 Critical parameters with JP8 (with EGR) at 5 bar IMEP.

As the heating value on volumetric basis of JP8 is slightly lower than ULSD, the throttle is increased to 48%. As the bulk modulus is less than ULSD, the peak of the rail pressure is slightly less than ULSD. The peak of rail pressure is 1069 bars (instead of 1130 bars) and its location is 5.6° ATDC. However, in order to maintain the same injection pressure, the rail pressure starts building up 5 CAD earlier than ULSD due to a lower value of bulk modulus as compared to ULSD. Due to a lower cetane number, there is a longer ignition delay and there is a larger fraction of premixed combustion which increases the value of the rate of heat release. The ignition delay for JP8 (with EGR) is 3.9°. Due to longer ignition delay, the combustion gets retarded. The maximum in-cylinder bulk gas temperature is 1316 K and its location is 21.1° ATDC.In order to optimize the system closer to ULSD running conditions, the injection of the fuel could be advanced so that the LPPC shifts closer to the TDC.

www.manaraa.com

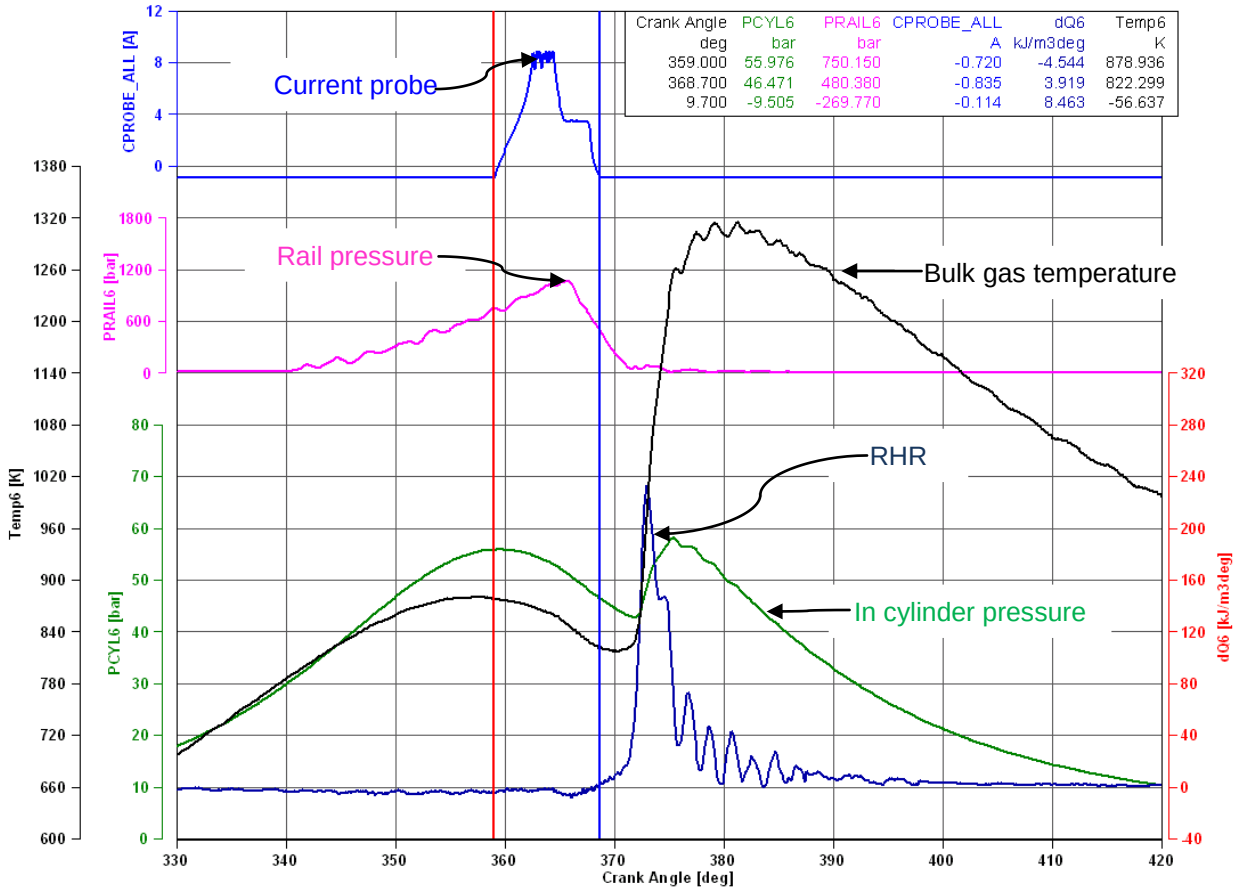

Figure 6.5 (5 bar) data point with JP8 (with EGR)

Figure 6.6 shows the exploded view of apparent RHR of the run made with JP8 (with EGR) at 5 bar IMEP.

www.manaraa.com

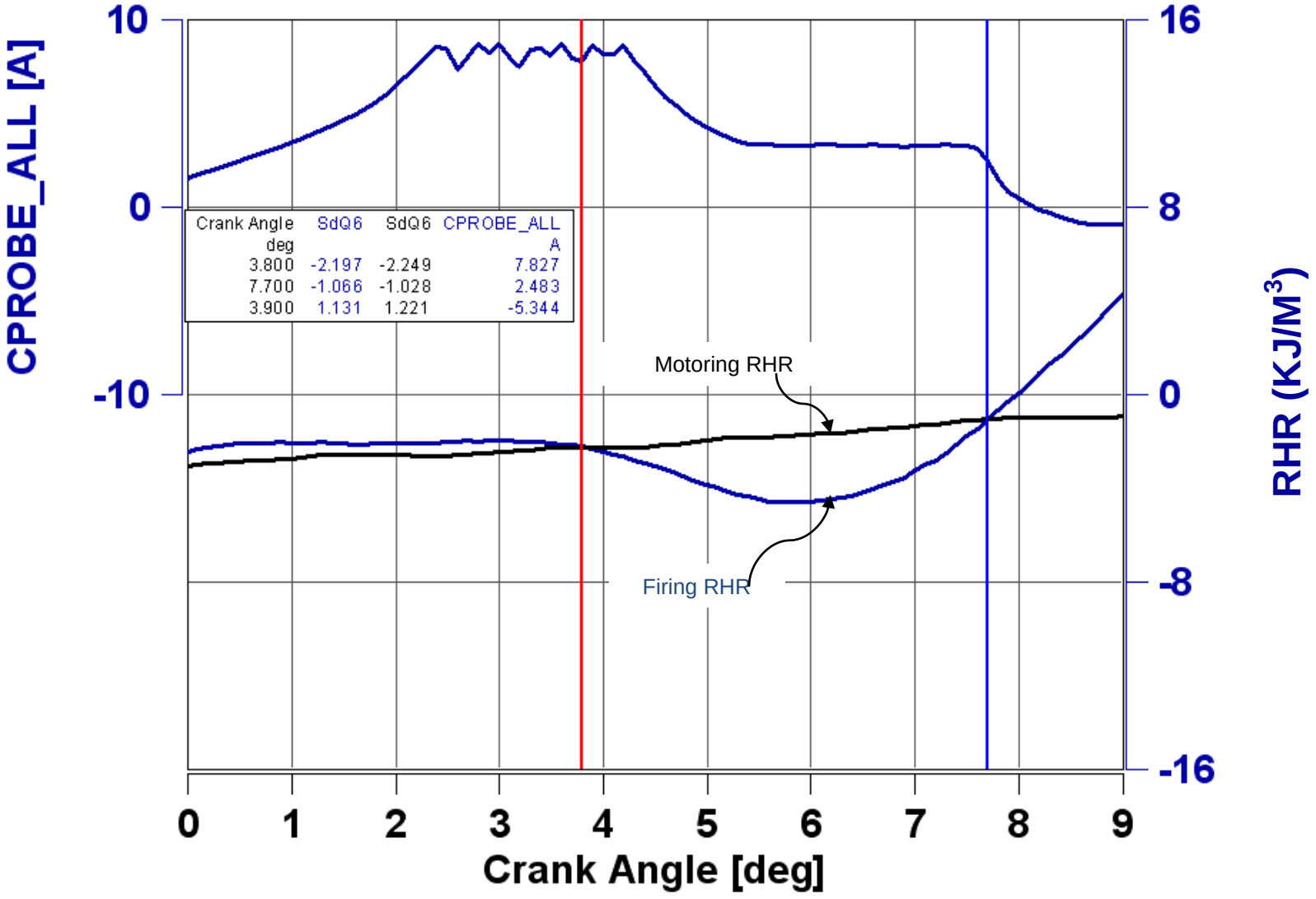

Figure 6.6 Exploded view of Apparent RHR for JP8 (withEGR)

www.manaraa.com

Figure 6.7 shows the run made with JP8 (without EGR) at 5 bar IMEP. Table 6.4 illustrates the few critical parameters at this running point.

Running point	Throttle valve opening	LPPC	RHR peak	Peak compression pressure	Peak combustion pressure	Fuel Consumption	Exhaust gas temperature
JP8 (Without EGR)	49%	10^0 ATDC.	251 KJ/m^3	65bars	69 bars	8.0 kg/hr	278 ^{0} C

Table 6.4 Critical parameters with JP8 (without EGR) at 5 bar IMEP.

As expected, a higher peak compression pressure and a higher combustion pressure (compared to JP8 with EGR) are obtained. Figure 6.8 shows the exploded view of RHR for JP8 (without EGR) at 5 bar IMEP. The maximum in-cylinder bulk gas temperature is 1239 K and its location is 18.5° ATDC. The ignition delay in this case is 3.6°.

However, as mentioned earlier, the injection timing is not optimized for these conditions.

www.manaraa.com

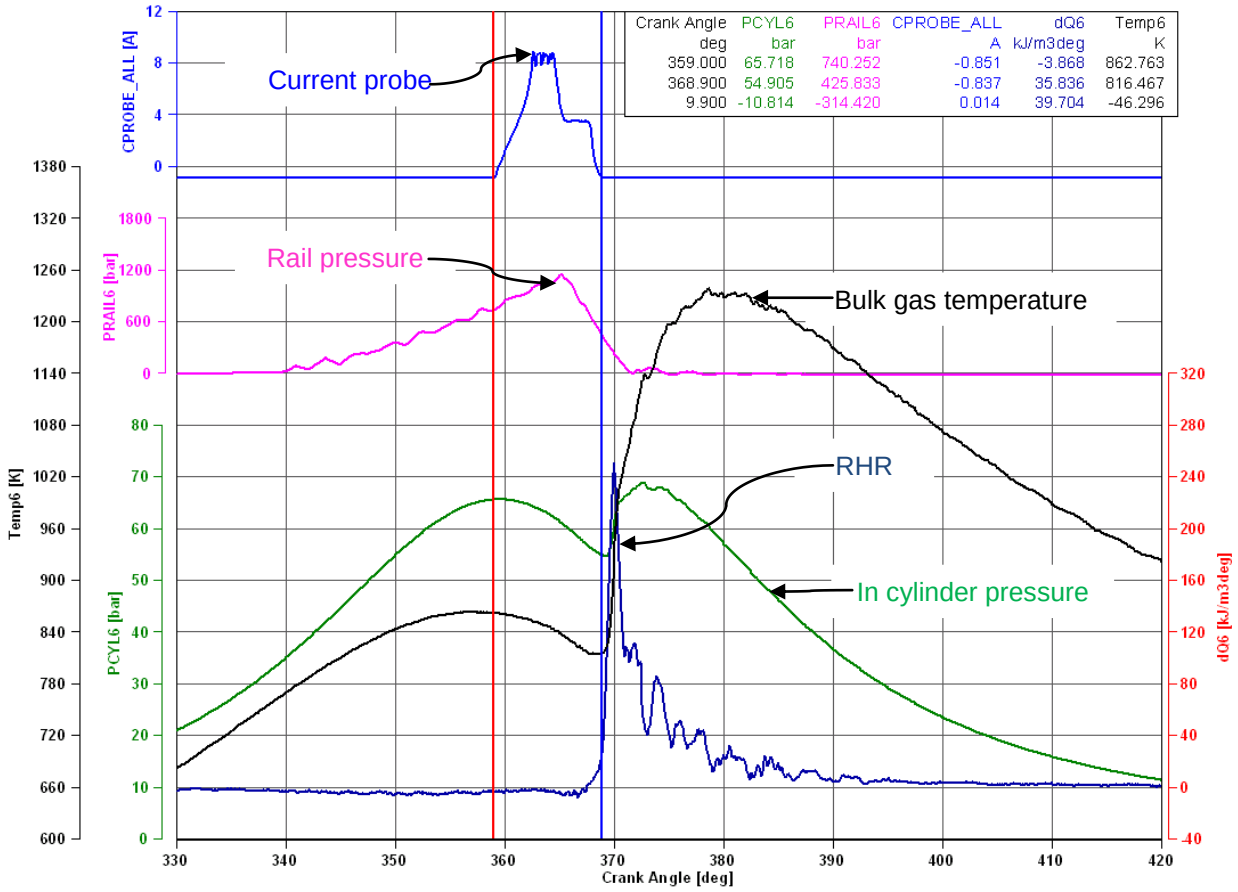

Figure 6.7 (5 bar) data point with JP8 (without EGR)

www.manaraa.com

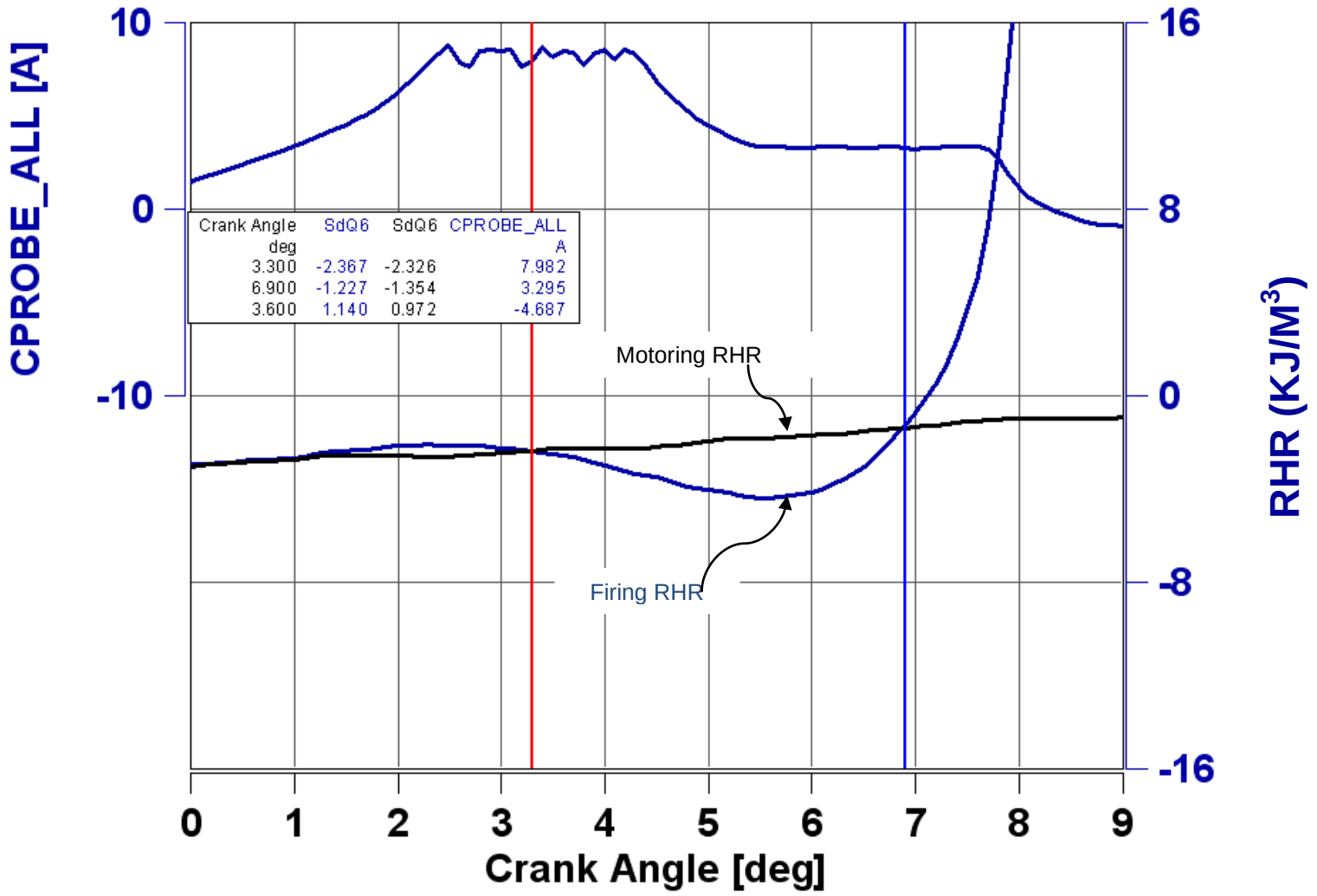

Figure 6.8 Exploded view of Apparent RHR for JP8 (without EGR)

www.manaraa.com

Figure 6.9 shows the run made with B20 (with EGR) at 5 bar IMEP. Table 6.5 illustrates the few critical parameters at this running point.

Running point	Throttle valve opening	LPPC	RHR peak	Peak compression pressure	Peak combustion pressure	Fuel consumption	Exhaust gas temperature
B20 (With EGR)	44%	10.7^{0} ATDC.	200 KJ/m^3	56bars	60 bars	7.8 kg/hr	307 ^{0} C

Table 6.5 Critical parameters with B20 (with EGR) at 5 bar IMEP.

As the heating value of the fuel on volumetric basis is almost the same, the throttle opening is the same as of ULSD (44%). As the bulk modulus of B20 is pretty close to ULSD, therefore, the peak of rail pressure is 1119 bars (instead of 1130 bars) and its location is same as of ULSD 4.8° ATDC. Due to higher cetane number, the ignition delay is shorter, which limits the peak of premixed combustion to a relatively lower value as compared to ULSD. Also, due to higher cetane number, the LPPC gets advanced with respect to crank angle degree. Figure 6.10 shows the exploded view of RHR for B20 (with EGR) at 5 bar IMEP. The maximum in-cylinder bulk gas temperature is 1246 K and its location is 21.4° ATDC.

The ignition delay for B20 (with EGR) is 3.2°. In order to optimize the system closer to ULSD running conditions, the injection of the fuel could be retarded.

www.manaraa.com

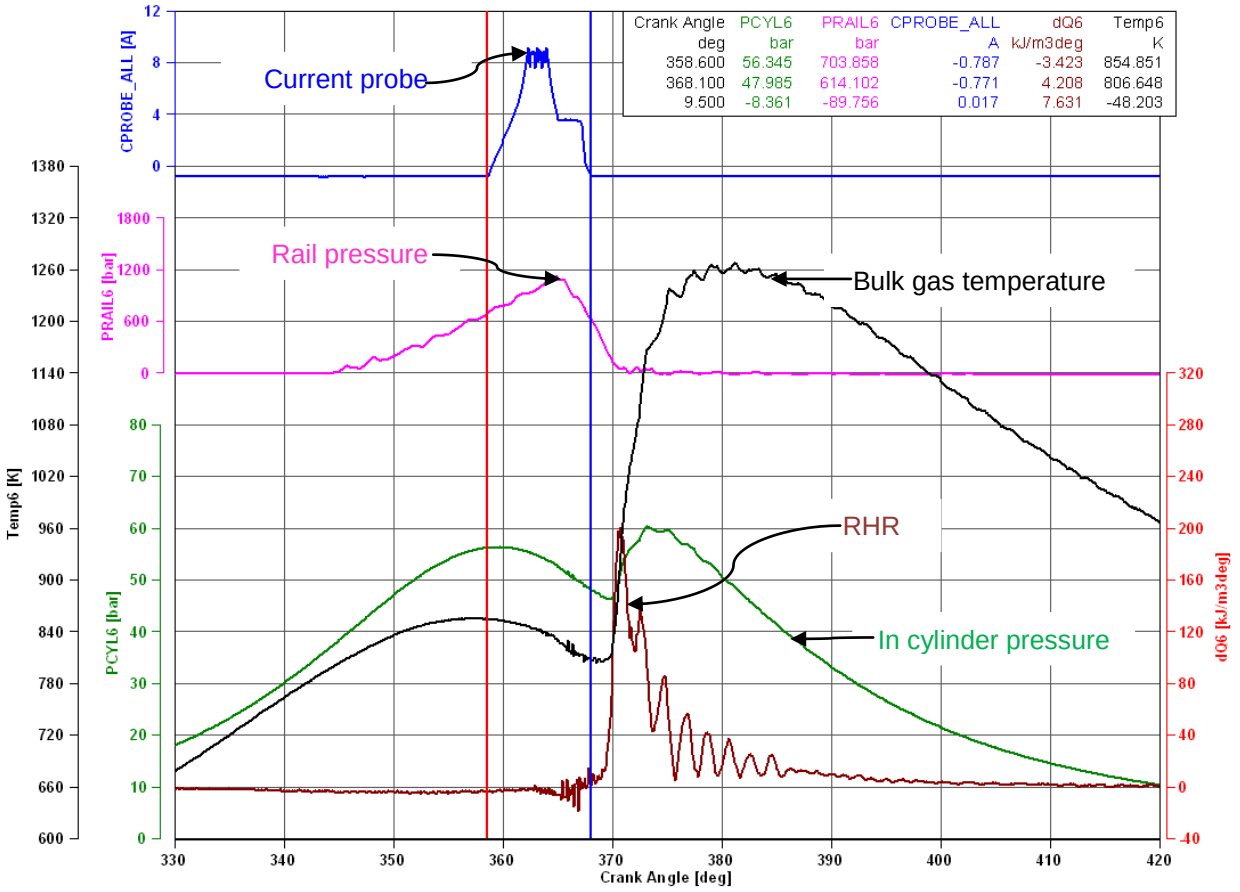

Figure 6.9 (5 bar) data point with B20 (with EGR)

www.manaraa.com

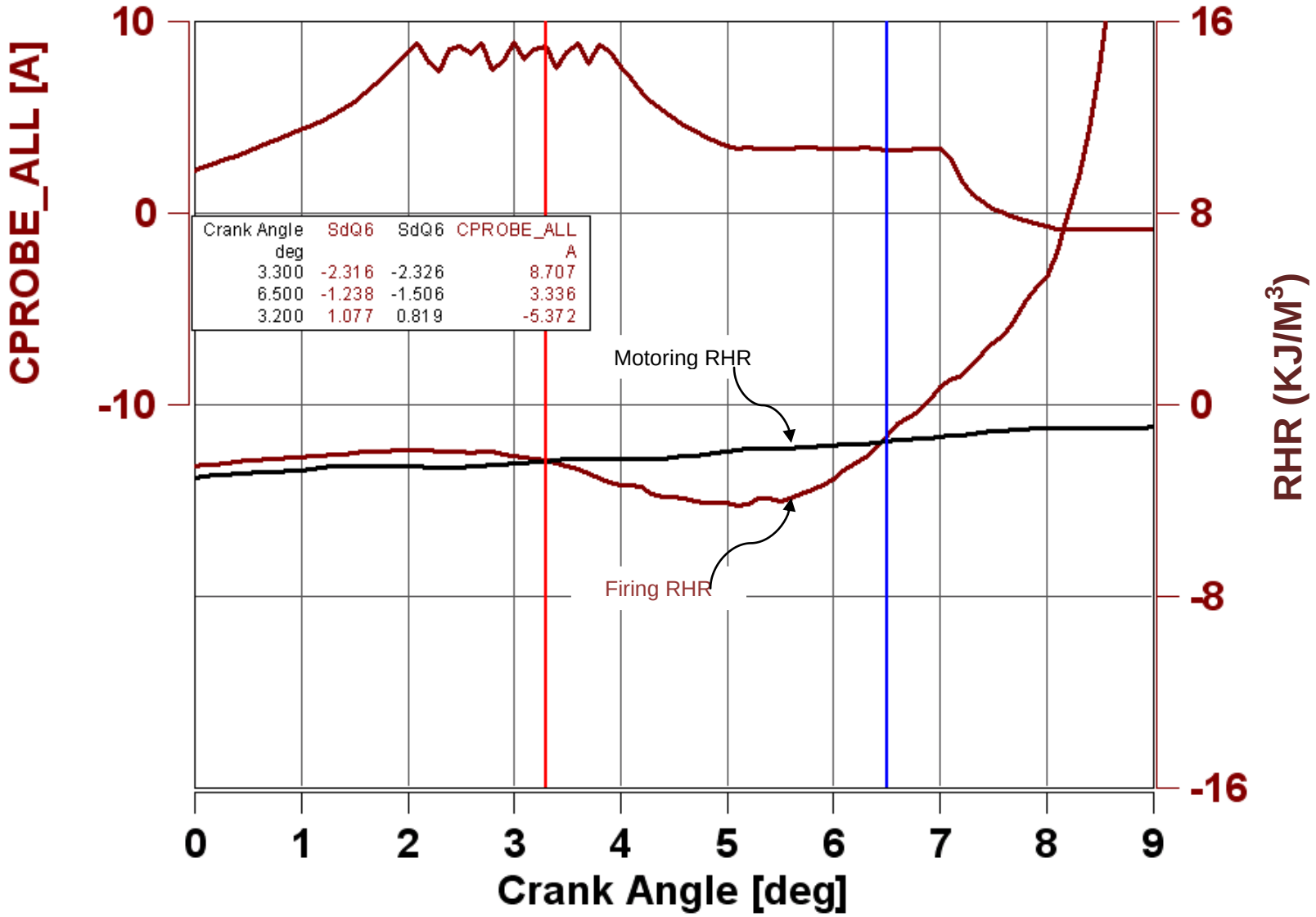

Figure 6.10 Exploded view of Apparent RHR for B20 (with EGR)

www.manaraa.com

Figure 6.11 shows the same running point (without EGR). Table 6.6 illustrates the few critical parameters at this running point.

Running point	Throttle valve opening	LPPC	RHR peak	Peak compression pressure	Peak combustion pressure	Fuel Consumption	Exhaust gas temperature
B20 (Without EGR)	46%	8.6^0 ATDC.	194 KJ/m^3	67bars	70 bars	8.3 kg/hr	283 ^{0} C

Table 6.6 Critical parameters with B20 (without EGR) at 5 bar IMEP.

As expected, a higher peak compression pressure and a higher combustion pressure (compared to B20 with EGR) are achieved. The exploded view of apparent RHR is shown in figure 6.12. The ignition delay is 3.0 CAD. The maximum in-cylinder bulk gas temperature is 1231 K and its location is 20.6° ATDC.

However, as mentioned earlier, the injection timing is not optimized for these conditions.

www.manaraa.com

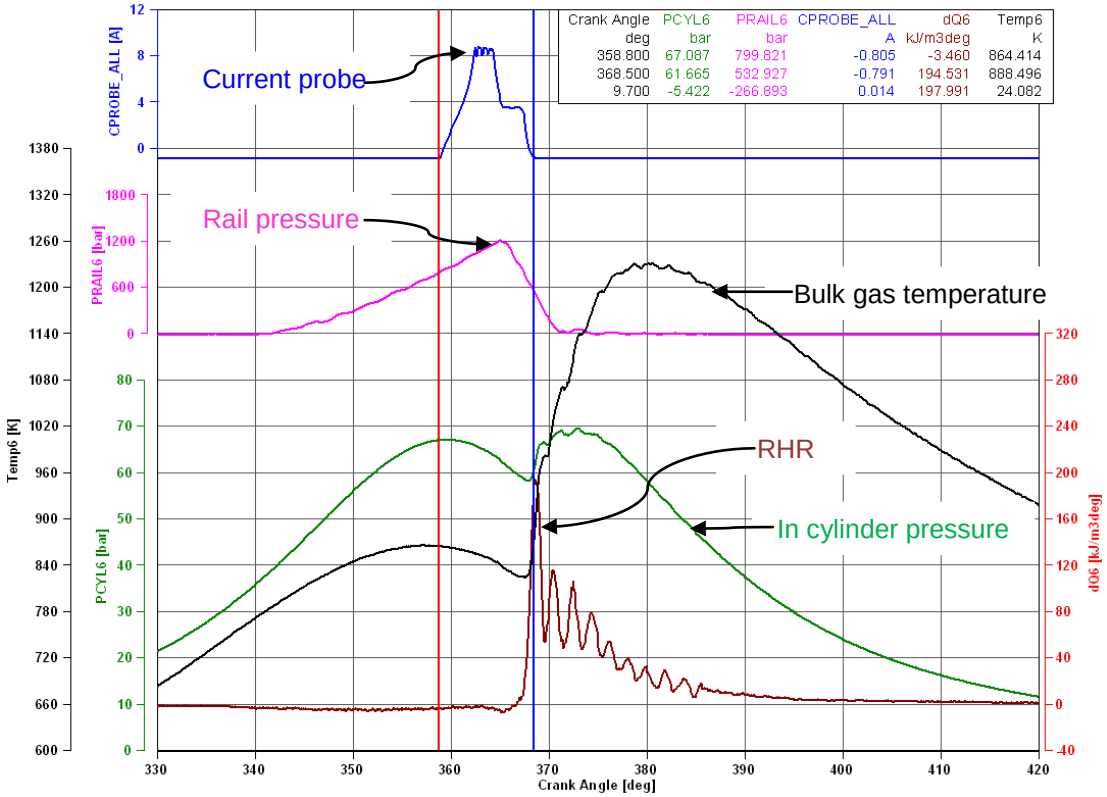

Figure 6.11 (5 bar) data point with B20 (without EGR)

www.manaraa.com

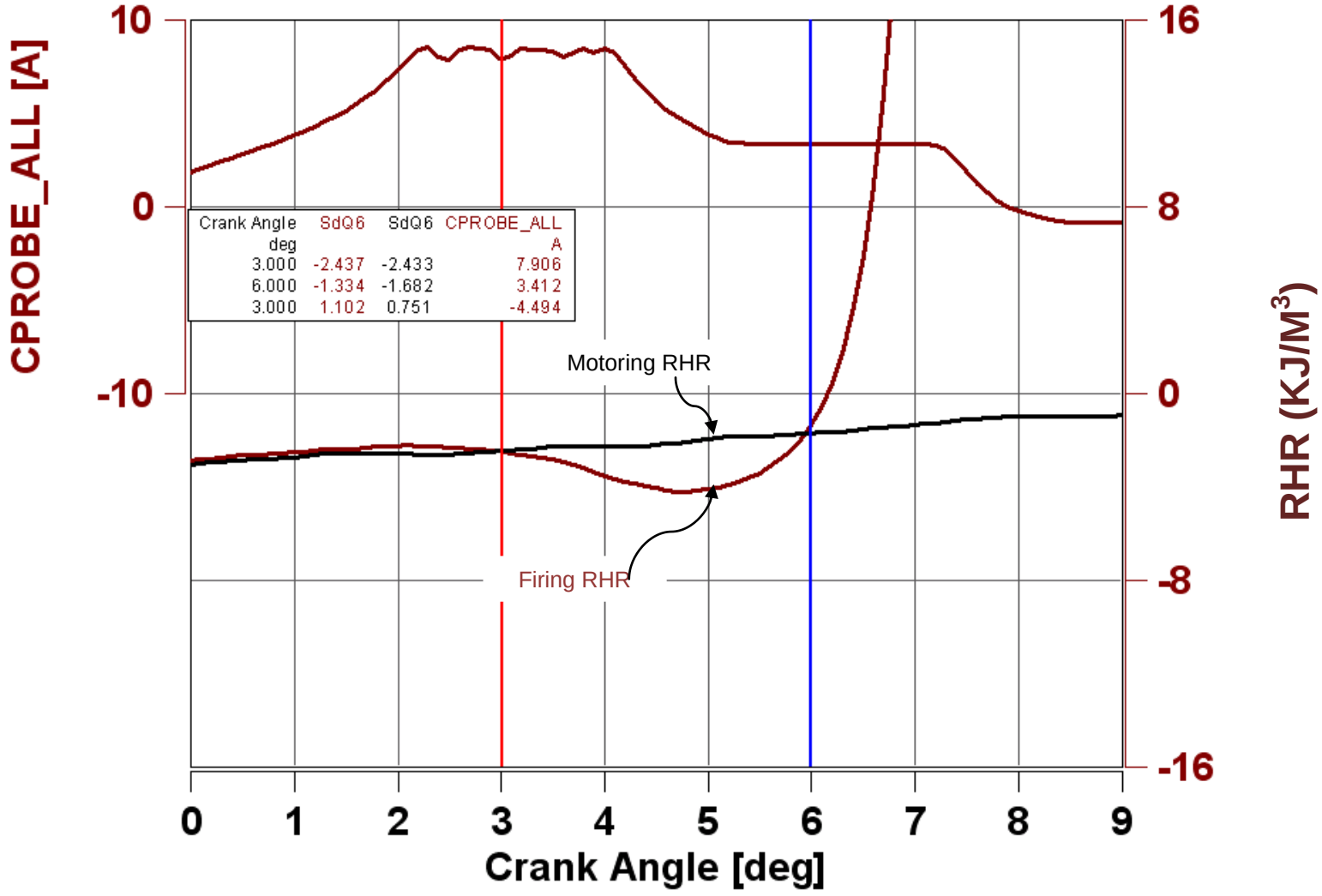

Figure 6.12 Exploded view of Apparent RHR for B20 (without EGR)

www.manaraa.com

Figure 6.13 shows the run made with S8 (with EGR) at 5 bar IMEP. Table 6.7 illustrates the few critical parameters at this running point.

Running point	Throttle valve opening	LPPC	RHR peak	Peak compression pressure	Peak combustion pressure	Fuel Consumption	Exhaust gas temperature
S8 (With EGR)	50%	10^0 ATDC.	137 KJ/m^3	56bars	54 bars	7.7kg/hr	300 ^{0} C

Table 6.7 Critical parameters with S8 (with EGR) at 5 bar IMEP.

As the heating value on volumetric basis of S8 is lower than ULSD, therefore the throttle is increased to 50%. As the bulk modulus of S8 is less than ULSD, the peak of the rail pressure is less than ULSD. The peak of rail pressure is 1015 bars (instead of 1130 bars) and its location is 5.3° ATDC. However to maintain the same fuel injection pressure, the rail pressure starts building up 5 CAD earlier than ULSD Higher cetane number of S8 ensures better and faster combustion and shortens ignition delay. The LPPC is advanced with respect to crank angle degree and its location is 10° ATDC. The combustion in this case is similar to constant pressure with a long expansion stroke. The maximum in-cylinder bulk gas temperature is 1246 K and its location is 21.4° ATDC. In order to optimize the system closer to ULSD running conditions, the injection of the fuel could be retarded.

www.manaraa.com

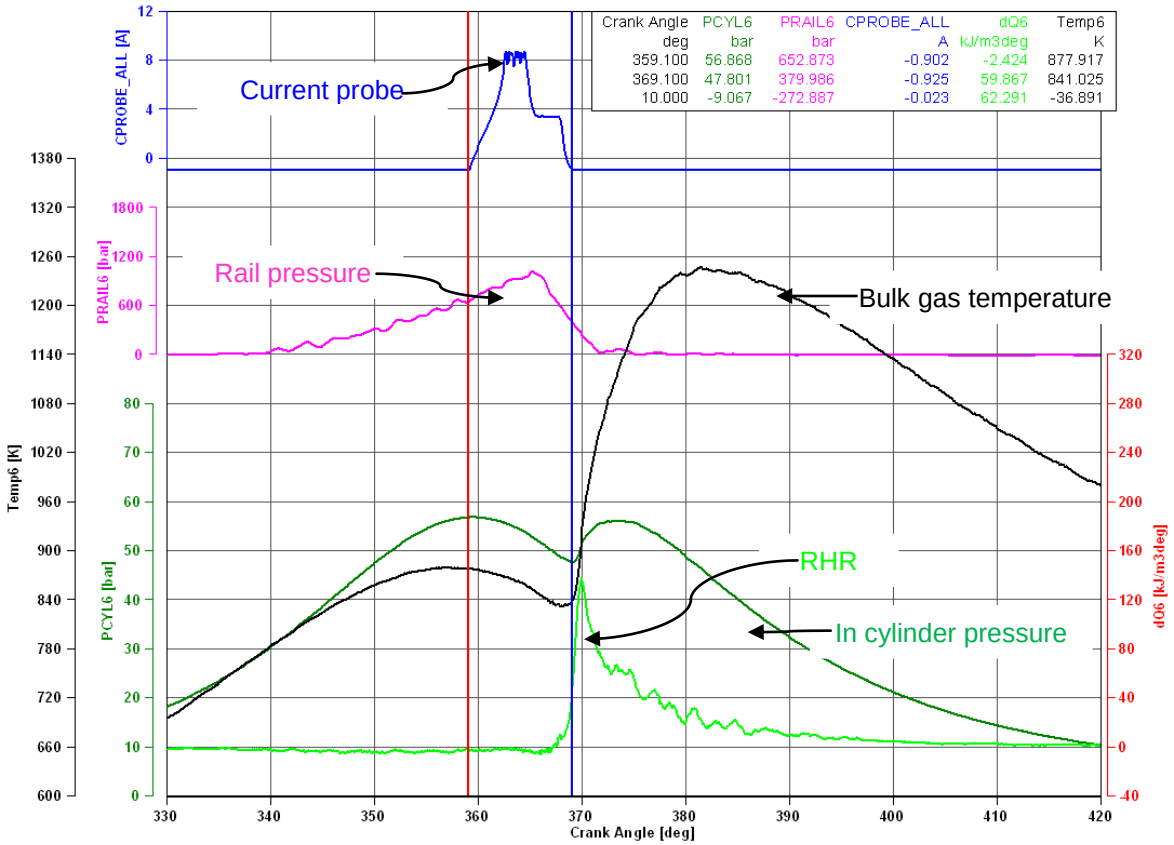

Figure 6.13 (5 bar) data point with S8 (with EGR)

Figure 6.14 shows the exploded view of RHR of the run made with S8 (with EGR) at 5 bar IMEP. The ignition delay is 2.6 CAD.

www.manaraa.com

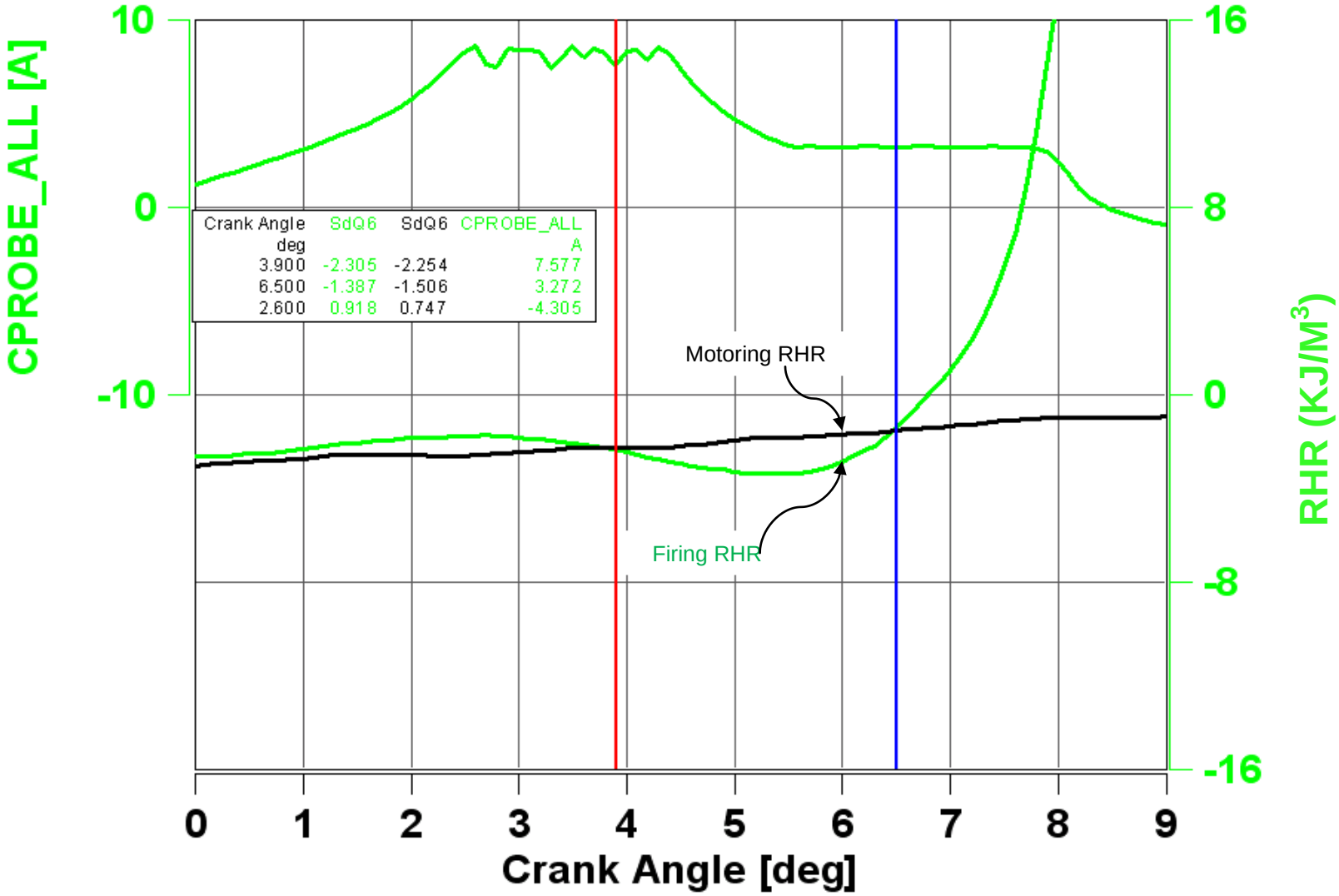

Figure 6.14 Exploded view of Apparent RHR for S8 (withEGR)

www.manaraa.com

6.1.3. Effect of fuel cetane number on ignition delay:

The cetane number of the fuel also has a great impact on the ignition delay. Higher the cetane number of the fuel, the shorter is the ignition delay. Figure 6.15 shows the impact of volatility and of cetane number on the ignition delay of the respective fuel. From this experimental result, it is quite clear that S8 has the shortest ignition delay, followed by B20, followed by ULSD, and then by JP8.

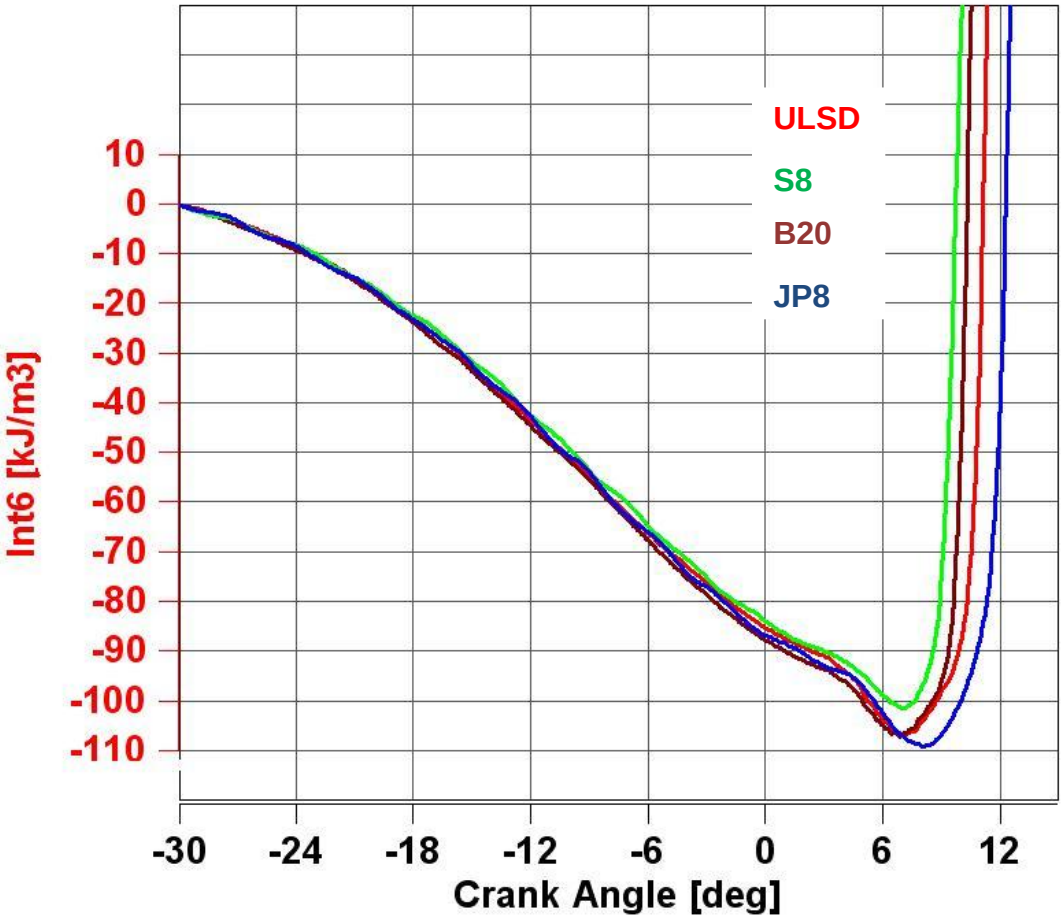

Figure 6.15 Effect of cetane number on the ignition delay

www.manaraa.com

6.2 Emissions at 5 bar IMEP

This investigation involves the effect of alternative fuels and the effect of EGR on emissions. The emissions were recorded before and after the aftertreatment device. The emissions obtained using ULSD are set as a benchmark and all the emissions using alternative fuels are compared with ULSD emissions.

6.2.1. Emissions using ULSD:

The effect of ULSD on the emissions at 5 BAR IMEP (with EGR) is illustrated in figure 6.2.1.

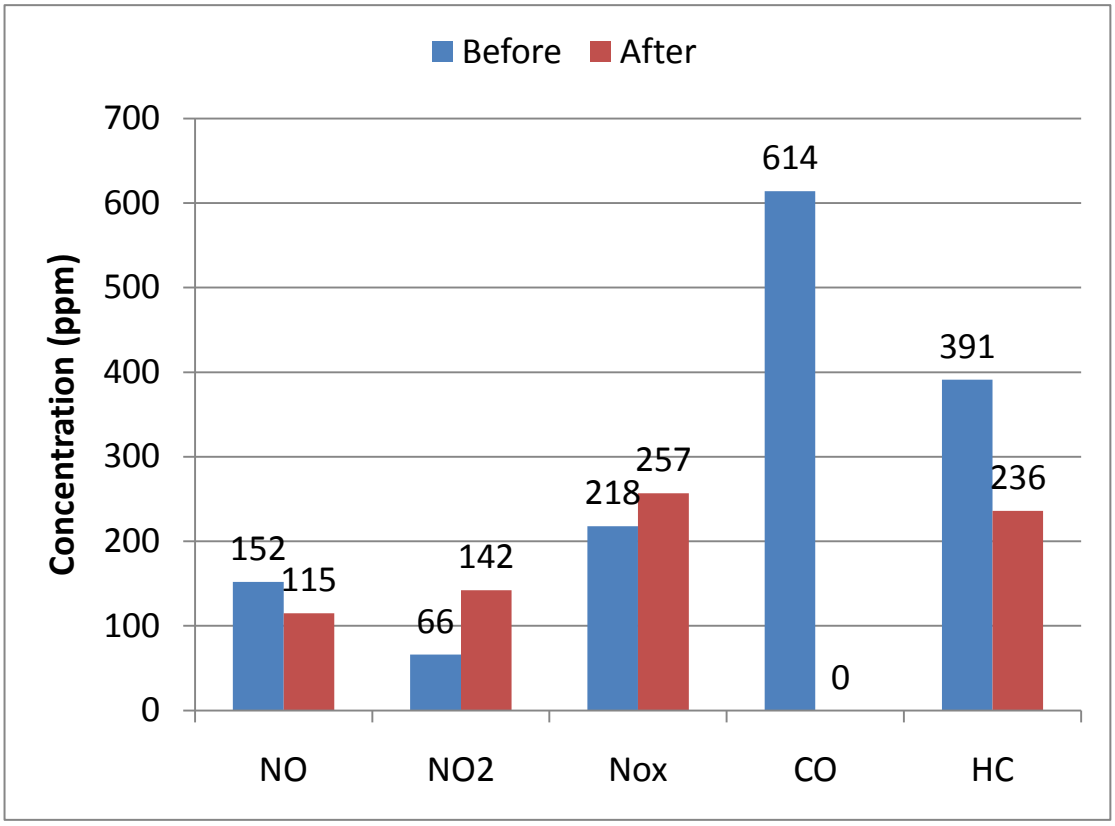

Figure 6.2.1 ULSD emissions at 5 BAR IMEP with EGR

www.manaraa.com

It is very clear from the experimental result that D.O.C. is very effective in reducing the CO emissions, but not that effective in reducing HC emissions. The D.O.C. is almost 100% efficient in reducing the CO emissions and only 40% for HC emissions. There could be two causes for this trend:

1. First is that the CO oxidation is better over the catalyst due to better adsorption of the CO on the active catalyst sites.
2. Second, FTIR may not be the best instrument for measuring HC emissions. The FTIR only measures the hydrocarbons with confidence up to four carbon atoms, and there may be higher/heavier components in the exhaust. Therefore, the measurement reading obtained from this instrument cannot be ascertained with a good confidence level.

Also, 85 to 95% of the NO_X emitted by diesel engine is NO. The D.O.C. converts part of the NO emissions to NO_2. Due to this reason NO_X emissions actually increase after the aftertreatment device.

Figure 6.2.2 illustrates the soot concentration emissions using ULSD at 5 BAR IMEP.

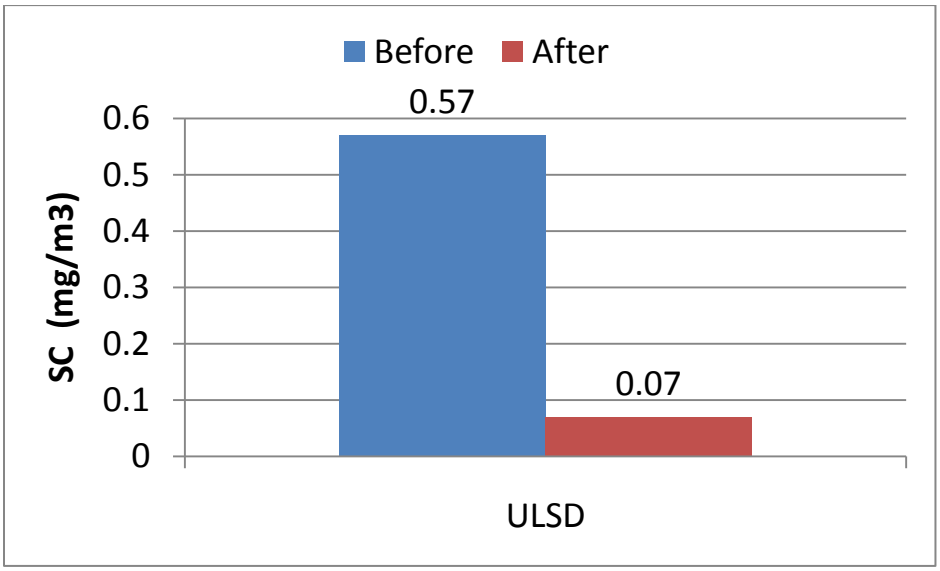

Figure 6.2.2 Soot concentration with ULSD at 5 BAR IMEP (with EGR)

www.manaraa.com

It is quite clear from the experimental results that the D.P.F. is very efficient in reducing the soot emissions. The efficiency of D.P.F. in reducing the soot emissions is about 99%.

The ULSD emissions without EGR at 5 BAR IMEP are illustrated in figure 6.2.3.

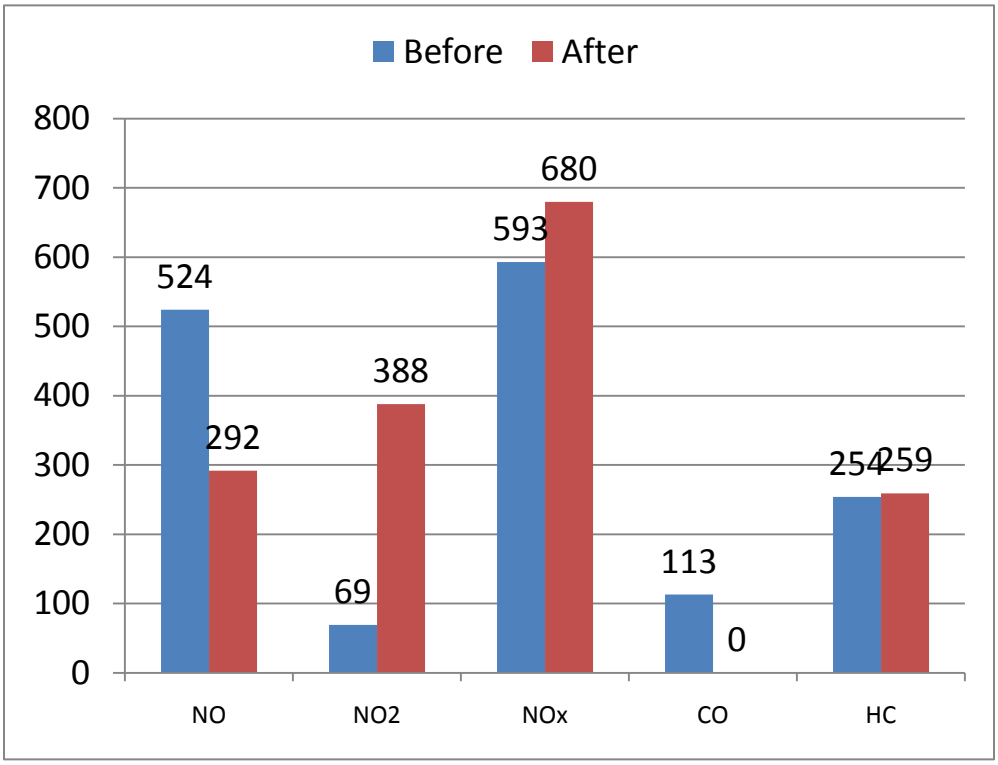

Figure 6.2.3 ULSD emissions at 5 BAR IMEP without EGR

In this case, the efficiency of the D.O.C. in reducing CO emissions is also close to 100%. As, the FTIR may not be the best instrument for measuring HC emissions, therefore the confidence level of the results obtained cannot be ascertained. D.O.C. is also effective in converting the NO to NO_2.

www.manaraa.com

Figure 6.2.4 illustrates the soot concentration emissions with ULSD (without EGR).

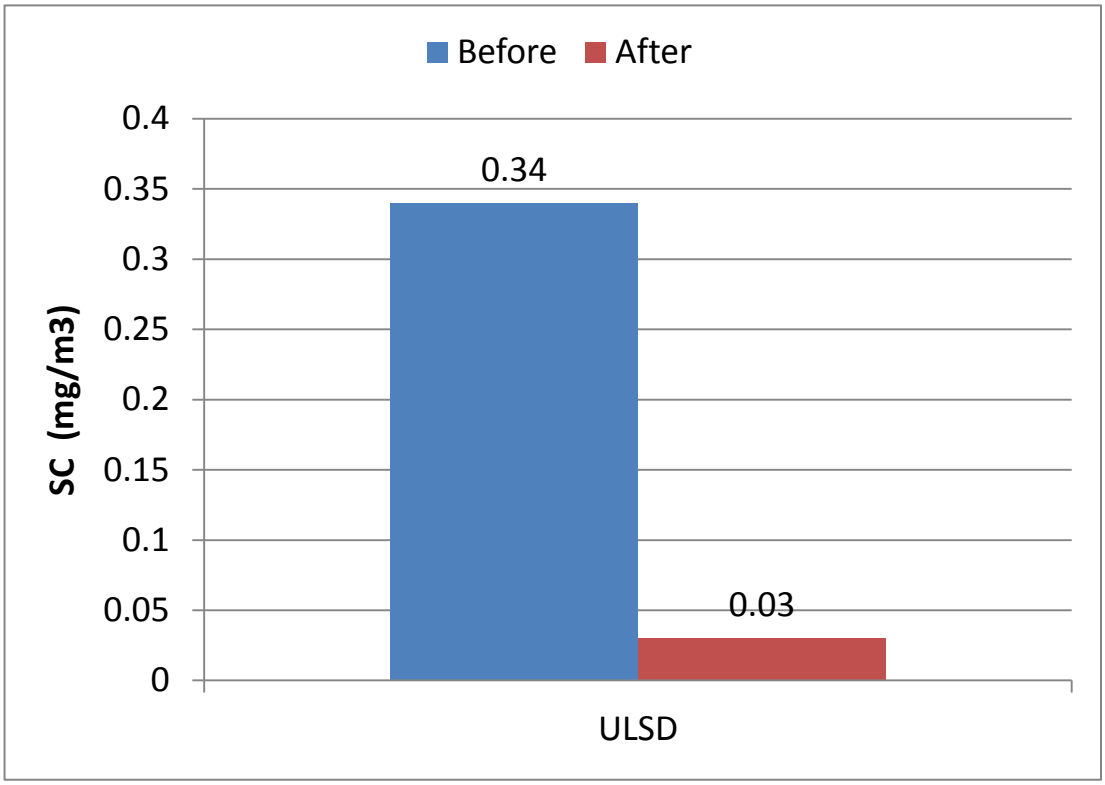

Figure 6.2.4 Soot concentration with ULSD at 5 BAR IMEP (without EGR)

Without EGR, combustion process is much more complete. Therefore, the mass fraction burned by pre mixed combustion of the two combustion fractions is increased and there is a considerable reduction in soot concentration. It is quite clear from the experimental results that the D.P.F. is very efficient in reducing the soot emissions. The efficiency of D.P.F. in reducing the soot emissions is about 91%.

6.2.1.1. Effect of EGR on ULSD emissions at 5 BAR IMEP:

With EGR, lesser amount of air goes into the cylinder and EGR also increases the specific heat of the charge inside the cylinder. Thus, it increases the ignition delay, reduces the in-cylinder temperature and the combustion is less complete. However, it is a very effective way

www.manaraa.com

to reduce the NO_X emissions. Here, only the engines out emissions (before the aftertreatment device) are considered.

6.2.1.1.1. Effect of EGR on engine out emissions:

The effect of EGR on engine out emissions is illustrated in figure 6.2.5.

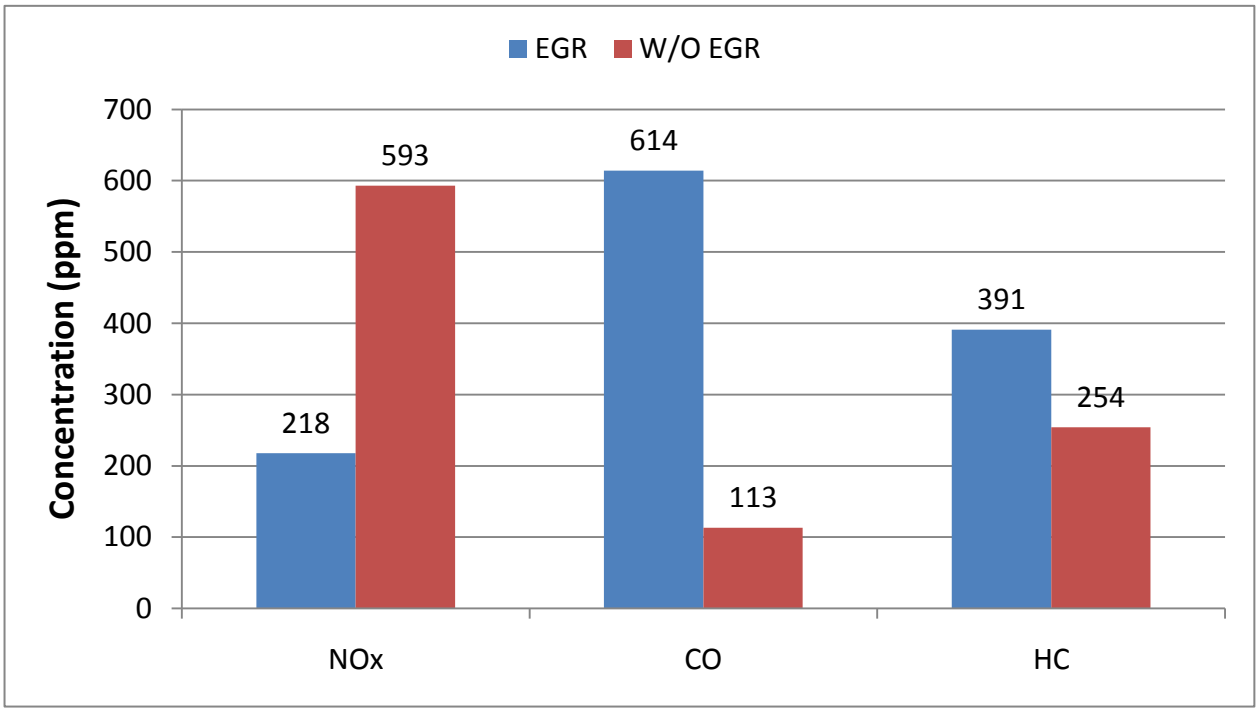

Figure 6.2.5 Effect of EGR on engine out emissions at 5 BAR IMEP (ULSD).

EGR lowers the peak of the pre-mixed combustion fraction which in return lowers the in-cylinder bulk gas temperatures. Because NOx formation is much faster at higher temperature range, EGR actually reduces the amount of NO_X generated by the combustion in the cylinder. The EGR reduces the NO_X emissions by about 63%.

It can be seen from the experimental result that EGR basically increases the CO emissions. EGR basically recycles some of the exhaust gases in the cylinder and therefore it

www.manaraa.com

displaces some amount of air. Therefore, EGR leads to incomplete combustion. It can be seen from the experimental result that EGR basically increases also the HC emissions.

6.2.1.1.2. Effect of EGR on particulate concentration:

The effect of EGR on particulate concentration is shown in figure 6.2.6.

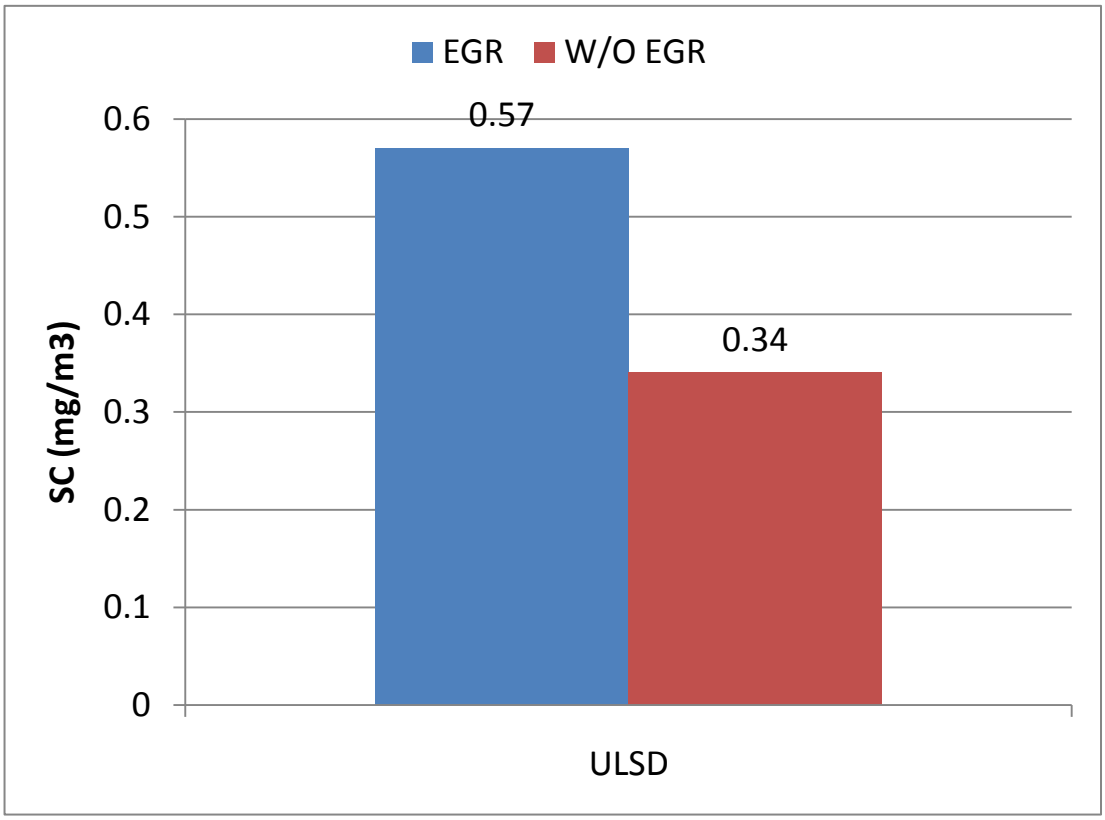

Figure 6.2.6 Effect of EGR on Particulate concentration (ULSD)

EGR basically increases the inert gas concentration inside the cylinder. Thus the in cylinder combustion is less complete and it produces more soot. As evident from the experimental results, EGR increases the soot concentration by about 67%.

www.manaraa.com

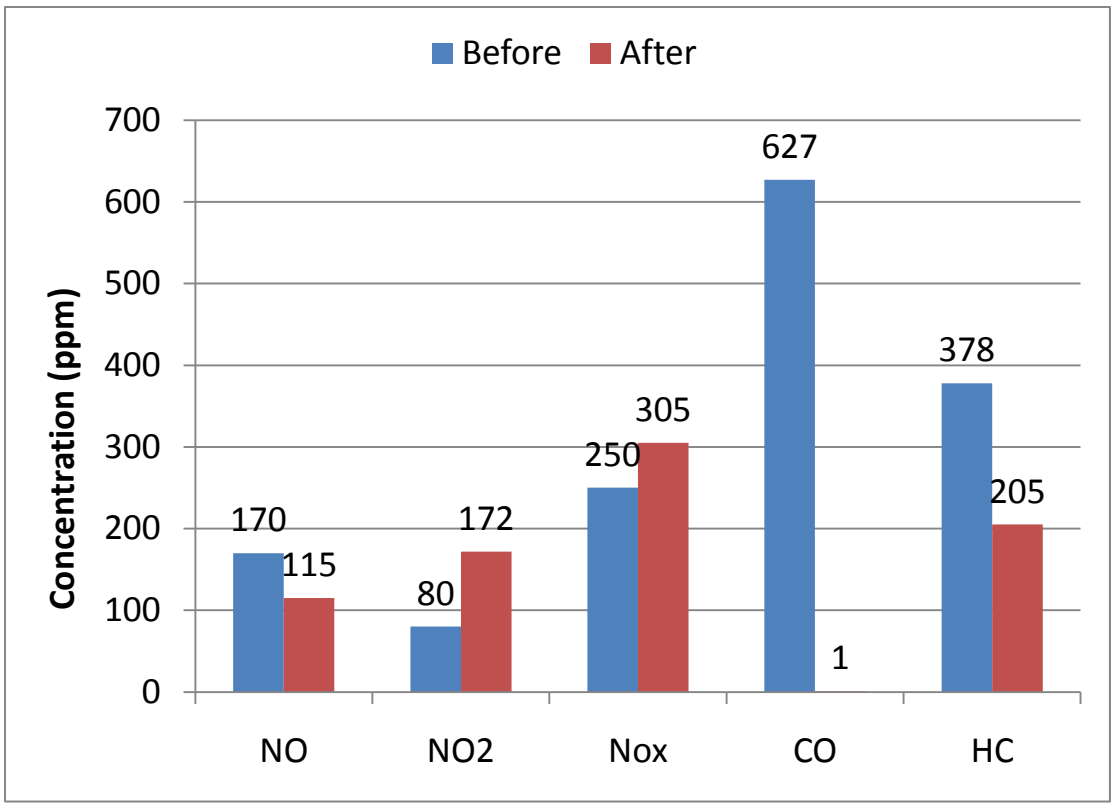

Figure 6.2.7 JP8 emissions with at 5 BAR IMEP with EGR

6.2.2 Emissions using JP8:

The engine was run using JP8 at 5 BAR IMEP to investigate the effect of JP8 on the emissions. The effect of ULSD on the emissions at 5 BAR IMEP (with EGR) is illustrated in figure 6.2.7.

The effect of D.O.C. has a similar trend on the emissions as compared to ULSD. The D.O.C. is very effective in reducing the CO emissions and not that effective in reducing HC emissions. Therefore, the D.O.C. has a similar effect in reducing CO and HC emissions as in the case of ULSD.

www.manaraa.com

Since the engine is equipped with a stock E.C.U. (engine control unit), the combustion phasing for different fuels is not the same due to different fuel properties and there is a significant change in the emissions. In order to get the same emissions as in the case of ULSD, the fuel injection in case of JP8 will have to be advanced with respect to crank angle degrees.

Figure 6.2.8 illustrates the soot concentration emissions using JP8 at 5 BAR IMEP.

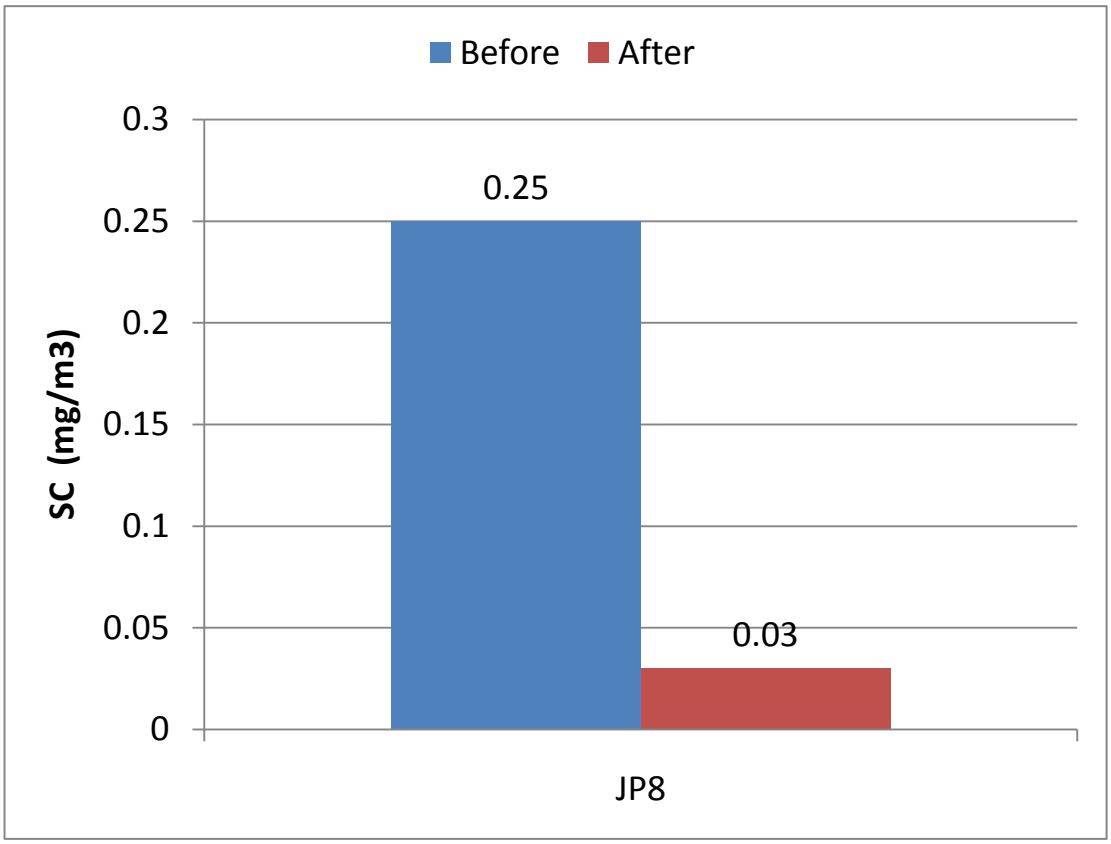

Figure 6.2.8 Soot concentration with JP8 at 5 BAR IMEP (with EGR)

JP8 has a longer ignition delay and the mass fraction burned by premixed combustion as compared to ULSD is also larger in magnitude. Consequently, there is a considerable reduction in soot concentration. Thus, JP8 produces less soot as compared to ULSD at the same running conditions. It is quite clear from the experimental results that the D.P.F. is very efficient in reducing the soot emissions.

www.manaraa.com

The JP8 emissions without EGR at 5 BAR IMEP are illustrated in figure 6.2.9.

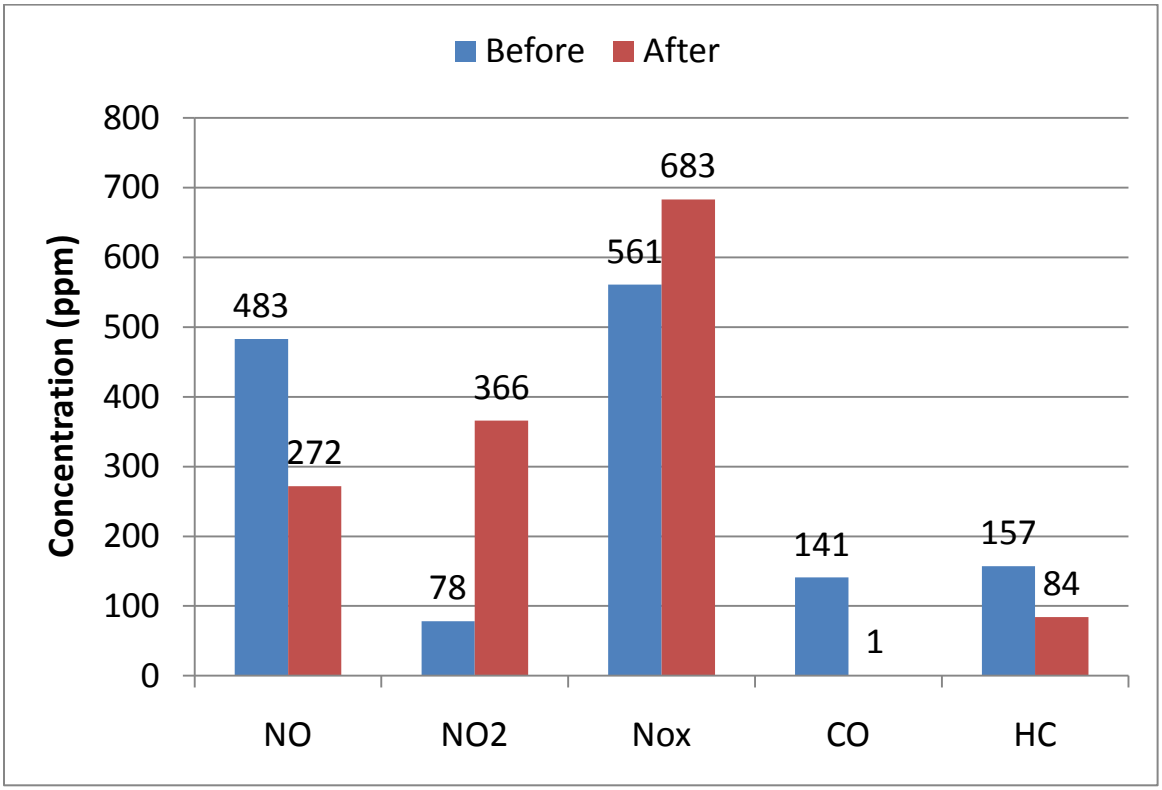

Figure 6.2.9 JP8 emissions at 5 BAR IMEP without EGR

The effect of D.O.C. has a similar trend on the emissions as compared to ULSD. Figure 6.2.10 illustrates the soot concentration emissions with JP8 (without EGR).

www.manaraa.com

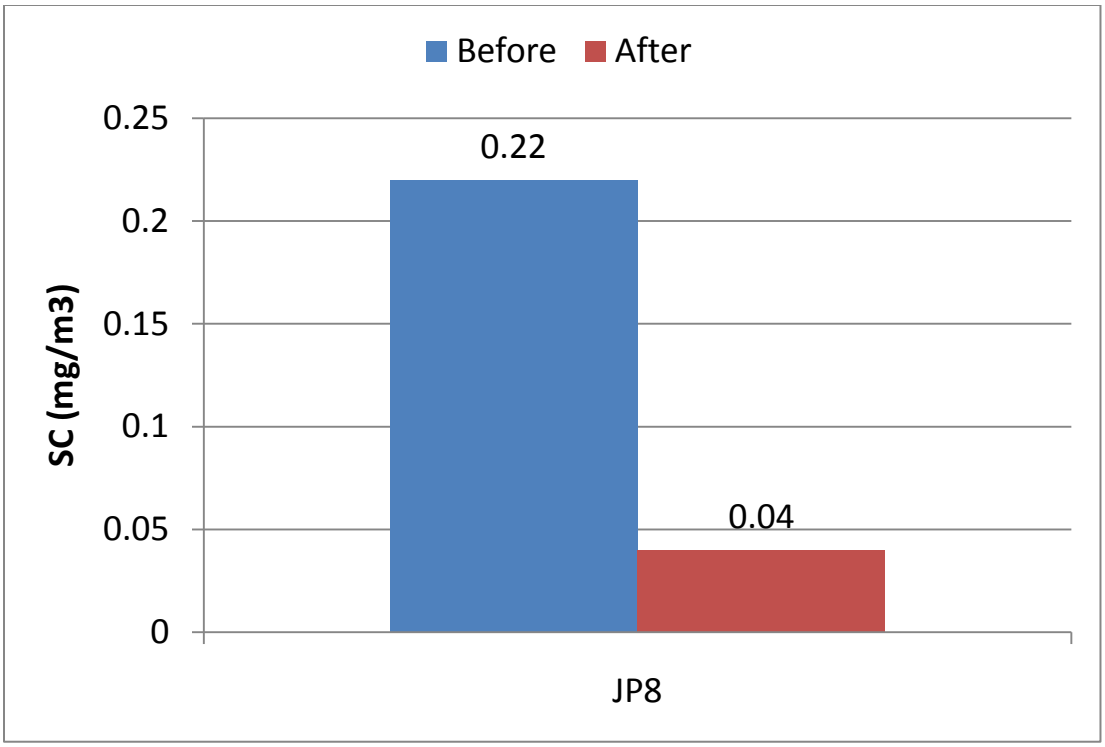

Figure 6.2.10 Soot concentration with JP8 at 5 BAR IMEP (without EGR)

Without EGR, the combustion process is much more complete. Therefore, the mass fraction burned by pre mixed combustion of the two combustion fractions is increased and there is a considerable reduction in soot concentration.

www.manaraa.com

6.2.2.1. Effect of EGR on JP8 emissions at 5 BAR IMEP:

6.2.2.1.1. Effect of EGR on engine out emissions:

The effect of EGR on engine out emissions is illustrated in figure 6.2.11.

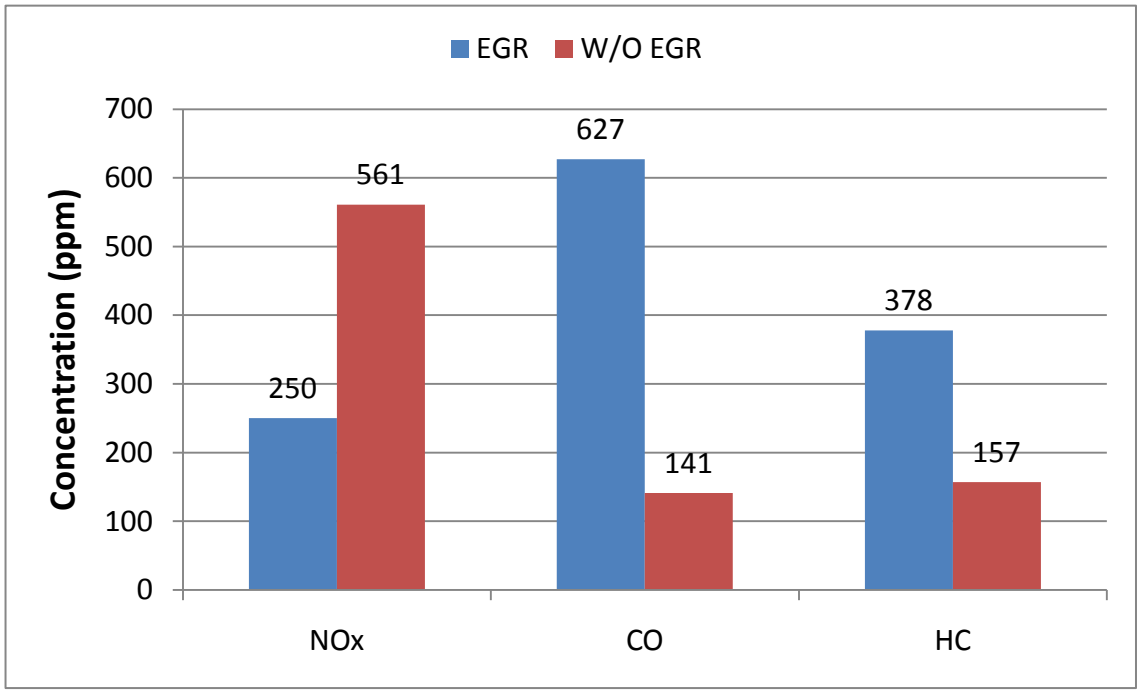

Figure 6.2.11 Effect of EGR on engine out emissions at 5 BAR IMEP (JP8).

The EGR reduces the NO_X emissions by about 55%. The EGR has a similar trend but has a reduced effect on NO_X emissions as in the case of ULSD. As seen from the experimental results, EGR increases the HC emissions by 140%.

www.manaraa.com

6.2.2.1.2. Effect of EGR on particulate concentration:

The effect of EGR on particulate concentration is shown in figure 6.2.12.

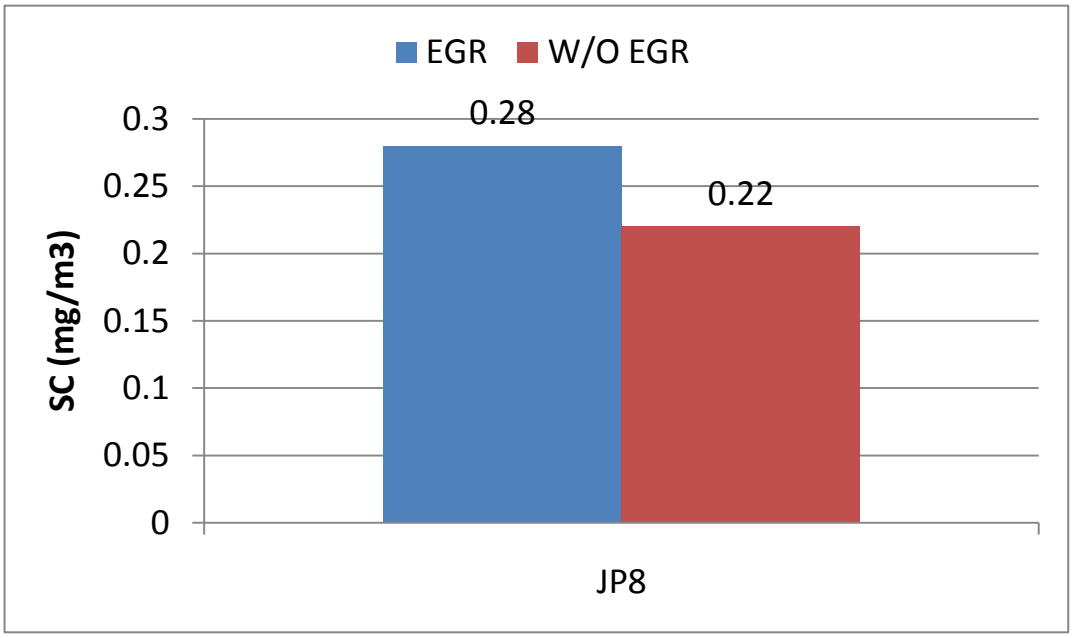

Figure 6.2.12 Effect of EGR on Particulate concentration (JP8)

EGR has a similar effect on JP8 soot concentration emissions as in the case of ULSD. As evident from the experimental results, EGR increases the soot concentration by about 27%.

www.manaraa.com

6.2.3. Emissions using B20:

The effect of B20 on the emissions at 5 BAR IMEP (with EGR) is illustrated in figure 6.2.13.

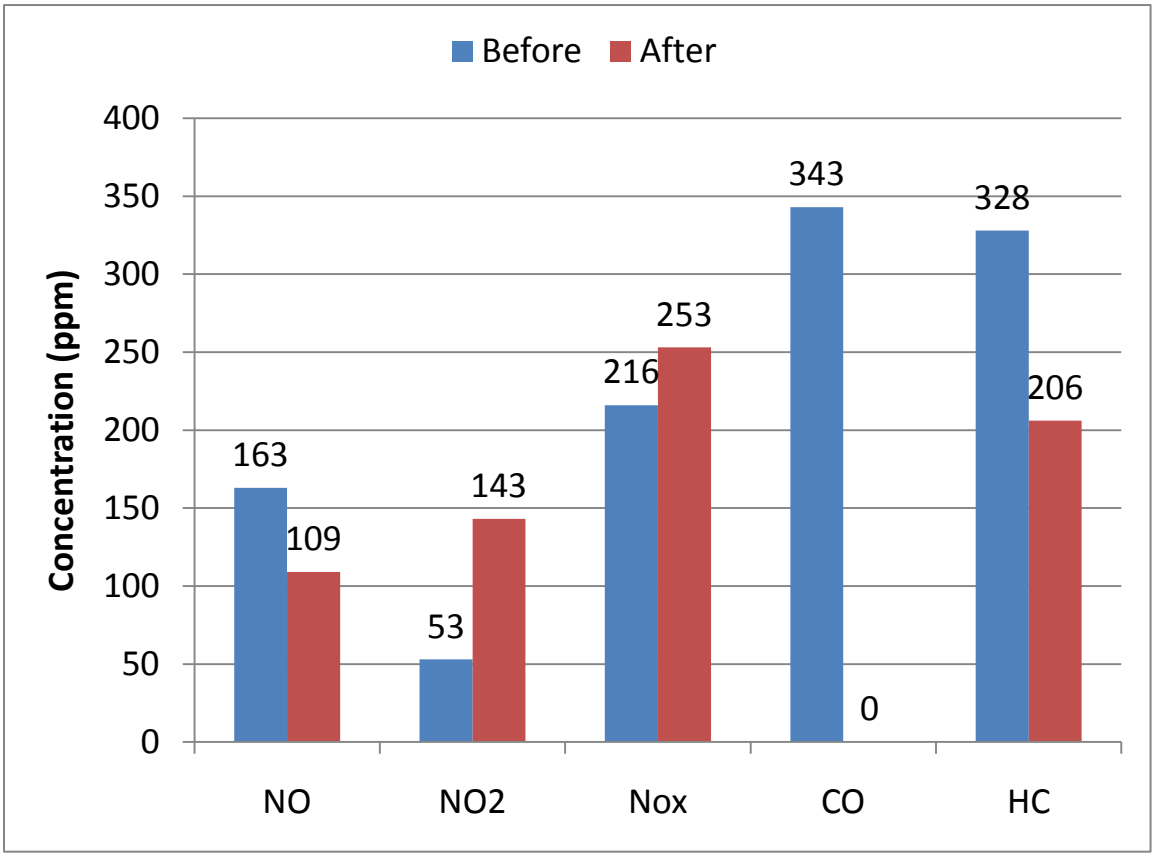

Figure 6.2.13 B20 emissions at 5 BAR (WITH EGR)

The effect of D.O.C. has a similar trend on the emissions as compared to ULSD.

Since the engine is equipped with a stock E.C.U. (engine control unit), the combustion phasing for different fuels is not the same due to different fuel properties and there is a significant change in the emissions. However, the difference in the NO_X emissions as compared to ULSD is negligible. This is due to the fact that only the lighter components of the fuel (which

www.manaraa.com

is basically ULSD) contribute towards the premixed combustion and the heavier components are being treated in the diffusion combustion.

The CO emissions are significantly less than ULSD. This is due to the fact that B20 has a higher cetane number. Higher cetane number of B20 leads to faster combustion and consequently the combustion process is more complete as compared to ULSD. Also, Biodiesel may be considered as oxygen rich fuels, which consequently raises the local air/fuel ratio resulting in increased oxygen at the locations of fuel burning and providing a greater opportunity for soot oxidation and cleaner combustion.

The HC emissions are lesser than ULSD because of higher cetane number and due to the fuel being rich in oxygen. Figure 6.2.14 illustrates the soot concentration emissions using B20 at 5 BAR IMEP.

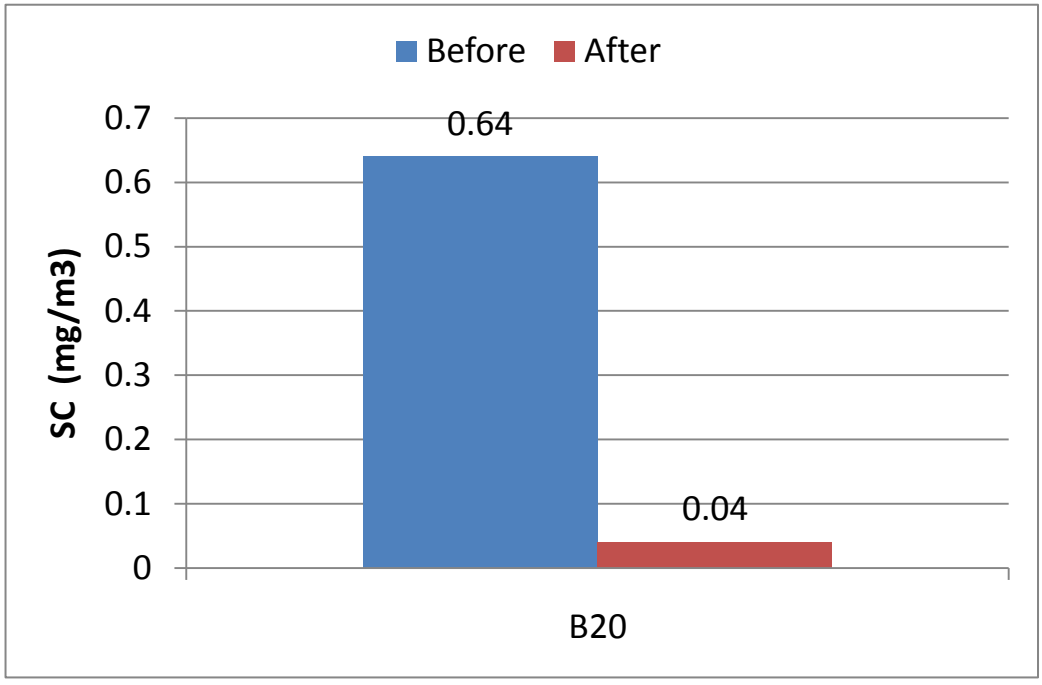

Figure 6.2.14 Soot concentration with B20 at 5 BAR IMEP (with EGR)

www.manaraa.com

B20 has a shorter ignition delay and thus the mass fraction burned by premixed combustion as compared to ULSD is also smaller in magnitude. Also, there is some amount of fuel injected in the flame. Therefore, B20 produces more soot as compared to ULSD at the same running condition.

The B20 emissions without EGR at 5 BAR IMEP are illustrated in figure 6.2.15.

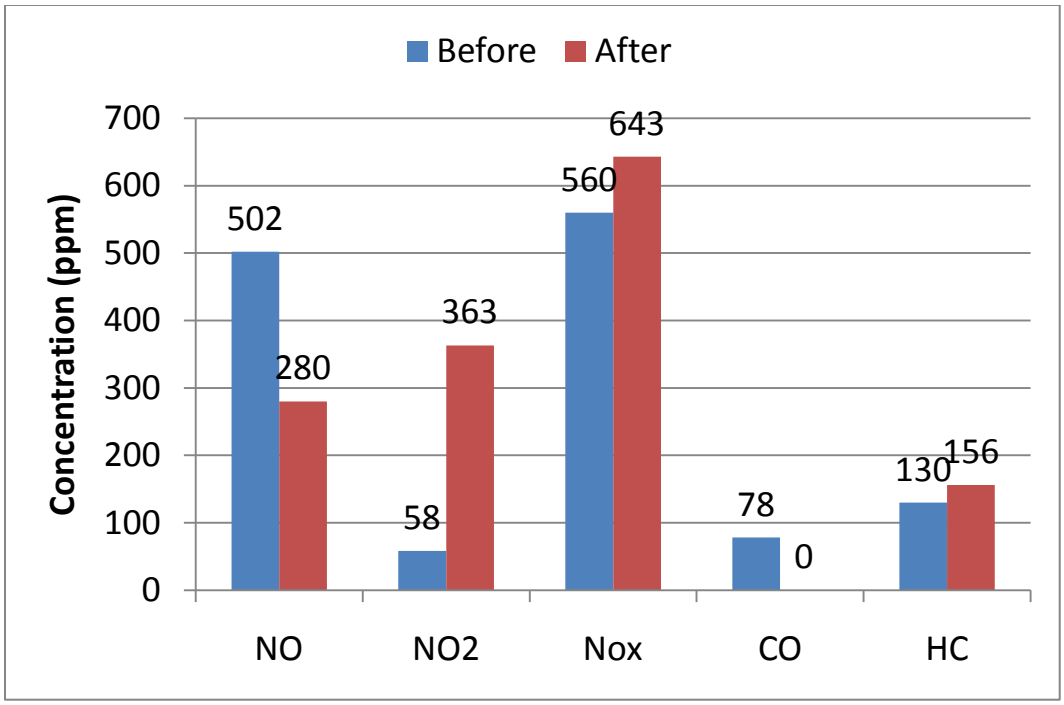

Figure 6.2.15 B20 emissions at 5 BAR IMEP without EGR

The effect of D.O.C. has a similar trend on the emissions as compared to ULSD. Figure 6.2.16 illustrates the soot concentration emissions with B20 (without EGR).

www.manaraa.com

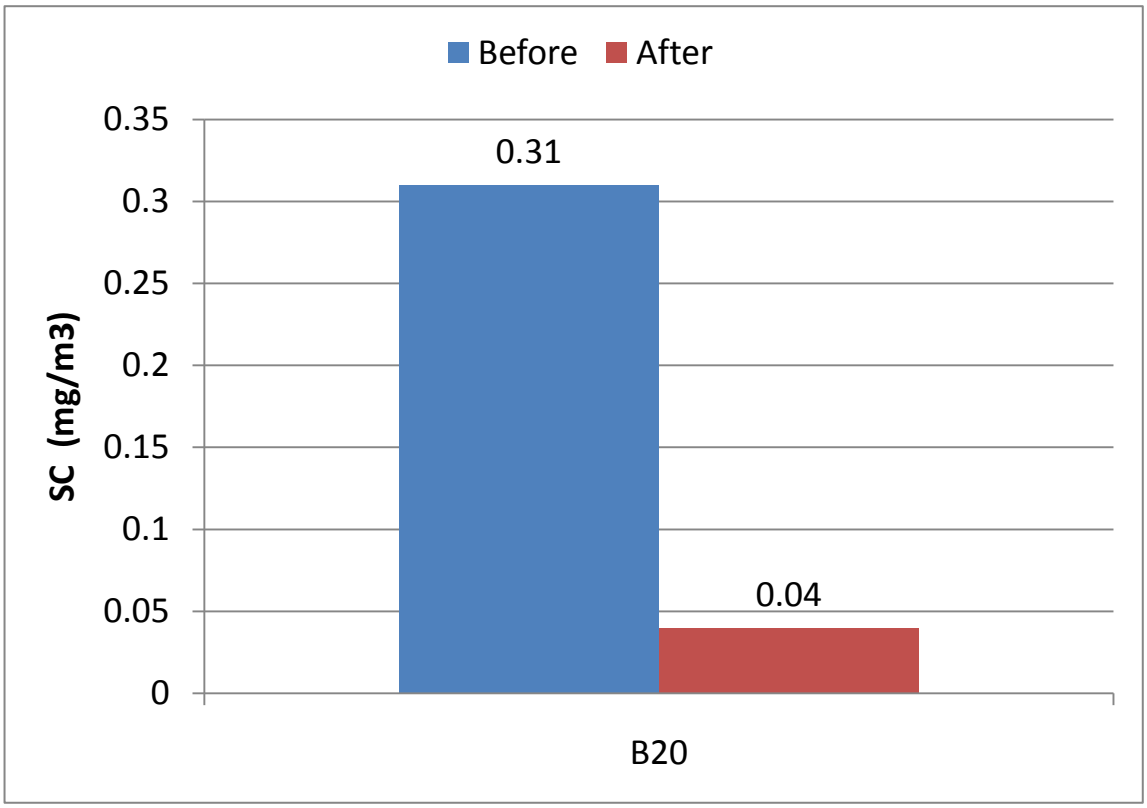

Figure 6.2.16 Soot concentration with B20 at 5 BAR IMEP (without EGR)

Without EGR, the combustion process is much more complete. Therefore, the mass fraction burned by pre mixed combustion of the two combustion fractions is increased and therefore there is a considerable reduction in soot concentration. Also, B20 has a lesser amount of aromatic content, no sulfur content and is oxygen rich as compared to ULSD.

www.manaraa.com

6.2.3.1. Effect of EGR on B20 emissions at 5 BAR IMEP:

6.2.3.1.1. Effect of EGR on engine out emissions:

The effect of EGR on engine out emissions is illustrated in figure 6.2.17.

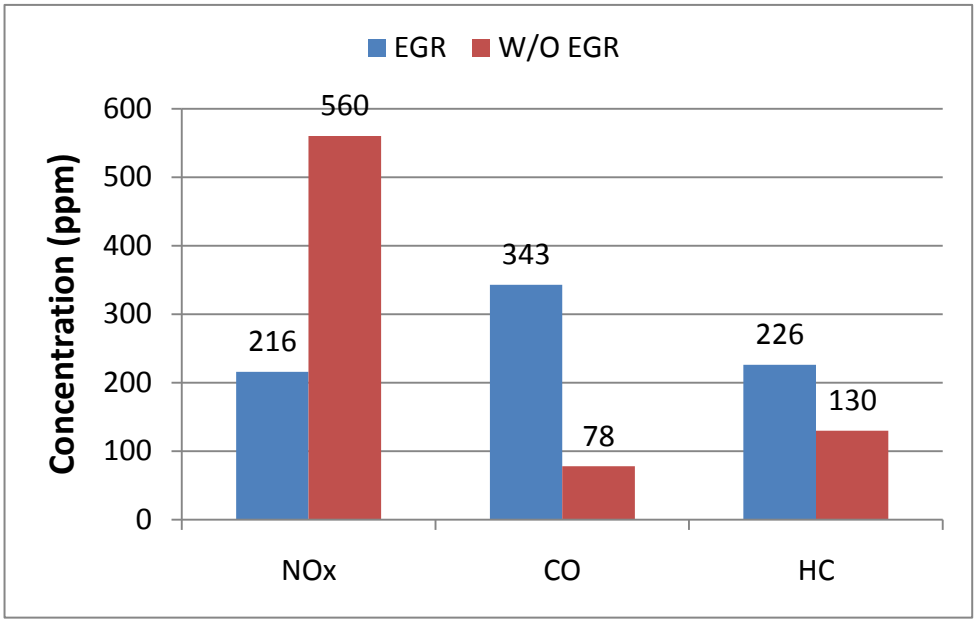

Figure 6.2.17 Effect of EGR on engine out emissions at 5 BAR IMEP (B20).

The EGR has a similar effect on B20 emissions as in the case of ULSD emissions.

www.manaraa.com

6.2.3.1.2. Effect of EGR on particulate concentration:

The effect of EGR on particulate concentration is shown in figure 6.2.18.

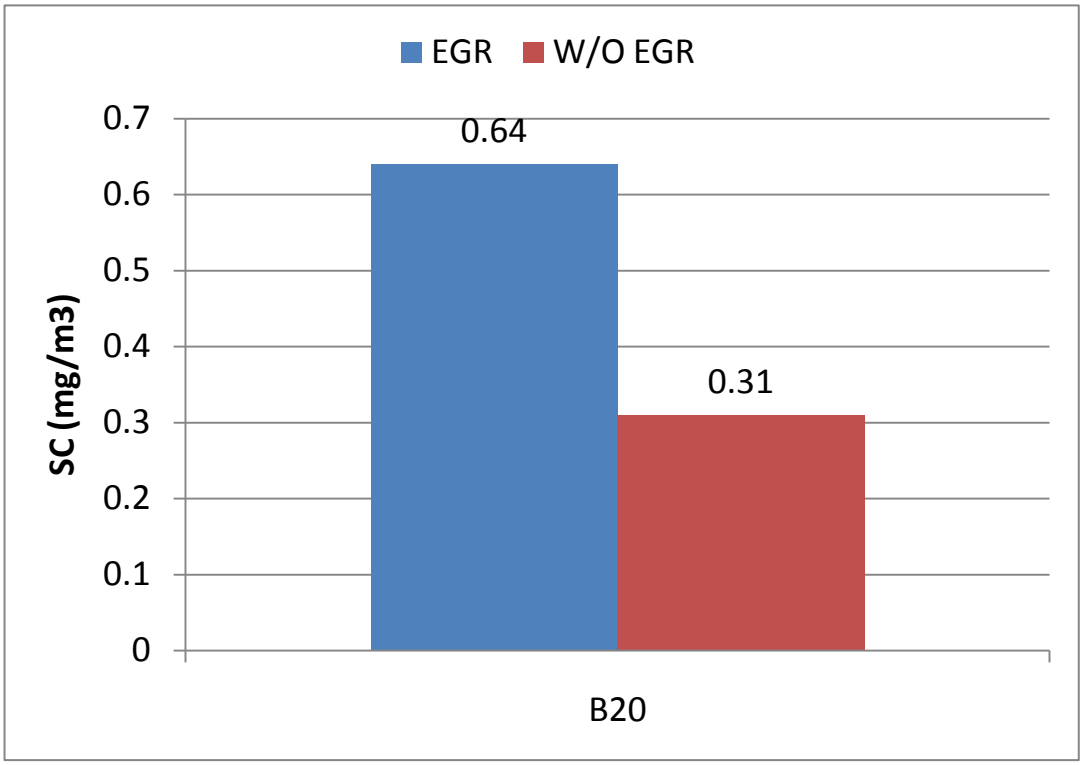

Figure 6.2.18 Effect of EGR on Particulate concentration

EGR has a similar effect on B20 soot concentration emissions as in the case of ULSD. As evident from the experimental results, EGR increases the soot concentration by about 106%.

www.manaraa.com

6.2.4. Emissions using S8:

The effect of S8 on the emissions at 5 BAR IMEP (with EGR) is illustrated in figure 6.2.19.

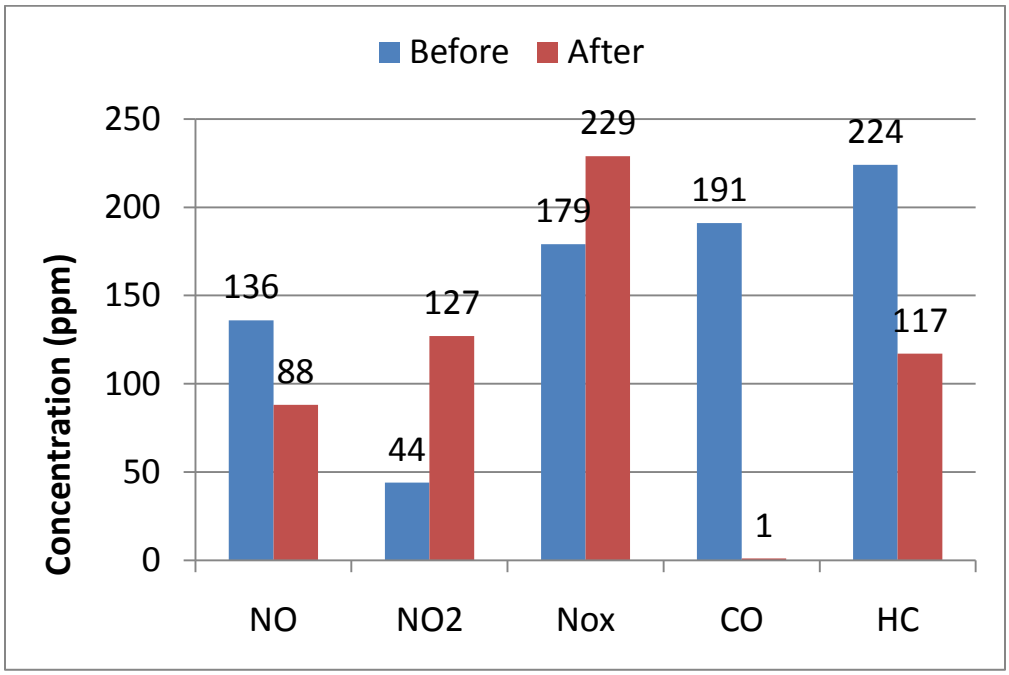

Figure 6.2.19 S8 emissions at 5 BAR IMEP (with EGR)

In this case, the NO_X emissions are lower as compared to ULSD. Due to a fairly high cetane number, the start of combustion is much earlier as compared to ULSD. This limits the peak of premixed combustion to a lower value and consequently leads to a lower in cylinder bulk gas temperature.

The CO and HC emissions are significantly less than ULSD. S8 has a fairly high cetane number and volatility as compared to ULSD. Due to higher cetane number, the combustion process is more complete as compared to ULSD. Higher volatility of the S8 leads to better evaporation and mixing which also leads to a cleaner and a better combustion as compared to ULSD.

www.manaraa.com

Figure 6.2.20 illustrates the soot concentration emissions using B20 at 5 BAR IMEP.

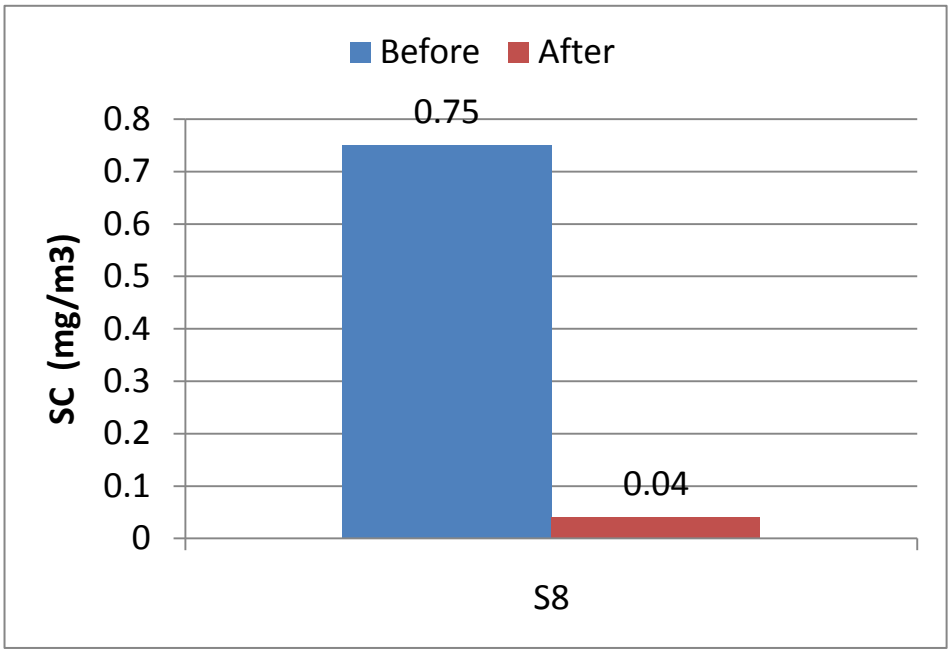

Figure 6.2.20 Soot concentration with B20 at 5 BAR IMEP (with EGR)

S8 has the highest cetane number and consequently the shortest ignition delay. Therefore, a large portion of the fuel is injected in the flame and produces the highest soot amongst all the fuels.

www.manaraa.com

6.3. Conclusions:

1. At 5 bar IMEP, the commercial engine (Mercedes series 900) runs normal with ULSD, JP8, S8 and B20 in the tested load range. However, the engine runs smoother with S8, JP8 and B20 as compared to ULSD.
2. The EGR concentration is assumed to be same with the same running conditions (same speed and torque). However, in order to develop the same power requirements, the throttle valve opening is different for different fuels. Therefore, the overall EGR effect varies with different fuels. Thus, the overall EGR effect is less in case of S8 and JP8 as compared to ULSD. Due to this effect, NO_X in case of JP8 is higher with EGR as compared to ULSD but when the engine is made to run without EGR, the trend becomes the other way around. The overall EGR effect in case of B20 is almost similar as compared to ULSD. This is because only the lighter components (which are mainly diesel) contribute towards premixed combustion.
3. B100 is characterized by cetane number of 56. By blending 20% of B100 and 80% of ULSD by volume, Cetane number of B20 will be higher than ULSD. This is confirmed by the effect that the ignition delay measured for B20 is shorter as compared to ULSD.
4. S8 has the shortest ignition delay amongst all the fuels. This trend is followed by B20, followed by ULSD, and then by JP8. This trend is in a strong correlation with the cetane number of the respective fuels. The effects of the ignition delay on the engine out emissions are summarized below:

❖ At 5 bar (with EGR), JP8 produced the highest oxides of nitrogen followed by ULSD, than by B20 and then by S8. JP8 has a longest ignition delay which leads to a higher peak of premixed combustion. Also the overall EGR effect reduces in case of JP8 as compared

www.manaraa.com

to ULSD because of increase in throttle valve opening. However, the difference between ULSD and B20 pertaining to the oxides of nitrogen is negligible. In case of S8, due to a fairly shorter ignition delay, the start of combustion is much earlier as compared to ULSD which limits the peak of premixed combustion to a lower value and consequently leads to a lower in cylinder bulk gas temperature.

- At 5 bar (with EGR), JP8 produced the highest carbon monoxide emissions followed by ULSD, than by B20 and then by S8. JP8 has the longest ignition delay and has a larger fraction of premixed combustion and has the least post oxidation reactions amongst all fuels. In case of B20, due to a shorter ignition delay, the start of combustion is much earlier as compared to ULSD which results in a more complete combustion. In case of S8, due to the shortest ignition delay amongst all fuels, the start of combustion is much earlier as compared to ULSD which results in a much more complete combustion.
- At 5 bar (with EGR), S8 produced highest soot concentration emissions, followed by B20, followed by ULSD, and then by JP8. In case of S8, due to a fairly shorter ignition delay, the combustion starts much earlier. Therefore, a large amount of fuel is injected in the flame which produces the highest soot. In case of B20, also due to a shorter ignition delay than ULSD, certain amount of fuel is injected in the flame which produces higher soot as compared to ULSD. In case of JP8, due to a long ignition delay, a higher fraction of premixed combustion is observed, therefore the in cylinder combustion is much more complete. Also, there is no fuel injected in the flame. Due to these reasons, the soot concentration emissions in this case are lower than ULSD.

5. At 5 bar IMEP, B20 has the highest fuel consumption, followed by ULSD, followed by JP8 and then by S8. This trend is because of the respective lower heating values of the

www.manaraa.com

fuels. B20 has the lowest heating value, followed by the ULSD, followed by JP8 and then by S8.

6. Due to the lower value of bulk modulus of JP8 and S8 (as compared to ULSD), the pressure developed in the pumping process is lower. However to maintain the same injection pressure, the rail pressure starts building up 5 CAD earlier than ULSD. The throttle opening in case of JP8 and S8 is larger as compared to ULSD because of a lower heating value of JP8 and S8 on volumetric basis.
7. The pressure developed in the pumping process is lower for B20 as compared to ULSD in spite of the fact that the bulk modulus of B20 is higher as compared to ULSD. This trend may be attributed to some experimental error however the difference in the values of bulk modulus of the two fuels is negligible. The throttle opening in case of B20 is same as compared to ULSD.
8. The engine tries to maintain the same injection timing irrespective of different fuels at different running conditions. However, there is a difference in the combustion phasing depending upon the fuel properties of different fuels.
9. In order to optimize the system closer to the ULSD running conditions, fuel injection will have to be advanced in case of JP8 whereas fuel injection will have to be retarded in the case of B20 and S8.
10. In the range of existing operating conditions, the D.O.C. is very effective in the oxidation of CO for all the fuels being tested.
11. For all the fuels being tested, the D.O.C. is also efficient in converting NO to NO_2.
12. The FTIR may not be the best instrument for measuring HC emissions.

www.manaraa.com

13. In the range of existing operating conditions, the D.P.F. is fairly effective in reducing PM.
14. The testing with S8 (without EGR) was not conducted. It was assumed that this would have lead to even shorter ignition delay for S8 and more fuel would have been injected in the flame. Therefore, in order to avoid a smoky operation, this run was not conducted.

www.manaraa.com

7. Effect of speed on in cylinder combustion at 7.5 bar IMEP

7.1. Introduction:

The study is concentrated to investigate the effect of speed at the same load on the in cylinder combustion. The engine was run at four different speeds (1300 rpm, 1500 rpm, 2000 rpm and 2200 rpm) while maintaining the same torque at 360 Nm. The testing was done at 7.5 BAR IMEP. These sets of four runs were conducted using four different fuels (ULSD, S8, JP8 and B20). All the testing is conducted with EGR. As the engine is calibrated for ULSD, therefore, initially the engine was run on ULSD in order to know how the engine behaves with ULSD and to set the results as a benchmark in order to compare it with other results obtained using other alternative fuels.

7.2. Effect of speed on in cylinder combustion:

7.2.1. Effect of speed on ULSD in cylinder combustion:

Figure 7.1 shows the running point with ULSD (1300 rpm). Table 7.1 illustrates the few critical parameters at this running point.

Running point	Throttle valve opening	LPPC	RHR peak	Peak compression pressure	Peak combustion pressure	Fuel Consumption	Exhaust gas temperature
ULSD(With EGR)	53%	11.4^0 ATDC.	257 KJ/m^3	57 bars	68 bars	9.49 kg/hr	408 ^{0} C

Table 7.1 Critical parameters with ULSD (with EGR) at1300 rpm.

www.manaraa.com

In this case, the engine produced 49 KW of power. Figure 7.5 shows the exploded view of RHR. The ignition delay in this case is 3.7 CAD.

Figure 7.2 shows the running point at 1500 rpm. Table 7.2 illustrates the few critical parameters at this running point.

Running point	Throttle valve opening	LPPC	RHR peak	Peak compression pressure	Peak combustion pressure	Fuel Consumption	Exhaust gas temperature
ULSD(With EGR)	56%	9.8^0 ATDC.	216 KJ/m^3	63bars	71 bars	11.12 kg/hr	385 ^{0} C

Table 7.2 Critical parameters with ULSD (with EGR) at1500 rpm.

The engine produced 57 KW of power. Figure 7.6 shows the exploded view of RHR. Due to an increase in the engine speed, the peak compression temperature increases due to smaller heat losses during the compression stroke. The combustion takes place at a faster rate (evident from the slope of the curve) and the LPPC shifts closer to TDC. As the combustion sets off earlier in this case, therefore, the LPPC is limited to a lower value. There is an increase in the fuel consumption with the increase in engine speed. Due to the increase in engine speed, there is a rise in the peak of the rail pressure. The ignition delay gets shortened and it is reduced to 3.4 CAD.

www.manaraa.com

Figure 7.3 shows the running point at 2000 rpm. Table 7.3 illustrates the few critical parameters at this running point.

Running point	Throttle valve opening	LPPC	RHR peak	Peak compression pressure	Peak combustion pressure	Exhaust gas temperature
ULSD(With EGR)	57%	9.1^0 ATDC.	124 KJ/m^3	75bars	71 bars	395 ^{0} C

Table 7.3 Critical parameters with ULSD (with EGR) at 2000 rpm.

The engine produced 76 KW of power. It is interesting to note that the peak compression pressure is higher than the peak combustion pressure in this case. The possible cause for this kind of trend may be due to a higher percentage of EGR concentration in order to take care of emissions. Figure 7.7 shows the exploded view of RHR. In spite of the fact that the temperature of the in cylinder charge at the end of the compression stroke is higher in this case, the ignition delay is still 3.4 CAD (as in the case when the engine was run at 1500 rpm). This trend may be due to the higher concentration of EGR.

www.manaraa.com

Figure 7.4 shows the running point at 2200 rpm. Table 7.4 illustrates the few critical parameters at this running point.

Running point	Throttle valve opening	LPPC	RHR peak	Peak compression pressure	Peak combustion pressure	Exhaust gas temperature
ULSD(With EGR)	60%	8^0 ATDC.	111 KJ/m^3	82bars	76 bars	411 ^{0} C

Table 7.4 Critical parameters with ULSD (with EGR) at 2200 rpm.

The engine produced 83 KW of power. Figure 7.8 shows the exploded view of RHR. The peak of rail pressure gets reduced as compared to the run at 2000 rpm. This trend may be necessary in order to take care of emissions (to reduce the oxides of nitrogen). The ignition delay gets shortened and it is reduced to 2.4 CAD.

www.manaraa.com

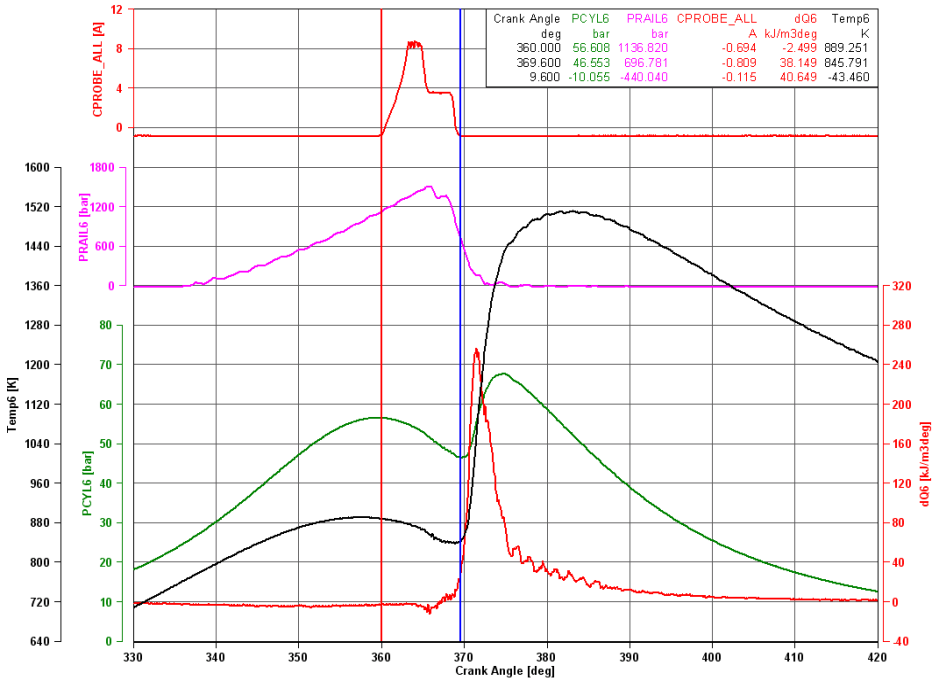

Figure 7.1 In cylinder combustion at 1300 rpm (ULSD).

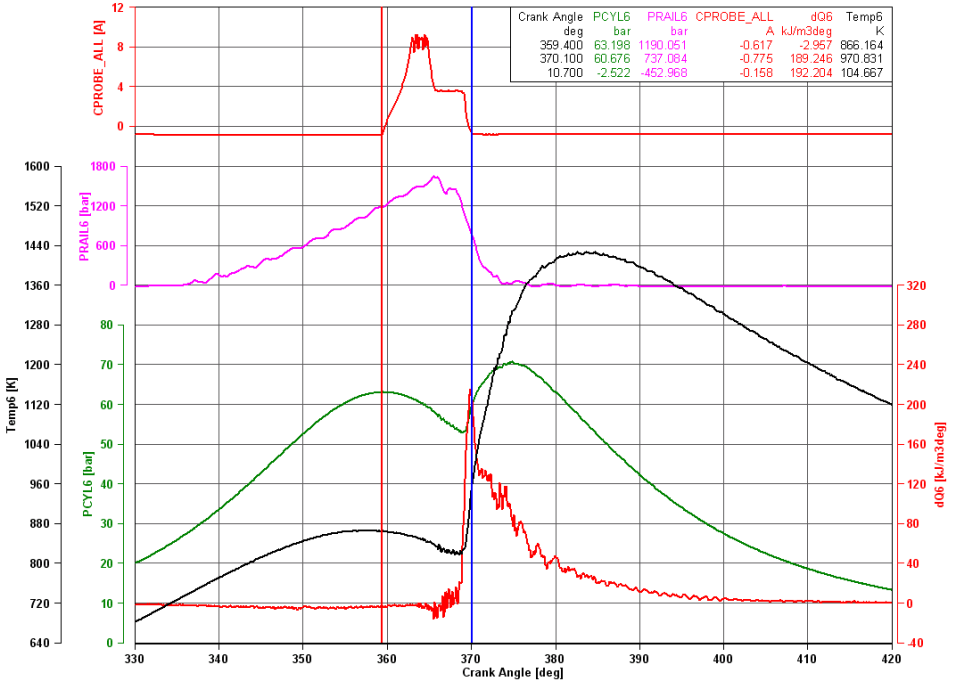

Figure 7.2 In cylinder combustion at 1500 rpm (ULSD).

www.manaraa.com

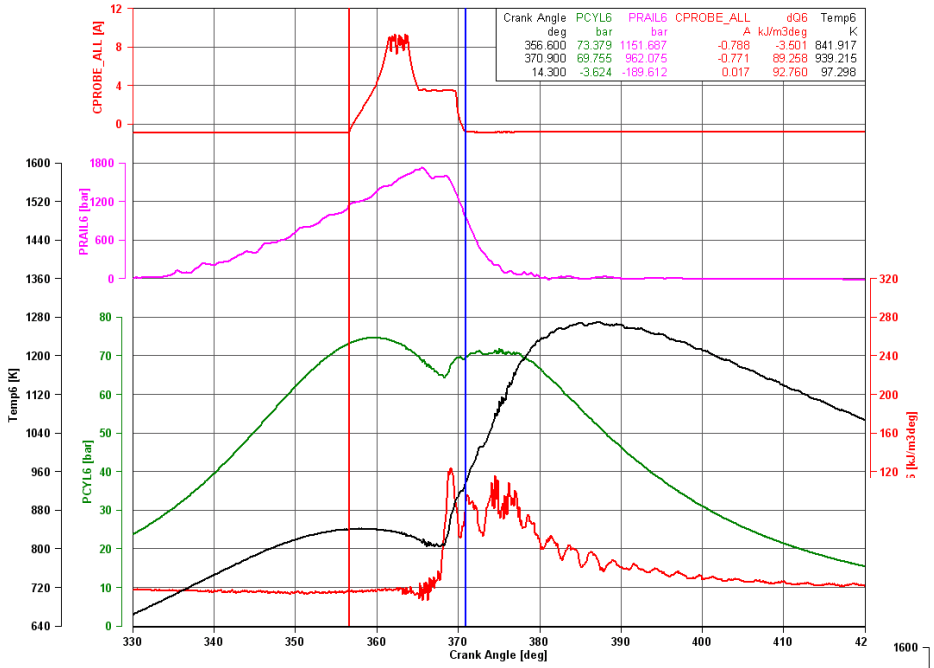

Figure 7.3 In cylinder combustion at 2000 rpm (ULSD).

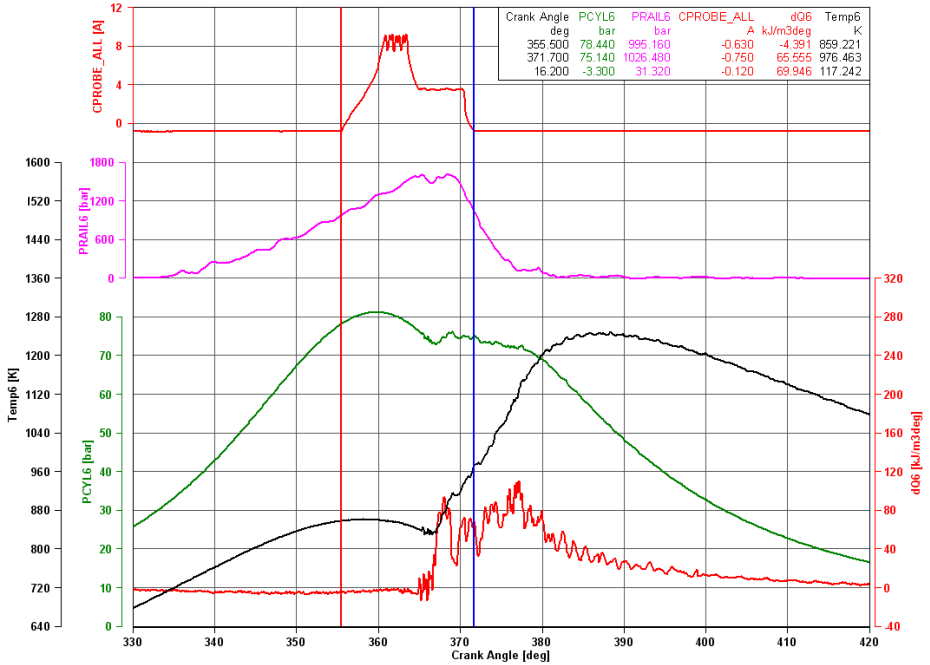

Figure 7.4 In cylinder combustion at 2200 rpm (ULSD).

www.manaraa.com

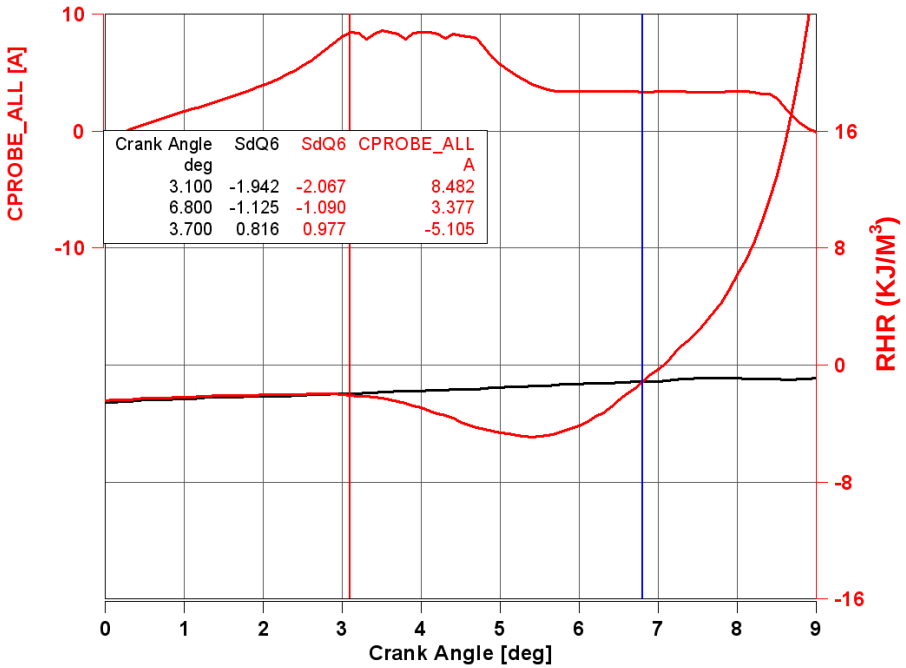

Figure 7.5 Ignition delay at 1300 rpm (ULSD).

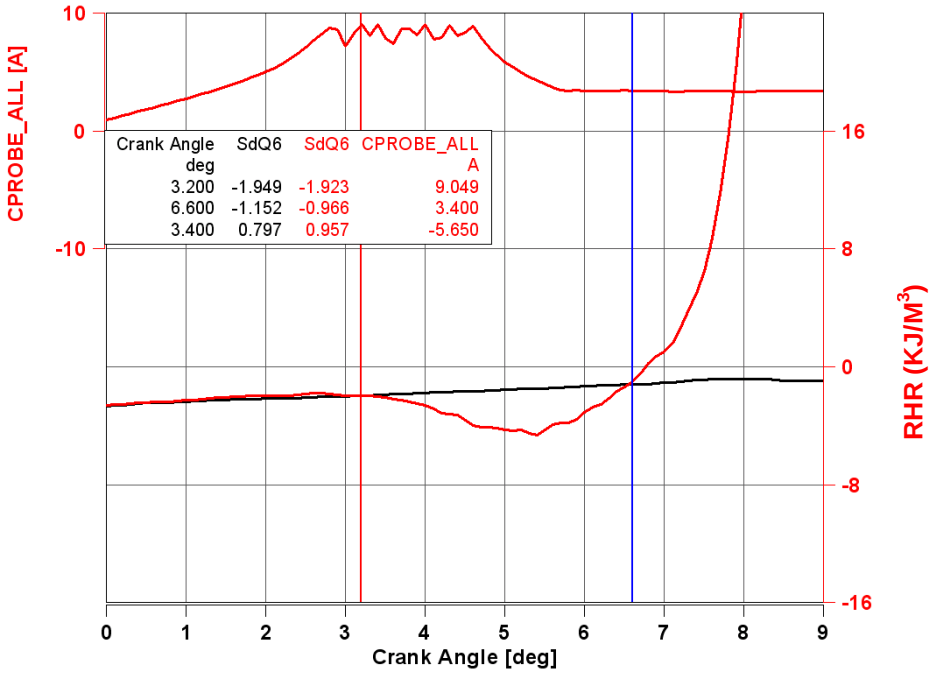

Figure 7.6 Ignition delay at 1500 rpm (ULSD).

www.manaraa.com

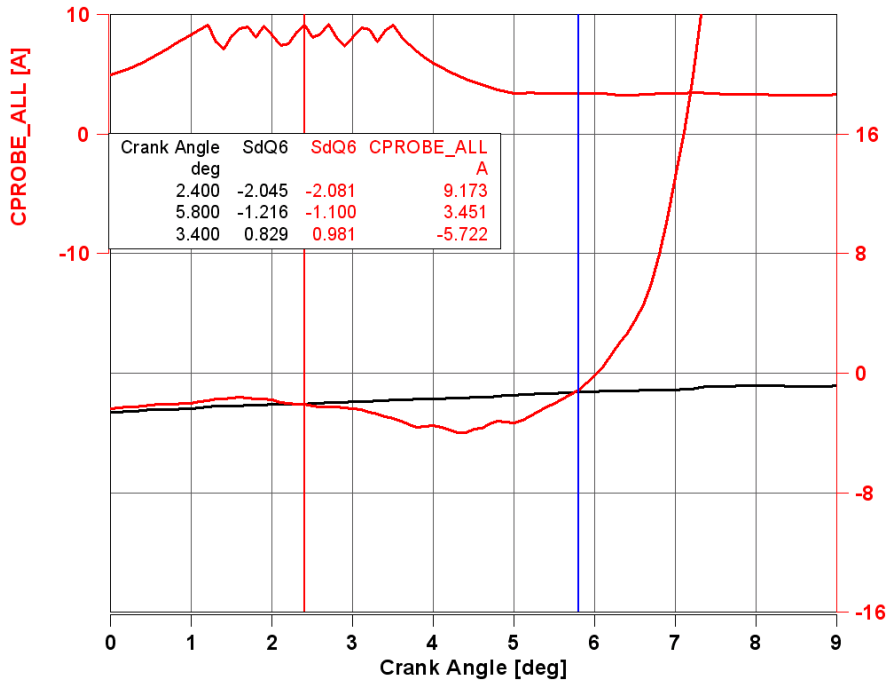

Figure 7.7 Ignition delay at 2000 rpm (ULSD).

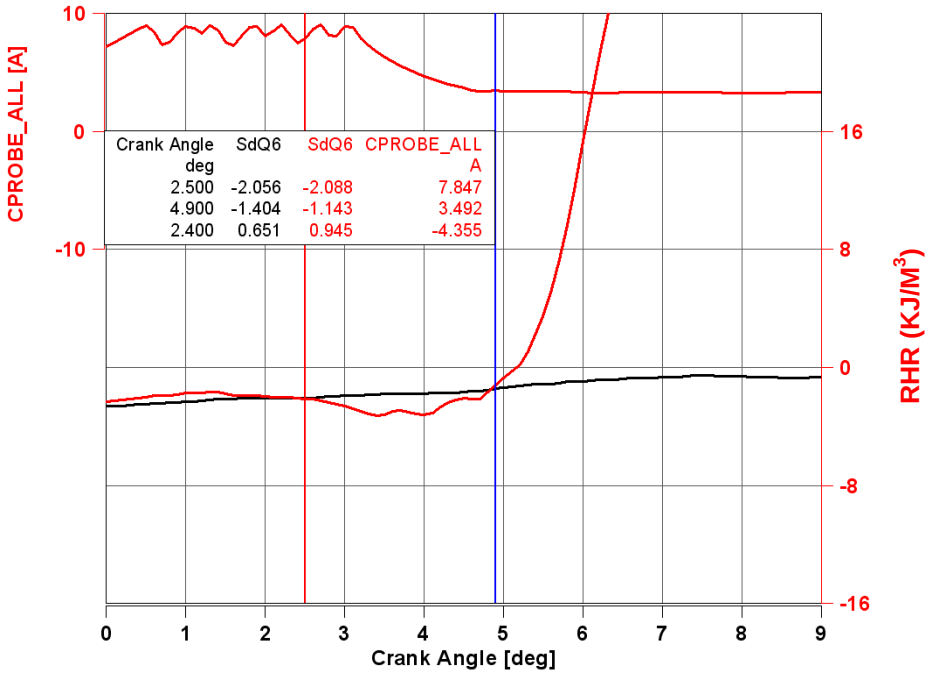

Figure 7.8 Ignition delay at 2200 rpm (ULSD).

www.manaraa.com

7.2.2. Effect of speed on JP8 in cylinder combustion:

Figure 7.9 shows the running point with JP8 (1300 rpm). Table 7.5 illustrates the few critical parameters at this running point.

Running point	Throttle valve opening	LPPC	RHR peak	Peak compression pressure	Peak combustion pressure	Fuel Consumption	Exhaust gas temperature
JP8(With EGR)	57%	12^0 ATDC.	250 KJ/m^3	58 bars	66 bars	9.38 kg/hr	390 ^{0} C

Table 7.5 Critical parameters with JP8 (with EGR) at 1300 rpm.

As the heating value on volumetric basis of JP8 is slightly lower than ULSD, the throttle is increased to 57%. As the bulk modulus is less than ULSD, the peak of the rail pressure is also less than ULSD for the same running point. Figure 7.13 shows the exploded view of RHR. The start of combustion gets retarded in case of JP8 due to lower cetane number and higher volatility as compared to ULSD. Therefore, JP8 has a longer ignition delay as compared to ULSD for the same running point. The ignition delay in this case is 4.2 CAD.

Figure 7.10 shows the running point at 1500 rpm. Table 7.6 illustrates the few critical parameters at this running point.

Running point	Throttle valve opening	LPPC	RHR peak	Peak compression pressure	Peak combustion pressure	Fuel Consumption	Exhaust gas temperature
JP8(With EGR)	58%	11.1^0 ATDC.	214 KJ/m^3	63 bars	68 bars	11.06 kg/hr	371 ^{0} C

Table 7.6 Critical parameters with JP8 (with EGR) at 1500 rpm.

www.manaraa.com

As the heating value on volumetric basis of JP8 is slightly lower than ULSD, the throttle is increased to 58%. Figure 7.14 shows the exploded view of RHR. As the bulk modulus is less than ULSD, the peak of the rail pressure is also less than ULSD for the same running point. The ignition delay gets shortened and it is reduced to 3.3 CAD.

Figure 7.11 shows the running point at 2000 rpm with JP8. Table 7.7 illustrates the few critical parameters at this running point.

Running point	Throttle valve opening	LPPC	RHR peak	Peak compression pressure	Peak combustion pressure	Fuel Consumption	Exhaust gas temperature
JP8(With EGR)	59%	9.2^0 ATDC.	140 KJ/m^3	77 bars	72 bars	16.20 kg/hr	384 ^{0} C

Table 7.7 Critical parameters with JP8 (with EGR) at 2000 rpm.

As the heating value on the volumetric basis of JP8 is slightly lower than ULSD, the throttle is increased to 59%. As the bulk modulus is less than ULSD, the peak of the rail pressure is also less than ULSD for the same running point. Figure 7.15 shows the exploded view of RHR. In spite of having a higher temperature of the charge trapped inside the cylinder at the end of the compression stroke, the ignition delay is 3.6 CAD due to a higher concentration of EGR.

www.manaraa.com

Figure 7.12 shows the running point at 2200 rpm. Table 7.8 illustrates the few critical parameters at this running point.

Running point	Throttle valve opening	LPPC	RHR peak	Peak compression pressure	Peak combustion pressure	Fuel Consumption	Exhaust gas temperature
JP8(With EGR)	62%	7.8^0 ATDC.	126 KJ/m^3	83 bars	77 bars	18.5 kg/hr	399 ^{0} C

Table 7.8 Critical parameters with JP8 (with EGR) at 2200 rpm.

As the heating value on the volumetric basis of JP8 is slightly lower than ULSD, the throttle is increased to 62%. Figure 7.16 shows the exploded view of RHR. The ignition delay gets shortened and it is reduced to 2.6 CAD.

www.manaraa.com

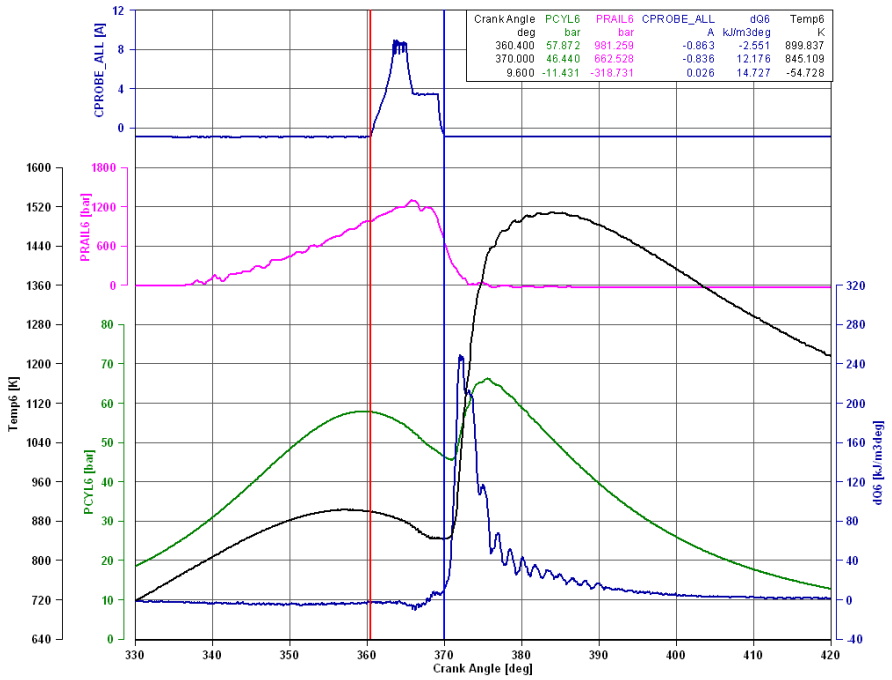

Figure 7.9 In cylinder combustion at 1300 rpm (JP8).

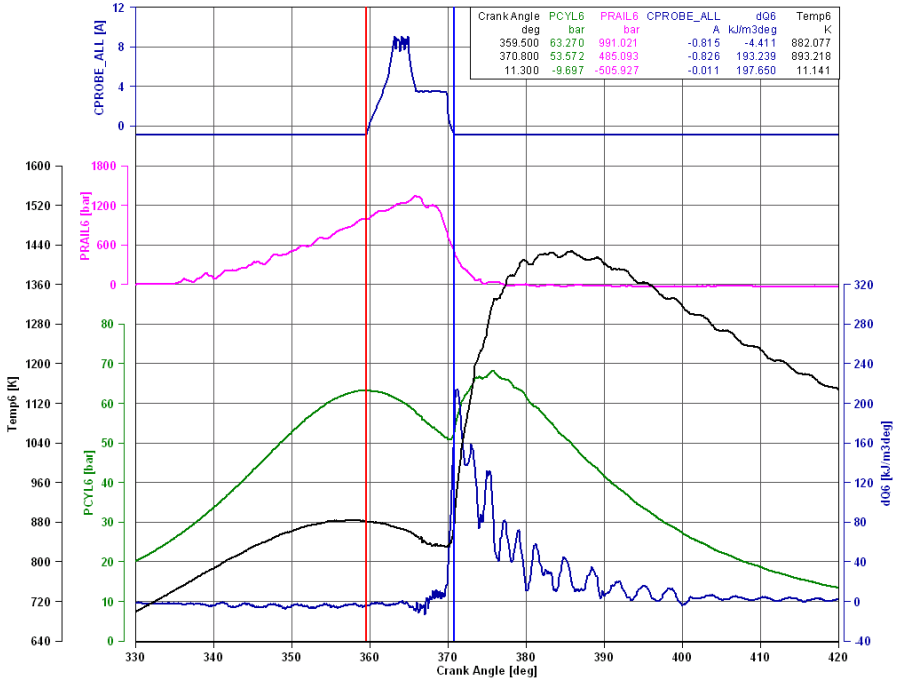

Figure 7.10 In cylinder combustion at 1500 rpm (JP8).

www.manaraa.com

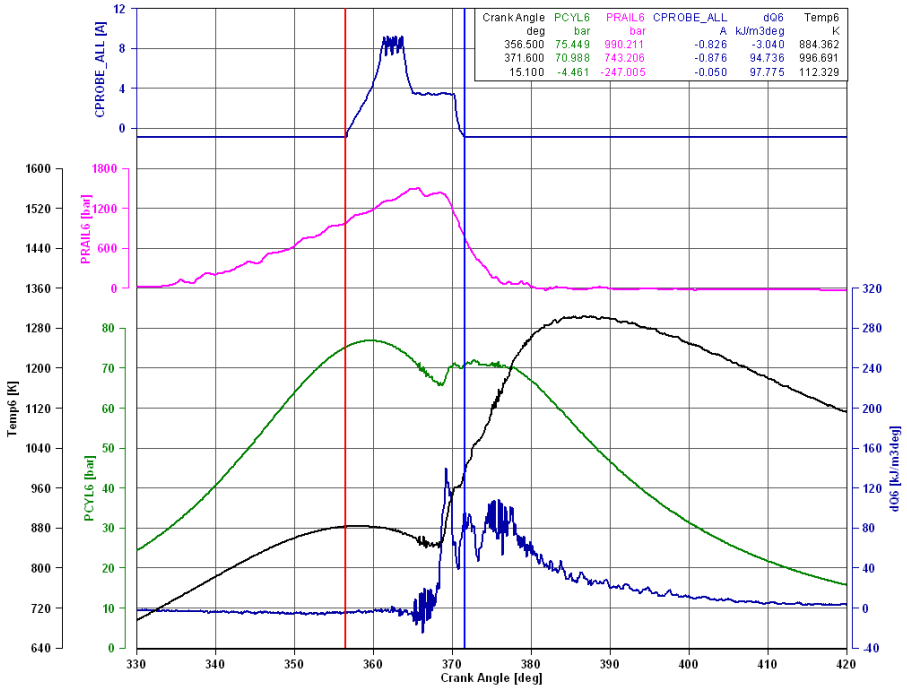

Figure 7.11 In cylinder combustion at 2000 rpm (JP8).

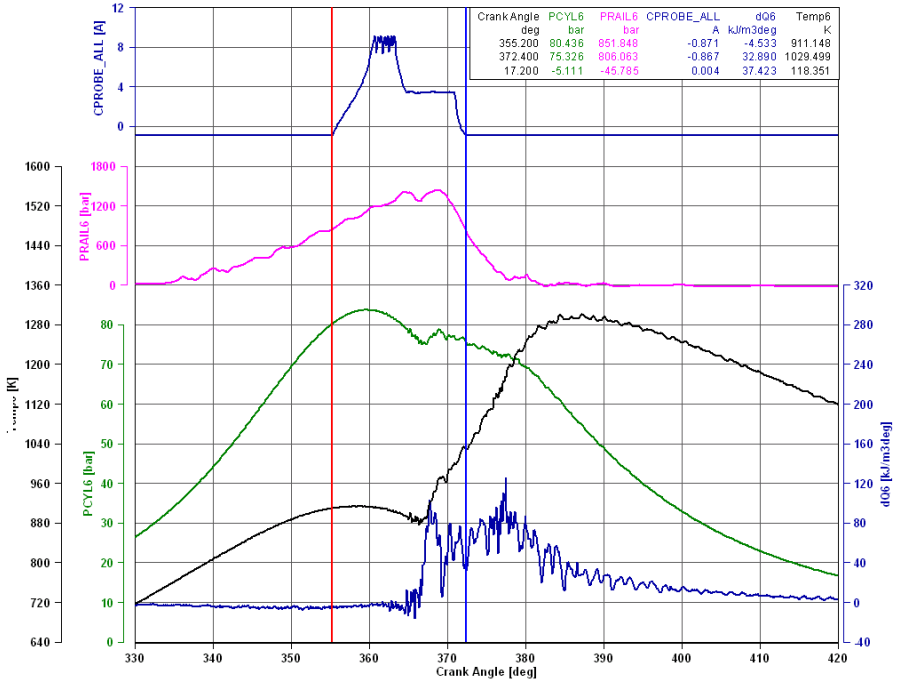

Figure 7.12 In cylinder combustion at 2200 rpm (JP8).

www.manaraa.com

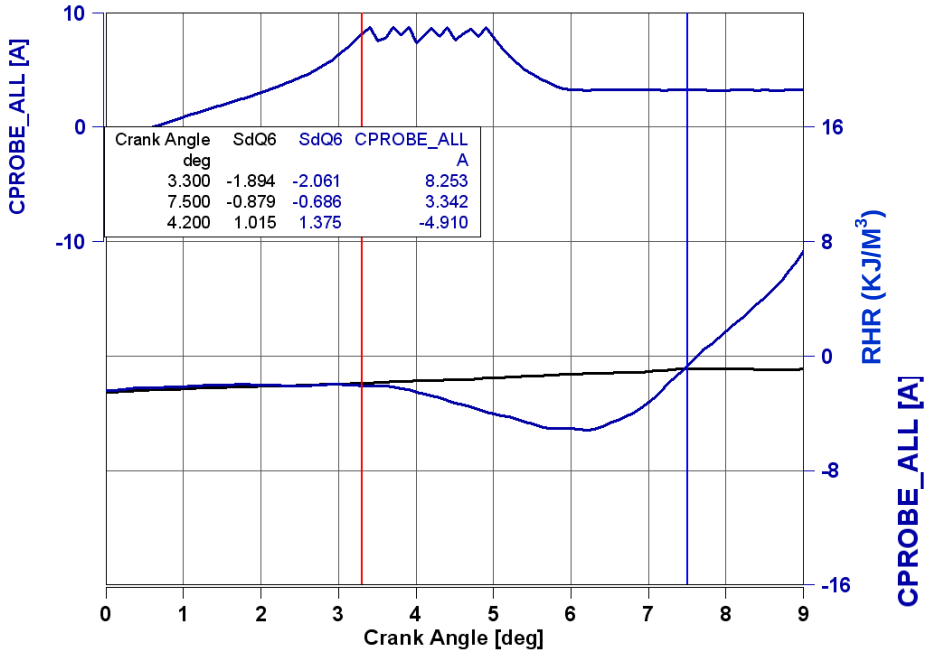

Figure 7.13 Ignition delay at 1300 rpm (JP8).

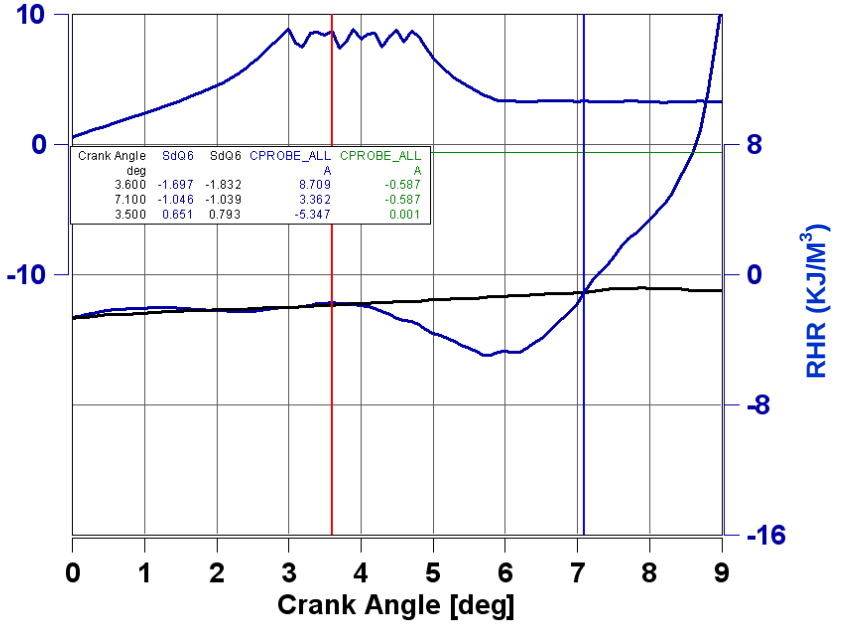

Figure 7.14 Ignition delay at 1500 rpm (JP8).

www.manaraa.com

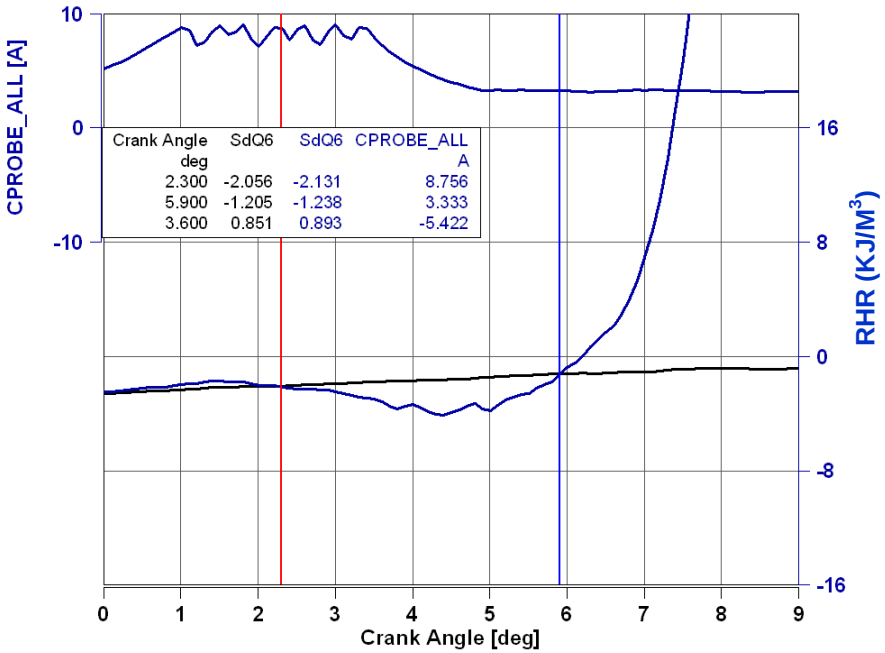

Figure 7.15 Ignition delay at 2000 rpm (JP8).

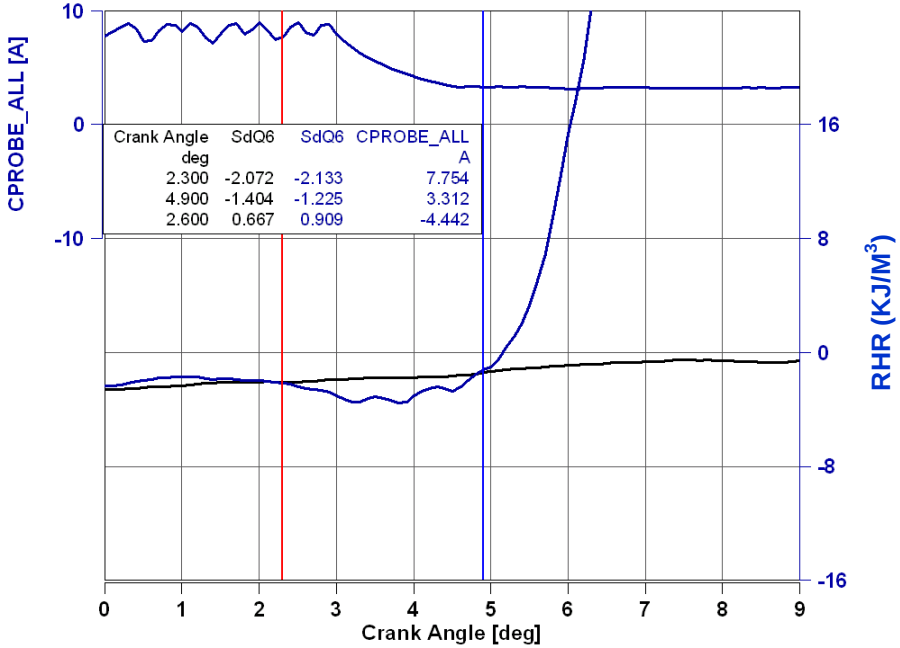

Figure 7.16 Ignition delay at 2200 rpm (JP8).

www.manaraa.com

7.2.3. Effect of speed on B20 in cylinder combustion:

The engine was also run at 7.5 bar IMEP at 1300 rpm using B20. The study was diverted to investigate the effect of speed on in cylinder combustion. Figure 7.17 shows the running point with B20 (1300 rpm). Table 7.9 illustrates the few critical parameters at this running point.

Running point	Throttle valve opening	LPPC	RHR peak	Peak compression pressure	Peak combustion pressure	Fuel Consumption	Exhaust gas temperature
B20(With EGR)	53%	10.7^0 ATDC.	261 KJ/m^3	58 bars	68 bars	9.67kg/hr	403 ^{0} C

Table 7.9 Critical parameters with B20 (with EGR) at 1300 rpm.

The throttle opening is the same as in the case of ULSD because only the lighter fraction of the fuel (which is diesel) participates in the premixed combustion at such a light load. As the cetane number of B20 is higher than ULSD, the combustion starts earlier and the LPPC shifts closer to the TDC. As the bulk modulus is higher than ULSD, the peak of the rail pressure is slightly more than ULSD for the same running point. Due to higher cetane number, the ignition delay is shorter. The ignition delay in this case is 3.5 CAD.

Figure 7.18 shows the running point at 1500 rpm. Table 7.10 illustrates the few critical parameters at this running point.

Running point	Throttle valve opening	LPPC	RHR peak	Peak compression pressure	Peak combustion pressure	Fuel Consumption	Exhaust gas temperature
B20(With EGR)	55%	10.2^0 ATDC.	208 KJ/m^3	62 bars	69 bars	11.39 kg/hr	373 ^{0} C

Table 7.10 Critical parameters with B20 (with EGR) at 1500 rpm.

www.manaraa.com

The throttle opening is the same as in the case of ULSD. Figure 7.22 shows the exploded view of RHR. The ignition delay gets shortened and it is reduced to 3.1 CAD.

Figure 7.19 shows the running point at 2000 rpm with B20. Table 7.11 illustrates the few critical parameters at this running point.

Running point	Throttle valve opening	LPPC	RHR peak	Peak compression pressure	Peak combustion pressure	Fuel Consumption	Exhaust gas temperature
B20(With EGR)	56%	8.6^0 ATDC.	123 KJ/m^3	75 bars	72 bars	16.56 kg/hr	400 ^{0} C

Table 7.11 Critical parameters with B20 (with EGR) at 2000 rpm.

The throttle opening is the same as in the case of ULSD. As the bulk modulus is slightly more than ULSD, the peak of the rail pressure is also slightly more than ULSD for the same running point. Figure 7.23 shows the exploded view of RHR. The ignition delay is 3.2 CAD.

Figure 7.20 shows the running point at 2200 rpm with B20. Table 7.12 illustrates the few critical parameters at this running point.

Running point	Throttle valve opening	LPPC	RHR peak	Peak compression pressure	Peak combustion pressure	Fuel Consumption	Exhaust gas temperature
B20(With EGR)	60%	8^0 ATDC.	121 KJ/m^3	82 bars	75 bars	19.06 kg/hr	413 ^{0} C

Table 7.12 Critical parameters with B20 (with EGR) at 2200 rpm.

www.manaraa.com

The throttle opening is the same as in the case of ULSD. Figure 7.24 shows the exploded view of RHR. The ignition delay gets shortened as compared to ULSD and it is reduced to 1.9 CAD due to a higher value of cetane number.

www.manaraa.com

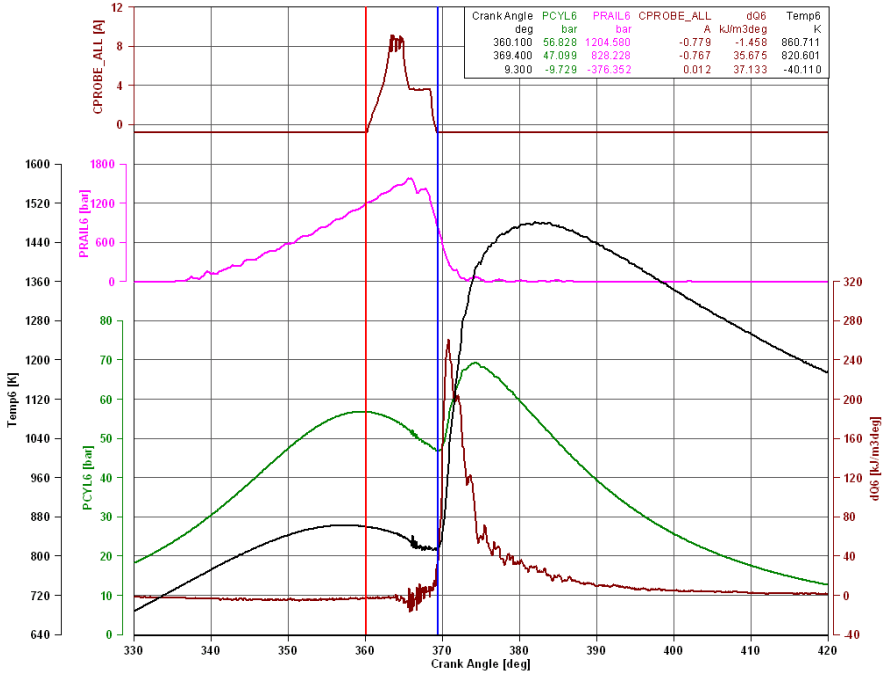

Figure 7.17 In cylinder combustion at 1300 rpm (B20).

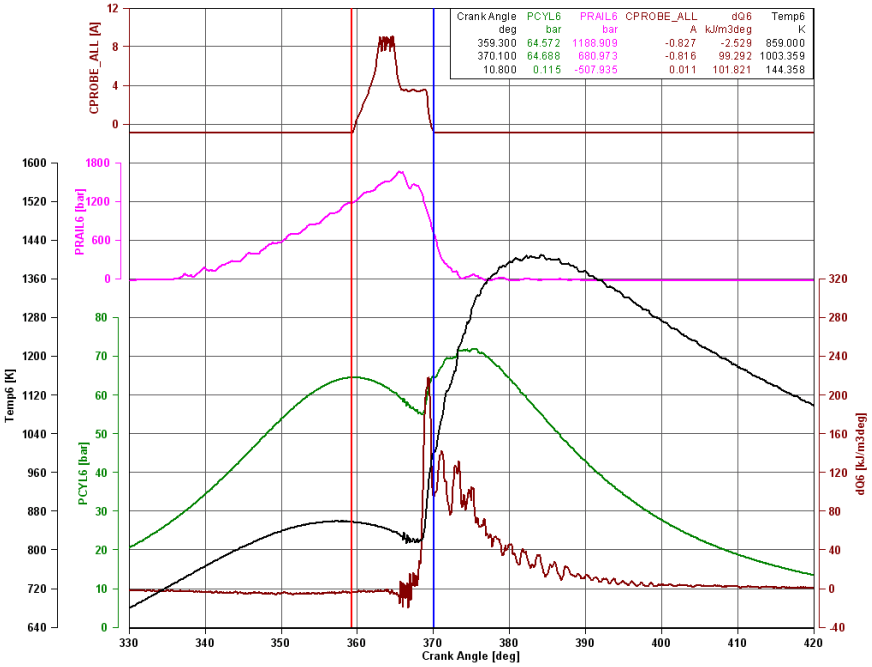

Figure 7.18 In cylinder combustion at 1500 rpm (B20).

www.manaraa.com

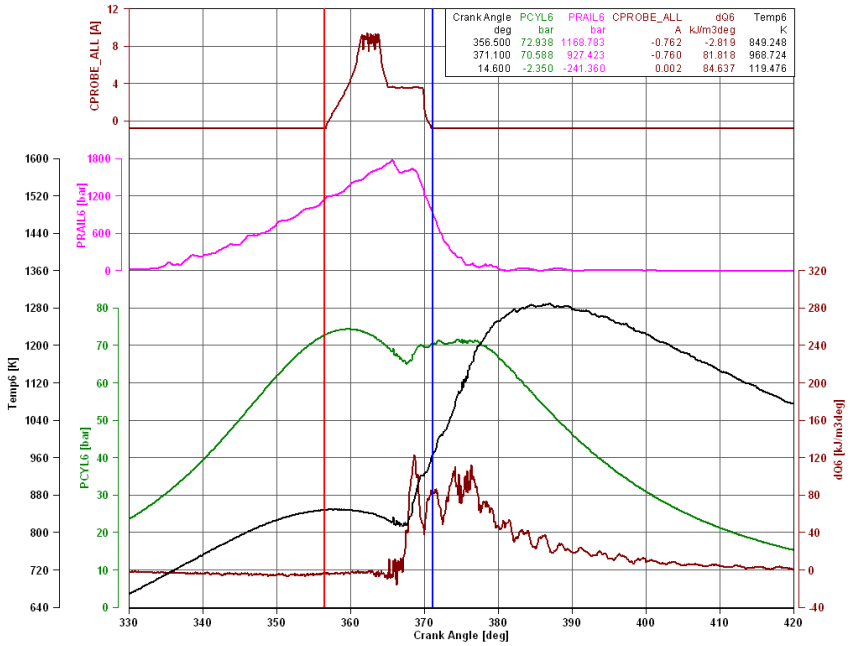

Figure 7.19 In cylinder combustion at 2000 rpm (B20).

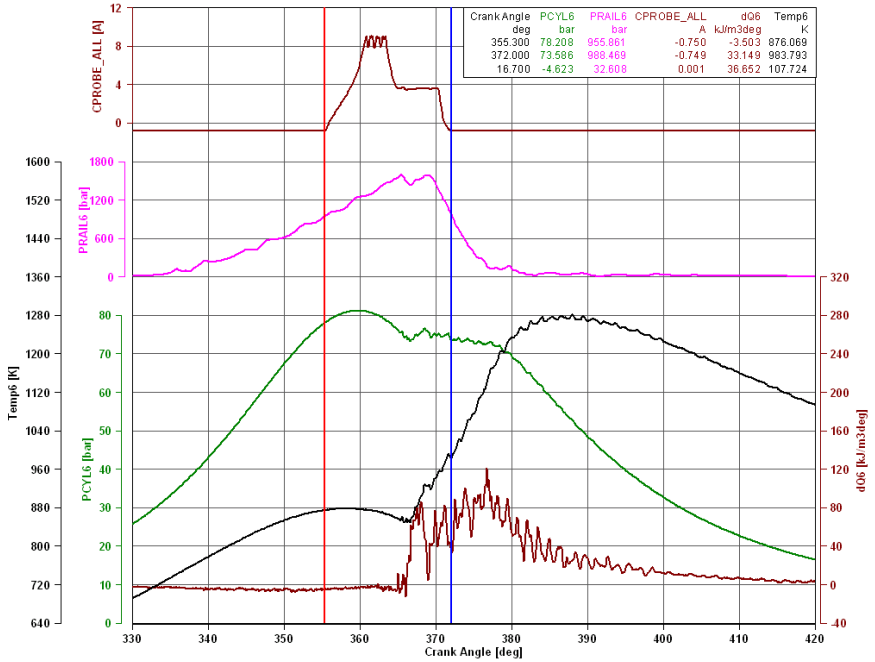

Figure 7.20 In cylinder combustion at 2200 rpm (B20).

www.manaraa.com

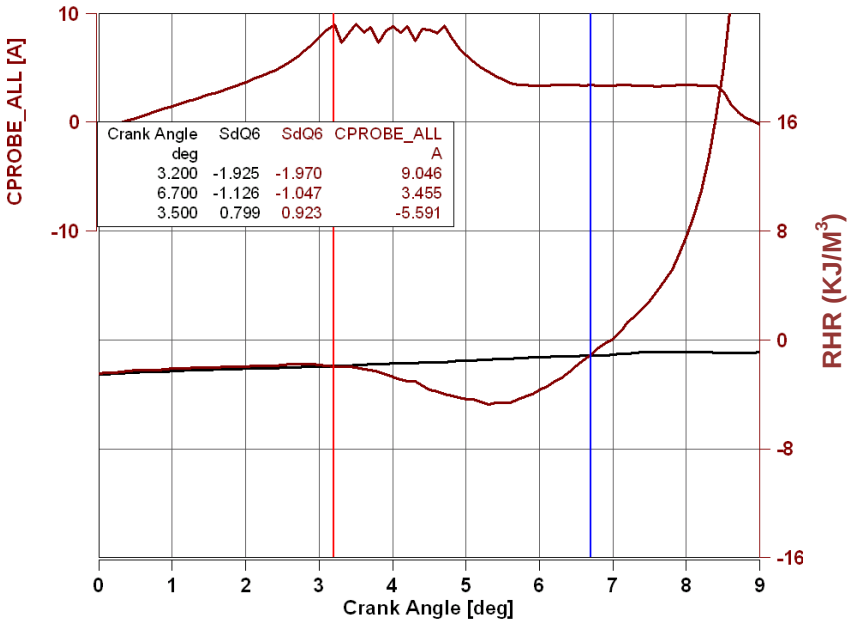

Figure 7.21 Ignition delay at 1300 rpm (B20).

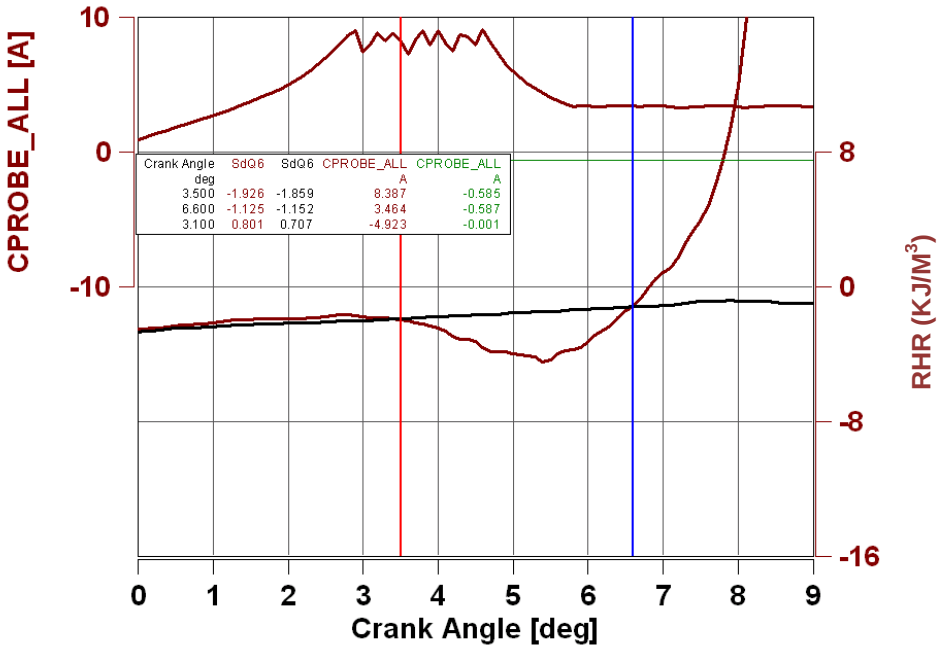

Figure 7.22 Ignition delay at 1500 rpm (B20).

www.manaraa.com

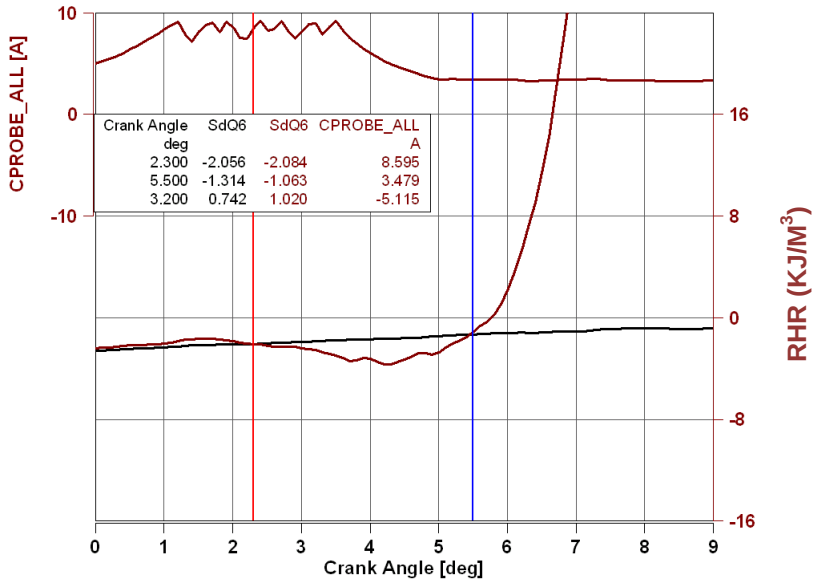

Figure 7.23 Ignition delay at 2000 rpm (B20).

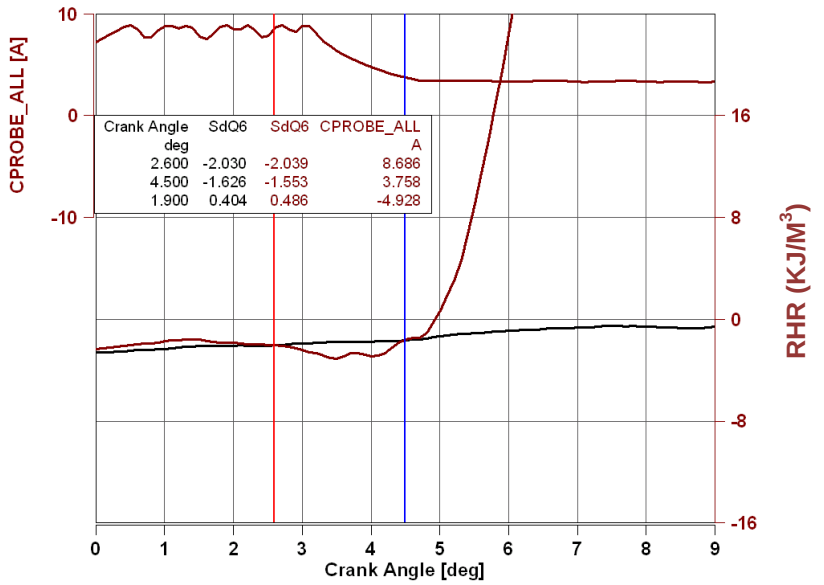

Figure 7.24 Ignition delay at 2200 rpm (B20).

www.manaraa.com

7.2.4. Effect of speed onS8 in cylinder combustion:

Figure 7.25 shows the running point with S8 (1300 rpm). Table 7.13 illustrates the few critical parameters at this running point.

Running point	Throttle valve opening	LPPC	RHR peak	Peak compression pressure	Peak combustion pressure	Fuel Consumption	Exhaust gas temperature
S8(With EGR)	57%	8.6^0 ATDC.	129 KJ/m^3	58 bars	65 bars	9.24 kg/hr	373 ^{0} C

Table 7.13 Critical parameters with S8 (with EGR) at 1300 rpm.

As the heating value on volumetric basis is lower than ULSD, the throttle is increased to 57%. As the bulk modulus is less than ULSD, the peak of the rail pressure is also less than ULSD for the same running point. Figure 7.29 shows the exploded view of RHR. The start of combustion gets advanced in case of S8 due to a higher cetane number. The ignition delay gets shortened to 2.9 CAD.

Figure 7.26 shows the running point at 1500 rpm. Table 7.14 illustrates the few critical parameters at this running point.

Running point	Throttle valve opening	LPPC	RHR peak	Peak compression pressure	Peak combustion pressure	Fuel Consumption	Exhaust gas temperature
S8(With EGR)	58%	8.9^0 ATDC.	143 KJ/m^3	63 bars	68 bars	11.06 kg/hr	356 ^{0} C

Table 7.14 Critical parameters with S8 (with EGR) at 1500 rpm.

As the heating value on volumetric basis is lower than ULSD, the throttle is increased to 58%. As the bulk modulus is less than ULSD, the peak of the rail pressure is also less than

www.manaraa.com

ULSD for the same running point. The ignition delay gets shortened and it is reduced to 2.5 CAD.

Figure 7.27 shows the running point at 2000 rpm with S8. Table 7.15 illustrates the few critical parameters at this running point.

Running point	Throttle valve opening	LPPC	RHR peak	Peak compression pressure	Peak combustion pressure	Fuel Consumption	Exhaust gas temperature
S8(With EGR)	59%	7.1^0 ATDC.	113 KJ/m^3	78 bars	72 bars	16.19 kg/hr	374 ^{0} C

Table 7.15 Critical parameters with S8 (with EGR) at 2000 rpm.

As the heating value on volumetric basis is lower than ULSD, the throttle is increased to 59%. Figure 7.31 shows the exploded view of RHR. The start of ignition takes place little earlier with respect to crank angle but due to EGR, the ignition delay is 2.7 CAD.

Figure 7.28 shows the running point at 2200 rpm. Table 7.16 illustrates the few critical parameters at this running point.

Running point	Throttle valve opening	LPPC	RHR peak	Peak compression pressure	Peak combustion pressure	Fuel Consumption	Exhaust gas temperature
S8(With EGR)	62%	6.7^0 ATDC.	110 KJ/m^3	84 bars	72 bars	18.61 kg/hr	387 ^{0} C

Table 7.16 Critical parameters with S8 (with EGR) at 2200 rpm.

As the heating value on volumetric basis is lower than ULSD, the throttle is increased to 62%. As the bulk modulus is less than ULSD, the peak of the rail pressure is also less than

www.manaraa.com

ULSD for the same running point. The ignition delay gets shortened and it is reduced to 1.7 CAD.

www.manaraa.com

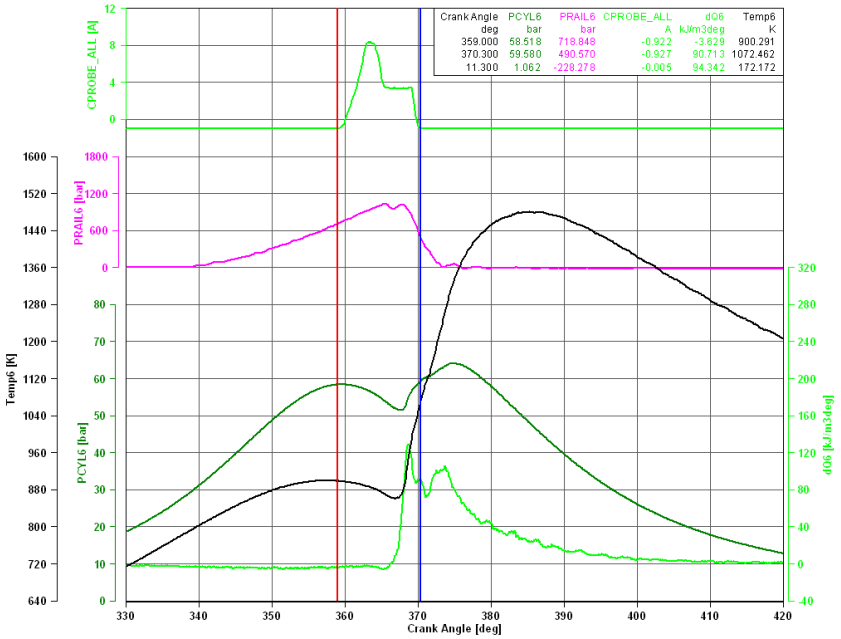

Figure 7.25 In cylinder combustion at 1300 rpm (S8).

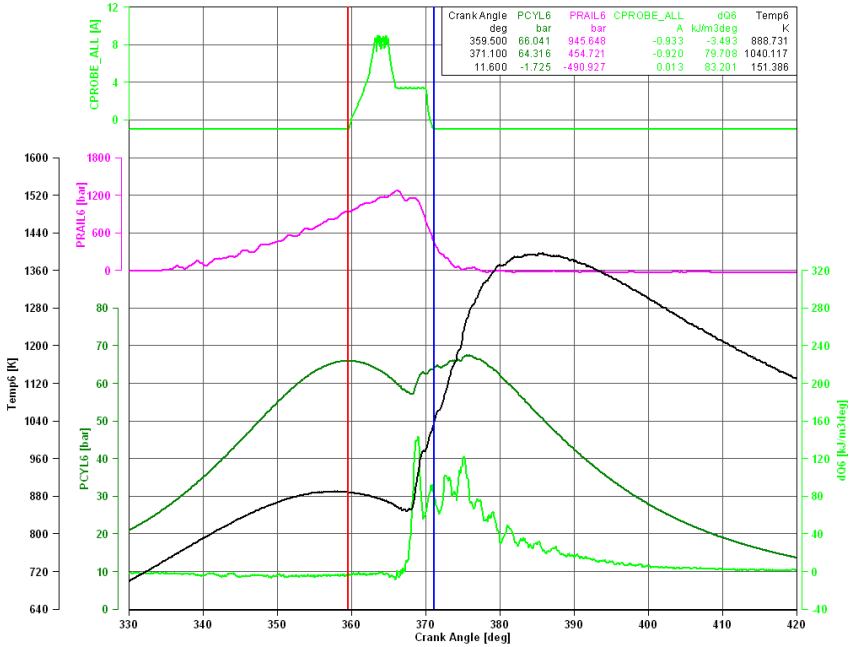

Figure 7.26 In cylinder combustion at 1500 rpm (S8).

www.manaraa.com

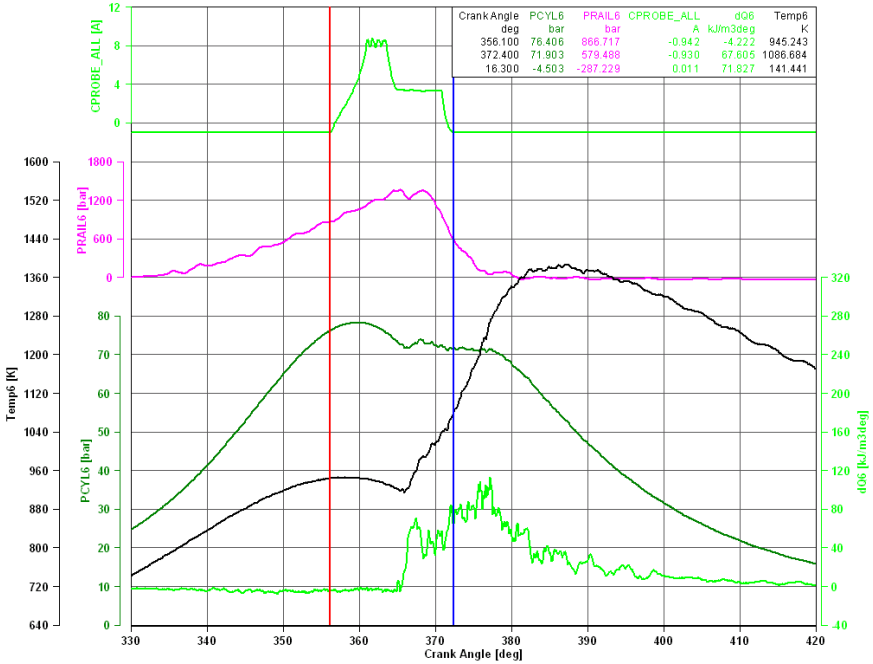

Figure 7.27 In cylinder combustion at 2000 rpm (S8).

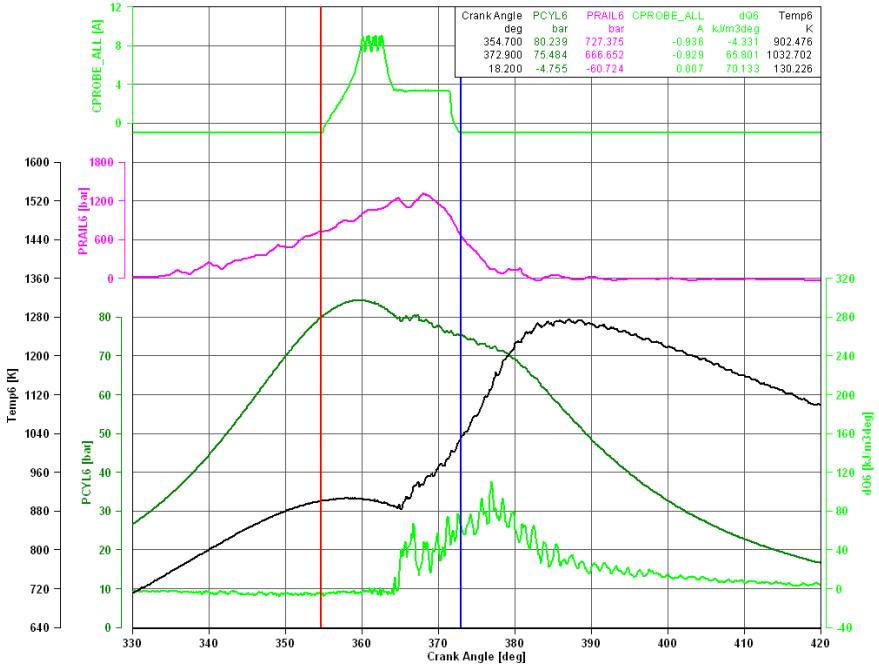

Figure 7.28 In cylinder combustion at 2200 rpm (S8).

www.manaraa.com

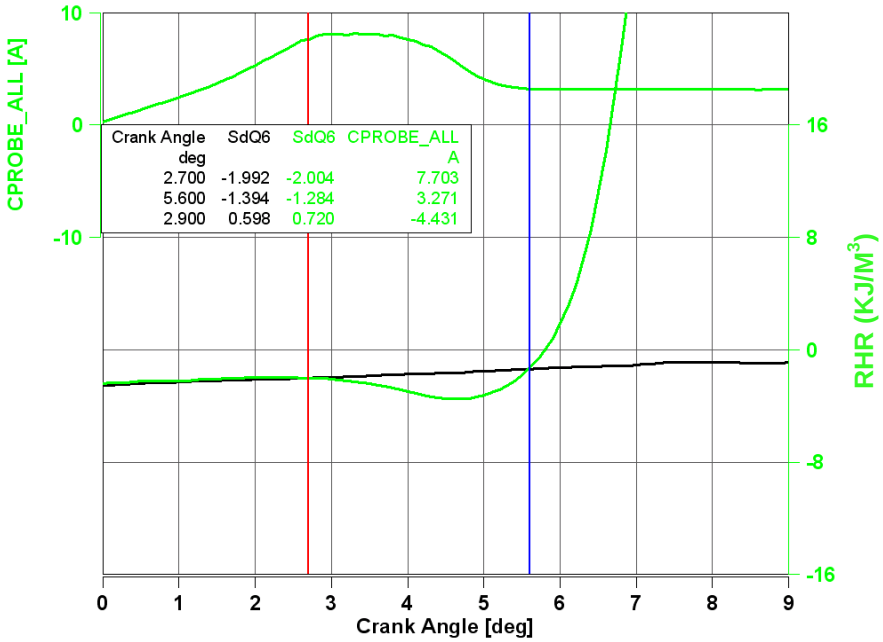

Figure 7.29 Ignition delay at 1300 rpm (S8).

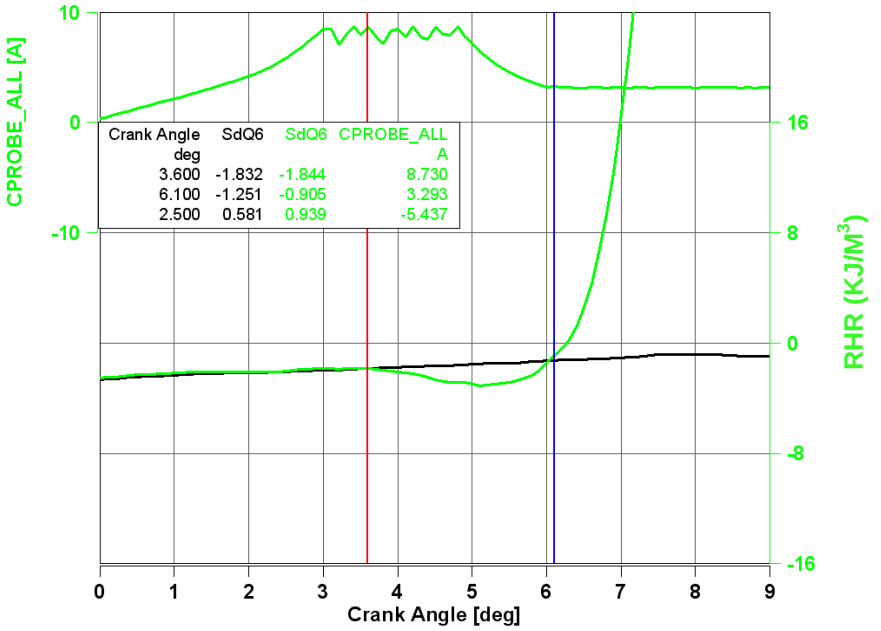

Figure 7.30 Ignition delay at 1500 rpm (S8**).**

www.manaraa.com

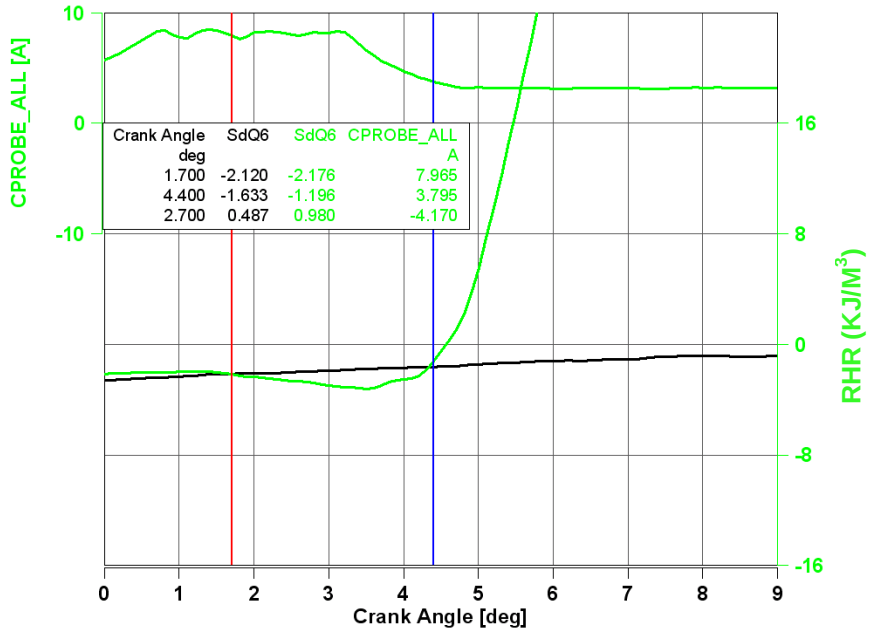

Figure 7.31 Ignition delay at 2000 rpm (S8).

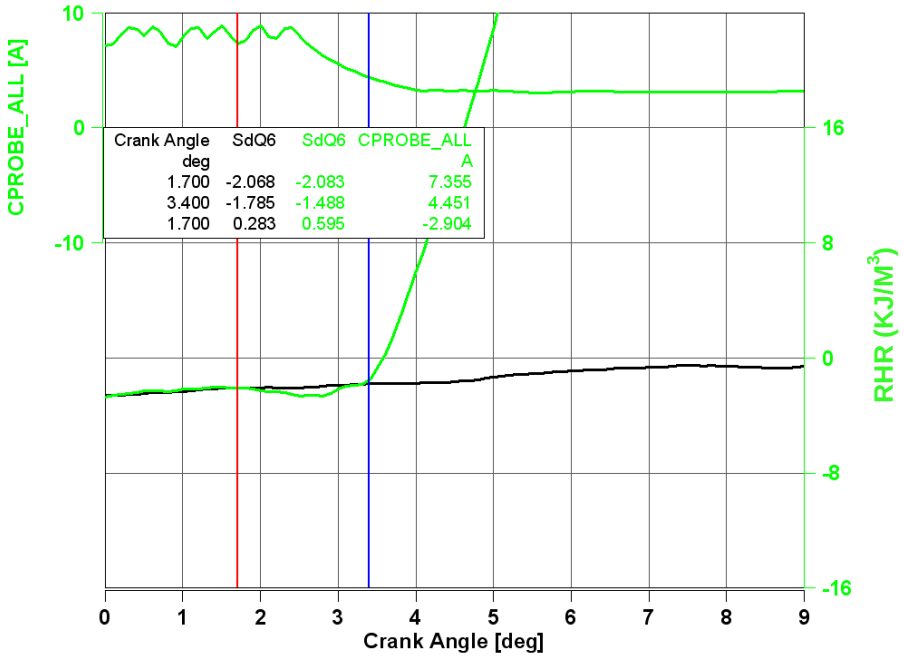

Figure 7.32 Ignition delay at 2200 rpm (S8).

www.manaraa.com

7.3 Effect of speed on emissions at 7.5 bar IMEP

7.3.1. Introduction:

The study is concentrated to investigate the effect of speed at the same load on emissions. As the engine is calibrated for ULSD, therefore, initially the engine was run on ULSD in order to know how the engine behaves with ULSD and to set the results as a benchmark in order to compare it with other results obtained using other alternative fuels.

7.3.2. Effect of speed on ULSD emissions:

Figure 7.3.1 shows the ULSD running point at 1300 rpm. It is very clear that from the experimental result that D.O.C. is very effective in reducing the CO emissions but not that effective in reducing HC emissions. The D.O.C. is almost 100% efficient in reducing the CO emissions and only 9% for HC emissions. There could be two causes for this trend:

1. First is that the CO oxidation is better over the catalyst due to better adsorption of the CO on the active catalyst sites.
2. Second, FTIR may not be the best instrument for measuring HC emissions. The FTIR only measures the hydrocarbons with confidence up to four carbon atoms, where as there may be higher/heavier components in the exhaust. Therefore, the measurement reading obtained from this instrument cannot be ascertained with a good confidence level.

Also, 85 to 95% of the NO_X emitted by diesel engine is NO. D.O.C. oxidizes part of the NO in the exhaust to NO_2. Therefore, there is an increase in the oxides of nitrogen after the aftertreatment device.

www.manaraa.com

Figure 7.3.5 illustrates the soot concentration emissions at 1300 rpm (ULSD). It is quite clear from the experimental results that the D.P.F. is very efficient in reducing the soot emissions. The efficiency of D.P.F. in reducing the soot emissions is about 99%.

Figure 7.3.2 shows the running point at 1500 rpm. The D.O.C. is almost 100% efficient in reducing the CO emissions but 16% for HC emissions.

From the experimental results at 1500 rpm, it is clear that the start of combustion gets advanced and the mass fraction burned by the premixed fraction of the two combustion fractions is increased. Also, the peak of bulk gas temperature is advanced with respect to crank angle degree as compared to 1300 rpm. Due to the above two reasons, there is an increase in the oxides of nitrogen at 1500 rpm. Due to lesser concentration of EGR, the CO and the unburnt hydrocarbons are lesser at 1500 rpm as compared to 1300 rpm.

Figure 9.6 illustrates the soot concentration emissions at 1500 rpm (ULSD). Due to lesser concentration of EGR, the soot concentration is lower at 1500 rpm as compared to 1300 rpm. The efficiency of D.P.F. in reducing the soot emissions is about 99%.

Figure 7.3.3 shows the running point at 2000 rpm. The D.O.C. is almost 100% efficient in reducing the CO emissions but 28% for HC emissions.

From the experimental results at 2000 rpm, it is clear that the start of combustion gets advanced but the mass fraction burned by the premixed fraction of the two combustion fractions is decreased. Increased concentration of EGR may have lead to this kind of trend. Also, the peak of bulk gas temperature is retarded with respect to crank angle degree. Due to the above two reasons, there is a decrease in the oxides of nitrogen at 2000 rpm. Also, due to the increase in speed, the residence time the combustion products spend in the cylinder is less and therefore, the CO emissions are high at 2000 rpm as compared to 1500 rpm.

www.manaraa.com

Figure 7.3.7 illustrates the soot concentration emissions at 2000 rpm (ULSD).As the premixed fraction of the two combustion fractions is less at 2000 rpm, therefore, the soot concentration emissions are more as compared to 1500 rpm. The efficiency of D.P.F. in reducing the soot emissions is 99%.

Figure 7.3.4 shows the running point at 2200 rpm. The D.O.C. is 100% efficient in reducing the CO emissions where as incase of HC emissions it is 37%.

From the experimental results at 2200 rpm, it is clear that the start of combustion gets advanced and the mass fraction burned by the premixed fraction of the two combustion fractions is decreased. Also, the peak of bulk gas temperature is retarded as compared to 2000 rpm. Due to the above two reasons, there is a decrease in the oxides of nitrogen at 2200 rpm. Also, due to the increase in speed, the residence time the combustion products spend in the cylinder is less and therefore, the CO emissions are high at 2200 rpm as compared to 2000 rpm.

Figure 7.3.8 illustrates the soot concentration emissions at 2200 rpm (ULSD). As the premixed fraction of the two combustion fractions is less at 2200 rpm, therefore, the soot concentration emissions are more as compared to 2000 rpm. The efficiency of D.P.F. in reducing the soot emissions is about 99%.

www.manaraa.com

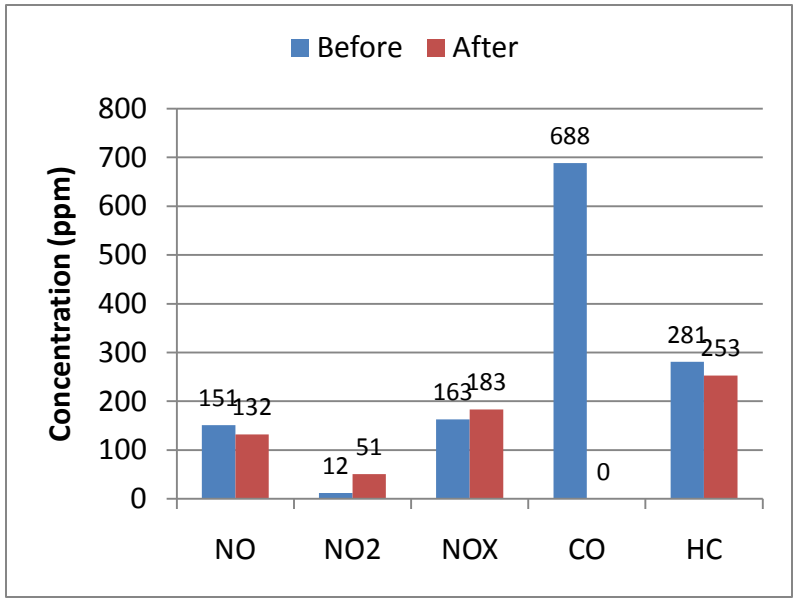

Figure 7.3.1 Emissions at 1300 rpm (ULSD).

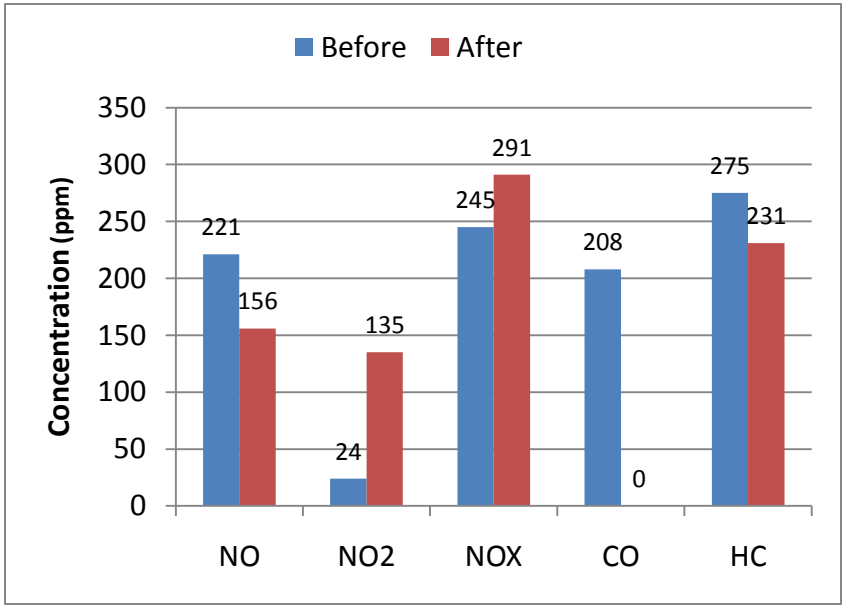

Figure 7.3.2 Emissions at 1500 rpm (ULSD).

www.manaraa.com

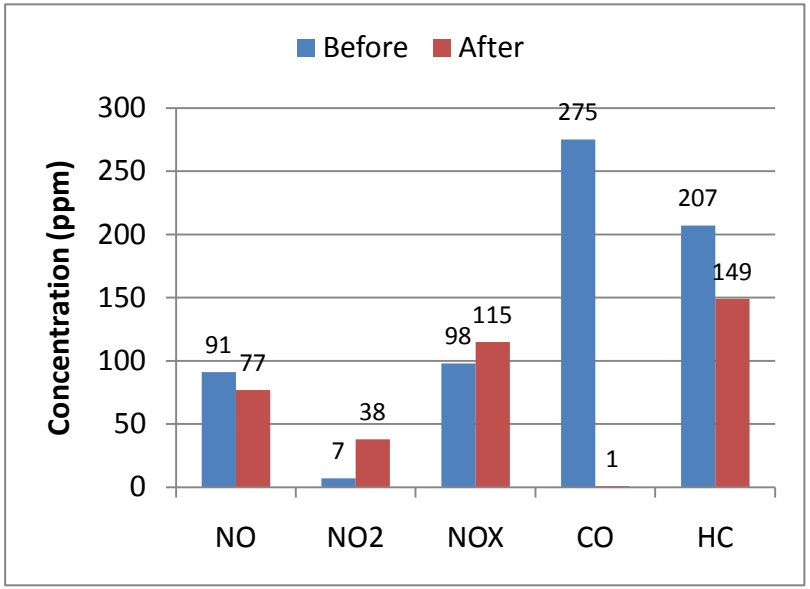

Figure 7.3.3 Emissions at 2000 rpm (ULSD).

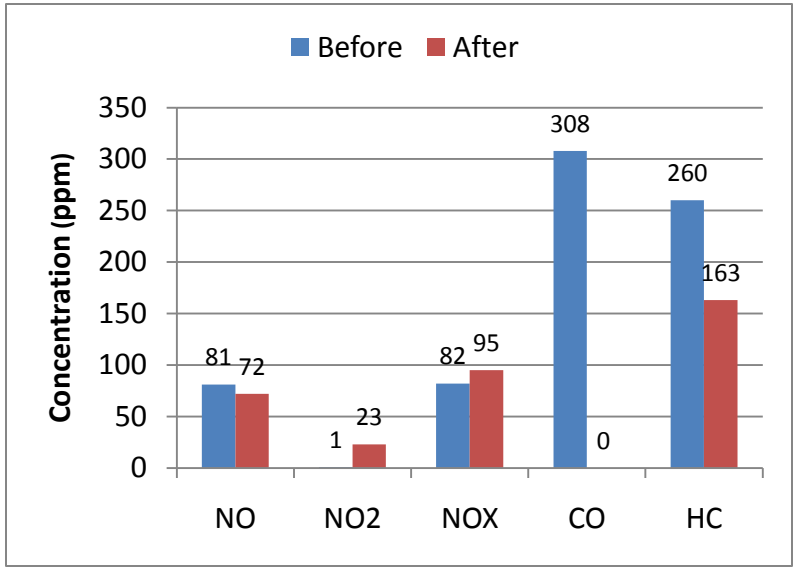

Figure 7.3.4 Emissions at 2200 rpm (ULSD).

www.manaraa.com

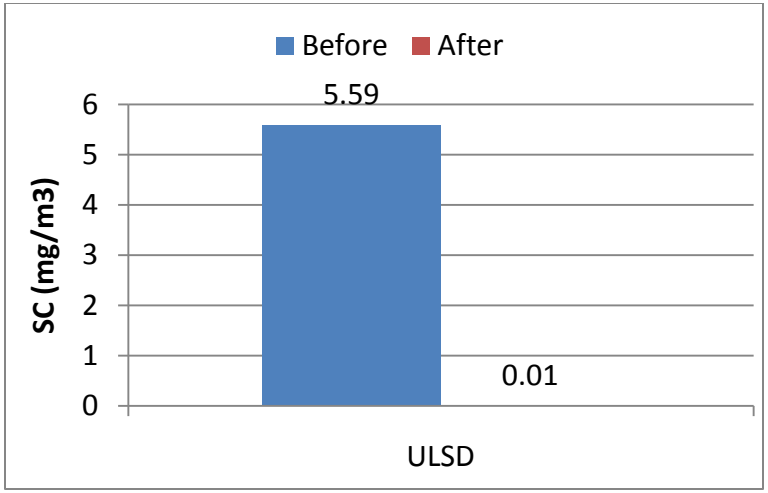

Figure 7.3.5 Soot concentration at 1300 rpm (ULSD).

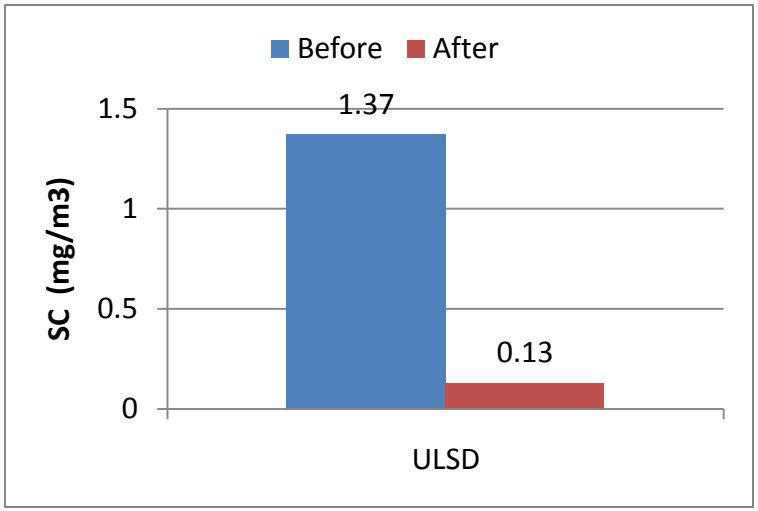

Figure 7.3.6 Soot concentration at 1500 rpm (ULSD).

www.manaraa.com

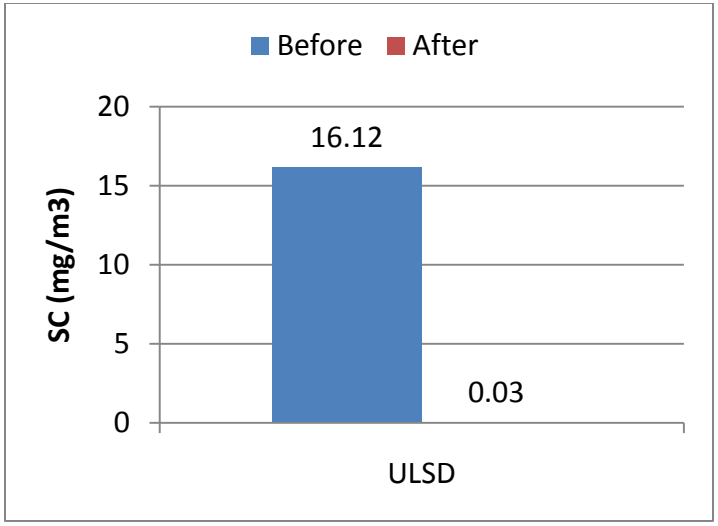

Figure 7.3.7 Soot concentration at 2000 rpm (ULSD).

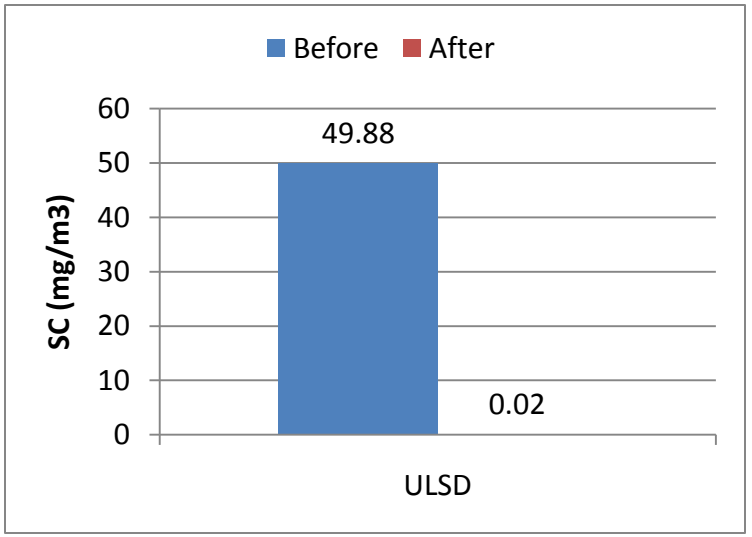

Figure 7.3.8 Soot concentration at 2200 rpm (ULSD).

www.manaraa.com

7.3.3. Effect of speed on JP8 emissions:

Figure 7.3.9 shows the JP8 running point at 1300 rpm. The effect of D.O.C. has a similar trend on the emissions as compared to ULSD.

NO_X emissions are higher in this case as compared to ULSD because of a higher fraction of premixed combustion burn of the two combustion fraction burns. CO and unburnt hydrocarbon emissions are less as compared to ULSD because JP8 fuel is more volatile and thus the in cylinder combustion is more complete in nature. In order to get almost the same engine out emissions as compared to ULSD emissions, the fuel injection in this case will have to be advanced.

Figure 7.3.13 illustrates the soot concentration emissions at 1300 rpm (JP8). The efficiency of D.P.F. in reducing the soot emissions is 94%. JP8 produces 77% less soot as compared to ULSD at this running condition because of higher premixed combustion and lower aromatic content.

Figure 7.3.10 shows the running point at 1500 rpm. The difference in NO_X emissions as compared to ULSD is negligible. CO and unburnt hydrocarbon emissions are higher as compared to ULSD.

Figure 7.3.14 illustrates the soot concentration emissions at 1500 rpm (JP8). JP8 produces 36% less soot as compared to ULSD at this running condition because of higher premixed fraction burn and lower aromatic content.

Figure 7.3.11 shows the running point at 2000 rpm. NO_X emissions are slightly higher in this case as compared to ULSD because in this case the magnitude of peak of in cylinder bulk gas temperature is higher as compared to ULSD. Also, the location of peak of in cylinder bulk gas temperature is slightly advanced as compared to ULSD. CO and unburnt hydrocarbon

www.manaraa.com

emissions are higher as compared to ULSD because of possibly lesser amount of post oxidation reactions in the expansion stroke

Figure 7.3.15 illustrates the soot concentration emissions at 2000 rpm (JP8). JP8 produces 18% less soot as compared to ULSD at this running condition because of higher premixed fraction burn and lower aromatic content.

Figure 7.3.12 shows the running point at 2200 rpm. NO_X emissions are slightly higher in this case as compared to ULSD in this case the magnitude of peak of in cylinder bulk gas temperature is higher as compared to ULSD. Also, the location of peak of in cylinder bulk gas temperature is slightly advanced as compared to ULSD. CO and unburnt hydrocarbon emissions are higher as compared to ULSD because of possibly lesser amount of post oxidation reactions in the expansion stroke

Figure 7.3.16 illustrates the soot concentration emissions at 2200 rpm (JP8). JP8 produces 8% less soot as compared to ULSD at this running condition because of higher premixed fraction burn and lower aromatic content.

www.manaraa.com

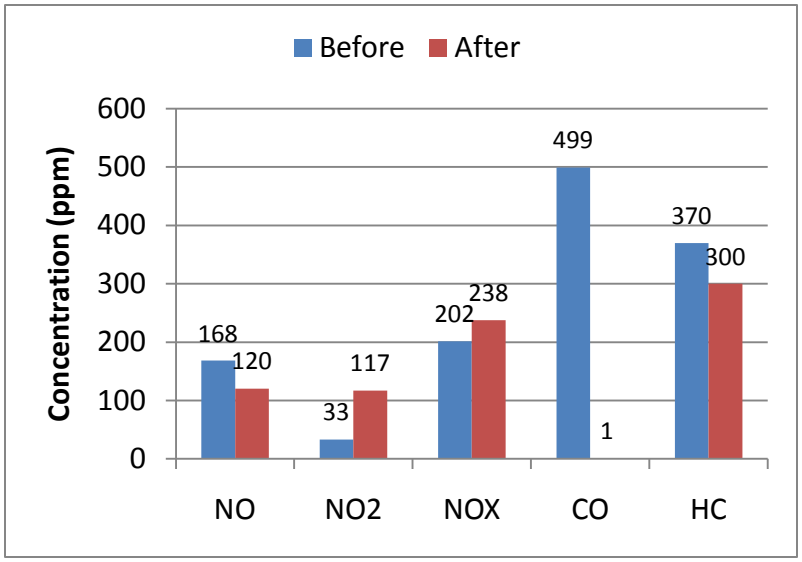

Figure 7.3.9 Emissions at 1300 rpm (JP8).

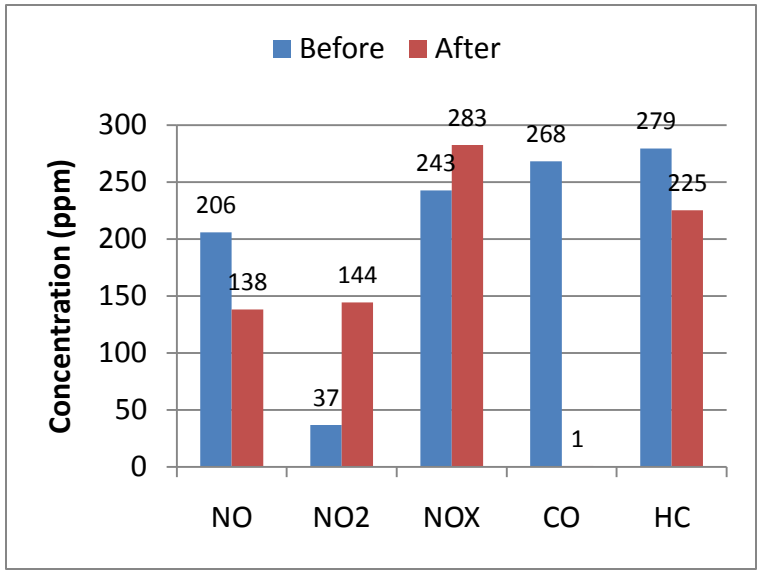

Figure 7.3.10 Emissions at 1500 rpm (JP8).

www.manaraa.com

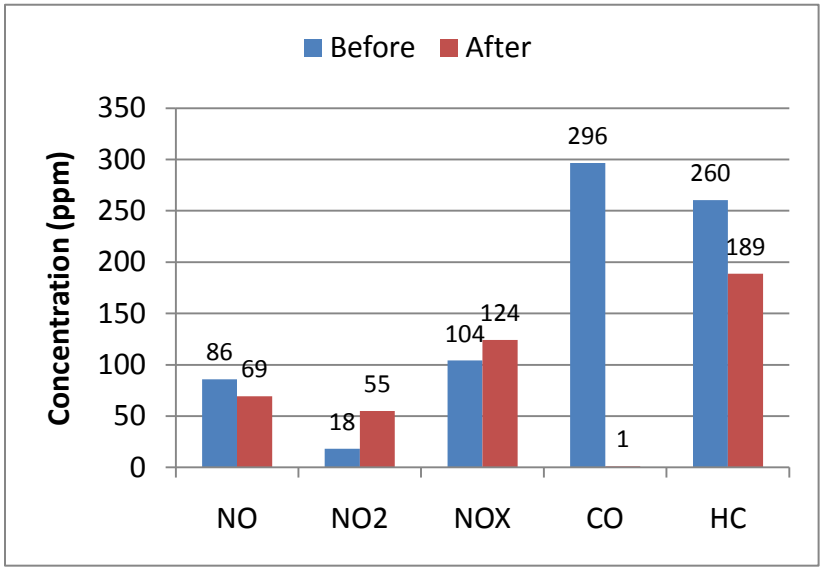

Figure 7.3.11 Emissions at 2000 rpm (JP8).

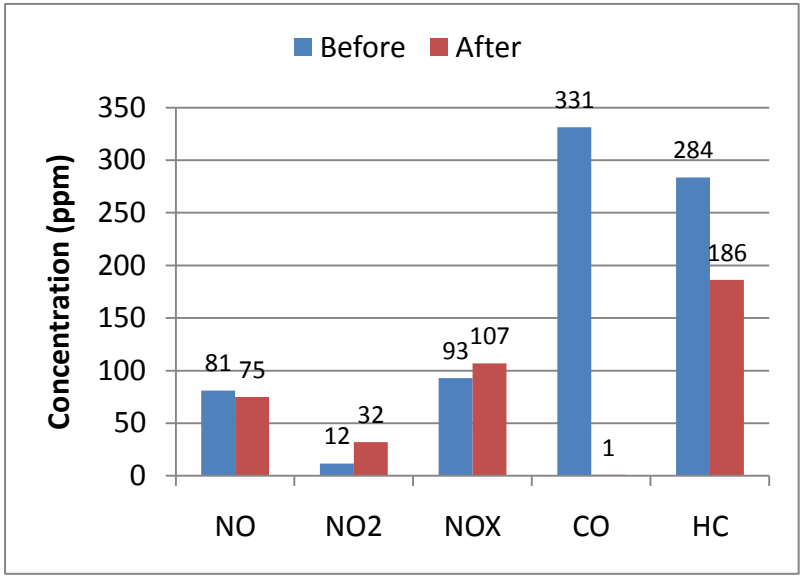

Figure 7.3.12 Emissions at 2200 rpm (JP8).

www.manaraa.com

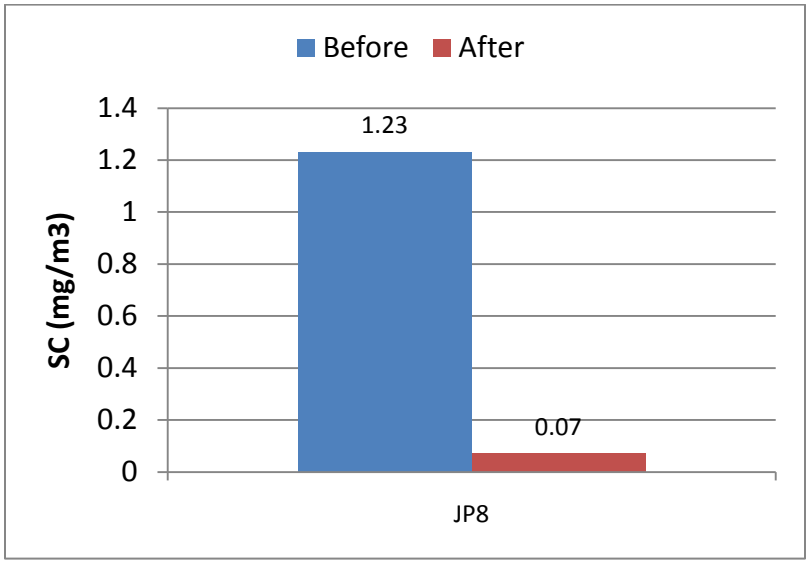

Figure 7.3.13 Soot concentration at 1300 rpm (JP8).

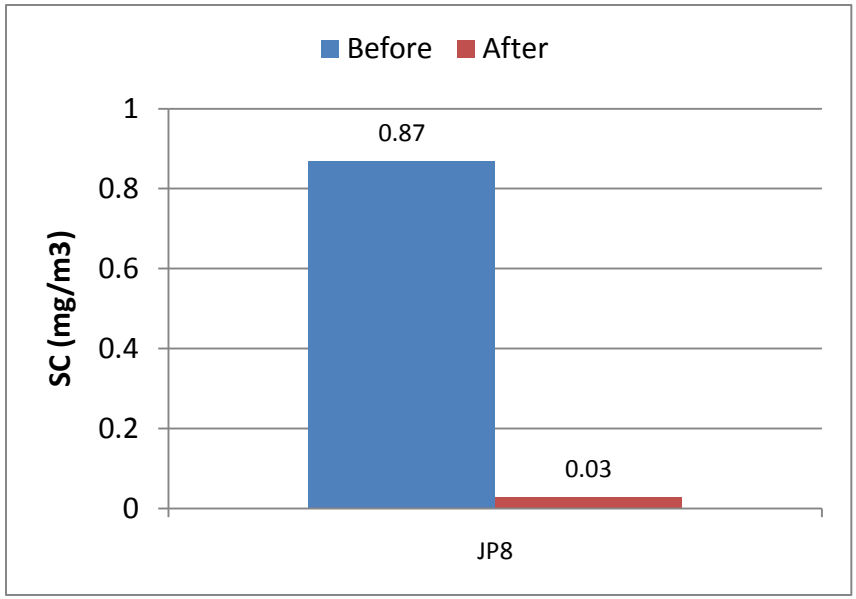

Figure 7.3.14 Soot concentration at 1500 rpm (JP8).

www.manaraa.com

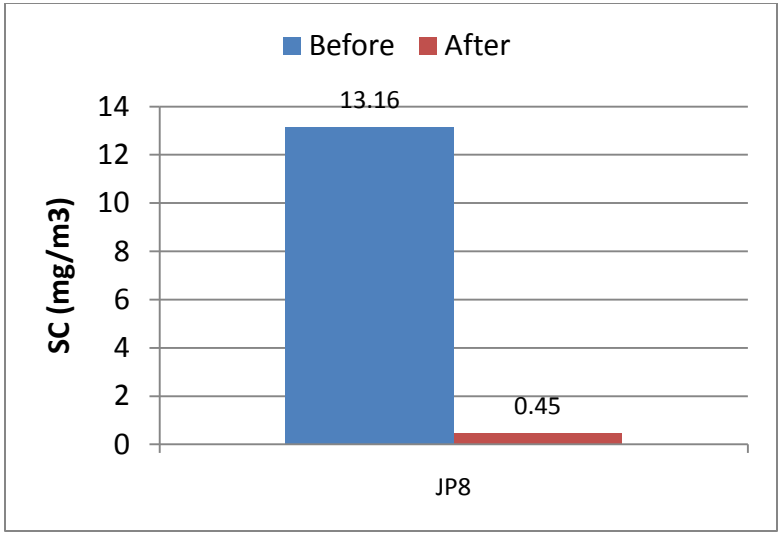

Figure 7.3.15 Soot concentration at 2000 rpm (JP8

.

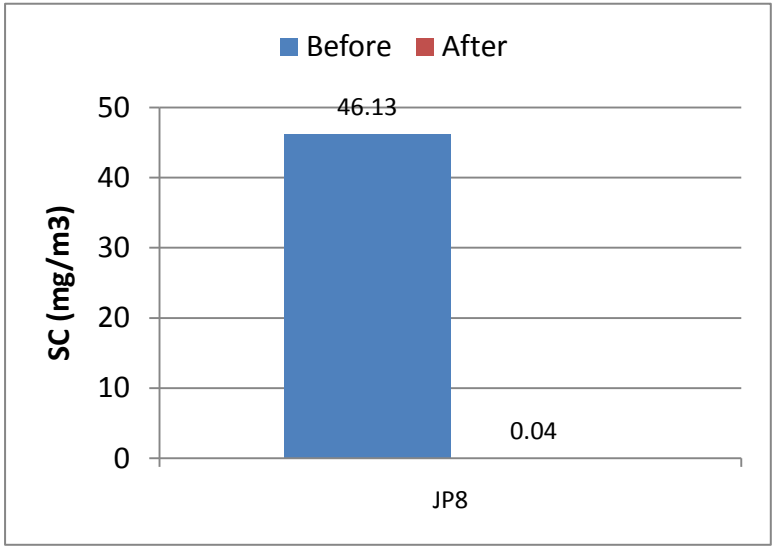

Figure 7.3.16 Soot concentration at 2200 rpm (JP8)

www.manaraa.com

7.3.4. Effect of speed on B20 emissions:

Figure 7.3.17 shows the B20 running point at 1300 rpm. The D.O.C. has a similar effect on emissions as in the case of ULSD. CO and unburnt hydrocarbon emissions are less as compared to ULSD because B20 fuel is oxygen rich. In order to get almost the same engine out emissions as compared to ULSD emissions, the fuel injection in this case will have to be retarded slightly.

Figure 7.3.21 illustrates the soot concentration emissions at 1300 rpm (B20). B20 produces 26% less soot as compared to ULSD at this running condition because it is an oxygen rich fuel.

Figure 7.3.18 shows the running point at 1500 rpm. At this running point B20 produces the lesser oxides of nitrogen as in the case of ULSD. CO and unburnt hydrocarbon emissions are less as compared to ULSD because B20 fuel is oxygen rich.

Figure 7.3.22 illustrates the soot concentration emissions at 1500 rpm (B20). B20 produces 44% less soot as compared to ULSD at this running condition because it is an oxygen rich fuel.

Figure 7.3.19 shows the running point at 2000 rpm. NO_X is higher for B20 as compared to ULSD because the combustion products spend more time in the critical temperature window. CO emissions are less as compared to ULSD because B20 fuel is oxygen rich.

Figure 7.3.23 illustrates the soot concentration emissions at 2000 rpm (B20). B20 produces 16% less soot as compared to ULSD at this running condition because it is an oxygen rich fuel.

www.manaraa.com

Figure 7.3.23 shows the running point at 2200 rpm. NO_X is higher for B20 as compared to ULSD because the combustion products spend more time in the critical temperature window. CO and unburnt hydrocarbon emissions are less as compared to ULSD because B20 fuel is oxygen rich.

Figure 7.3.24 illustrates the soot concentration emissions at 2200 rpm (B20). B20 produces 27% less soot as compared to ULSD at this running condition because it is an oxygen rich fuel.

www.manaraa.com

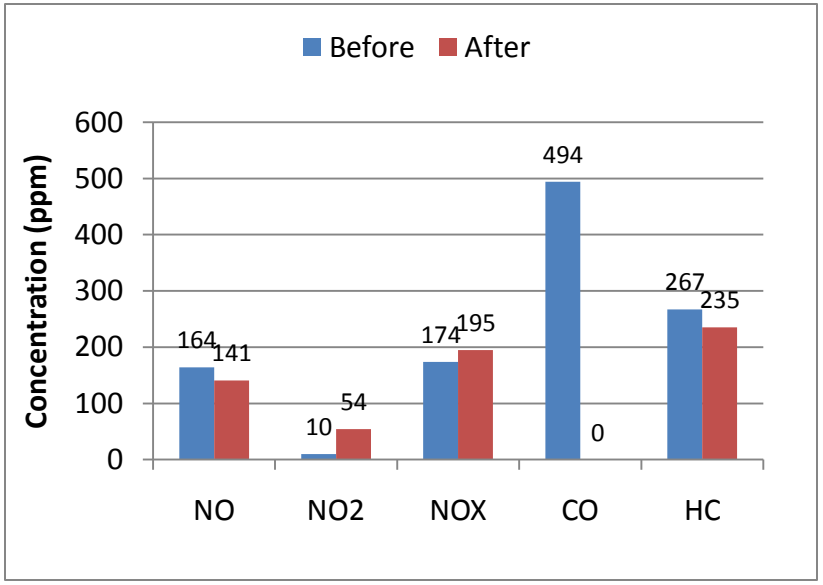

Figure 7.3.17 Emissions at 1300 rpm (B20).

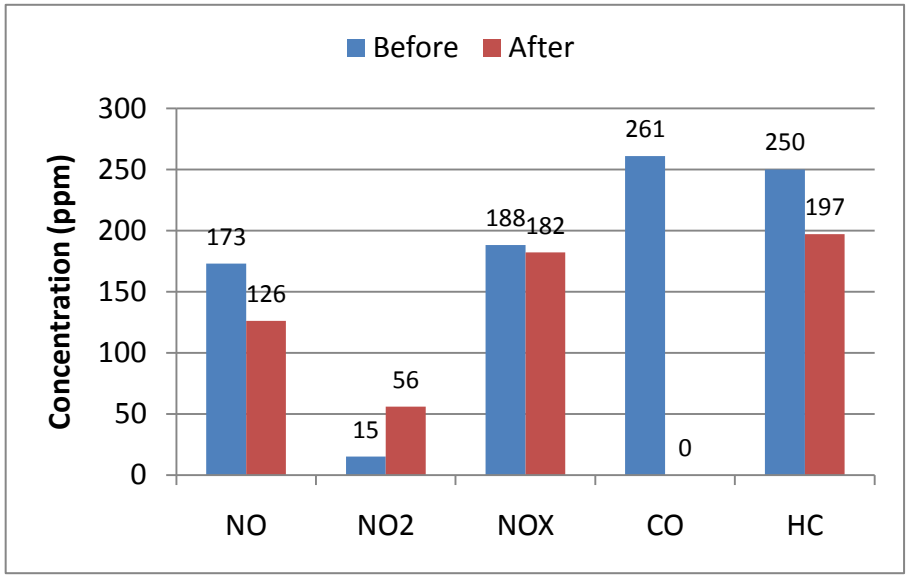

Figure 7.3.18 Emissions at 1500 rpm (B20).

www.manaraa.com

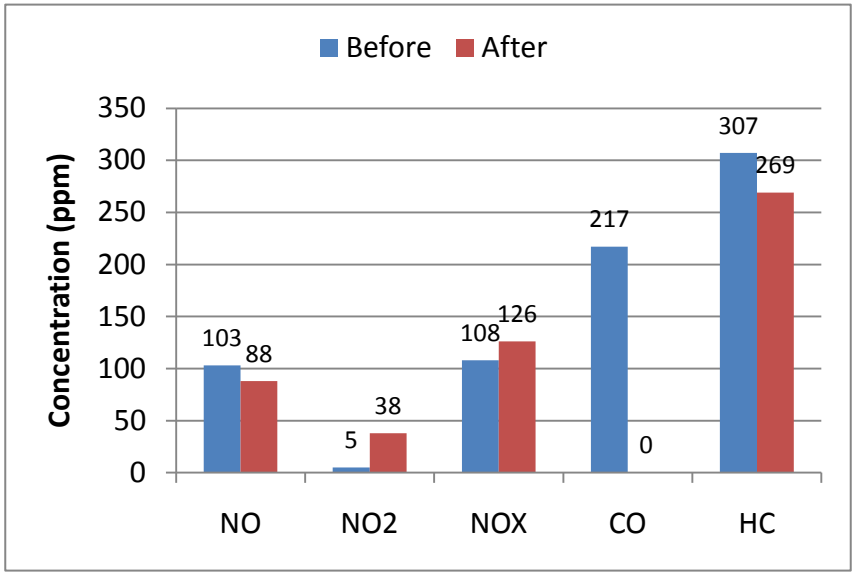

Figure 7.3.19 Emissions at 2000 rpm (B20).

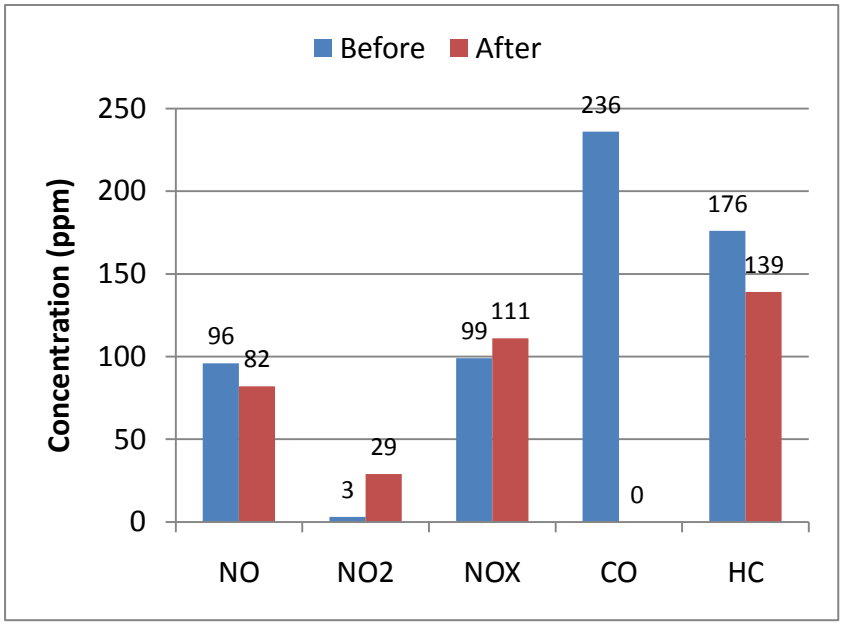

Figure 7.3.20 Emissions at 2200 rpm (B20).

www.manaraa.com

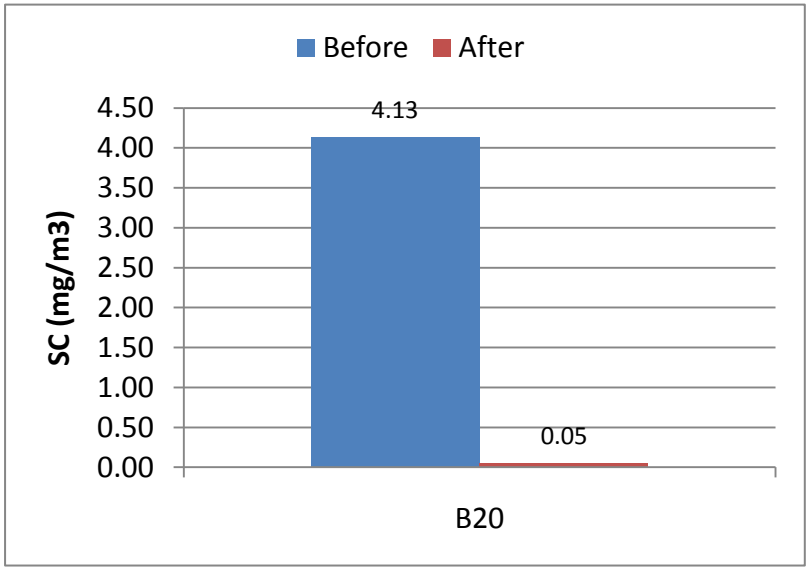

Figure 7.3.21 Soot concentration at 1300 rpm (B20).

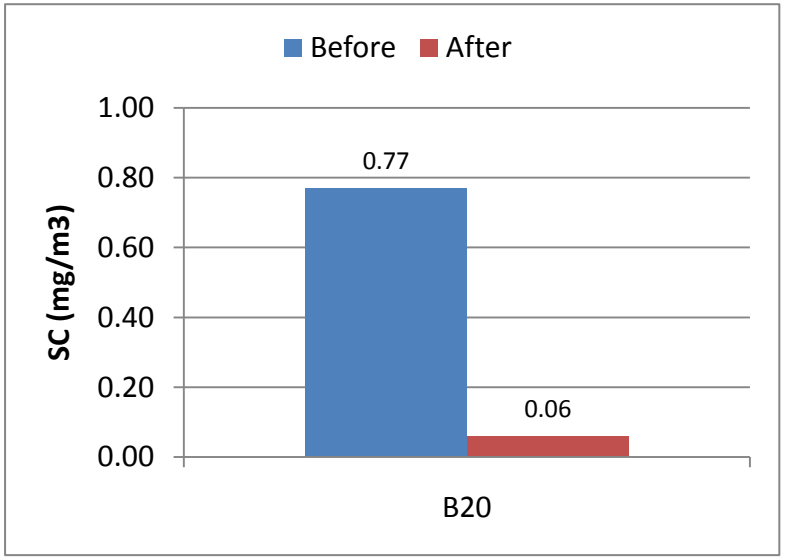

Figure 7.3.22 Soot concentration at 1500 rpm (B20).

www.manaraa.com

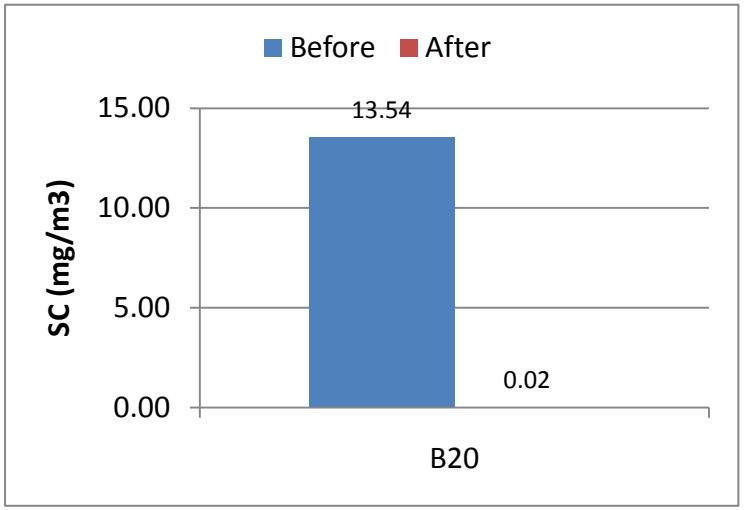

Figure 7.3.23 Soot concentration at 2000 rpm (B20).

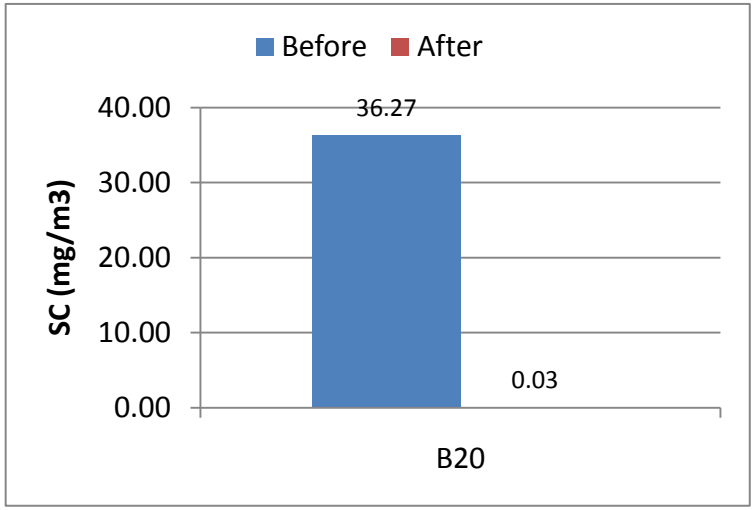

Figure 7.3.24 Soot concentration at 2200 rpm (B20).

www.manaraa.com

7.3.5. Effect of speed on S8 emissions:

Figure 7.3.25 shows the S8 running point at 1300 rpm. NO_X emissions are higher in this case as compared to ULSD because in this case the residence time the combustion products spent in the critical temperature window (for NO formation) is higher. CO and unburnt hydrocarbon emissions are less as compared to ULSD because S8 fuel is more volatile and has a fairly high cetane number. Therefore, the in cylinder combustion is much more complete. In order to get almost the same engine out emissions as compared to ULSD emissions, the fuel injection in this case will have to be retarded.

Figure 7.3.29 illustrates the soot concentration emissions at 1300 rpm (S8). S8 produces 39% less soot as compared to ULSD at this running condition because of lower aromatic content and higher volatility.

Figure 7.3.26 shows the running point at 1500 rpm. NO_X emissions are slightly higher in this case as compared to ULSD because in this case the residence time the combustion products spent in the critical temperature window (for NO formation) is slightly higher. CO and unburnt hydrocarbon emissions are less as compared to ULSD because S8 fuel is more volatile and has a fairly high cetane number.

Figure 7.3.30 illustrates the soot concentration emissions at 1500 rpm (S8). S8 produces 20% less soot as compared to ULSD at this running condition because of lower aromatic content higher volatility.

Figure 7.3.27 shows the running point at 2000 rpm. NO_X emissions are slightly higher in this case as compared to ULSD because in this case the residence time the combustion products spent in the critical temperature window (for NO formation) is slightly higher. CO emissions are less as compared to ULSD because S8 fuel is more volatile and has a fairly high cetane number.

www.manaraa.com

Figure 7.3.31 illustrates the soot concentration emissions at 2000 rpm (S8). S8 produces 42% less soot as compared to ULSD at this running condition because of lower aromatic content higher volatility.

Figure 7.3.28 shows the running point at 2200 rpm. NO_X emissions are slightly higher in this case as compared to ULSD because in this case the residence time the combustion products spent in the critical temperature window (for NO formation) is slightly higher. CO and unburnt hydrocarbon emissions are less as compared to ULSD because S8 fuel is more volatile and has a fairly high cetane number.

Figure 7.3.32 illustrates the soot concentration emissions at 2200 rpm (S8). As the premixed fraction of the two combustion fractions is less at 2200 rpm, therefore, the soot concentration emissions are more as compared to 2000 rpm. S8 produces 34% less soot as compared to ULSD at this running condition because of lesser aromatic content and higher volatility.

www.manaraa.com

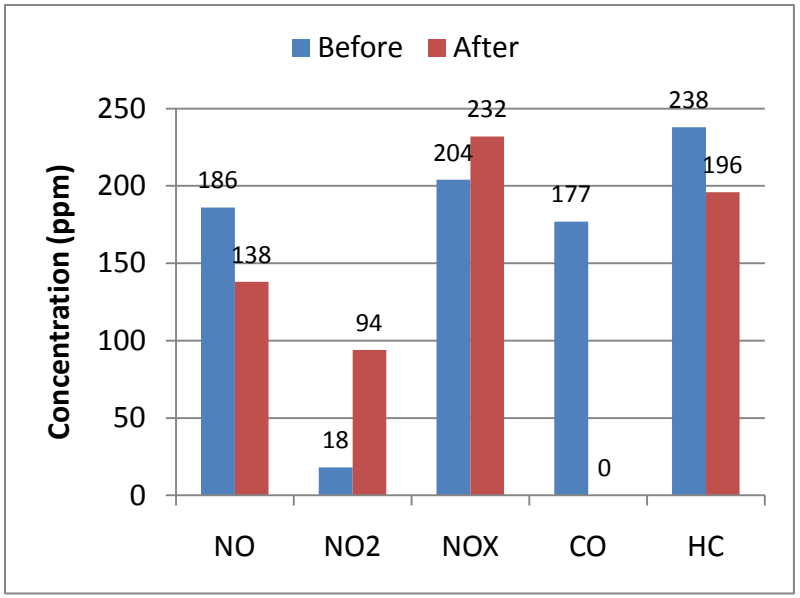

Figure 7.3.25 Emissions at 1300 rpm (S8).

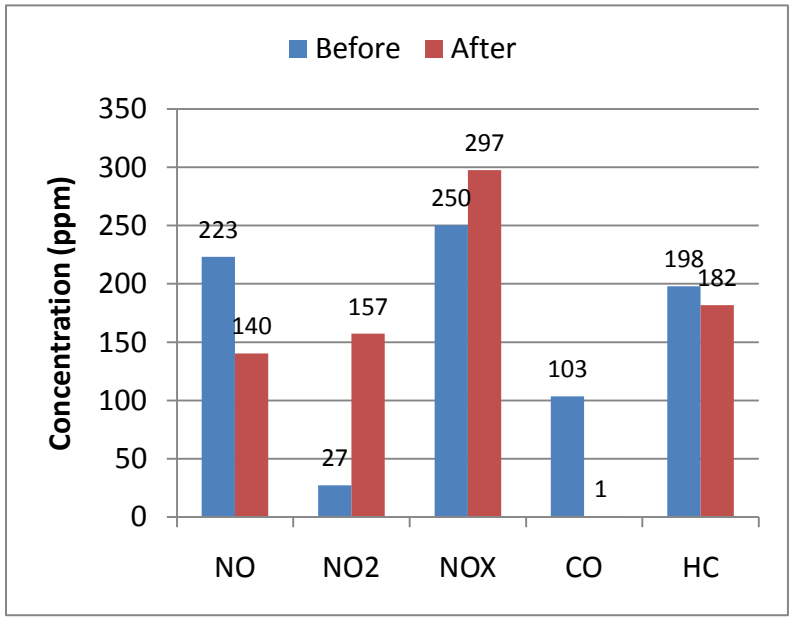

Figure 7.3.26 Emissions at 1500 rpm (S8).

www.manaraa.com

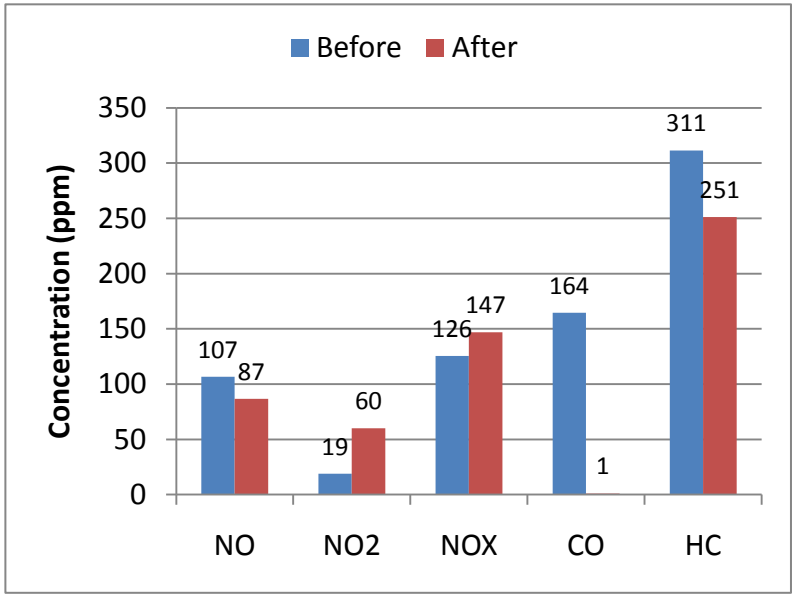

Figure 7.3.27 Emissions at 2000 rpm (S8).

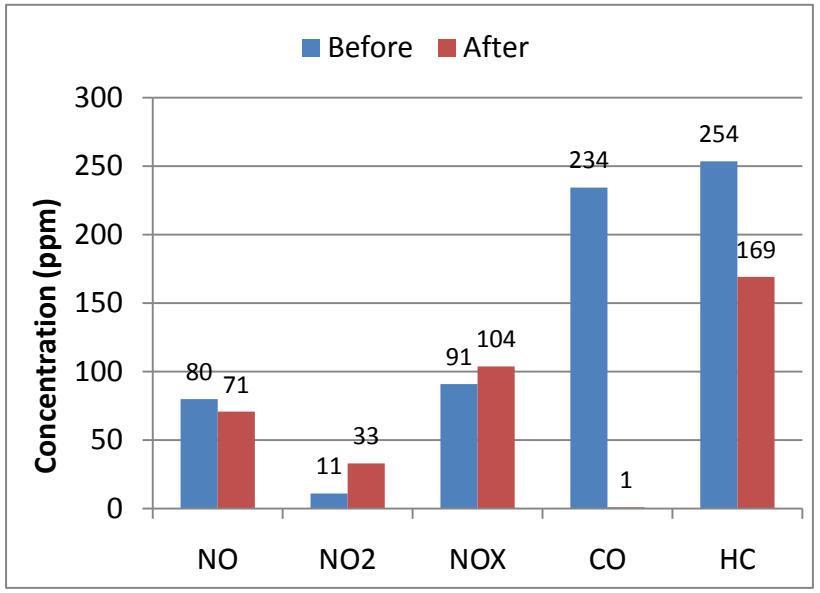

Figure 7.3.28 Emissions at 2200 rpm (S8).

www.manaraa.com

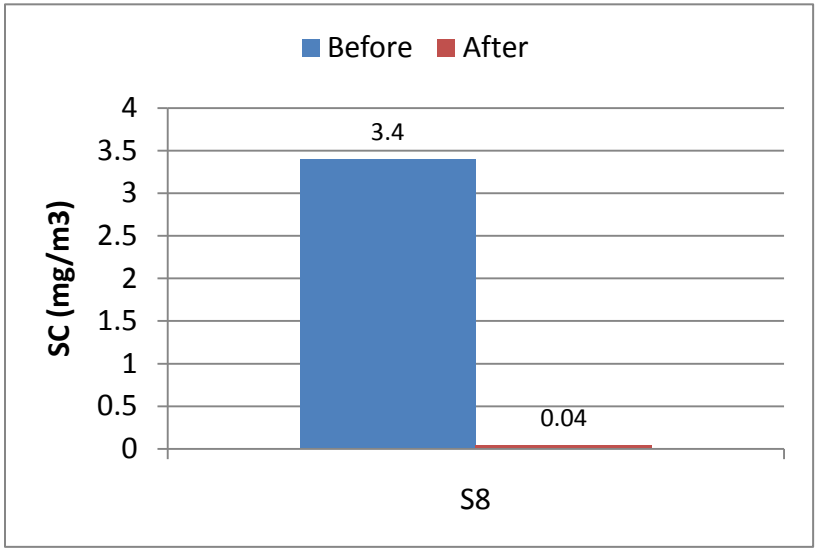

Figure 7.3.29 Soot concentration at 1300 rpm (S8).

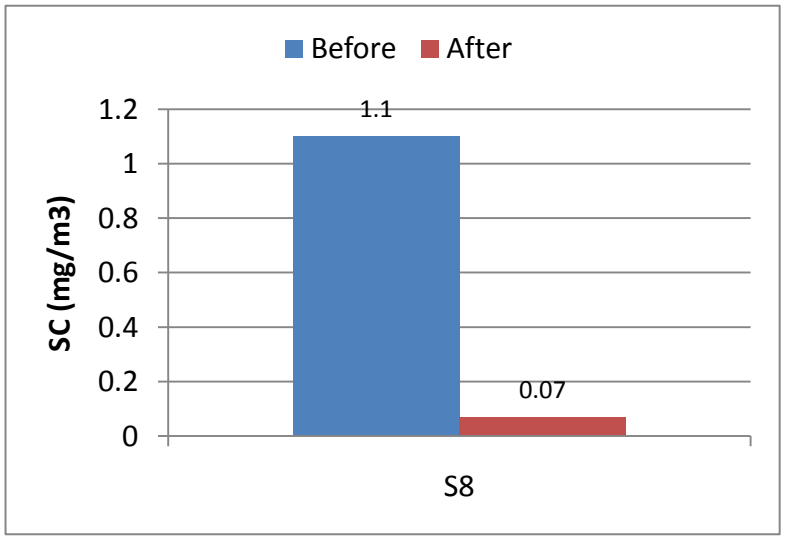

Figure 7.3.30 Soot concentration at 1500 rpm (S8).

www.manaraa.com

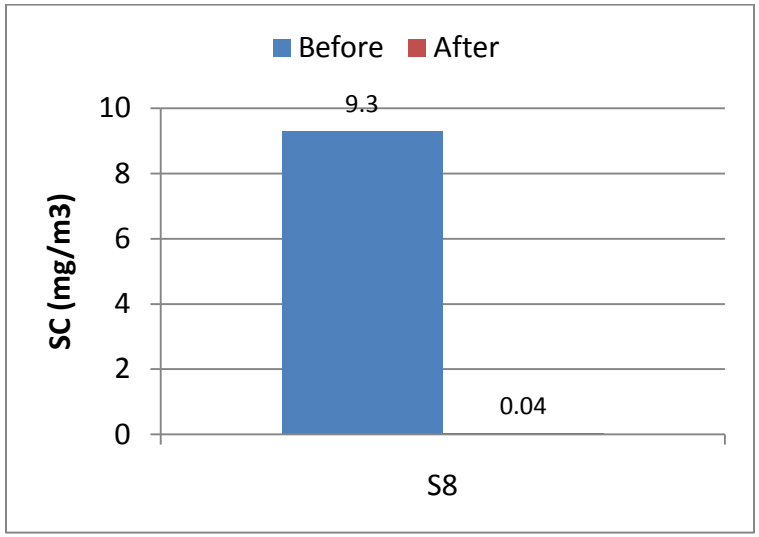

Figure 7.3.31 Soot concentration at 2000 rpm (S8).

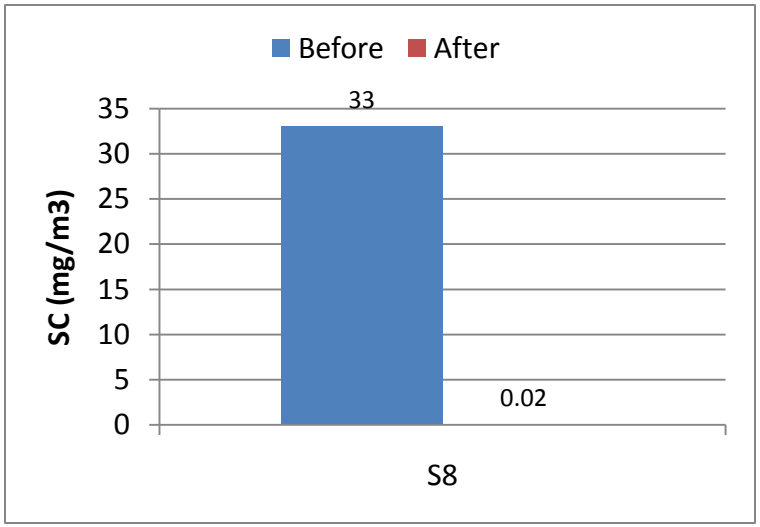

Figure 7.3.32 Soot concentration at 2200 rpm (S8).

www.manaraa.com

Conclusions:

1. The fuel rail pressure increases with the increase in speed for all the fuels. However, at 2200 rpm, the rail pressure reduces for all the fuels. The trend is necessary in order to take care of the oxides of nitrogen.
2. The engine tries to maintain the same injection timing irrespective of different fuels at different running conditions. However, there is a difference in the combustion phasing depending upon the fuel properties of different fuels.
3. The fuel consumption increases linearly with the increase in speed. There is a slight difference in the fuel consumption of different fuels depending upon the lower heating value of the fuels.
4. At all speeds, B20 has the highest fuel consumption, followed by ULSD, followed by JP8 and then by S8 as illustrated in figure 7.33. This trend is because of the respective lower heating values of the fuels. B20 has the lowest heating value, followed by the ULSD, followed by JP8 and then by S8.

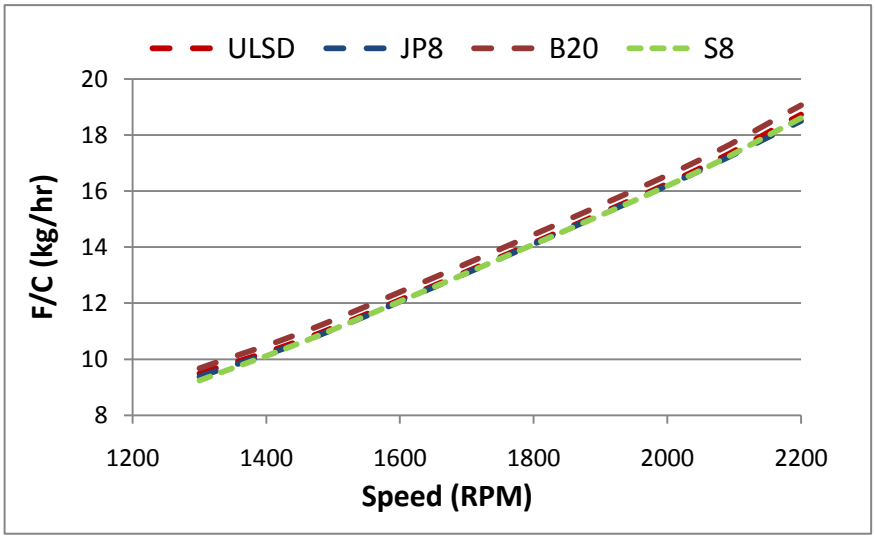

Figure 7.3.33 Effect of speed on fuel consumption.

www.manaraa.com

5. Due to a lower value of bulk modulus of JP8 and S8, the pressure developed in the pumping process is lower as compared to ULSD. The throttle opening in case of JP8 and S8 is more as compared to ULSD because of a lower density. Due to a higher value of bulk modulus of B20, the pressure developed in the pumping process is higher in case of B20 as compared to ULSD. The throttle opening in case of B20 is same as compared to ULSD.
6. At 7.5 bar IMEP, the diffusion combustion burn fraction is dominant as compared to the premixed combustion burn fraction. Therefore, the fuel properties such as the cetane number, aromatic content etc plays a very vital role in the engine out emissions.

. Figure 7.3.33 shows the effect of speed on NO_X emissions for all the tested fuels.

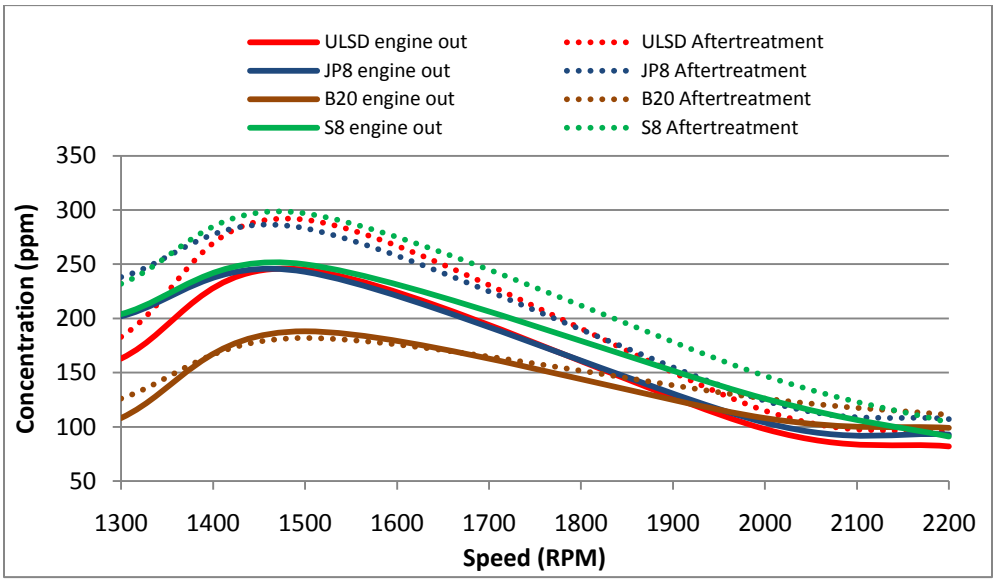

Figure 7.3.34 Effect of speed on NOx.

Figure 7.3.34 shows the effect of speed on CO emissions for all the tested fuels and figure 7.3.35 shows the effect of speed on soot concentration for all the fuels.

www.manaraa.com

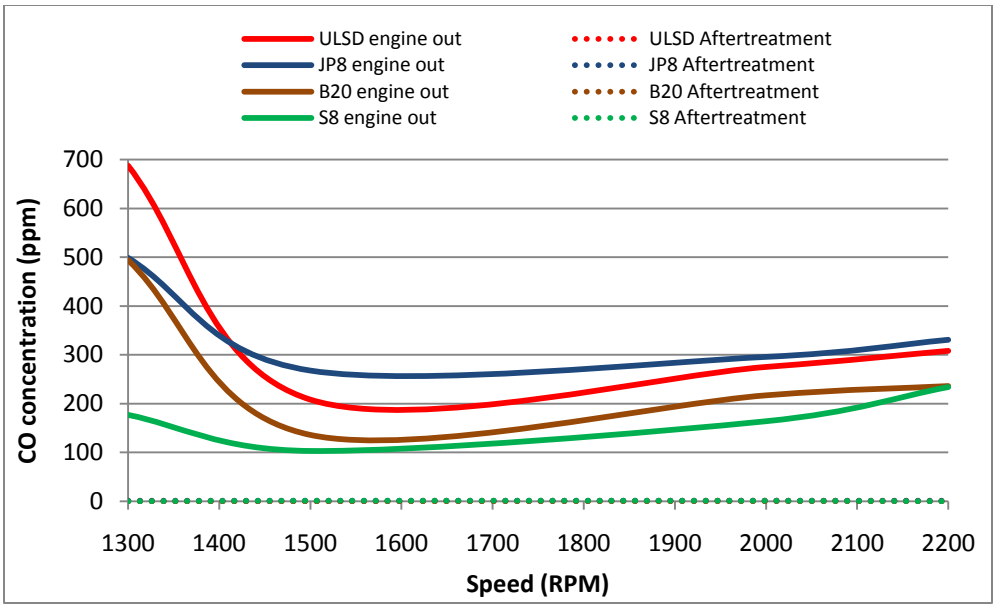

Figure 7.3.35 Effect of speed on CO emissions.

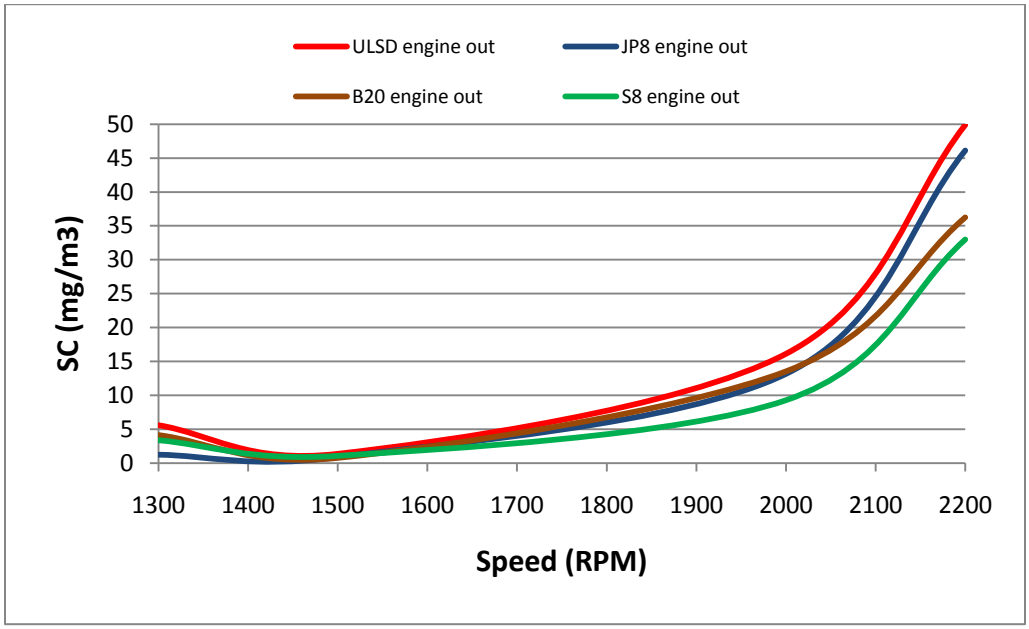

Figure 7.3.36 Effect of speed on soot concentration.

www.manaraa.com

1. The effect of alternative fuels on emissions:

a. The NO_X emission behavior at 7.5 bars is different from the one at 5 bars. S8 produced the highest oxides of nitrogen at 7.5 bars whereas it produced the least oxides of nitrogen at 7.5 bars. The residence time the combustion products spent in the critical temperature window at 7.5 bars for S8 is larger amongst all the fuels as compared to the emissions at 5 bars.

b. Amongst all the fuels, S8 produced highest oxides of nitrogen, followed by B20, followed by JP8 and then by ULSD. The residence time the combustion products spent in the critical temperature for S8 is largest, followed by B20. JP8 has higher oxides of nitrogen as compared to ULSD because of a higher fraction of premixed combustion burn of the two combustion fraction burns.

c. At 7.5 Bar IMEP ULSD produced the highest soot concentration emissions, followed byJP8, followed by B20 and then by S8. JP8 produced less soot as compared to ULSD because of higher amount of premixed fraction burn as compared to ULSD. B20 produced lesser soot then ULSD because the fuel is oxygen rich in nature. In case of S8, due to a high cetane number, the combustion is much more complete. Thus it can be concluded that at higher load (7.5 bar IMEP); fuel property such as the aromatic content plays an important role due to the dominance of the diffusion combustion burn.

d. Amongst all the fuels, CO emissions are highest with JP8, followed by ULSD, followed by B20 and then by S8. JP8 has the longest ignition delay and highest premixed fraction burn amongst all the fuels. Therefore the post oxidation reactions in this case are the least as compared to other fuels. ULSD has smaller fraction of premixed fraction burn as

www.manaraa.com

compared to JP8 and therefore it develops lesser CO emissions as compared to JP8. B20 has a higher fraction of diffusion combustion burn as compared to ULSD and JP8. S8 has the highest fraction of diffusion combustion burn amongst all the fuels.

2. The effect of speed on emissions:

a. There is an increase in the oxides of nitrogen at 1500 rpm as compared to 1300 rpm for all the fuels. There is a decrease in the EGR concentration at 1500 rpm.

b. There is a decrease in the oxides of nitrogen at 2000 rpm as compared to 1500 rpm. Although the start of combustion is advanced with respect to crank angle degree, the mass fraction burned by the premixed fraction is decreased due to the increase in EGR concentration. Also, the peak of bulk gas temperature is retarded as compared to 1500 rpm.

c. There is a decrease in the oxides of nitrogen at 2200 rpm as compared to 2000 rpm. Although the start of combustion is advanced with respect to crank angle degree, the mass fraction burned by the premixed fraction is decreased due to the increase in EGR concentration. Also, the peak of bulk gas temperature is retarded as compared to 2000 rpm.

d. The CO emissions at 1500 rpm are less as compared to 1300 rpm. There is a decrease in the EGR concentration at 1500 rpm

e. The CO emissions at 2000 rpm are high as compared to 1500 rpm. At 2000 rpm, the peak of compression pressure is higher than peak of combustion pressure. This is necessary in order to take care of oxides of nitrogen. Also, due to the increase in speed, the residence time the combustion products spend in the cylinder is less and therefore, the CO

www.manaraa.com

emissions are high at 2000 rpm as compared to 1500 rpm. Similarly, the CO emissions at 2200 rpm are less as compared to 2000 rpm.

f. The soot concentration emissions reduce at 1500 rpm but then it increases with the increase in speed. The EGR concentration at 1500 rpm is the least for all the fuels.

www.manaraa.com

8. CONCLUSIONS AND RECOMMENDATIONS:

8.1. Conclusions:

Since the engine is equipped with a stock E.C.U, the parameters cannot be controlled and it is not possible to isolate certain parameter. Therefore, the conclusions are purely based on the experimental results.

1. The oxides of nitrogen vary with the change in engine speed (load being the same). At 1500 rpm, the oxides of nitrogen attain the maximum value due to the decrease in the EGR concentration. The EGR concentration is the least at 1500 rpm for all the fuels. There is a decrease in the oxides of nitrogen at higher engine speeds due to the increase in EGR concentration.
2. The residence time the combustion products spend in the critical temperature window plays a very important role for engine out NO_X emissions. The emission behavior pertaining to the oxides of nitrogen is different at 7.5 bar IMEP from the one at 5 bar IMEP. S8 produced the highest oxides of nitrogen at 7.5 bar IMEP whereas it produced the least oxides of nitrogen at 5 bar IMEP. The residence time at 7.5 bar IMEP for S8 is larger amongst all the fuels as compared to the emissions at 5 bars.
3. At 7.5 bar IMEP, S8 produced highest oxides of nitrogen, followed by B20, followed by JP8 and then by ULSD. The residence time the combustion products spent in the critical temperature for S8 is largest, followed by B20. JP8 has higher oxides of nitrogen as compared to ULSD because of a higher fraction of premixed combustion burn of the two combustion fraction burns. At 5 bar (with EGR), JP8 produced the highest oxides of

www.manaraa.com

nitrogen followed by ULSD, than by B20 and then by S8. JP8 has a longest ignition delay which leads to a higher peak of premixed combustion. Also the overall EGR effect reduces in case of JP8 as compared to ULSD because of increase in throttle valve opening. However, the difference between ULSD and B20 pertaining to the oxides of nitrogen is negligible. In case of S8, due to a fairly high cetane number, the start of combustion is much earlier as compared to ULSD which limits the peak of premixed combustion to a lower value and consequently leads to a lower in cylinder bulk gas temperature.

4. The overall EGR effect varies with different fuels. The EGR concentration is assumed to be same with the same running conditions (same speed and torque). However, in order to develop the same power requirements, the throttle valve opening is different for different fuels. Thus, the overall EGR effect is less in case of S8 and JP8 as compared to ULSD. The overall EGR effect in case of B20 is almost similar as compared to ULSD. This is because only the lighter components (which are mainly diesel) contribute towards premixed combustion.
5. The CO emissions also vary with the change in engine speed (load being the same) and have a strong correlation with the EGR concentration. At 1500 rpm, the CO emissions attain the minimum value due to the decrease in the EGR concentration. The EGR concentration is the least at 1500 rpm for all the fuels. There is an increase in the CO emissions at higher speeds due to the increase in EGR concentration.
6. The CO emissions follow the same trend with the change in load (5 bar and 7.5 bar IMEP). Amongst all the fuels, CO emissions are highest with JP8, followed by ULSD, followed by B20 and then by S8. JP8 has the longest ignition delay and highest premixed

www.manaraa.com

fraction burn amongst all the fuels. Therefore, the post oxidation reactions in this case are the least as compared to other fuels. ULSD has smaller fraction of premixed fraction burn as compared to JP8 and therefore it develops lesser CO emissions as compared to JP8. B20 has a higher fraction of diffusion combustion burn as compared to ULSD and JP8. S8 has the highest fraction of diffusion combustion burn amongst all the fuels.

7. The PM emissions also vary with the change in engine speed (load being the same) and has a strong correlation with the EGR concentration. At 1500 rpm, the PM emissions attain the minimum value due to the decrease in the EGR concentration. The EGR concentration is the least at 1500 rpm for all the fuels. There is an increase in the PM emissions at higher speeds due to the increase in EGR concentration.
8. At 5 bar IMEP (with EGR), S8 produced highest soot concentration emissions, followed by B20, followed by ULSD, and then by JP8. However, at 7.5 bar IMEP, ULSD produced highest SC emissions, followed by JP8, followed by B20 and then by S8. At higher load, diffusion combustion burn is dominant and the rate of fuel burning is slow. Therefore, the fuel property such as the aromatic content of the fuel plays a very vital role in this case. ULSD has the highest aromatic content of all the fuels and therefore it registers the maximum SC emissions. On the other hand, S8 has the least aromatic content and therefore, it registers the minimum Soot Concentration emissions.
9. Efficiency of the aftertreatment system:
    a. In the range of existing operating conditions, the D.O.C. is fairly efficient in the oxidation of CO. The D.O.C. is also very effective in the oxidation of NO to NO_2. However, the F.T.I.R. is not so consistent with the analysis of unburnt hydrocarbons.

www.manaraa.com

b. In the range of existing operating conditions, the D.P.F. is fairly effective in reducing PM.

www.manaraa.com

8.2. Recommendations and future work:

1. A more accurate analyzer should be used in order to increase the accuracy of unburnt hydrocarbons emission measurements.
2. Develop a control system that will allow the override the stock ECU and optimize the injection strategy for each alternative fuel.
3. Develop a method to identify, on board, the type of fuel the engine is running on.

www.manaraa.com

APPENDIX

ABBREVIATIONS

ULSD: Ultra Low Sulfur Diesel Fuel

B-20: 20% Biodiesel blend with Ultra Low Sulfur Diesel Fuel

JP8: Jet Petroleum Fuel

S8: Synthetic Fuel

NO_X: Oxides of Nitrogen

CO: Carbon Monoxide

HC: Hydrocarbon

PM: Particulate Matter

SC: Soot Concentration

ARHR: Apparent Rate of Heat Release

LPPC: Location of Peak of Premixed Combustion

TDC: Top Dead Center

ATDC: After Top Dead Center

EGR: Exhaust Gas Recalculation

DOC: Diesel Oxidizing Catalyst

DPF: Diesel Particulate Filter

SCR: Selective Catalyst Reduction

IMEP: Indicated Mean Effective Pressure

ID: Ignition Delay

BSFC: Brake Specific Fuel Consumption

www.manaraa.com

RPM: Revolution per Minute

SOI: Start of Injection

SOC: Start of Combustion

CAD: Crank Angle Degree

SOF: Soluble Organic Fraction

www.manaraa.com

RERFERENCES

1. Timothy V. Johnson",Diesel Emission Control in Review",SAE 2009-01-0121.

2. David F. Merrion",Heavy duty diesel emission regulations - past, present and future", SAE 2003-01-0040.

3. Peter Wuensche, Franz X. Moser, Rolf Dreisbach and theodor sams",Can the technology for heavy duty diesel engines be common for future emission regulations in USA, Japan and Europe", SAE 2003-01-0344.

4. Robert Bosch",Automotive handbook, 7th edition; july 2007.

5 Aaron Williams, Robert McCormick, R.Robert Hayes, John Ireland, Howard L.Fang",Effect of biodiesel blends on diesel particulate filter performance", SAE 2006-01-3280.

6. H.E. Saleh", Effect of exhaust gas recirculation on diesel engine nitrogen oxide reduction operating with jojoba methyl ester", Renewable energy journal 34 (2009 2178-2186.).

7. Leo L. Stavinoha", Alternative fuels: Gas to liquids as potential 21st century truck fuels", SAE:2000-01-3422.

8. Atkinson, Christopher M., et al.," In cylinder combustion pressure characteristics of Fischer-Tropsch and conventional diesel fuels, "SAE: 1999-01-1472.

9. Lee, Rob, et al., " Fuel quality impact on heavy duty diesel emissions: A literature review", SAE: 982649.

10. Yoshimoto, Yasufumi, et al., "NOx reduction with EGR in a diesel engine using emulsified fuel",SAE: 982490.

11. Tamanouchi, Mitsuo, et al., "Effects of fuel properties and oxidation catalyst on exhaust emissions for heavy duty diesel engines and diesel passenger cars", SAE: 980530.

www.manaraa.com

12. Daisuke Kawano, Hajime Ishii, Yuichi Goto and Akira Noda," Application of biodiesel fuel to modern diesel engine", SAE: 2006-01-0233.

13. M.A. Ahmed, C.E. Ejim, B.A. Fleck, A. Amirfazli," Effect of biodiesel fuel properties and its blends on atomization", SAE: 2006:01:0893.

14. Hitoshi Shiotani, Shinichi Goto," Studies of fuel properties and oxidation stability of biodiesel fuel", SAE: 2007-01-0073.

15. Heinrich Prankl", Oxidation stability of fatty acid mthyl esters", 10th european conference on biomass for energy and industry, 8-11 june 1998, Wurzburg, Germany.

16. Piotr Bielaczyc, Andrzej Szczotka," Astudy of RME- based biodiesel blend influence on performance, reliability and emissions from modern light-duty diesel engines:, SAE: 2008-01-1398.

17. Aaron Williams, Robert L.McCormick, R.Robert Hayes, John Ireland," Effect of biodiesel blends on diesel paryiculate filter performance",SAE: 2006-01-3280.

18. David B.Kittelson," Engines and nanoparticles", PII: S0021-8502(97)10037-4.

19. Wayne A. Eckerle, Edward J. Lyford-Pike, Donald W. Stanton, Leon A.Lapointe, Shawn D. Whitcare and John C.Wall," Effects of methyl ester biodiesel blends on NOx emissions", SAE: 2008-01-0078.

20.Effects of biodiesel blends on vehicle emissions: NREL/MP-540-40554, October 2006.

21. Valerie L.Stringer, Way Lee Cheng, Chia-fon F.Lee, Alan C.Hansen," Combustion and emissions of biodiesel and diesel fuels in direct injection compression ignition engines using multiple injection startegies", SAE: 2008-01-1388.

22. Peter Eastwood," Critical topics in exhaust gas aftertreatment".

www.manaraa.com

23. Ken Nagashima, Yasuyuki Banno, Yasuharu Kanno, Makota Nagata," SOF combustion behaviour in flow-thru diesel oxidation catalysts", SAE: 2004-01-1942.

24. Stephane Zinola, Jacques Lavy, Anne Jaecker-voirol," Towards CO and HC aftertreatment devices for the next generation of diesel engines", SAE: 2008-01-1543.

25. W. Addy Majewski," Nitrogen oxides reactions in diesel oxidation catalyst", SAE: 950374.

26. T.V.Johnson,"Diesel emission control in review", SAE: 2003-01-0039.

27. Yougen Kong, Chris Huffmeyer, Randy Johnson, Bill Taylor, Wilbur Crawley, Granville Hayworth," Applications of an active diesel particulate filter regeneration system", SAE: 2004-01-2660.

28. Z. Gerald Liu, Matthew D.Skemp, Joseph C. Lincoln," Diesel particulate filters: Trends and implications of particle size distribution measurement", SAE: 2003-01-0046.

29. EPA07 MBE900 Service Manual.

30. AVL 415 S Variable Sampling Smoke Meter – Operating Manual.

www.manaraa.com

ABSTRACT

EFFECT OF ALTERNATIVE FUELS ON THE AFTERTREATMENT DEVICE

by

BUNPREET SINGH

December 2010

Advisor: Dr. Dinu Taraza

Major: Mechanical Engineering

Degree: Master of Science

There is no doubt that globally, alternative fuels have attained the center of attention in order to reduce the dependency on fossil fuels. A lot of research has been conducted on the alternative fuels in the automotive industry pertaining to the sustainability, engine performance and the emission characteristics.

The focus of this study is to investigate the effect of alternative fuels (JP8, Soy-based B20, and S8) on the aftertreatment device. Different fuel properties (both physical and chemical properties) affect the in cylinder combustion and engine out emissions. The research is conducted on a multi-cylinder commercial diesel engine (MBE 926) and the aftertreatment device is comprised of a Diesel Oxidizing Catalyst (D.O.C.) followed by a Diesel Particulate Filter (D.P.F.). The engine has a stock Electronic Control Unit (E.C.U.) and is calibrated to run on Ultra Low Sulfur Diesel (U.L.S.D.).

The testing at 5 bar IMEP was done in order to compare the data with a high speed single cylinder diesel engine in one of the test cells (lab 1356) at center of automotive research. On the other hand, at 7.5 bar IMEP, the investigation pertains to the effect of speed on in-cylinder

www.manaraa.com

combustion and the emissions. The emissions were recorded both before and after the aftertreatment device.

The study involves the effect of engine speed, engine load, fuel type, EGR concentration on the in-cylinder combustion and the emissions. Also, the study involves the effect of the aftertreatment device on the engine out emissions.

www.manaraa.com

AUTOBIOGRAPHICAL STATEMENT

I was born in Meerut, India on 29th December 1979. I finished my schooling from "Army Public School, Dagshai" located at himachal Pradesh in the year 1997. I completed my Bachelor of Technology in Mechanical Engineering from "G.Z.S.C.E.T", Bathinda, India in the year 2001. After my bachelor's, I did one year post graduation diploma in marine engineering from" Marine Engineering and Research Institute" Mumbai, India in the year 2002. Thereafter, I joined a merchant shipping company "Wallem Shipmanagement" in 2003 and worked as a training marine engineer for one year. After that I did certification course in marine diesel engines from "Mercantile Marine Department", Kolkatta, India in the year 2005 and joined back as 4th engineer. I worked for five years as a marine engineer officer. On board a ship, I was an officer in full charge of the operation, performance, maintenance, and complete overhauling of diesel engines. I worked extensively with marine diesel engines, planned and performed maintenance and repair of marine engine components including piston rings, cylinder head, cylinder liner, engine driven pumps, fuel system and injectors, turbocharger and marine boiler. I also worked on air compressors, purifiers, pumps, refrigeration plants, marine pneumatic and hydraulic control systems and other marine machineries.

In May 2007 I quit shipping as 3rd engineer and joined "Wayne State University", Detroit to pursue MS in Mechanical Engineering. Along with coursework I also got an opportunity to work under Dr. Dinu Taraza at the Center of Automotive Research. There as a graduate research assistant I did my research work for more than two years. Thereafter, I joined Caterpillar and am working as a performance analyst on C15 Tier4 rating development program.

www.manaraa.com